ISSN 1977-5296

ESARDA

European Safeguards Research and Development Association

Bulletin

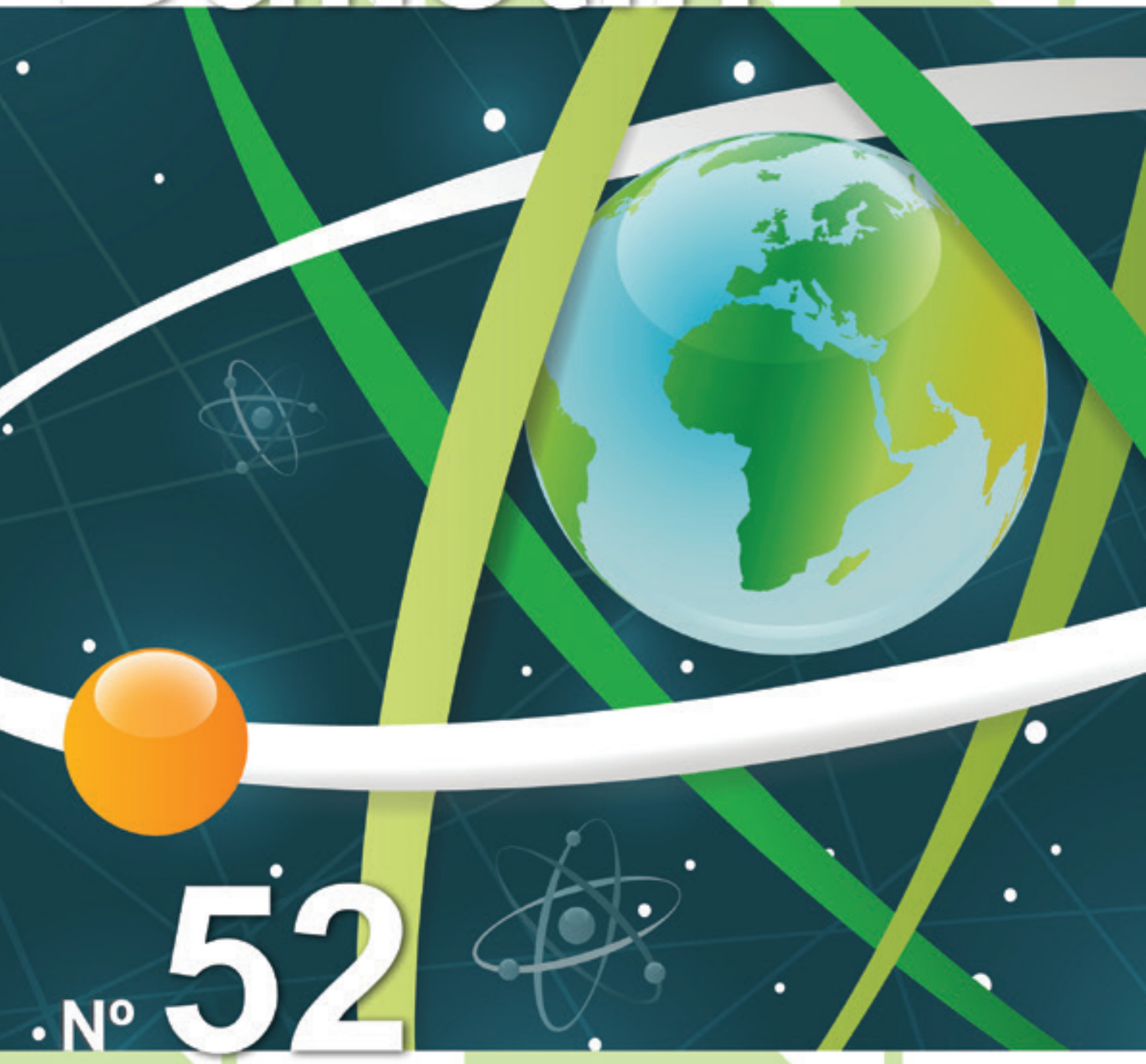

Nº 52

June 2015

ISSN 1977-5296

Number 52
June 2015

Editor
Hamid Tagziria

European Commission, Joint Research Centre,
ITU - Nuclear Security Unit
T.P. 800, I-21027 Ispra (VA), Italy
Tel. +39 0332-786324
esarda-bulletin@jrc.ec.europa.eu
hamid.tagziria@jrc.ec.europa.eu

Cover designed by Laura Spirito,
(JRC Ispra in Italy),

Printed by
IMPRIMERIE CENTRALE, Luxembourg

ESARDA
European Safeguards Research and Development Association

Bulletin

Table of Content Issue n° 52

Editorial

Hamid Tagziria

Dear Readers,

I am pleased to provide you with the 52nd edition of the Esarda bulletin predominantly containing the papers which have been selected by the chairperson of the 37th Esarda symposium in Manchester as best papers in each session, in addition to other papers independently submitted in recent months.

Once again and on behalf of the Editorial committee, I am grateful to authors for allowing their good work to be published in our journal and to the reviewers for their most valuable and important contributions to this process thus ensuring that good quality is maintained and continuously improved.

Each paper has generally been peer-reviewed by two independent experts and in some rare cases three when the two opinions were opposing and contrasting on important issues. The timing of the publication (i.e. issue 52 or 53) shall mostly depend on the readiness as regards the peer-review process bearing in mind the very tight schedule following the symposium.

I would like to thank all authors for submitting their papers to the bulletin, which they can also do anytime during the year and, in order to help with the ongoing process towards indexing and citation I encourage everybody to cite the work published in the bulletin by giving the following:

- Name of authors
- Title of article
- Page from-to
- ESARDA Bulletin, Issue and year

I am also pleased to announce that the ESARDA Bulletin has been submitted to Scopus for indexation in their academic database of publications.

Following the successful ESARDA symposium in Manchester attended by more than 200 participants with 139 papers submitted, it is my pleasure to include in this issue the symposium opening statement made by the ESARDA president James Tushingham and the after dinner speech by Graham Andrew.

I wish you all a very good summer break.

Hamid Tagziria
Editor and Editorial Committee Chairman

https://esarda.jrc.ec.europa.eu
Esardabulletin@jrc.ec.europa.eu
hamid.tagziria@jrc.ec.europa.eu

Esarda Symposium Opening Statement by the ESARDA President

James Tushingham

Good morning Ladies and Gentlemen, and welcome to Manchester.

For those of you who do not know me, my name is James Tushingham. I have the honour to be the current President of ESARDA and, in this capacity, it is my pleasure to welcome you to this, the 37th Annual Meeting of ESARDA: a symposium on safeguards and nuclear non-proliferation.

Manchester dates back to Roman times: a small settlement that grew in size to a modest town through the Middle Ages. It was the industrial revolution of the 19th century that saw the expansion of Manchester into the city that you see around you today. Manchester had the world's first inter-city passenger railway station, whilst the opening of the Manchester ship canal in 1894 – at the time the longest river navigation canal in the world – created the port of Manchester and linked the city to the sea. So, Manchester has long been a centre for communication.

Of course, Manchester has not only an industrial but an academic history. It was at today's University of Manchester that Ernest Rutherford pioneered his model of the atom. He is widely credited with first "splitting the atom" here, in Manchester, in 1917.

A generation later, the Manchester Small-Scale Experimental Machine was the world's first stored-program computer. It was built at the same university, and ran its first program in 1948. It was the first working machine to contain all of the elements essential to a modern electronic computer.

So, now, we have the background to split the atom; and to enable the efficient processing of safeguards-relevant information.

If those links appear a little tenuous, the UK has quite a history of more direct nuclear development, with a civil nuclear industry centred here in the North West of England.

Approximately 200km to the North West of Manchester lies the Sellafield reprocessing site, incorporating the original Windscale Piles and the Calder Hall reactor site. Construction of nuclear facilities commenced at Sellafield in 1947, under the UK Government's Ministry of Supply, with the first of four MAGNOX reactors becoming operational at Calder Hall in 1956. By then, the United Kingdom Atomic Energy Authority had been created, and Calder Hall and the Windscale works continued operation under UKAEA until the Authority divided into research and production divisions in 1971. The major part of the site then operated under British Nuclear Fuels Ltd, whilst UKAEA retained a number of laboratories. Today, Sellafield Ltd operates the site under contract to the Nuclear Decommissioning Authority, whilst the National Nuclear Laboratory operates its own nuclear laboratories on site.

Considerably closer to Manchester, around 60km to the Northwest, is the Springfields site - which has provided conversion and fuel fabrication services since the 1940s. Springfields was the first site in the world with plant providing nuclear fuel for a commercial reactor: Calder Hall. Its history is similar to that of Sellafield, in that it progressed from the Ministry of Supply, through UKAEA and BNFL, but is now operated by Springfields Fuels Ltd. Again, the National Nuclear Laboratory has a laboratory on site.

An equivalent distance away to the South West of Manchester, lies the site of the UK's uranium enrichment capacity, at Capenhurst. Some of you will have the opportunity to visit Capenhurst on Friday, and learn more about its history and the production of enriched uranium within a gas centrifuge enrichment facility.

To complete this brief historical and geographical tour of Manchester and the North West, I would like to add, unfortunately…

…that the Maldives lie approximately 8,700km to the South West.

Significantly closer to Manchester, and providing another historical perspective, is the Hack Green Nuclear Bunker. This facility was developed first as an underground radar bunker in the 1940s. It was as recent as 1976 – six years after entry into force of the Non-Proliferation Treaty - that the original bunker was converted into a vast underground complex: containing its own generating plant; air conditioning and life support; nuclear fallout filter rooms; communications; emergency water supply; and all the support services that would be required to enable 135 civil servants and military personnel to survive a sustained nuclear attack. There are opportunities to visit this "attraction" on the Tuesday and Thursday evenings of this week, and further details can be obtained from the ESARDA Reception desk.

Alongside the achievements of Ernest Rutherford and Manchester's computer pioneers, and as a contrast to the civil nuclear industry's achievements, the bunker serves as a sober reminder of why we are here today, and the importance of effective nuclear safeguards.

On the subject of sobriety, we should, of course, celebrate our achievements! The photograph above was taken in February 1970: not in anticipation of the entry into force of the Non-Proliferation Treaty, but to celebrate the first uranium hexafluoride mass spectrometer ion source at Capenhurst to complete 1,000 working hours – a major achievement at the time.

How times change, with other alcoholic and non-alcoholic drinks now available! More importantly, the Non-Proliferation Treaty has survived, and matured as the safeguards community has adapted - and continues to adapt - to new challenges. From the Non-Proliferation Treaty of 1970, successive generations have seen the Model Additional Protocol and now the State-Level Approach. The next generation will, I hope, see further technical challenges in arms control verification: a subject that ESARDA is beginning to address. The UK itself is, of course, already involved in ground-breaking verification work with Norway and with the United States on this subject.

As you know, the 2015 NPT Review Conference is scheduled to conclude this Friday. I am sure that you will join me in wishing a successful conclusion to the conference, and continued progress towards all of the commitments made under the NPT.

Personally, I began work at UKAEA's Harwell Laboratory in 1987 – a second generation in the nuclear industry and the son of one of those celebrating in 1970. I began to work in the field of nuclear safeguards in the early 1990s, and benefitted throughout my career from the support of those often older, and certainly wiser, than myself. I remember being welcomed to ESARDA as "new blood", with comments that it was good to see "someone young" entering the field of safeguards. No one says this to me anymore.

Which brings me to my point. Following the pioneers of nuclear science of a century ago; the development of nuclear energy in the 1950s; the NPT in the 1970s; my own involvement in nuclear safeguards and the purely coincidental development of the Model Additional Protocol in the 1990s, we should now be looking to the next generation.

Following shortcomings identified within a United Nations study on disarmament and non-proliferation education in 2002, ESARDA responded with the creation of a Working Group on Training and Knowledge Management. In March 2005, this Working Group presented a prototype course on nuclear safeguards and non-proliferation.

Ten years on, the 14th course has been completed. The course is open to master's degree students, in particular nuclear engineering students, but also to young professionals and International Relations and law students. It seeks to complement nuclear engineering studies by including nuclear safeguards within the academic curriculum. The course addresses aspects of the efforts to create a global nuclear non-proliferation system and how this system works in practice, dealing in particular with technical aspects and application of safeguards.

Now, the Training and Knowledge Management Working Group wishes to develop further, and a paper to be presented this Wednesday morning will propose a new strategy for how ESARDA might work with education, training and knowledge management in nuclear safeguards.

The establishment of an ESARDA Young Generation is an initiative intended to tie in to this strategy. Proposed by Riccardo Rossa, the ESARDA Young Generation is intended to provide a meeting point for students and young professionals involved in different aspects of nuclear safeguards, with the aim to contribute to the promotion of nuclear safeguards and enable a new generation to engage with ESARDA.

In part in anticipation of this new initiative, the National Nuclear Laboratory was pleased yesterday to host a session intended to provide a basic introduction to safeguards, and to inform academia of opportunities primarily within the UK safeguards community. This was in recognition that, increasingly, we need to look outside the traditional areas of expertise associated with ESARDA in order to explore synergies and potential benefits of new approaches and verification practices. As many of you will know, NNL is my employer and I should therefore say a few words about who we are and what we do, although there is much more information available on the exhibition stand outside. NNL was established by the UK Government with the intention to preserve and develop key research and development capabilities, and now operates as a Government-Owned laboratory. This essentially returns NNL to the roots of the UK nuclear industry and, I hope, to the enthusiasm of the generation at the time. NNL is proud to host the 2015 ESARDA Symposium.

There are, of course, challenges in engaging potential “new recruits” to nuclear safeguards. Not least is the financial burden: for example, of hosting and attending a symposium such as this one. I would like to express my gratitude to you all for your contribution to this symposium: to the authors, delegates, exhibitors, sponsors and the Parties of ESARDA.

Of course, the challenge extends to progressing the careers of those involved in the nuclear industry, particularly in a scenario where progress and promotion may be dependent upon a change in role rather than development in-post. It is incumbent upon all of us who have achieved our personal goals to remember how we benefitted from the previous generation, and to seek the means to ensure that we can assist those who will take our place.

So, I hope that we can take this week as an opportunity to respect the past, celebrate our current successes but look to the future: and welcome and support a new generation of safeguards practitioners.

With this, I would like to open the 37th ESARDA Symposium. I hope you will have a fruitful week, and I thank you very much for your attention.

37th Annual Meeting of ESARDA After Dinner Conference Speech, 20 May 2015

Graham Andrew CMG

Ladies and Gentlemen, it's a real honour for me to be asked to address this distinguished gathering. It is good to see some familiar faces and many new ones.

I'll focus today on safeguards. My own connection with safeguards began some 45 years ago – doesn't time fly when you are having fun – working at AWE Aldermaston developing Cf-252 neutron interrogation equipment for the non destructive assay of, for example, kilogram quantities of Pu and HEU metal. In the safeguards field working at Harwell I went on to develop hybrid K-edge and X-ray fluorescence techniques, and neutron measurement equipment (coincidence counting, and differential die away neutron interrogation for measuring waste streams in reprocessing plants). It's interesting for me to see papers on DDA and hybrid K-edge/XRF at this symposium.

The focus on physics measurements was quite a change from my chemistry focus at university, but as many of you here will know safeguards often tends to cross the boundaries of scientific and other disciplines. Safeguards is indeed a fascinating and a unique blend of science, policy and international diplomacy. ESARDA, the Joint Research Centre and national efforts have played a crucial role in helping to develop that science and policy base.

In regard to policy development it was a great honour for me – particularly coming from a Nuclear Weapon State – to be entrusted for five years as Chairman of the IAEA's Standing Advisory Group on Safeguards Implementation (SAGSI). This was in the late 90s at a key time for the development and introduction of the Model Additional Protocol (INFCIRC/540) and Integrated Safeguards (as it was known then).

Regarding ESARDA, I recall the 2nd symposium held in Edinburgh that I attended in 1981 (now we are on the 37th!). Some of the founding fathers of Safeguards were there: Fred Brown, Roger Marsh, Bob Keepin, Marizo Zifererro, Guy Dean (pronounced Gee Deeean, or "Giey Deeen" as a hotel clerk always called him during a SAGSI visit to Australia!), Adolf von Baeckmann and Sven Thorstensen from the IAEA, Marc Cuypers, Jon Harry, Gotthard Stein, to name just a few.

One of my fondest memories of ESARDA – sometimes also known in the early days as the "European Sustainable Reflection and Dining Association" – was the 13th symposium, which was held in 1991 in the Palais du Pape in Avignon, France. The evening meal came complete with jugglers and jousting from horseback in the dining room! OK you can bring the horses on now, Jim.

In complete contrast, I recall as Head of the UK safeguards Office, when I hosted an ESARDA international meeting of senior officials. With a very limited hospitality budget to hand, I gave a trusted member of staff the guidance of "please go easy with the food". I meant not to overdo the supply of fine meats, vintage wine etc. It was to my horror when I saw the individual in the background with his thumbs up. He had taken my guidance rather literally and before the assembled senior guests were just three small bowls of peanuts, a bowl of crisps and a few jugs of water (UK hospitality at its best). I'm pleased to see from this evening that things have improved.

I'd also like to briefly recall two other occasions concerning ESARDA and Euratom Safeguards:

- At the 15th ESARDA symposium in Rome held in 1993 I had a brief audience, together with Guy Dean from France, with no less than His Holiness Pope John Paul II. He had heard about the symposium and was intrigued about the work of safeguards and its mission, given its connection with nuclear non-proliferation, and asked to meet representatives. Guy and I were chosen – it was a great honour to meet His Holiness and brief him about international efforts such as "Programme 3+2" related to the Additional Protocol;
- The other occasion was in the late 1990s, where I found my name mentioned in an article in Platts Nuclear Fuel/Nucleonic week referencing a leak of a private conversation the then Director of Euratom Safeguards, my good friend Wilhelm Gmelin, had had with German representatives in which he mentioned my role as a "CEMO salesman". Many of you will know that CEMO is an acronym for the continuous enrichment monitor developed by the UK for use in gas centrifuge enrichment plants. It seems that I pushed its merits a little too hard – not everyone warmed to the idea of a device continuously monitoring enrichment and transmitting results in real time to Vienna and Luxembourg. C'est la vie!

As in all areas of human endeavour, you'll appreciate the importance of continuing to challenge established boundaries even if sometimes it's in the face of criticism and resistance. I recall well in the '80s and '90s the first mentions in the safeguards community of particle analysis and

satellite imagery – with some saying at the time "these are from the world of spies and aren't safeguards".

Thanks to your and others' efforts both are now bedrocks of the safeguards system (I don't mean the spies …. or do I …) and I note with pleasure that at the symposium this week there are papers on particle analysis, satellite imagery and other familiar topics. It's good to see that a really high technical standard of presentations has been maintained over the years.

The importance in safeguards of detecting undeclared nuclear activities in a State is of course now very well recognised. It can provide a significant deterrent: pushing a State that is seeking to proliferate towards conducting a separate clandestine programme, fuel cycle and procurement activities - at great cost and much increased risk of detection by inspectors and others.

Of course, not all endeavours bear fruit. I recall with some humour, the blue sky efforts of a few colleagues at the then BNFL Sellafield considering the use in the THORP Receipt and Storage spent fuel pool of a submarine, or remotely piloted submersible, for checking ultrasonic seals of Multi Element Bottles (storage flasks) containing spent fuel. The concept was ahead of its time and the assessed risk of an accident was too great so the submarine idea was quickly torpedoed.

If I can now indulge in sharing a few quick personal reflections on a couple of topics where I think the safeguards community may want to explore further in the future in the key area of improving capabilities to detect undeclared nuclear activities and facilities in a country as a whole (the difficult one).

Firstly, I believe that the use of Wide Area Environmental Sampling techniques (e.g. Kr-85 monitoring, and techniques for longer range detection of enrichment facilities) on a limited regional or country-specific basis is worth further consideration. If a country truly has nothing to hide and wants and needs, in special cases, to build international confidence it might be open to permitting the use of such technology on its soil. The Model Additional Protocol already has a relevant placeholder in Article 9.

Secondly, I also believe time has come to start the process of revisiting the technical Annexes to the Model Additional Protocol. In particular, Annex II is out of date and could, at least from a technical perspective, be modified quite quickly. In my humble view, it is worth the admittedly not inconsiderable bureaucratic, political and administrative burden of getting this done. There's no gain without pain.

More generally, perhaps one of the most disturbing lessons of previous proliferation attempts was the existence of an extensive illicit market for the supply of nuclear items, which thrived on demand. As we know, nuclear components designed in one country can be manufactured in another, shipped through a third and assembled in a fourth and used in a fifth.

Some would argue that the ease of which a multinational illicit network was set up and operated demonstrates the need to bolster some of the present informal non-binding arrangements. Personally, I think this could include providing for more comprehensive systematic sharing of information, such as exports denials and requests, with the IAEA – for example through and by the Nuclear Suppliers Group. Much of the hardware of interest is 'dual use' and the sheer diversity of technology makes it difficult to control or even track procurement attempts and sales. More needs to be done and I note that the JRC in particular has done some very good work to help strengthen this system.

My job in the IAEA, working for two very different but equally effective Director Generals, also emphasised to me the essential role of international diplomacy in safeguards. It's one thing having the technical and financial wherewithal but in the final analysis little can be achieved on the ground, even with binding legal undertakings, without the real willingness and cooperation of the parties concerned.

This showed up in the development of the so-called State Level Concept by the Agency and in negotiations on implementation of safeguards more generally. This is clearly not the main focus of an essentially technical (R&D) organisation like ESARDA but I leave the thought with you: time spent early on to consult and involve the wider safeguards community (industry, regulators, State representatives, academia, media, etc.) on developing policy and the associated emerging scientific developments is usually time very well spent.

In my time, I recall the successful efforts to communicate and consult widely with respect to the LASCAR project (for large-scale reprocessing plant safeguards) and the sensitive topic of Alternative Nuclear Materials (such as Np-237). It was interesting to hear today of the work in Belgium to include social science students and not just nuclear specialists in their safeguards training courses. Effective communication and consultation takes a lot of effort and patience: I wish you all well in explaining for example the complexities of 'Game Theory and Nash Equilibrium' (as presented at this symposium) to a sceptical IAEA board and member States. I jest!

During the past 13 years I worked with Agency colleagues in relation to Iraq, North Korea, Libya, Iran and other countries - some more successfully than others. The inspectors role was - and I'm sure still is – always to act as the impartial honest broker wanting to get to the facts and not taking sides in the process.

Overall, my time working in the UK and Vienna demonstrated to me that the interaction of safeguards, intelligence

efforts, export controls, diplomacy can be extremely powerful when properly leveraged: the whole together being greater than the individual parts working in isolation. All elements of the non-proliferation system are needed with their distinct and different roles and constraints duly respected. I also observed there is great power in the international community speaking with one voice - for example, a single united message to a member State from the IAEA Board.

I'm sure all here wish the very best for the recent fledgling deal currently being further negotiated between the EU3+3 and Iran, and for the vital verification job that will need to be undertaken. An important message for the international community to bear in mind is that the process of clarifying and drawing conclusions on the outstanding issues ('possible military dimensions', etc.) will take time to be credible; and to fulfil a key objective of easing tensions – you know the countries concerned – it must be credible and be seen to be. Even with the full engagement of both parties, it cannot be rushed. The negotiations also exemplify the necessity of continuing political dialogue among concerned States to address underlying insecurities and misunderstandings, and to build mutual confidence and in turn that very very fragile commodity, "trust".

As ever, key elements are the willingness of the State concerned to provide access (to information, to documents, to individuals, to locations) and at the same time for all involved to protect scrupulously the confidentiality of information.

In closing, I would like on your behalf to take this opportunity to add my voice to thank the organisers of the symposium here in Manchester - in particular Jim Tushingham, Adrian Bull and their team.

I look forward to following future developments in ESARDA and associated partners in the EU, the Agency, and internationally. On a light note, if I could leave one message with colleagues in the EU to take home: it's simply not true that the only reason the UK is holding an in/out referendum is to free itself from the oversight of EURATOM safeguards inspectors!

I hope you will enjoy the rest of the evening and the symposium. Thank you.

Tatton Park, UK, 20 May 2015

Real-time, fast neutron detection for stimulated safeguards assay

Malcolm J. Joyce[1], Justyna Adamczyk[2], Michael D. Aspinall[3], Francis D. Cave[3], and Romano Plenteda[2]

[1] Department of Engineering, Lancaster University, United Kingdom
E-mail: m.joyce@lancaster.ac.uk
[2] Department of Safeguards, International Atomic Energy Agency, Vienna, Austria
[3] Hybrid Instruments Ltd., Birmingham Research Park, United Kingdom

Abstract:

The advent of low-hazard organic liquid scintillation detectors and real-time pulse-shape discrimination (PSD) processing has suggested a variety of modalities by which fast neutrons, as opposed to neutrons moderated prior to detection, can be used directly to benefit safeguards needs. In this paper we describe a development of a fast-neutron based safeguards assay system designed for the assessment of ^{235}U content in fresh fuel. The system benefits from real-time pulse-shape discrimination processing and auto-calibration of the detector system parameters to ensure a rapid and effective set-up protocol. These requirements are essential in optimising the speed and limit of detection of the fast neutron technique, whilst minimising the intervention needed to perform the assay.

Keywords: neutron; assay; scintillator; fast

1. Introduction

Neutrons constitute the main route by which nuclear material might be assayed, non-destructively and remotely. Generally they can be considered to exist in two groups in terms of their energy: *fast* and *thermal*, wherein the former can be considered for most purposes to be limited to a maximum of ~5 MeV whilst the latter is usually defined by the ambient conditions at 0.0253 eV. Epithermal neutrons, ostensibly between 0.5 eV - 10 keV, are, like thermal neutrons, undetectable in the liquid scintillators used in this research due to the low-energy cut-off. Hence, they are, for the purposes of this paper, considered together. Thermal neutrons are often considered easier to detect because of the significant capture cross sections on materials containing ^{10}B and ^{3}He compared to higher energies. Fission neutrons emitted by isotopes that might provide useful signatures of nuclear materials are almost always emitted in the fast domain. Hence, if a thermal neutron detection modality is to be used, this requires that the neutrons are thermalized by hydrogenous materials (usually polyethylene) prior to detection. Such materials are bulky and can restrict the portability of such measurements. Thermal detection media, such as boron trifluoride and ^{3}He gas, are often considered either hazardous in use or supply limited, respectively; although these limitations have not prevented many forms of apparatus based on them being developed and used for nuclear materials assay over the last 50 years or so.

However, as the world seeks alternative sources of energy (and especially electricity) in light of depleted oil stocks and the desire to decarbonise electricity supplies, the nuclear industry is under renewed focus in terms of novel reactor design i.e. small modular reactors, Generation IV systems and alternative fuels. The latter includes revised thinking about such matters as fuel reuse, recycling, mixed-oxide variants and thorium. Whilst nuclear fission remains the only proven technology for massive production of carbon-free electricity, it is also being considered as an energy source for desalination, hydrogen production and bulk chemical synthesis. This multi-faceted nuclear renaissance heralds an era in which there is likely to be an escalation in international nuclear fuel trading and transportation, and all of these matters present challenges for the nuclear safeguards analyst. Such challenges go beyond the need to ensure that new capabilities are grasped to ensure the continuous improvement of safeguards assay and to encompass the need to replace and seek alternatives to established methods, particularly those based on thermal neutron detection.

Neutron detection is often preferred for fissile materials assay because it enables those neutrons emitted simultaneously in fission to be detected providing, in some cases, an *a priori* measurement of quantity of nuclear material present. The detection of neutrons in coincidence enables these neutrons to be discriminated from *single* neutrons that originate from a variety of other, competing contaminant sources and processes. An important example in this context are the isotopes that are susceptible to fission, such as ^{235}U, ^{238}U, ^{239}Pu, ^{240}Pu etc. which constitute sources that emit neutrons that are emitted simultaneously, whilst neutrons that result from the interaction of a particles (usually arising from a decay in actinide species) on light isotopes are emitted independently of each other.

To a thermal neutron detector, neutrons arising from a,n reactions or from fission are identical since the moderation process wipes out any information available associated with their initial energy. The discrimination is done instead by the processing electronics using the time correlation information associated with the fission neutrons. To isolate the coincident signature of fission neutrons from those not

correlated in time, a time window is usually applied, either electronically or in subsequent analysis; this time window is usually referred to as the coincidence gate. The uncorrelated neutron fluence constitutes a random, accidental contribution to the total number of coincident neutron events that fall within this gate. Coincident neutrons arising from a fission event are distributed very close to the first neutron detected (depending on the detector characteristic), exhibiting the so-called "Rossi-Alpha distribution". These neutrons are usually referred to as 'reals' in common parlance to reflect that they are real products of the fission event. Neutrons that are not products of the fission event or have scattered in the environment have a constant probability at whatever time they occur and are termed 'accidentals' due to their tendency to fall *accidentally* within the coincidence gate. Hence, the larger the gate, the larger the probability of a random accidental contribution. In order to account for these random accidental events, a delayed gate with the same width as the coincident gate is opened far from the first event. This technique is usually carried out within hardware or firmware referred to as a shift register and is a well-established means for identifying the accidental contribution. In certain conditions in which the amount of real coincidences is very small in comparison to the accidental contribution, the statistical uncertainty in the mass estimate required will be too large for a practical acquisition time to be achieved.

It is hence very clear that a significant factor that governs the uncertainty in coincidence measurements is the gate width. In thermal neutron detection systems the average delay between two coincident detections is due mainly to the time necessary for the thermalisation prior to detection. In sharp contrast, in the case of fast neutron detection, the delay between two coincident events is not driven by the time needed for thermalisation but only by the difference in time of flight of the two fission neutrons. This can be three orders of magnitude lower in comparison with a thermal detector.

This can be depicted by comparing the Rossi-Alpha distributions for a thermal system that requires moderation prior to detection, and a fast system that does not. This are shown in Figure 1, and illustrate the basis on which it is possible to move from an unavoidably wide time window of the order of ~100 μs for thermal systems to a much shorter, ~ 100 ns window for fast systems; the latter inferring significantly-reduced accidentals rates relative to the former.

This paper concerns the use of fast neutrons for neutron coincidence assay in contrast to long-established thermal neutron assays, the latter reliant predominantly on the use of ^{3}He. It describes measurements made in collaboration with the International Atomic Energy Agency (IAEA). This paper is focussed on development of the electronics that has been necessary to promote the use of long-established liquid scintillator detectors into a field-deployable active interrogation assay of uranium materials.

2. Concept outline and system architecture

Nuclear safeguards assay based on fast neutrons has been made possible by two developments: i) the availability of low-hazard, organic scintillation detectors and ii) electronic hardware and firmware that is sufficiently fast to enable real-time discrimination of neutrons from g-ray contamination.

A single neutron detector cannot detect two coincident neutrons due to the dead time (100-300 ns) in the detector and electronics. Therefore a number of distinct, single detection cells is necessary for coincidence assays. On the other hand, it is known that a large single liquid scintillator cell would distort the pulse too much to apply pulse shape discrimination between neutron and g effectively [3]. Detector systems comprising a limited number of detectors i.e. a pair of detectors are, by definition, no use for multiplicity measurements but they serve as a useful basis with which to introduce the system architecture for fast-neutron safeguards assay. A twin-detector arrangement is shown in Figure 2.

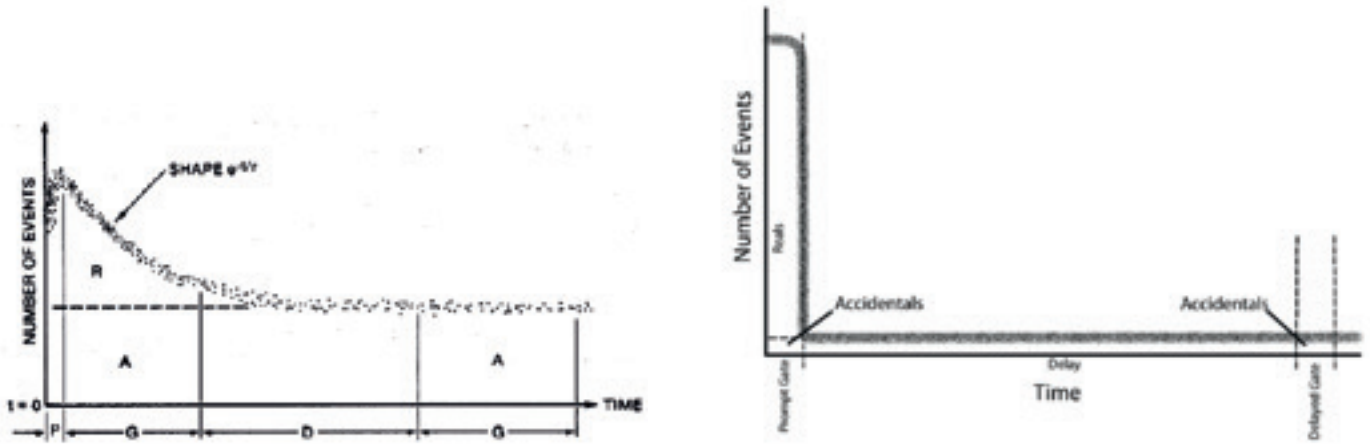

Figure 1: Rossi-alpha distribution for thermal systems (left) [1] and for fast systems (right) [2].

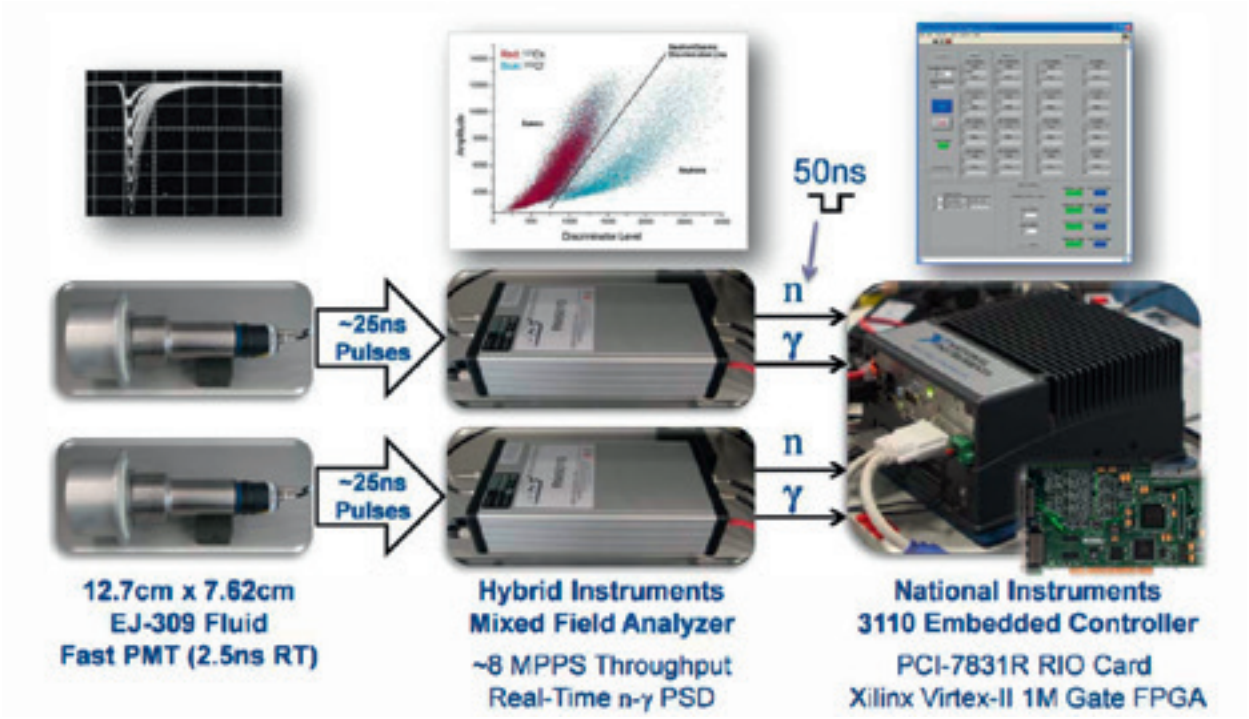

Figure 2: The fundamental system architecture for fast-neutron assay [2].

This comprises two high-flashpoint, low-hazard EJ309 detectors (Scionix, Netherlands) connected through to two single-channel mixed-field analysers (Hybrid Instruments Ltd.). The analyser comprises the high-voltage supply to drive the photomultiplier tube of a given detector and the firmware to discriminate the long-tailed neutron pulses from the shorter g ray events; it is a single-unit alternative to laboratory-based rack modules. The discriminated signals from these analysers are fed into a shift register configured on a field-programmable gate array on an embedded controller (National Instruments Ltd.).

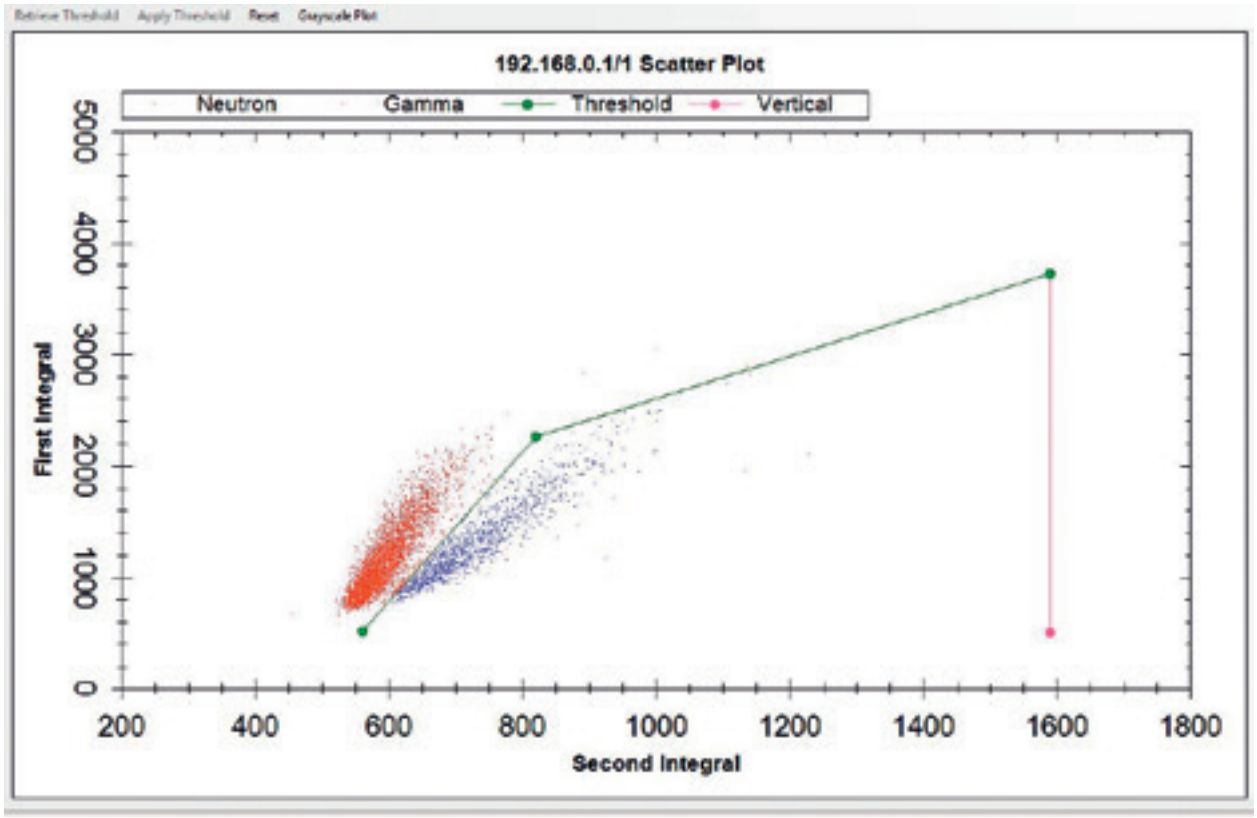

Figure 3: An exemplar scatter plot for one detector showing g rays in red and neutrons in blue, with a threshold separation line in green obtained with a ^{252}Cf source.

Neutrons and g rays interact with the organic scintillant differently; the former lose their energy predominantly via proton recoil whilst the latter interact with the electron structure of the scintillant molecules. This distinction in interaction processes results in a well-known albeit subtle difference in profile of the light pulse that results, with the neutron pulses exhibiting a longer falling edge than that of the g-ray events. When the data are plotted in terms of a first- and second integral of the area under the pulse the data separate into two clear loci which can then be used as a basis for separating the neutrons from the total field detected. The PSD method used in this case is the pulse gradient analysis method [4] in which discrimination is performed via the on-the-fly comparison of a sample in the falling edge of the digitized event profile with that of the pulse peak, following processing by a moving average filter. The specific advantage of this approach over digital alternatives is that it enables events to be processed in real-time, without the need for post-processing whilst maintaining satisfactory levels of figure-of-merit performance and data throughput. An exemplar depiction of the separation of events or *scatter plot* is given in Figure 3.

The distinction of this arrangement from long-established, laboratory-based methods of pulse-shape discrimination (PSD) is that it enables *real-time* PSD i.e. radiation incident on the detector is processed immediately, without the need for post-processing but retaining the synchronisation with pulse arrival time to enable the essential coincidence function. This is an important requirement for the application to be used autonomously in commercial fuel production facilities because post-processing would introduce a delay, thus interfering with the manufacturing process which is highly undesirable. Also the availability of a digital signal corresponding to each neutron event synchronised in time with the detection of the incident event renders the system compatible with existing acquisition systems at the IAEA. The mixed-field analyser also offers very high levels of throughput to enable the requisite levels of sensitivity to be reached with a practical number of detectors and within a reasonable period of acquisition. A more comprehensive description of the approach is available in [5].

In support of the research reported here, three significant developments have been made to the electronics and firmware:

- The high-voltage supply systems have been upgraded to provide for much greater stabilisation in use, to optimise the consistency of the gains across a significant number of detector cells, as necessary in this application.
- Events that result in pulses of significant amplitude can saturate the processing electronics. This has in the past contributed to an extensive and erroneous source of high-amplitude noise in the scatter plot data have been identified in firmware and removed. This leaves behind much better localised plumes that enables the better separation of neutrons and g rays, and has the potential for simpler PSD thresholding.
- The matching of gains across a significant number of detector cells i.e. >10 has been enabled by the real-time acquisition of pulse-height spectra for each cell. The auto-calibration of these spectra is enabled via the graphical user interface, providing a quick and effective approach to setting up arrays of detector systems of this type.

3. System design for fuel assembly assay

3.1 Detector system design: the IAEA Liquid Scintillator Uranium Neutron Collar (LS-UNCL)

The detector system used for this research is shown in Figure 4. It comprises 12 individual VS-1105-21 EJ309 detectors (Scionix, Netherlands). Each of these detectors is

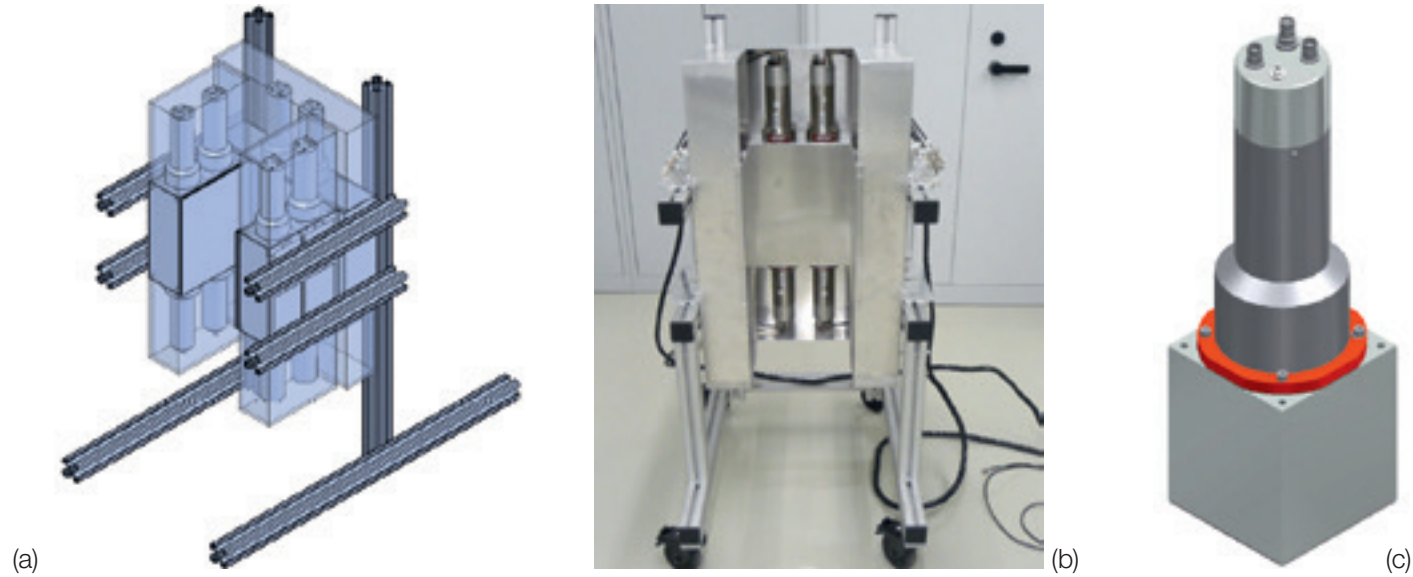

(a) (b) (c)

Figure 4: The detector system used in this research. Schematic design showing the vacant face where the stimulating source is positioned (a), physical embodiment (b) and a single detector (c).

a cube of dimensions of 100 mm × 100 mm × 120 mm with a photomultiplier tube of type 9821 FLB (ADIT Electron Tubes, Sweetwater, TX). The detectors are positioned in three gangs of four, with the detector cells facing one another and the PMTs aligned vertically, opposite one another. The pulse-shape discrimination is provided by three, 4-channel mixed-field analysers (Hybrid Instruments, UK) and the acquisition system to perform the shift register processing is as described in Section 2. The design of the detector arrangement was influenced by simulations that were performed by the Joint Research Centre, Ispra, Italy.

3.2 Multiple-channel real-time pulse-shape discrimination

An extended number of single-channel units is clearly not a satisfactory practical arrangement to process the pulses from a significant number of detectors. Therefore for this application three 4-channel analysers from a bank of four were configured, as shown in Figure 5.

This unit provides processing capability for 16 detectors ensuring that there is redundancy for 4 extra detectors if they are needed. As in the case of the system architecture discussed in Section 2, these analysers provide for 500 MHz processing per channel, 6 ns jitter between events and a processing period of 333 ns per event from detection through to output. They output discriminated 50 ns TTL pulses for each neutron and g ray, with the former being fed to the shift register firmware. A comprehensive description of the analyser is available in [6,7].

Figure 5: A bank of MFAx4.3 4-channel analysers used in this research.

3.3 System control

The MFAX4.3 systems are controlled via a graphical user interface, and the system can operate in two modes. The first of these is as a multi-channel analyser (MCA) in order to match the gain of all detection cells through the control of the high-voltage settings for each of the detectors; the user interface displays plots of counts versus channel for each of the channels in use and these are integrated in real time to enable quick and simple configuration on the fly. Two examples of these plots are given in Figure 6 below; one for ^{137}Cs (the usual choice of calibration source due to its single, 662 keV g ray), and ^{252}Cf, the latter a popular choice for configuring PSD thresholds. The other mode is as a PSD analyser, the unit's main role, in which it provides scatter plots for diagnostic purposes which are once again updated in real-time, as depicted in Figure 3. The user interface, as shown in Figure A1.1 in the appendix, allows high-voltage levels, trigger thresholds, pre-amplifier gains and pulse-shape discrimination thresholds to be adjusted. Once configured, these settings are written to the FPGA on the MFAX4.3 analyser so that after powering off, the settings for each channel are set in firmware, allowing for autonomous operation independent of the user interface.

The FPGA-based shift register is configured via a separate user interface, and an example screen shot of this is shown in Figure A1.2 in the appendix. This provides information for each pod (i.e. collection of four detectors), detection rates for each detector including GARRN estimates and doubles detection rates as a function of position in terms of time bins which is also displayed in terms of events versus bin number for each pod.

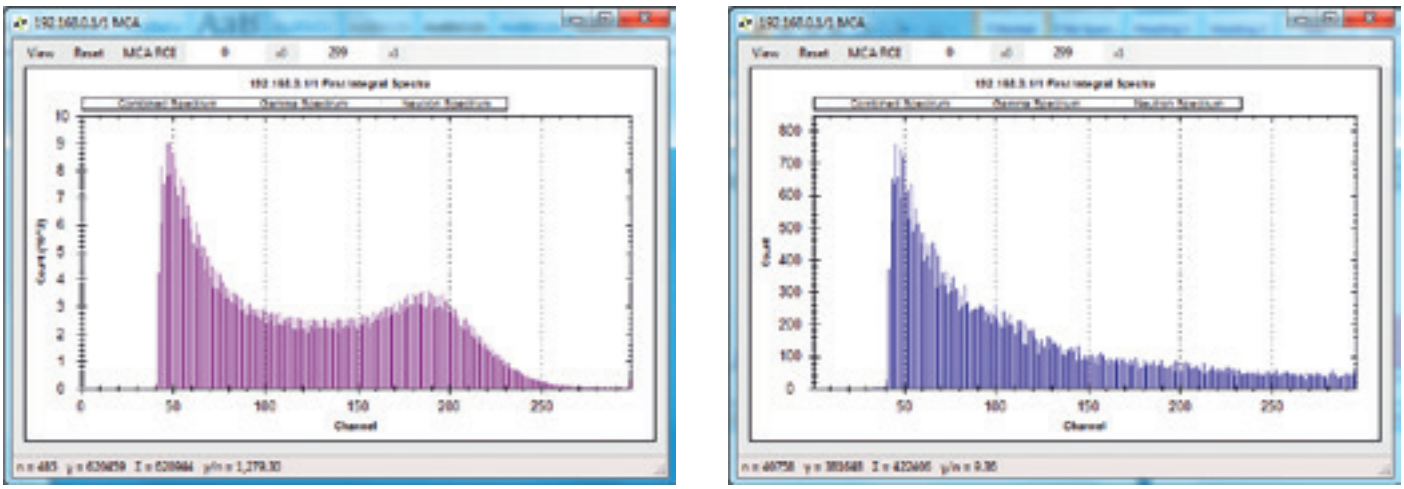

Figure 6: MCA plots for ^{137}Cs (left) and ^{252}Cf (right) provided in real-time by the MFAX4.3.

3.4 Combatting cross-talk

One consequence of using an array of fast neutron detectors is that to ensure satisfactory levels of detection efficiency the detectors are best positioned near to the sample under scrutiny. However, this exacerbates the possibility that neutrons might scatter from one detector to another. This is shown schematically in Figure 7.

The significance of a cross-talk event is that it results in a single neutron stimulating two counts in neighbouring detectors and, in the case of a single scatter from one detector to another, a coincident event despite in reality there only being one neutron, not two. If left uncorrected this contribution to the dataset would lead to an overestimate in the reals and a corresponding overestimate in the amount of material under assay.

In the system used in this work a filter has been constructed to reduce this possibility, which comprises a 1 cm polyethylene layer separating the detectors from one another, and a software function which discounts coincident events in neighbouring detectors.

4. Experimental details

4.1 Premise for the measurement

We have previously reported the assay of plutonium with a real-time fast neutron system, comprising 4 detectors and based on the detection of coincident events [7]. In this paper we describe an application for enriched uranium fresh fuel. Nuclear fuel of this type that has yet to be irradiated is a challenge to safeguards because the ^{235}U (for which the level of enrichment is of safeguards concern) emits a very weak radiation signature that does not provide for a quick and accurate measurement of the quantity of material present. Hence, for this aspect of the fuel cycle active methods are often employed in which a neutron source is used to stimulate ^{235}U fission in the fuel. The radiation that arises as a result is measured to infer fuel quantity and, ideally, enrichment (usually the neutron component of the stimulated field is the focus of the measurement). In certain conditions, when the stimulating neutrons are above the absorption energy for gadolinium (to be independent of the presence of this component), the neutron fluence from stimulated fission is very small compared with the interrogating source (i.e. 1:1000) and design challenges can arise in the context of the use of thermal detectors. The premise for this measurement is described in more detail in [8].

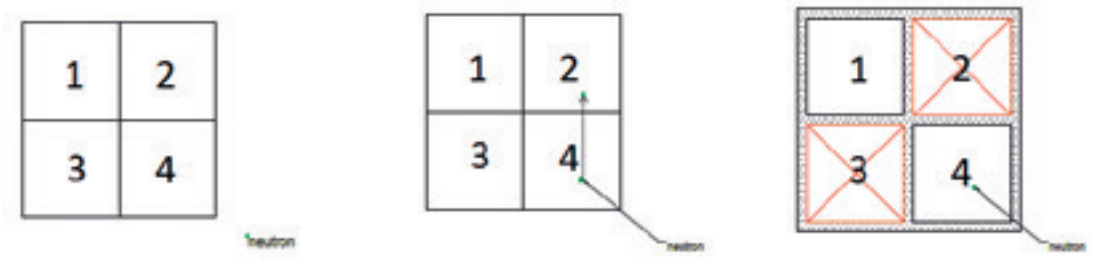

4 detectors without separation

Probability that one neutron will give a coincidence

1cm polyethylene layer + Anticrosstalk filter implemented in FPGA

Figure 7: A schematic depicting the cross-talk phenomena between four detectors arranged adjacent to one another.

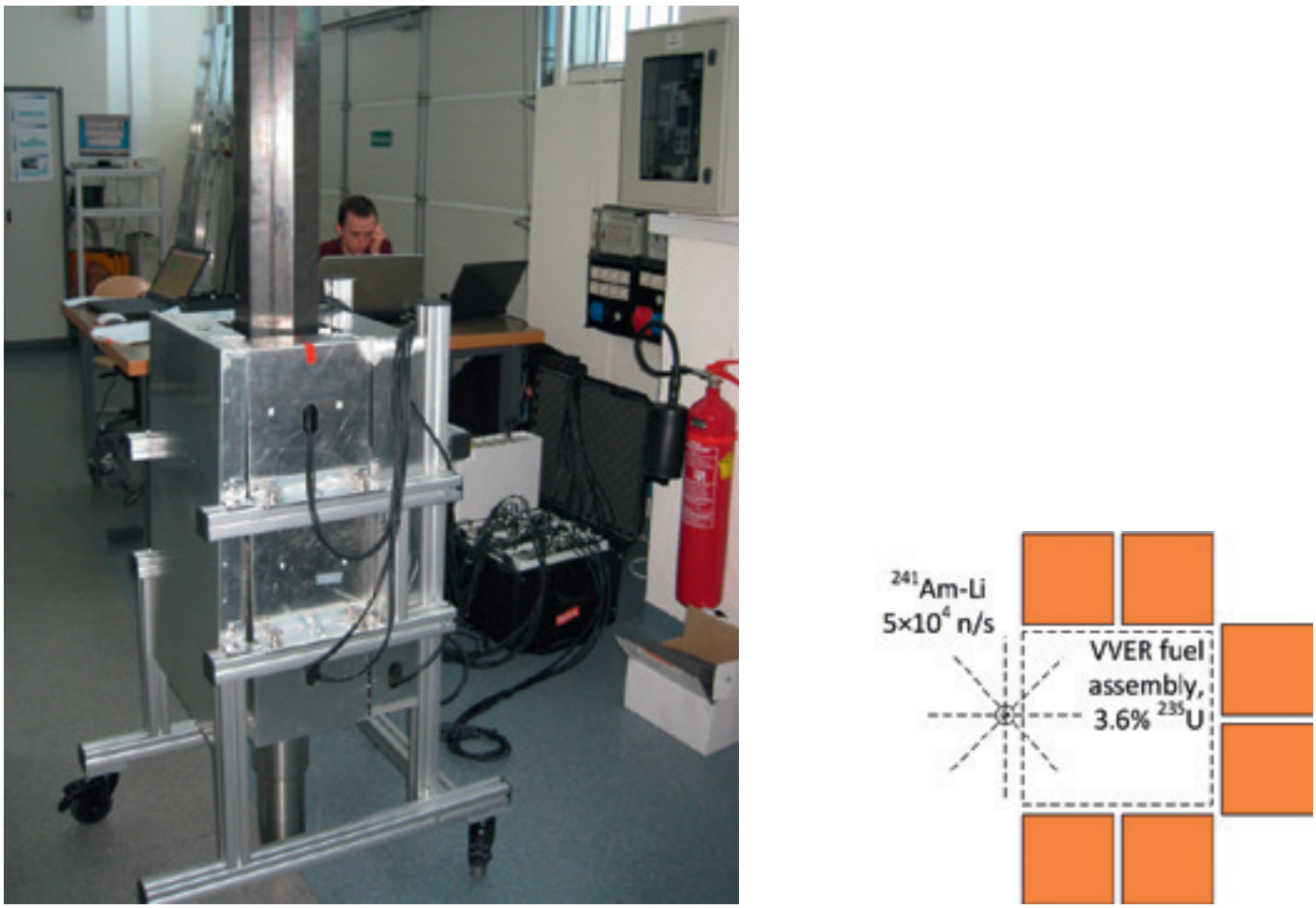

Figure 8: LS-UNCL system in use in Vienna (left) and a plan-view schematic of the system depicting the position of the source and assembly under test (right).

In this work we have adopted a similar rationale, with a ^{241}Am-Li source as the stimulus but with the combination of the liquid scintillator UNCL detector system, the MFAX4.3 analyser and the FPGA-based shift register instead of a thermal neutron detection system. This approach has two significant advantages in principle. Firstly, the coincidence counting approach with a shorter coincidence gate allows for data corresponding to the true coincident neutrons detected with significantly-reduced accidentals rates. Secondly, the system can also discriminate the stimulating source from the fission source on the basis of energy since it still preserves the original emission energy. In order to reduce the cross-talk contribution from the ^{241}Am-Li to negligible levels, the low-energy cut-off of the organic liquid scintillation materials (EJ309) in neutron energy is raised to approximately 400 keV. This ensures that the same neutron surviving the first detection is very unlikely to have enough have energy to be detected again.

4.2 Experimental set-up

The experiments central to the research described in this paper were carried out at the Atominstitut, TU-Wien, Vienna, Austria. The LS-UNCL was positioned near to the MFAx4.3 units and the associated HV, signal-input, and signal-output (neutron and g-ray) cables were connected to the MFAx4.3. The gains of the detectors were matched over Ethernet using a ^{137}Cs source and the signal output cables were connected to the National Instruments ® industrial controller for the multiplicity data collection. The ^{241}Am-Li source (neutron emission rate 5×10^4 per second) was placed in the vacant face of the LS-UNCL detector system i.e. the face void of any detectors. The source was removed to allow for passive measurements to be made of the material under test (predominantly of the ^{238}U content present in the sample) and then active measurements were made (stimulating neutrons from the ^{235}U content).

The sample was a WWER-440 fuel assembly, of 3.6% enrichment as shown with the LS-UNCL system and MFAx4.3 in Figure 10. The total mass of uranium in this assembly was 61.965 kg comprising 2.232 kg ^{235}U. Data were acquired for 15 minutes, both passive and active. The threshold was set to 400 keV neutron-equivalent energy with a coincidence gate width of 100 ns.

4.3. Results

Duration of measurement	Neutron detection rates (totals) per second			Uncertainty
	Passive reals	Active reals	Net reals	
15 minutes	1.28	5.57	4.28	2%

Table 1: Data recorded for the passive and active measurement of a 3.6%-enriched WWER-440 fuel assembly.

The results from a 15-minute measurement of the WWER-440 fuel assembly are given in Table 1. These include the passive-real neutron rates (without the source) and the active-reals neutron rates (with the source). The net reals rate is obtained via subtraction, giving a 2% uncertainty in the measurement.

5. Conclusions

The research described in this paper demonstrates that liquid organic scintillators can be used effectively for the analysis of enrichment levels in a nuclear fuel assembly, in this case a 3.6%-enriched WWER-440 assembly. In particular, three advancements made to the electronics in terms of high-voltage stabilisation, removal of saturated pulse profiles and auto-calibration of detector gains have yielded significant advantages in operation. The use of liquid scintillators, coupled with real-time digital pulse-shape discrimination, results in extremely low accidentals rates offering the potential for the assay of a wider range of nuclear materials than previously considered possible. The approach offers the benefits of faster assay of fresh fuel than was previously considered possible as a result of the very low accidentals rates or conversely, measurements with smaller stimulating sources where this presents benefits in terms of radiation protection and ease of use.

6. References

[1] N. Ensslin, *Principles of neutron coincidence counting, chapter 16, Passive non-destructive assay manual,* pp. 457-492, http://www.lanl.gov/orgs/n/n1/panda/00326411.pdf

[2] A. Lavietes, R. Plenteda, N. Mascarenhas, L. M.Cronholm, M. Aspinall, M. Joyce, A. Tomanin, P. Peerani *Liquid Scintillator-Based Neutron Detector Development* Nuclear Science Symposium and Medical Imaging Conference (NSS/MIC), 2012 IEEE, Anaheim, pp. 230-234.

[3] A. Lavietes, Private communication, International Atomic Energy Agency, Vienna, Austria, June 2011.

[4] M. D. Aspinall, B. D'Mellow, R. Mackin and M. J. Joyce, 'Digital n-g discrimination in liquid scintillators using pulse gradient analysis', Nuclear Instruments and Methods **A578** (1) 191-197 2007

[5] M. J. Joyce, 'Fast neutron multiplicity assay', Nuclear Future 9 (6) 43-46 Nov./Dec. 2013.

[6] M.J. Joyce, M.D. Aspinall, F.D. Cave, A. Lavietes, *A 16-channel real-time digital processor for pulse-shape discrimination in multiplicity assay*, IEEE Trans. Nuc. Sci. 61 (4) pp. 2222-2227 (2014).

[7] M.J. Joyce, K.A.A. Gamage, M.D. Aspinall, F.D. Cave, A. Lavietes, *Fast Neutron Coincidence Assay of Plutonium with a 4-Channel Multiplexed Analyzer and Organic Scintillators*, IEEE Trans. Nuc. Sci. 61 (3) pt. 2 pp. 1340-1348 (2014).

[8] A. Lavietes, R. Plenteda, N. Mascarenhas, M. Cronholm. M. Aspinall, F. Cave and M.J. Joyce, 'Development of a liquid scintillator–based active interrogation system for LEU fuel assemblies', oral paper for the IEEE Advancements in Nuclear Instrumentation, Measurement Methods and Analysis (ANIMMA), Marseille (June 2013), paper #1257, DoI: 10.1109/ANIMMA.2013.6728037.

7. Acknowledgments

This work was funded by the UK Department of Energy and Climate Change through the UK Safeguards Technical Support Programme in support of IAEA safeguards. We acknowledge the support of P. Peerani and A. Tomanin at the JRC ISPRA, Italy, for supporting calculations.

Appendix

A.1

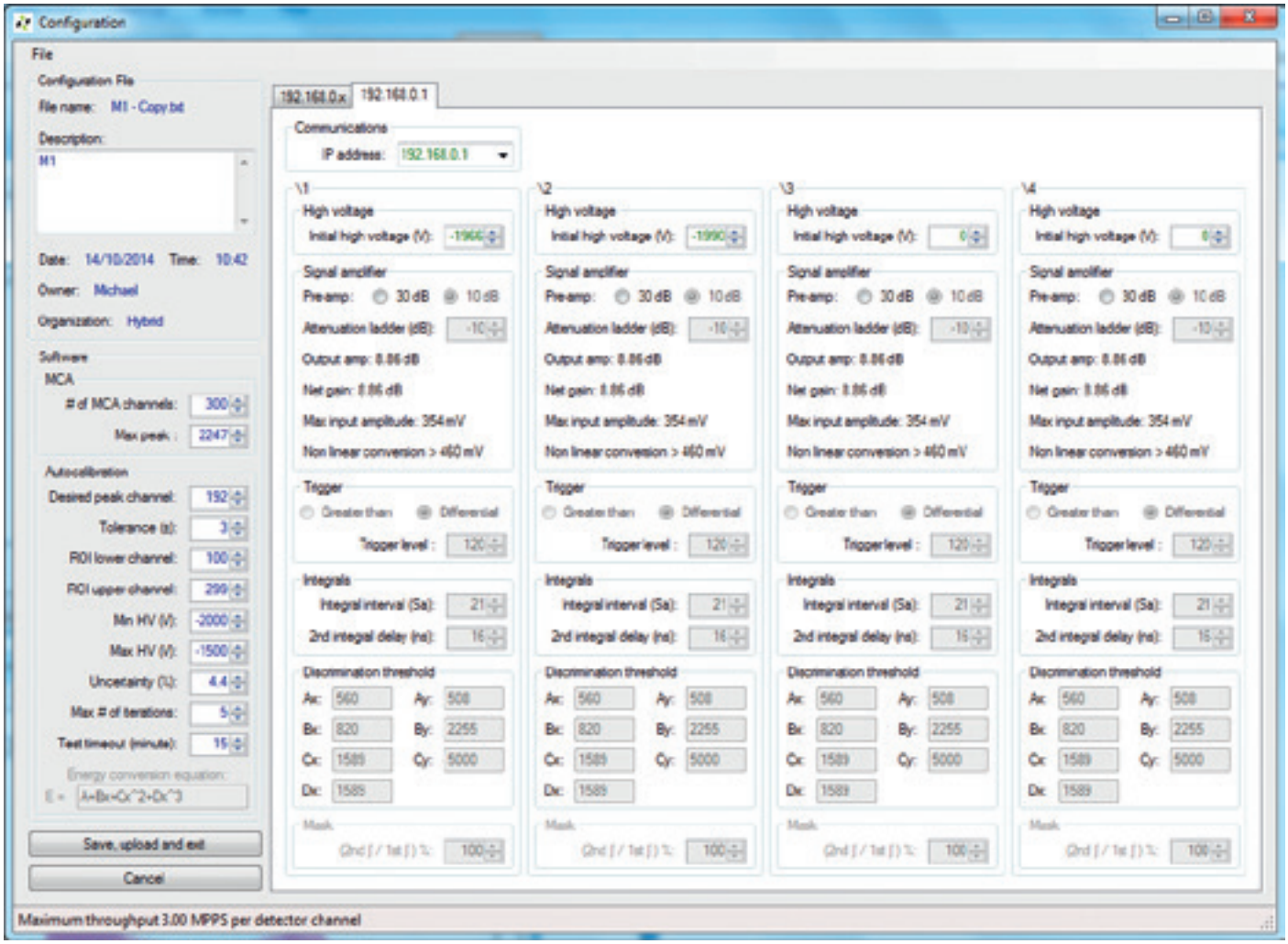

Figure A1.1: A screen shot from the control laptop of one of the control environments on the MFAX4.3.

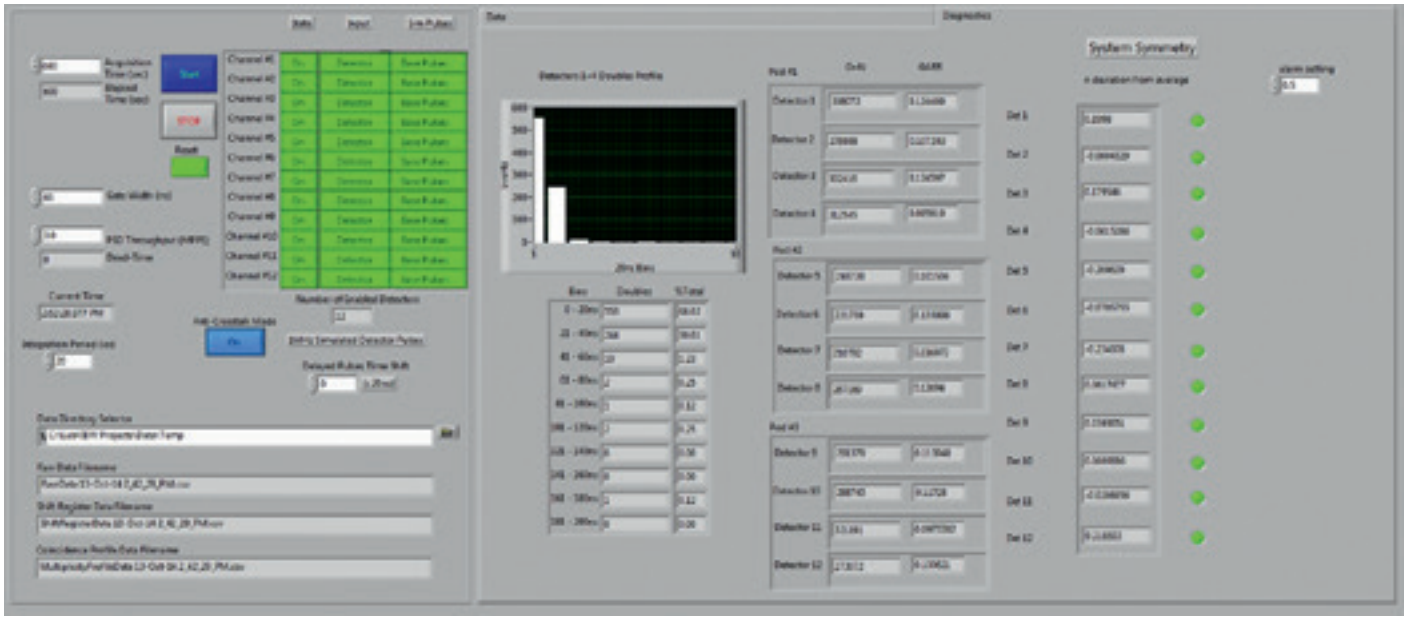

Figure A1.2: A screen shot from the control laptop of LabView ® environment configured to control the shift register.

Influence of fuel composition on the spent fuel verification by Self-Interrogation Neutron Resonance Densitometry

Riccardo Rossa[1,2], Alessandro Borella[1], Pierre-Etienne Labeau[2], Nicolas Pauly[2], Klaas van der Meer[1]

[1] SCK•CEN, Belgian Nuclear Research Centre, Boeretang, 200 - B2400 Mol, Belgium
[2] Université libre de Bruxelles, Ecole polytechnique de Bruxelles - Service de Métrologie Nucléaire (CP 165/84), Avenue F.D. Roosevelt, 50 - B1050 Brussels, Belgium
E-mail: rrossa@sckcen.be

Abstract:

The Self-Interrogation Neutron Resonance Densitometry (SINRD) is a passive Non-Destructive Assay (NDA) that is developed for the safeguards verification of spent nuclear fuel. The main goal of SINRD is the direct quantification of ^{239}Pu by estimating the SINRD signature, which is the ratio between the neutron flux in the fast energy region and in the region close to the 0.3 eV resonance of ^{239}Pu. The resonance region was chosen because the reduction of the neutron flux within 0.2-0.4 eV is due mainly to neutron absorption from ^{239}Pu, and therefore the SINRD signature can be correlated to the ^{239}Pu mass in the fuel assembly.

This work provides an estimate of the influence of ^{239}Pu and other nuclides on the SINRD signature. This assessment is performed by Monte Carlo simulations by introducing several nuclides in the fuel material composition and by calculating the SINRD signature for each case. The reference spent fuel library developed by SCK•CEN was used for the detailed fuel compositions of PWR 17x17 fuel assemblies with different initial enrichments, burnup, and cooling times.

The results from the simulations show that the SINRD signature is mainly correlated to the ^{239}Pu mass, with significant influence by ^{235}U. Moreover, the SINRD technique is largely insensitive to the cooling time of the assembly, while it is affected by the burnup and initial enrichment of the fuel. Apart from ^{239}Pu and ^{235}U, many other nuclides give minor contributions to the SINRD signature, especially at burnup higher than 20 GWd/t$_{HM}$.

Keywords: SINRD, neutron resonance densitometry, reference spent fuel library, Non-Destructive Assay, spent fuel verification

1. Introduction

The International Atomic Energy Agency (IAEA) has the task to ensure that all nuclear activities in the Member States are devoted exclusively to peaceful applications. In order to achieve this objective, the Nuclear Material Accountancy (NMA) is the primary verification tool, and it is supported by Containment and Surveillance (C/S) measures [1].

As part of the NMA for spent nuclear fuel, the non-destructive assays (NDA) are playing an important role for the verification of operator data. Moreover, they can be used for the characterization of spent fuel both for safeguards verification and for other applications such as the disposal of spent fuel in a geological repository [2]. Many NDA methods are currently under investigation to improve the capabilities of current NDA techniques [3], and the Self-Interrogation Neutron Resonance Densitometry (SINRD) is proposed to directly quantify the ^{239}Pu mass in a fuel assembly [4].

However, in addition to ^{239}Pu, spent fuel contains a wide variety of radioactive elements that are resulting from the irradiation in the reactor core. In order to evaluate the influence of several nuclides on the results of the SINRD technique, a set of simulations were carried out considering fuel with different fuel compositions. The impact of single nuclides included in the fuel composition was evaluated following a multi-step procedure. Starting from fuel containing only ^{238}U and ^{16}O other nuclides were added sequentially to estimate the effects of each isotope on the SINRD signature and on the neutron energy distribution. Moreover, the SINRD signature was calculated for fuel with different initial enrichment, burnup, and cooling time, to evaluate the sensitivity of SINRD to the fuel irradiation history. In fact the contributions of individual nuclides on the spent fuel neutron emission, evaluated in this paper by calculating the SINRD signature using Monte Carlo simulation, are not straightforward to quantify during the measurement of an actual spent fuel assembly [5].

The background information on the SINRD technique is given in Section 2, followed by the description of the Monte Carlo model developed for the simulations and the details of the fuel compositions used in the study. Then the influence of single nuclides on the SINRD signature is evaluated in Section 4, whereas the impact of the fuel irradiation history is analyzed in Section 5. Finally the conclusions of this study are drawn at the end of the paper.

2. Background on the SINRD technique

The SINRD technique is a passive NDA method that has the unique feature to directly quantify the ^{239}Pu content in a spent fuel assembly, and this goal is achieved by measuring the attenuation of the neutron flux in the 0.2-0.4 eV energy region. This energy region is close to the significant

resonance of ^{239}Pu, and therefore the reduction of the neutron flux is expected to be correlated to the ^{239}Pu concentration in the fuel [6], [7], [8], [9].

The ^{239}Pu content is estimated by using the SINRD signature, which is defined in Formula (a) as the ratio between the neutron flux in the fast energy region (*FAST*) and in the region close to the resonance (*RES*).

$$SINRD = \frac{FAST}{RES} \qquad (a)$$

A ^{238}U fission chamber and a ^{239}Pu fission chamber are envisaged to measure the fast neutron flux and the flux around the 0.3 eV resonance region, respectively. The term "self-indication" can also be used in the acronym of SINRD instead of "self-interrogation" because the isotope quantified with the technique is also used as active material in the detector to increase the detection of neutrons in the resonance region. Apart from the SINRD technique, self-indication measurements are a well-established method for cross-section measurements [10], [11], [12]. In the approach proposed for SINRD the ^{239}Pu resonance region is selected by wrapping a foil of Gd or Cd around the ^{239}Pu fission chamber. These elements are also called filters because they exhibit a cut-off energy for neutron absorption slightly below and above 0.3 eV. Therefore by taking the difference between the neutron fluxes transmitted through each filter, the estimation of the neutron flux around 0.3 eV is possible.

3. Description of the model

3.1 Monte Carlo model of the fuel assembly and detector

The PWR 17x17 fuel assembly geometry was taken as reference for the development of the Monte Carlo model. The MCNPX code [13] was used to create the model of the fuel assembly and of the 12 cm thick slab of polyethylene surrounding it, and the geometrical dimensions of the fuel assembly were taken from [14]. By simulating this configuration the neutron moderation occurred mainly outside the fuel assembly and this leads to a clearer reduction of the neutron flux at 0.3 eV due to ^{239}Pu absorption. In fact, the neutron moderation within the fuel pins occurring when the fuel assembly is stored under water is detrimental for the SINRD technique, because it reduces the indication of the neutron absorption due to ^{239}Pu as mentioned in [15], [16].

The neutron flux (j_{in}) was calculated in the central guide tube of the assembly by computing a F4 flux tally in a void cavity that can host the neutron detector and filter. The void cavity extended over the 2 m in the central axial location of the fuel assembly to consider the axial region with constant burnup [16]. No model of detector or filter was placed at this stage in the simulation, and the flux transmitted through the filter (j_{tr}) used for the calculation of *RES* was estimated as:

$$\varphi_{tr} = \varphi in * exp(-d*l*\sigma_{tot}^{D}) \qquad (b)$$

where *d* is the atom density, *l* is the thickness, and is the Doppler broadened total cross-section of the filter. Therefore, the transmitted flux is directly related to the total cross section and the area density of the elements present in a sample [17]. Considering the results in [18], a 0.1 mm Gd filter and a 1.0 mm Cd filter were used in the calculations to achieve a good balance between significant sensitivity to ^{239}Pu and large total neutron counts.

For the estimation of *FAST*, Formula (b) was modified by neglecting the exponential term since a bare ^{238}U fission chamber is used for the measurement.

The source term in the Monte Carlo simulations was modelled by using the parameters for the ^{244}Cm Watt fission spectrum included in [13], and $5*10^8$ neutrons were run for each simulation to reach a statistical uncertainty of about 0.1% on the total neutron flux tally.

3.2 Characteristics of the spent fuel compositions

Fuel compositions containing the 50 main neutron absorbers were selected for this study in order to account for the influence of single nuclides on the SINRD signature. The reference spent fuel library was developed for more than 1600 case studies according to several variables such as initial enrichment, fuel burnup, and cooling time after discharge [19], [20].

In this paper the fuel compositions calculated for 4 values of initial enrichment (i.e. 3.5, 4.0, 4.5, 5.0%), 6 values of burnup (i.e. 5, 10, 15, 20, 40, 60 GWd/t_{HM}), and 5 values of cooling time (i.e. direct discharge, 30 days, 5, 10, 50 years) were included in the Monte Carlo simulations.

The simulations in Section 4 evaluated the influence of single nuclides on the SINRD signature, and the ^{239}Pu concentration was selected first as additional nuclide apart from ^{238}U and ^{16}O. Then several nuclides were added sequentially and the SINRD signature was calculated for each case. The concentration of each nuclide added in the fuel composition was taken from the reference fuel library, and the quantity of ^{238}U was adjusted to keep a constant total fuel mass. The study in Section 5 compared the SINRD signature calculated for fuel with different irradiation histories, and the fuel composition for these simulations contained the 50 main neutron absorbers as calculated in the reference spent fuel library. The ENDF/B-VII.0 nuclear data library [21] was used for the neutron cross-sections values used in all simulations.

4. Influence of single nuclides on the SINRD technique

4.1 SINRD signature

One of the objectives of this paper is to investigate the influence that single nuclides have on the SINRD signature. To reach this goal, several simulations were performed starting from fuel containing only ^{238}U and ^{16}O, and then adding one nuclide sequentially as described in Section 3.2. The nuclides chosen in this section represent the nuclides that have the highest macroscopic cross-section in the energy region around 0.3 eV and therefore are expected to give the major contributions to the SINRD signature [16].

Figure 1 shows the normalized SINRD signature as a function of the ^{239}Pu content for the cases selected in this study. The simulations considered fuel with 3.5% initial enrichment, 10 years of cooling time, and burnup up to 60 GWd/t_{HM} as indicated in the plot. The values of the SINRD signature were normalized to the case obtained for fuel containing only ^{238}U and ^{16}O. Several groups of data points can be identified on the plot as a function of the ^{239}Pu content, and they reflect the different fuel burnup considered in this study.

At low burnup fuel the SINRD signature obtained with a detailed fuel composition is almost the same as the signature obtained with only ^{239}Pu and ^{235}U as additional nuclides. Moreover, the ^{235}U gives the major contribution up to 20 GWd/t_{HM}. By increasing the burnup the contribution from other nuclides becomes more relevant, and Table 1 shows the share of SINRD signature due to the single nuclides added in the fuel composition for fuel with 3.5% initial enrichment, 10 years cooling time, and 60 GWd/t_{HM} burnup. For the cases reported in Table 1 the two main fissile isotopes in spent fuel, namely ^{239}Pu and ^{235}U, account only for about 60% of the SINRD signature. The influence of the nuclides included in Table 1 was also observed in [22] by using the perturbation method.

Nuclide	SINRD signature	Share of full material card
^{239}Pu [1]	4.3	57 %
[1] + ^{235}U [2]	4.7	62 %
[2] + ^{241}Pu [3]	5.2	68 %
[3] + ^{240}Pu [4]	5.9	78 %
[4] + ^{241}Am [5]	6.4	83 %
Full card	7.6	100 %

Table 1: Normalized SINRD signature and share compared to the full material card. The values refer to fuel with burnup of 60 GWd/t_{HM} and the uncertainty associated to the SINRD signature was always lower than 0.1%.

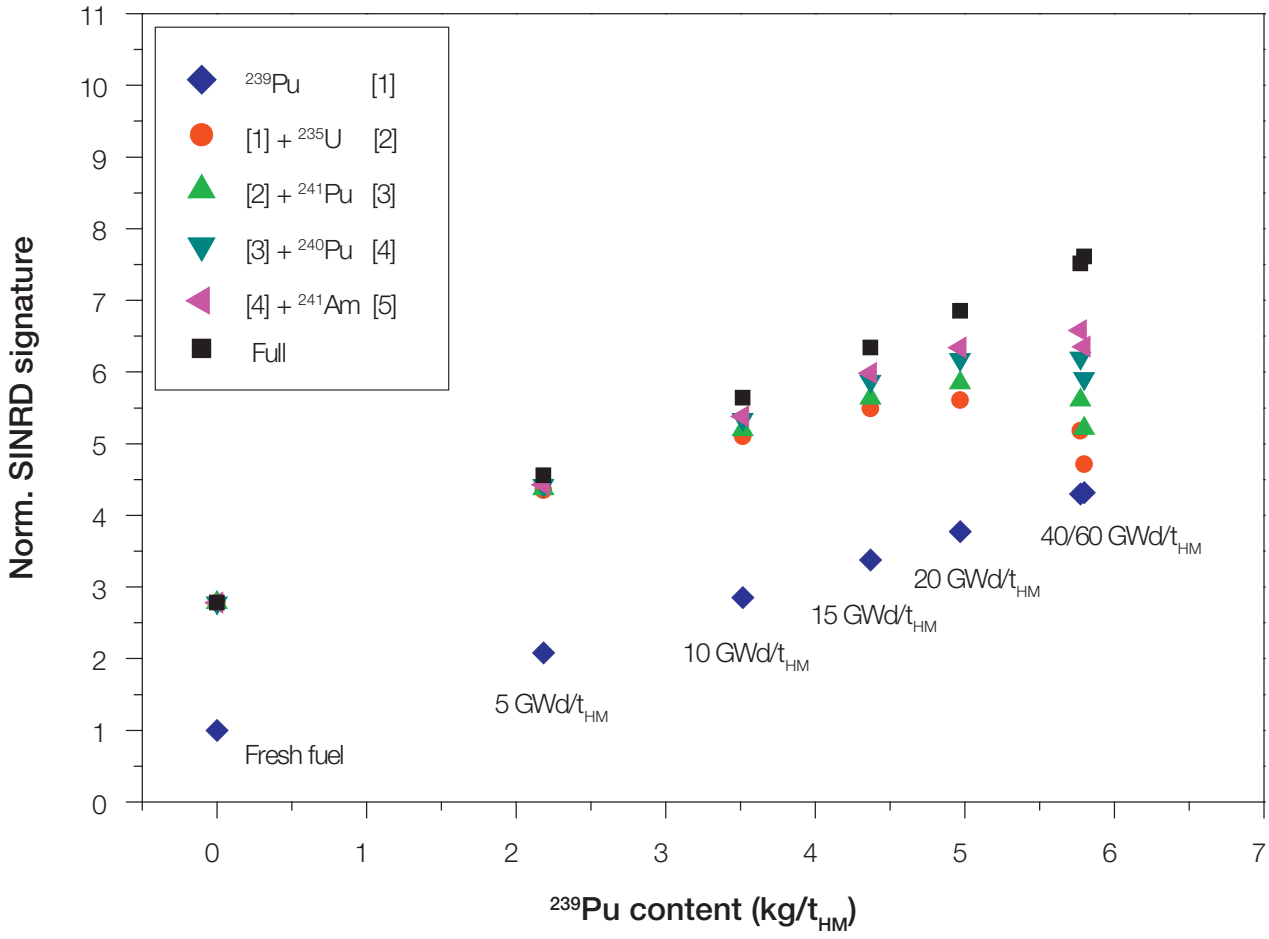

Figure 1: Normalized SINRD signature as a function of the ^{239}Pu content. The legend shows the additional nuclide added in the simulation starting from ^{238}U and ^{16}O. The values reported close to the data points refer to the fuel burnup.

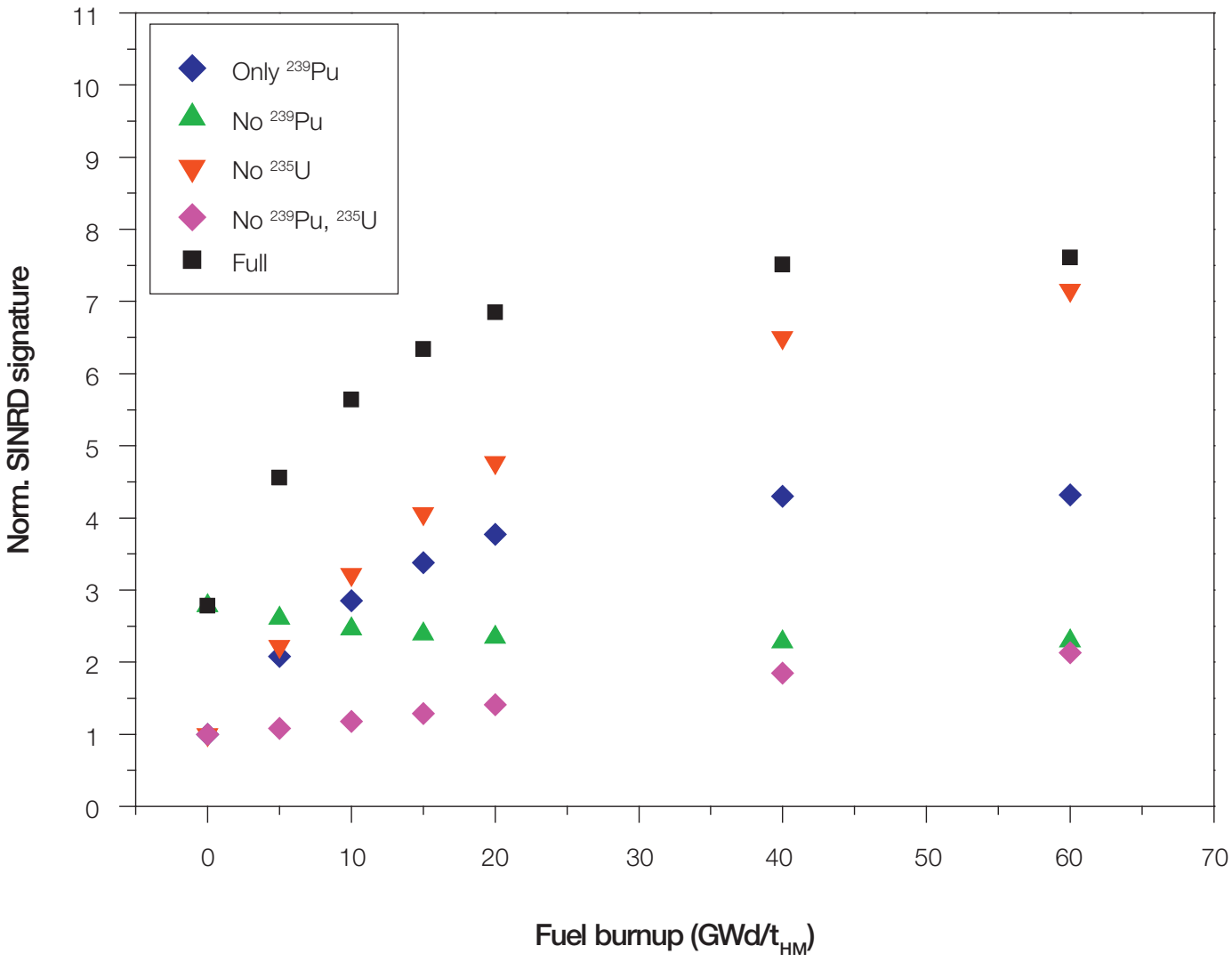

Figure 2: Normalized SINRD signature as a function of the fuel burnup for different fuel compositions.

Starting from the results in Figure 1, additional simulations were performed to evaluate the influence of both ^{239}Pu and ^{235}U on the SINRD signature. For this purpose, the simulations included a set of fuel compositions containing the fissile nuclides, as well as compositions where those nuclides are removed from the material card. Figure 2 shows the normalized SINRD signature as a function of the fuel burnup for several fuel compositions. The plot contains the results obtained for full material cards and for fuel with only ^{239}Pu, ^{238}U, and ^{16}O. In addition, the SINRD signature was calculated for fuel where ^{239}Pu, ^{235}U, or both ^{239}Pu and ^{235}U were removed from the material composition. All cases reported in the figure show almost constant SINRD signatures for fuel with burnup higher than 40 GWd/t_{HM}, because the ^{239}Pu content in the fuel used in the simulations reaches a constant value at high burnup. Moreover, the figure shows that by excluding the ^{239}Pu from the fuel composition the SINRD signature is almost independent from the fuel burnup, and this supports the concept that the SINRD signature is mainly affected by the ^{239}Pu fuel content.

4.2 Energy distributions of the neutron flux

As shown in Figure 1 the SINRD signature is influenced by several nuclides, and the mass of each nuclide in the fuel composition depends on the fuel burnup. To investigate the results included in the previous section, Figures 3 and 4 show the energy distributions of the neutron fluxes in the resonance and in the fast energy regions for fuel with burnup of 15 GWd/t_{HM} and 60 GWd/t_{HM} respectively. The color scheme used in the figures to indicate the fuel composition is the same of Figure 1.

The energy distribution in the resonance region was calculated as the difference between the transmitted fluxes through Gd and Cd filters, and by considering ^{239}Pu as active material in the detector, while for the fast energy region the response of a bare ^{238}U fission chamber was calculated.

The plots of the resonance region show a decrease when nuclides are added to fuel containing only ^{238}U and ^{16}O, while an opposite trend is shown in the graphs of the fast

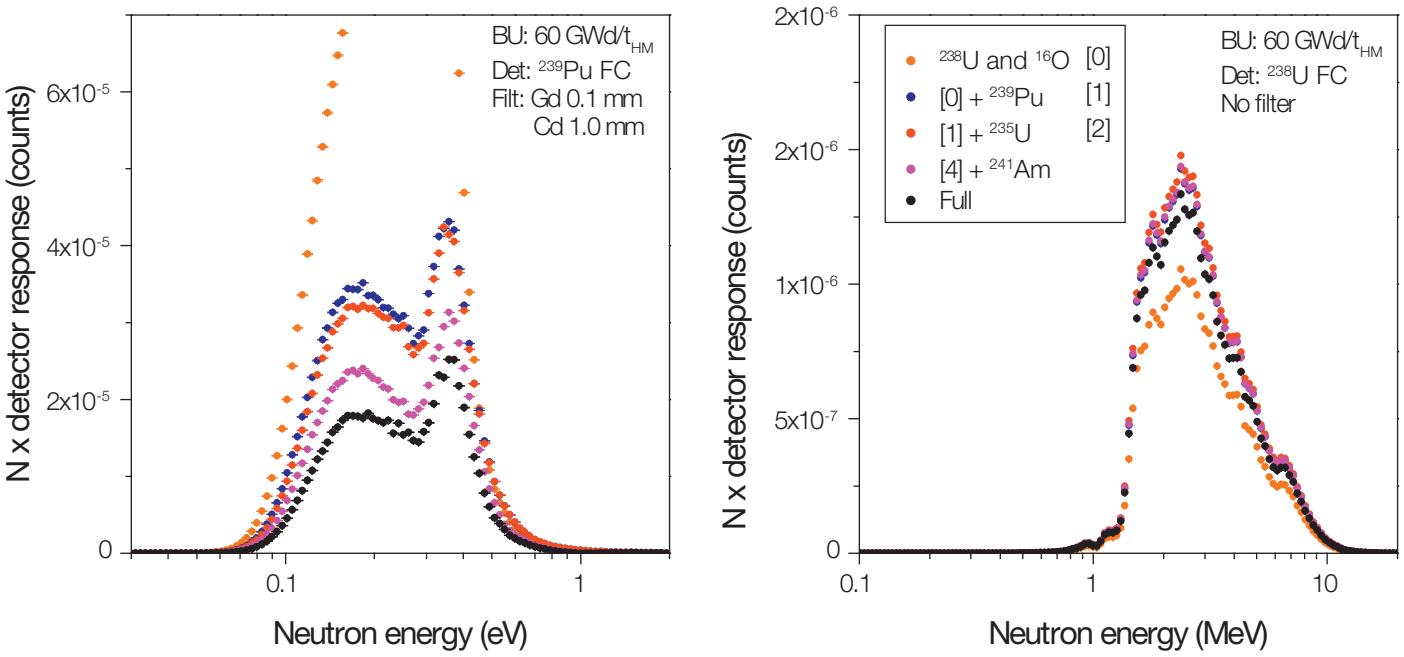

Figure 3: Energy distributions of the neutron fluxes in the resonance *(left)* and fast *(right)* energy regions. The color scheme used to indicate the fuel composition is the same as Figure 1 and the compositions refer to fuel with burnup of 15 GWd/t$_{HM}$.

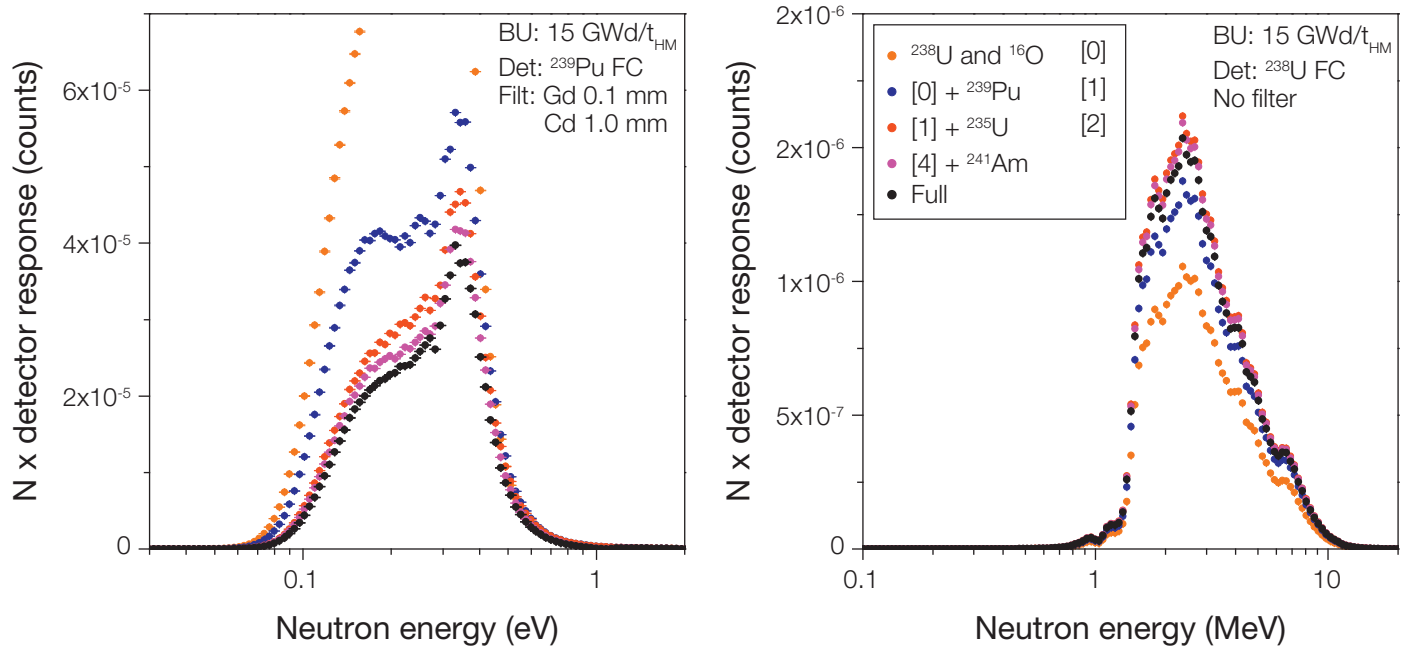

Figure 4: Energy distributions of the neutron fluxes in the resonance *(left)* and fast *(right)* energy regions. The color scheme used to indicate the fuel composition is the same as Figure 1 and the compositions refer to fuel with burnup of 60 GWd/t$_{HM}$.

energy region. The reduction of the neutron flux in the resonance region is due to the neutron absorptions from different nuclides, while the increase in the fast energy region is linked to the increase of the total fissile material in the fuel. For both burnup values there is a significant decrease of the neutron flux in the resonance region due to ^{239}Pu absorption, while significant effect is due to ^{235}U only for fuel with burnup of 15 GWd/t$_{HM}$. Moreover, for fuel with burnup of 60 GWd/t$_{HM}$ several nuclides are responsible for the reduction of the neutron flux in the resonance region, while the curves for fuel with burnup of 15 GWd/t$_{HM}$ and containing only ^{239}Pu and ^{235}U are rather similar to the results obtained with full material composition.

Focusing on the fast energy region, this region is less influenced by the fuel composition compared to the resonance region. However, still significant contributions can be seen from ^{239}Pu and ^{235}U for fuel with burnup of 15 GWd/t$_{HM}$, while ^{239}Pu alone gives the main influence for fuel with higher burnup.

5. Impact of the fuel composition on the SINRD signature

The nuclides included in the fuel composition have an influence on the energy distribution of the neutron flux and therefore result also in a variation of the SINRD signature.

Figure 5 shows the SINRD signature calculated for the fuel compositions mentioned in the previous section starting from data obtained in the reference spent fuel library. The values are normalized to the SINRD signature calculated for fuel containing only ^{238}U and ^{16}O.

A significant trend can be observed with the initial enrichment and burnup of the fuel; the increase of the SINRD signature with the initial enrichment is due to the increasing ^{235}U content, while the increase with the fuel burnup is due to the increasing ^{239}Pu concentration. Only the results from simulations with burnup of 40 and 60 GWd/t$_{HM}$ give similar SINRD signatures because the ^{239}Pu content in these cases is similar.

The SINRD signature is reported in Figure 5 for several cooling times only for the fuel with 3.5% initial enrichment. As shown in the figure, the cooling time of the fuel assembly does not influence significantly the SINRD signature, and this is because both ^{235}U and ^{239}Pu concentrations are not affected by this parameter. Therefore, the SINRD signature shown in Figure 5 for other initial enrichments refers only to the cooling time of 10 years.

The results from these simulations agree with previous results [16], [22] that concluded that the SINRD signature was mainly influenced by the ^{239}Pu and ^{235}U concentrations and minor effects were due to other nuclides.

6. Conclusions

The SINRD technique aims at the direct quantification of ^{239}Pu in a fuel assembly by measuring the attenuation of the neutron flux close to 0.3 eV due to the neutron absorptions of this nuclide. However, since all isotopes present in the fuel assembly determine a variation in the energy distribution of the neutron flux, this paper estimated the influence that single nuclides have on the SINRD technique.

By using the results of the reference spent fuel library developed by SCK•CEN, ^{239}Pu and ^{235}U were the isotopes

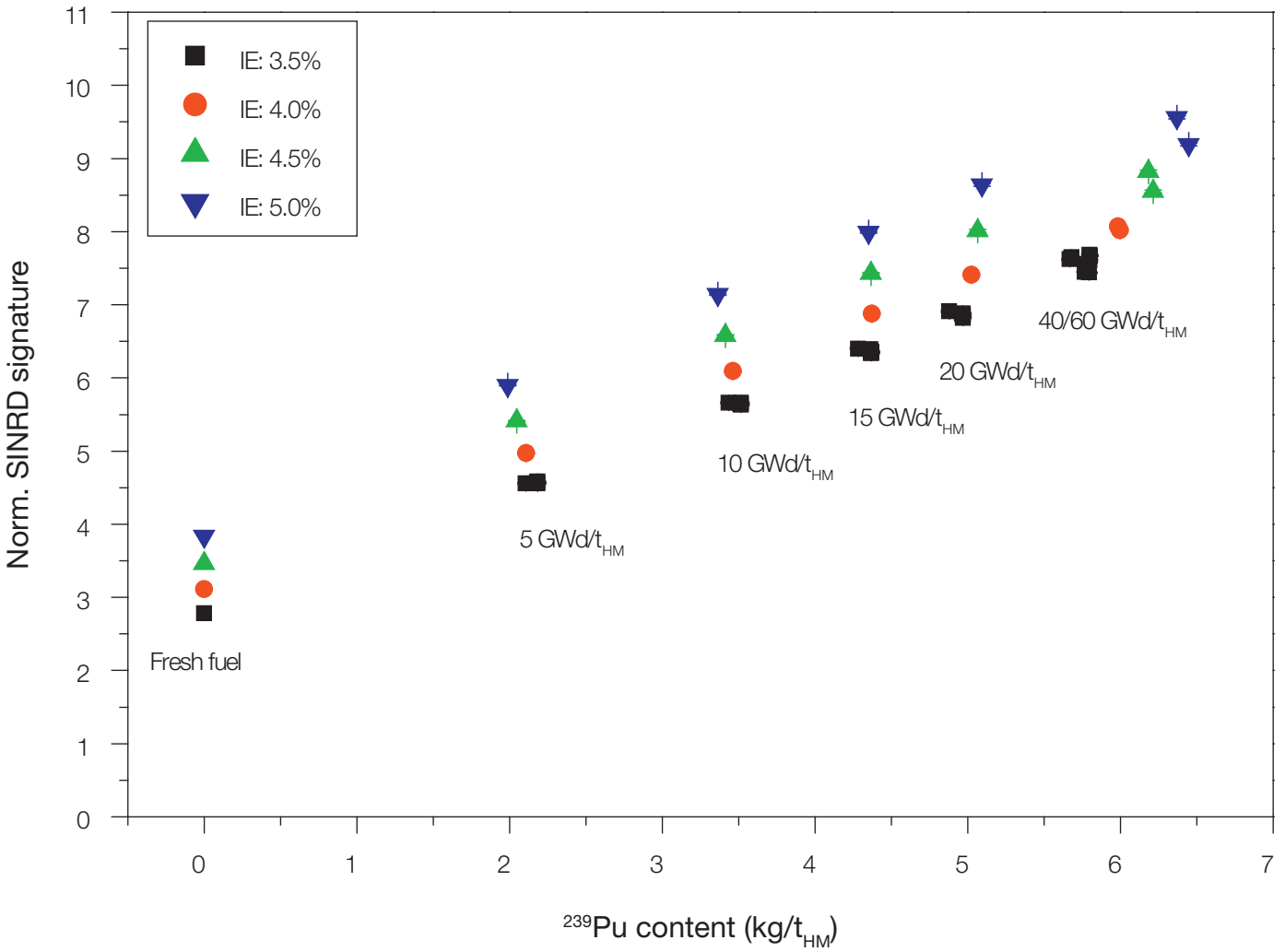

Figure 5: Normalized SINRD signature as a function of the ^{239}Pu content for several fuel compositions. The burnup values corresponding to different data groups are reported in the figure.

that influenced mostly this parameter, but for burnup higher than 20 GWd/t_{HM} significant contributions from other nuclides such as ^{240}Pu, ^{241}Pu, and ^{241}Am were observed. Finally, the correlation between the SINRD signature and the ^{239}Pu fuel content was confirmed because the simulations of fuel without ^{239}Pu did not show any significant trend for the SINRD signature.

The energy distribution of the neutron flux calculated with different fuel composition confirmed the major role of ^{239}Pu and ^{235}U on the SINRD signature, and highlighted the balance between the neutron absorptions in the resonance region due to multiple nuclides and the increase of the fast neutron flux due to the presence of fissile material.

Considering the 50 main neutron absorbers present in the spent fuel, the SIRND signature was calculated for fuel compositions reflecting several combinations of initial enrichment, burnup, and cooling time. It was found that the SINRD signature increases with initial enrichment and burnup because of the increase of the ^{235}U and ^{239}Pu concentrations respectively. On the other hand, the cooling time did not influence significantly the results because the ^{235}U and ^{239}Pu contents are not affected by this parameter.

7. Acknowledgment

This work is sponsored by GDF SUEZ in the framework of the cooperation agreement CO-90-07-2124 between SCK•CEN and GDF SUEZ.

8. Legal matters

8.1 Privacy regulations and protection of personal data

"I agree that ESARDA may print my name/contact data/photograph/article in the ESARDA Bulletin/Symposium proceedings or any other ESARDA publications and when necessary for any other purposes connected with ESARDA activities."

8.2 Copyright

The authors agree that submission of an article automatically authorises ESARDA to publish the work/article in whole or in part in all ESARDA publications – the bulletin, meeting proceedings, and on the website.

The authors declare that their work/article is original and not a violation or infringement of any existing copyright.

9. References

[1] International Atomic Energy Agency (IAEA), 2011. *"Safeguards Techniques and Equipment: 2011 Edition"*, IAEA/NVS/1/2011 (Rev. 2). Vienna, IAEA.

[2] International Atomic Energy Agency (IAEA), 2008. *"Spent Fuel Reprocessing Options"*, IAEA-TECDOC-1587. Vienna, IAEA.

[3] Tobin S. J., et al., 2013. *"Prototype Development and Field Trials under the Next Generation Safeguards Initiative Spent Fuel Non-Destructive Assay Project"*, proceedings of the 35th ESARDA Symposium.

[4] Menlove H. O., et al., 1969. *"A Resonance Self-Indication Technique for Isotopic Assay of Fissile Materials"*. Nuclear Applications Vol. 6.

[5] Phillips J. R., 1991. *"Irradiated fuel measurements"*. Passive Nondestructive Assay of Nuclear Materials – Chapter 18. Los Alamos National Laboratory – LA-UR-90-732.

[6] LaFleur A. M., 2011. *"Development of Self-Interrogation Neutron Resonance Densitometry (SINRD) to Measure the Fissile Content in Nuclear Fuel"*. PhD dissertation at Texas A&M University.

[7] LaFleur A. M., et al., 2012. *"Comparison of Fresh Fuel Experimental Measurements to MCNPX Calculations Using Self-Interrogation Neutron Resonance Densitometry",* Nuclear Instruments and Methods Section A, 680 (2012) 168-178.

[8] LaFleur A. M., et al., 2013. *"Development of Self-Interrogation Neutron Resonance Densitometry to Improve Detection of Partial Defects in PWR Spent Fuel Assemblies",* Nuclear Technology, 181, (2013) 354 – 370.

[9] LaFleur A. M., et al., 2015. *"Analysis of experimental measurements of PWR fresh and spent fuel assemblies using Self-Interrogation Neutron Resonance Densitometry",* Nuclear Instruments and Methods Section A, DOI:10.1016/j.nima.2015.01.029.

[10] Fröhner F. H., et al., 1966. *"Accuracy of Neutron Resonance Parameters from Combined Area and Self-Indication Ratio Measurements".* Proceedings of the Conference on Neutron Cross Section Technology, P. Hemmig (ed.), CONF-660 303, Washington D.C. (1966) Book 1, pp. 55-66.

[11] Bakalov T., et al., 1980. *"Transmission and self-indication measurements with U-235 and Pu-239 in the 2 eV-20 keV energy region"*, NBS Special Publications, (594), 692-697.

[12] Massimi C., et al., 2011. *"Neutron resonance parameters of 197Au from transmission, capture and self-indication measurements"*, J. Korean Phys. Soc. 59, 1689 – 1692.

[13] Pelowitz D., 2011. *"MCNPX User's Manual Version 2.7.0"*. Los Alamos National Laboratory. LA-CP-11-00438.

[14] I. Gauld, S. Bowman, J. Horwedel. *"Origen-ARP: automatic rapid processing for spent fuel depletion, decay, and source term analysis."* ORNL/TM-2005/39. January 2009

[15] Hu J., et al., 2012. *"The performance of self-interrogation neutron resonance densitometry in measuring spent fuel"*. Journal of Nuclear Material Management, Volume XL, No.3.

[16] Rossa R., et al., 2015. *"Investigation of the Self-Interrogation Neutron Resonance Densitometry applied to spent fuel using Monte Carlo simulations"*, Annals of Nuclear Energy 75 (2015) 176-183.

[17] Schillebeeckx P., et al., 2011. *"Neutron resonance spectroscopy for the characterization of materials and objects"*. 2nd International Workshop on Fast Neutron Detectors and Applications.

[18] Rossa R., et al., 2015. *"Neutron absorbers and detector types for spent fuel verification using the Self-Interrogation Neutron Resonance Densitometry"*, submitted for publication in Nuclear Instruments and Methods Section A, forthcoming.

[19] Rossa R., et al., 2013. *"Development of a reference spent fuel library of 17x17 PWR fuel assemblies"*, ESARDA Bulletin Issue 49.

[20] Borella A., et al., 2014. *"Sensitivity Studies on the Neutron Emission of Spent Nuclear Fuel by Means of the Origen-ARP Code"*. Proceeding of the 55th INMM Annual Meeting, Atlanta, Georgia, United States.

[21] Chadwick M. B., et al., 2006. *"ENDF/B-VII.0: Next Generation Evaluated Nuclear Data Library for Nuclear Science and Technology"*. Nuclear Data Sheets Volume 107, Issue 12, 2931–3060.

[22] Hu J., et al., 2013. *"Performance assessment of self-interrogation neutron resonance densitometry for spent nuclear fuel assay"*. Nuclear Instruments and Methods in Physics Research A 729 (2013) 247–253.

Analytical estimate of high energy gamma-ray emissions from neutron induced reactions in U-235, U-238, Pu-239 and Pu-240

Frederik Postelt, Fabio Zeiser, Gerald Kirchner

University of Hamburg
Carl Friedrich von Weizsäcker-Centre for Science and Peace Research
Beim Schlump 83, 20144 Hamburg, Germany
E-Mail: Frederik.Postelt@physik.uni-hamburg.de

Abstract:

The verifiability of nuclear dismantlement depends on robust measurement techniques to characterise fissile material. The isotopic vector can be determined with passive gamma spectroscopy, but only in the absence of significant shielding. Prompt gamma-ray emissions from neutron capture reactions in fissile material have energies above 3 MeV. Due to these high energies, they show a higher penetrability through external shielding than passive gamma-rays and are less subject to self-absorption. The current work presents a new approach to estimate the isotopic vector of uranium or plutonium by the measurement of prompt gamma-rays following neutron capture. Several neutron sources have been considered and analytical estimates for the spectra following neutron irradiation are presented.

Gamma emission rates of neutron interrogated fissile material are calculated. From the variety of possible neutron sources, a DD-generator and a research reactor are selected. The application of a chopper, neutron-gamma anti-coincidence counters and moderation of the fast neutrons have been considered to improve the peak-to-background ratio. Our analytical estimates are compared to the few published measured spectra available.

It is shown that the transition probabilities of highly enriched uranium are too low for being used for enrichment measurements. However, the determination of the isotopic vector of plutonium with thermal neutrons from either a research reactor or a moderated DD-source appears to be feasible.

Keywords: dismantlement; verification; PGAA; plutonium; uranium

1. Introduction

It is possible to determine the isotopic vector of special nuclear material (SNM) with passive gamma-ray spectroscopy. However, the emitted photons are subject to strong self-attenuation and absorption. This is particularly obstructive for dismantlement verification of nuclear warheads and detecting illicit trafficking of SNM, where significant (self-)shielding effects cannot be excluded.

Active measurements present a promising alternative, especially if Information Barriers (IB) are required and a black box is measured as usually assumed for dismantlement verification [1-3]. Radiative neutron capture reactions in SNM isotopes lead to a gamma spectrum up to energies of 6.5 *MeV*. These photons are much less attenuated than the generally regarded passive gamma radiation below 6.5 *MeV*.

Challenges to implementing this measurement technology are low transition probabilities, low detector efficiencies at high gamma energies, a high background of gammas from induced fission in the fissile material, and delayed gammas from both radiative capture and induced fission. In addition, only few radiative neutron capture lines can be resolved, while most form a quasi-continuum.

In this paper, the potential of (n,γ)-measurements for characterising the isotopic composition of fissile material is assessed. After documenting the state of research, the radiative neutron capture gamma-ray yield is analytically estimated to prepare measurements and open questions are addressed.

2. State of research

The bulk of research into radiative neutron capture reactions was done in the 1990s. The focus was on low-Z materials, with the intent of identifying explosives[1]. In the last decade research in the US has shifted its focus to SNM. Unfortunately, only little information has been published. Examples of research in the SNM are the “Nuclear Materials Identification System” (NMIS, which uses (n,γ) to identify explosives [4]), the “Nuclear Car Wash” (NCW, which uses (n,f) [5, 6]), Chemical Warfare Agents and Explosives PGAA (which focuses on (n,γ) to identify explosives [7-10]) and the Nuclear Resonance Fluorescence (NRF, which uses gammas to activate the SNM [11]). Runkle *et al.* give an overview on active interrogation of SNM [12].

Most papers on (n,γ) in plutonium date back to the 1970s and 1980s and do not discuss isotopic vectors [13-20]. The measured intensities vary between one and two orders of magnitude between the different publications and

1 personal communication with Volker Dangendorf, PTB, in November 2011

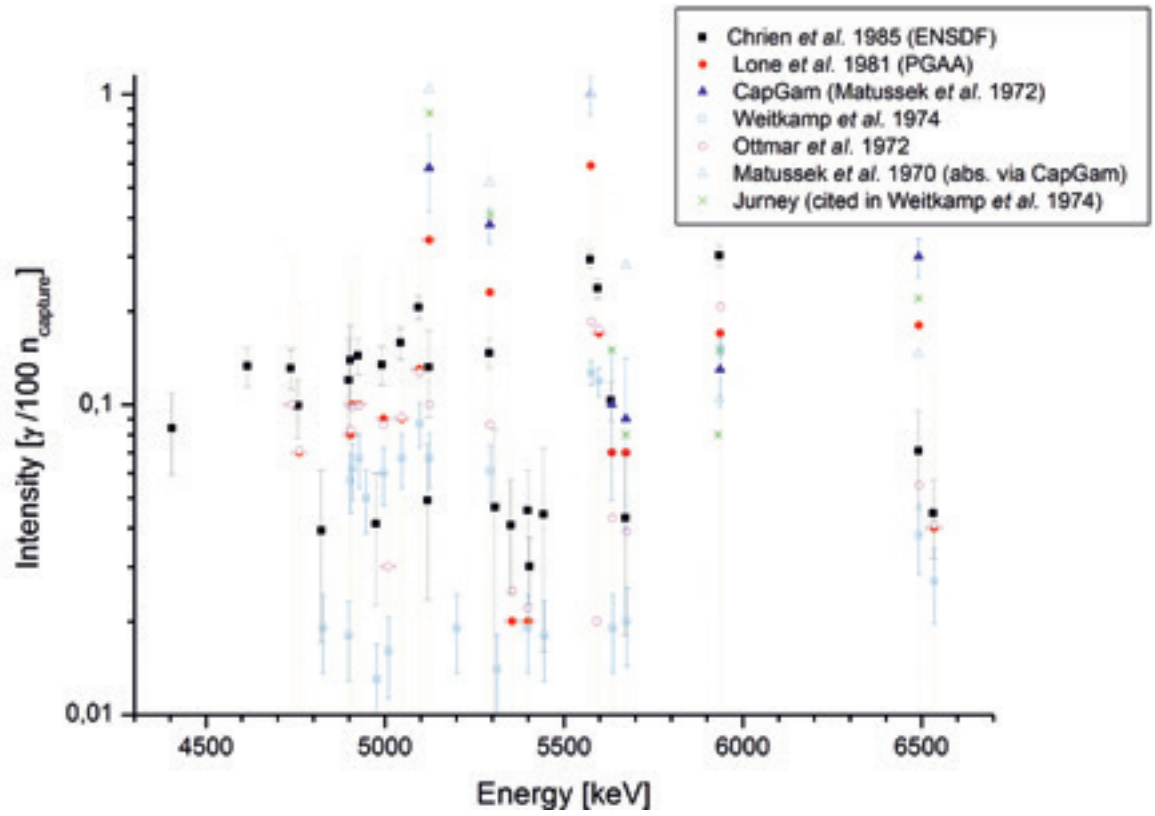

Figure 1: Measured plutonium-239 (n,γ)-intensities. The references are specified in the plot legend.

databases, see Figure 1. However, uranium has been researched as recently as the 2010s: Molnár *et al.* were able to assess the enrichment up to 36% U-235 [21] and Chichester *et al.* showed that a simple DD-generator set-up is not fit to identify highly enriched uranium [22].

There are two databases, which summarise (n,γ)-intensities and specific cross sections, respectively. The Prompt Gamma-ray neutron Activation Analysis database (PGAA [23]) was created from 1999 to 2003 by the International Atomic Energy Agency Nuclear Data Service (IAEA NDS) and contains the natural elements (up to uranium with Z=92). Plutonium is not included, but the PGAA database refers to Lone *et al.* [15]. The Thermal Neutron Capture gamma's database (CapGam [24]) by the Brookhaven National Laboratory National Nuclear Data Center (BNL NNDC) was last updated in 2013 and goes up to berkelium. Most publications and both databases refer to thermal neutron capture.

3. Simulations

A Mathematica code has been written to analytically calculate the neutron induced gamma spectra of fissile material above 3 *MeV*. Two different neutron sources and three different targets will be compared.

3.1 Neutron source

Two neutron sources are considered, a nuclear research reactor and a Deuterium-Deuterium Electronic Neutron Generator (DD-ENG) [22, 25-27]. The research reactor estimates are oriented towards the existing PGAA set-ups in Garching and Budapest [28-34]. The FRM-II reactor has a thermal equivalent neutron flux density of $2.7 \cdot 10^{10}$ s^{-1} cm^{-2} at the target position, with a cold source made of 25 *K* liquid D_2 [28]. In the following, we use the thermal equivalent flux density Φ_0 because no comprehensive neutron flux density spectrum is available. It is derived with the thin sample approximation [35]:

$$\int_0^\infty \sigma_\gamma(E_n)\,\Phi(E_n)dE_n = \sigma_{\gamma,0}\Phi_0$$

where σ_γ is the capture cross section (b), Φ the neutron flux density (s^{-1} cm^{-2}), E_n the neutron energy (*MeV*) and $\sigma_{\gamma,0}$ the capture cross section for thermal neutrons (b).

Deviations from the 1/v dependence are accounted for with the Westcott *g* factors [36]. Their high neutron flux densities and low neutron energies are major advantages of research reactors, especially of the FRM-II.

For the DD-generator the continuous neutron energy distribution given by Fantidis *et al.* [25] is used. The total neutron flux density is 10^5 s^{-1} cm^{-2} at the target position and the peak energy 2.5 *MeV* [26, 27]. The DD-source generates fast neutrons and a lower flux density, but has the decisive asset of being portable.

3.2 Fissile material target

Target	Mass	ΔMass	Isotope	wt.%	Δwt.%
HEU [22]	610 g	1 g	U-235	90	1
			U-238	10	1
HEU	100 g	1 g	U-235	90	0.01
			U-238	10	0.01
WGPu	100 g	0.01 g	Pu-239	95	0.01
			Pu-240	5	0.01

Table 1: Characteristics of the simulated fissile material samples.

The assumed fissile material samples are summarised in Table 1. Due to its small isotopic fraction, U-234 plays a minor roll and is not taken into account. The first target is identical to a measured Highly Enriched Uranium (HEU) sample to allow comparison [22]. The masses of the other two samples are generic to facilitate extrapolation. All targets are assumed to have a cross sectional area of 1 cm^2 perpendicular to the neutron beam and are approximated as point source in respect to the HPGe detector.

3.3 Gamma detector efficiency

A point source in 10 *cm* distance in front of a HPGe detector (50% NaI) is assumed. The following efficiency calibration curve has been provided by Helmut Fischer, University of Bremen[2]:

$$\ln(\varepsilon) = \begin{cases} -294.7+273.70\ ln(E)-96.6700\ ln^2(E) \\ \quad +15.18\ ln^3(E)-0.89420\ ln^4(E) \end{cases}, \quad E \leq 100\ keV$$

$$\ln(\varepsilon) = \begin{cases} -28.50+16.260\ ln(E)-3.83000\ ln^2(E) \\ \quad +0.382\ ln^3(E)-0.01423\ ln^4(E) \end{cases}, \quad E \geq 100\ keV$$

Its uncertainty (including geometrical uncertainties) is set to 10%.

To consider the most important physical effect in the HPGe detector, each gamma-ray is broadened to a Gaussian distribution with a constant Full Width at Half Maximum (FWHM) of 4 *keV* [3]. In addition an adapted continuous background is superposed as discussed in Subsection 3.4.3.

3.4 Nuclear reactions

Of primary interest here is the radiative neutron capture. In addition, the background from neutron capture, prompt fission gamma-rays, and delayed fission gammas are considered and added to the signal. All other nuclear reactions, e.g. spontaneous fission and neutron scattering are neglected. Non-elastic scattering with uranium and plutonium occurs only at neutron energies above 1 *keV*. Even at a neutron energy of 2.5 *MeV*, the induced gamma-rays contribute only to the gamma radiation background up to 2.5 *MeV*, while the prompt gammas have energies above 3 *MeV*.

3.4.1 Radiative neutron capture

Most gamma-rays from radiative neutron capture in fissile material form a quasi-continuum. Relatively few gamma-rays, mainly at the extremes of the spectrum, are distinct [35].

The radiative neutron capture signal is assessed by the (n,γ)-reaction rate. Their cross sections are taken from ENDF/B-VII.1 (duplicates were manually deleted[4]). As discussed in Section 2, the published intensities vary significantly. The gamma-ray intensities used here are from Chrien *et al.* [13] for Pu-239 and from the CapGam database [24] for U-235, U-238[5] and Pu-240[6]. These are the most reliable data sets in the view of the authors.

Only gamma-rays with energies ≥3 *MeV* are considered here. A selection is presented in Table 2. The highest gamma energy is at 6.5 *MeV* emitted by Pu-239, the lowest at 3.0 *MeV*, emitted by U-238. The gamma-ray energies for thermal neutron capture in plutonium can be seen in Figure 5. Ottmar *et al.* propose that the gamma peaks have higher energies with higher incident neutron energies [19]. Since experimental data are missing, this effect is not considered here [19].

Isotope	$\frac{E}{\mathrm{MeV}}$	$\frac{\Delta E}{\mathrm{MeV}}$	$\frac{I_\gamma}{n_{capture}}$	$\frac{\Delta I_\gamma}{n_{capture}}$
Pu-239	5.935	2.0E-04	3.02E-03	2.39E-04
	5.574	1.3E-04	2.94E-03	1.85E-04
	5.094	2.0E-04	2.06E-03	1.81E-04
	4.616	3.0E-04	1.33E-03	1.95E-04
Pu-240	5.080	2.0E-05	2.76E-02	1.44E-03
	5.072	1.0E-03	5.80E-03	2.41E-03
	4.472	4.0E-05	3.70E-02	3.05E-03
	4.400	1.0E-04	2.12E-02	1.54E-03
U-235	6.396	2.0E-04	3.20E-03	2.84E-03
	4.974	6.0E-04	8.99E-04	8.10E-04
	4.647	6.0E-04	4.00E-04	4.12E-04
	6.396	2.0E-04	3.20E-03	2.84E-03
U-238	4.661	2.0E-04	3.07E-04	1.58E-04
	4.060	1.5E-04	1.32E-02	6.79E-03
	3.983	2.0E-04	2.39E-03	1.23E-03
	3.583	2.0E-04	3.88E-03	2.00E-03

Table 2: Selection of thermal neutron capture prompt gamma lines with their energies in *MeV* (and 1σ uncertainty) and intensities per neutron capture (and 1σ uncertainty) [13, 24].

The gamma-ray intensities per neutron capture range from $3.79 \cdot 10^{-6}$ (U-238) to $1.3 \cdot 10^{-1}$ (Pu-240). The sums of all regarded discrete (n,γ)-intensities for the four isotopes U-235, U-238, Pu-239 and Pu-240 are $8.49 \cdot 10^{-3}$, $4.09 \cdot 10^{-2}$, $3.06 \cdot 10^{-2}$ and $9.37 \cdot 10^{-1}$, respectively. On average, 3.78 gammas are emitted per radiative neutron capture [37] (for E_n<1.09 *MeV*), but most of these form a quasi-continuum and only very few gamma-rays at both ends of the (n,γ)-spectrum can be observed [35].

2 personal communication, June 2013

3 Since no detector specific data was available, we contacted the manufacturer who recommended a FWHM of 4 *keV* at an energy of 8 *MeV*. To be conservative, this FWHM is used for all peaks.

4 There exist more than one cross section for some energies

5 The gamma-rays at 3913.1 keV and at 3406.9 keV are adapted from the according PGAA-database intensities by the authors.

6 might be originally from White *et al.* [44], then arbitrary intensities

The count-rate is estimated as

$$R_{n,\gamma}(E_\gamma) = N_{AX} I_\gamma(E_\gamma)\, \varepsilon(E_\gamma) \int_0^\infty \Phi(E_n)\, \sigma_{n,\gamma}(E_n)\, dE_n \,,$$

where N_{AX} is the number of target atoms, I_γ (E_γ) the gamma-ray intensity, $\varepsilon(E_\gamma)$ the detector efficiency, $\Phi(E_n)$ the neutron flux density ($s^{-1}\, cm^{-2}$), $\sigma_{n,\gamma}(En)$ the (n,γ)-cross section (b), E_γ the gamma energy (*MeV*) and E_n the neutron energy (*MeV*).

3.4.2 *Prompt fission gammas*

The prompt fission background is assessed by the (n,f)-rate. Their cross sections are taken from ENDF/B-VII.1 [38][7]. On average, each neutron induced fission in Pu-239 and Pu-240 leads to the emission of 8.095 photons [37] (for E_n<1.09 *MeV*). Most fission gammas have energies smaller than 1*MeV*. The gamma energy distributions used in the following have been measured by [37, 39, 40]. Spontaneous fission and induced fission by secondary neutrons are neglected. With the gamma multiplicity of 8.095 [37], the prompt fission gamma background count-rate is calculated analogous to the (n,γ)-count-rate:

$$R_{n,f}(E_\gamma) = 8.095\, N_{AX} I_f(E_\gamma) \varepsilon(E_\gamma) \int_0^\infty \Phi(E_n) \sigma_{n,f}(E_n) dE_n$$

3.4.3 *Delayed fission gammas and continuous capture gammas*

An additional background is caused by delayed gammas from fission. To our knowledge no such data is recorded in ENDF. Thus, an estimate for the delayed fission gamma spectrum was obtained by calculating the ratio of delayed fission to prompt gammas for the spectra given in Matussek *et al.* [16]. This energy dependent ratio is then multiplied by the intensities estimated for prompt gammas. To reassess this approach for thermal incident neutrons, the fission and delayed background was calculated for all peaks[8]. The cumulative yield for neutron induced and spontaneous fission [41] and secondary gammas [42] not farther than 10 *keV* from neutron capture peaks were considered and then compared to the simulated background (without continuous capture). The calculations do not consider detector specific secondary effects, e.g. the Compton effect, and therefore underestimate the background as can be seen in Figure 2.

Most gamma-rays from radiative neutron capture form a continuum [35]. This additional background is estimated analogously to the delayed fission gammas, see paragraph above.

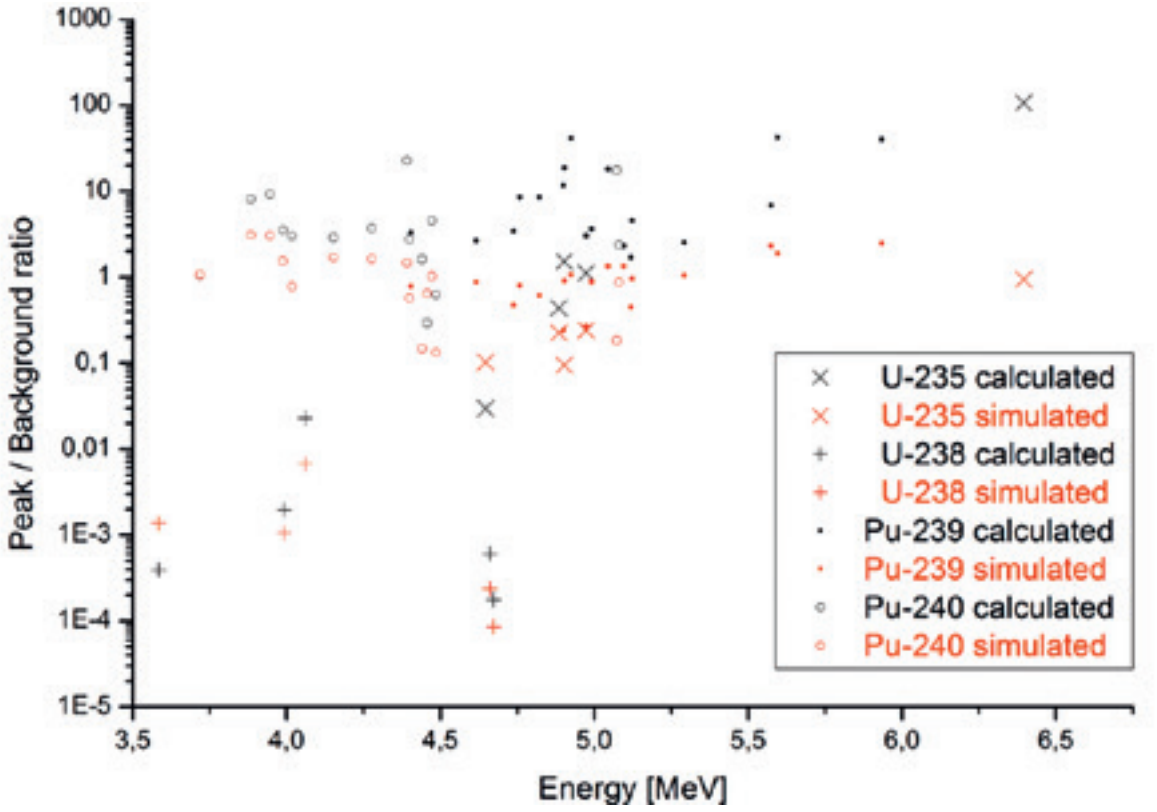

Figure 2: Peak-background ratio of thermal neutron capture gamma-rays in uranium and plutonium. Red: simulated with measured spectra [16]. Black: calculated with nulclear data [41, 42].

7 Again, after deleting duplicate entries

8 The help of Erik Buhmann (ZNF) is much appreciated

A limitation of our approach is the incomplete data base of measured spectra. First of all, only Weapons-Grade Plutonium (WGPu) and HEU were measured by Matussek *et al.*, but not Pu-240 and U-238. Hence, here the WGPu data had to be used for Pu-239 and Pu-240 and the HEU data for U-235 and U-238. Secondly, the energy ranges covered only 4 *MeV* to 6 *MeV* and 4.2 *MeV* to 6.5 *MeV*, respectively. Therefore the ratio had to be linearly extrapolated to include all gamma lines (from 3.0 *MeV* to 6.5 *MeV*). The uncertainties are accordingly high.

4. Results

This section is divided in three subsections. First, the application of a chopper and n-γ-anti-coincidence set-up is discussed; second, the estimate with a DD-generator; third, the estimate with a thermal reactor neutron spectrum. For measurement times of 1000 *seconds* count-rates above ca. 1 *cps* are statistically significant, taking into account background.

4.1 Chopper and n-γ-anti-coincidence

It is possible to separate the (n,γ)-signal from part of the background by the use of a chopper and n-γ-anti-coincidence measurements as successfully applied by Matussek *et al.* [16]. A chopper or pulsed neutron beam allows a differentiation between prompt and delayed fission gammas, the n-γ-coincidence/-anti-coincidence method between fission and (n,γ)-reactions.

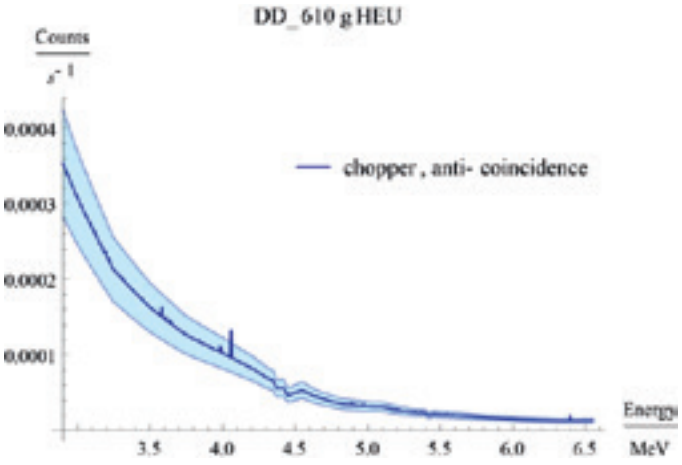

Figure 3: Theoretical (n,γ)-spectrum of a 610 *g* 90% enriched HEU sample and a DD-generator with chopper and n-γ-anti-coincidence differentiation. Shaded areas represent 1σ uncertainties.

Figure 3 shows the simulated spectrum of the HEU target with 90% enrichment and a DD-source without delayed fission and prompt fission gammas. This corresponds to the application of a chopper and anti-coincidence set-up as used by Matussek *et al.* As a result, the (n,γ)-peaks become significantly more visible. These effects are more intense for lower energies, i.e. they favour the nuclei with an even number of neutrons, Pu-240 and U-238. Therefore, the U-238 peak at 4.060 *MeV* is visible. The systematic reassessment described in Subsection 3.4.3 identifies the fission product Rb-90 with its decay line at 4.062 *MeV* [42] as the main contributor to the background (considered here only indirectly through the Matussek *et al.* delayed background). Molnar *et al.* also recognise this gamma line as the main obstacle in determining the isotopic composition of highly enriched uranium [21]. The U-235 peak at 6.4 *MeV* is also significantly more distinct, but still weak. This is due to the continuous (n,γ)-background. In addition, the overall count-rate is very low. All (n,γ)-peaks above 4.81 *MeV* are from U-235 and all below 4.64 *MeV* are from U-238.

For all four simulated set-ups (HEU/WGPu with DD-ENG/FRM-II) the application of a chopper and the anti-coincidence method increases the signal to background ratio significantly, but does not change the general picture.

4.2 4.2. DD-generator

4.2.1 Comparison with measurement of uranium

For a 610 *g* 90% enriched HEU sample our estimated (n,γ)-spectrum does not show any significant peak. Applying the thin sample approximation to a target of 610 *g* uranium with a cross section of 1 cm^2 is hypothetical and neglects self-absorption. Therefore, it gives an upper limit of the expected count-rates. Our estimations are in agreement with the finding of Chichester *et al.*, who used a similar set-up [22]. The background is mostly due to the delayed fission background, and to a lesser degree due to prompt gammas from induced fission in uranium-235, as well as the continuous capture background.

4.2.2 Plutonium

The following results are produced with generic targets to allow easy extrapolation.

The identical set-up with the same DD-generator, but a 1 *g* WGPu target shows a lower count-rate, even if the mass difference is accounted for. No single Pu-239 (n,γ)-line can be identified, at most some Pu-240 lines. For plutonium, the three different background contributors (Pu-239 fission, delayed fission and neutron capture gammas) are in the same order of magnitude up to 4 *MeV*. Thereafter, the delayed fission gammas become dominant.

4.2.3 Moderated DD-generator

The previous results indicate that an unmoderated DD neutron source does not allow for the determination of the isotopic vector of SNM.

Moderation of the fast neutrons shifts the ratio between prompt fission (and following delayed fission) and neutron capture gammas to more desirable values.

MCNP (Monte Carlo N-Particle code, [43]) simulations are used to establish a moderated neutron energy distribution

spectrum[9]. An isotropic, mono-energetic 2.5 *MeV* neutron point source is assumed, located in the centre of 7 *cm* by 7.01 *cm* by 30.8 *cm* of polyethylene (PE), just next to the target (5 *cm* by 5 *cm* by 5 *cm*). In addition, a neutron loss factor is derived, because only 0.5% of the emitted neutrons reach the target.

The shapes of the gamma spectra resulting from simulations with moderated neutrons are similar to the reactor spectra due to the fact, that many neutrons are thermalised, and because the reaction cross sections are significantly higher for slow neutrons. The count-rate is significantly lower due to the weaker neutron source, and additional effects such as scattering in the PE.

4.3 Reactor spectra

4.3.1 Uranium

As expected from the much higher neutron flux density of the neutron source, the overall count-rate is much higher than with the DD-generator. It is so high that dead time effects will dominate and the detector might even be damaged. Therefore, additional shielding will be necessary, see Subsection 4.3.3. However, the fission background is still suppressing most (n,γ)-peaks. The U-235 peak at 6.4 *MeV* is by far the strongest peak. The U-238 4.06 *MeV* peak visible in the DD-spectrum (Figure 3) is not visible here, due to a shift in the cross sections ratio $^{\sigma_{U-235}}/_{\sigma_{U-238}}$ with the energy of the incident neutron and a high background from neutron capture and fission in U-235.

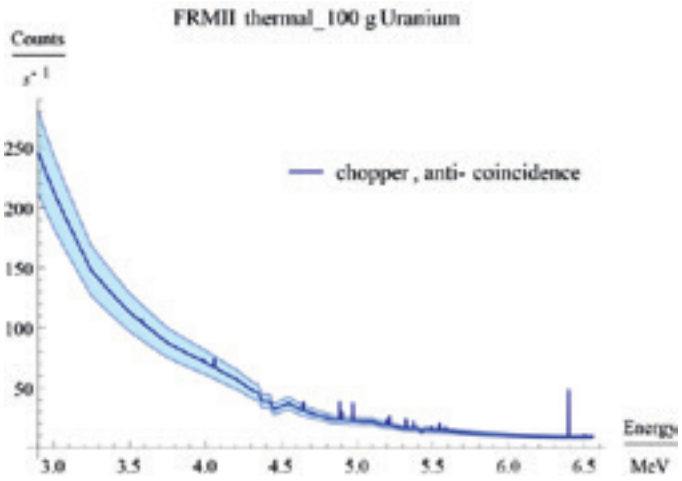

Figure 4: Theoretical (n,γ)-spectrum of a 100 *g* 90% enriched HEU sample and neutrons from the FRM-II research reactor with "chopper" and n-γ-anti-coincidence differentiation. Shaded areas represent 1σ uncertainties.

By the application of a chopper and an anti-coincidence set-up the (n,γ)-peaks become more distinct, see Figure 4. However, the general picture does not change. The U-238 peaks are still suppressed and the U-235 peak at 6.4 *MeV* clearly dominates. This is consistent with Matussek *et al.* [16], who identified only this peak. All (n,γ)-peaks above 4.81 *MeV* are from U-235 and all below 4.64 *MeV* from U-238.

As discussed, these results are transferable to an ideal moderated DD neutron source.

4.3.2 Plutonium

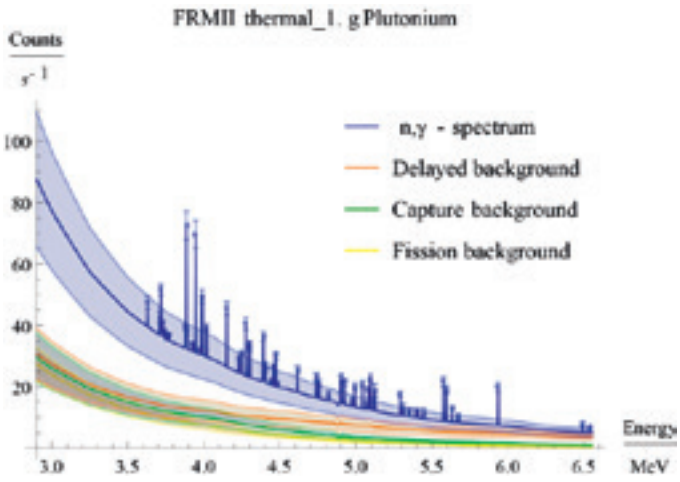

Figure 5: Theoretical (n,γ)-spectrum of a 1 *g* WGPu sample with 95% Pu-239 and 5% Pu-240 and the FRM-II research reactor as neutron source (uppermost curve). Shaded areas represent 1σ uncertainties.

Figure 5 shows the simulated (n,γ)-spectrum of a 1 *g* WGPu target with 95% Pu-239 and 5% Pu-240 and the FRM-II research reactor as neutron source. All (n,γ)-peaks above 5.08 *MeV* are from Pu-239, all below 4.40 *MeV* from Pu-240. The background is due to induced fission gammas in Pu-239, subsequent delayed fission gammas, and continuous neutron capture gammas.

Again, the overall count-rate is much higher than with the DD-generator. Therefore, additional shielding will be required. For plutonium, most (n,γ)-lines are visible for both isotopes: Pu-239 and Pu-240.

4.3.3 Attenuation of prompt and delayed fission gammas

The application of a chopper and anti-coincidence set-up does not sufficiently reduce the high gamma count-rates for the research reactor spectra. Therefore, the gamma-rays should be attenuated by additional shielding. Figure 6 compares the FRM-II plutonium spectrum in Figure 5 with the same spectrum attenuated by 3 *cm*, 10 *cm* and 20 *cm* of Pb[10]. The spectrum is extrapolated below 4 *MeV*, see Subsection 3.4.3, resulting in high uncertainties. The peak/background ratio between 33 and 6.5 *MeV* changes very little. This is also true for the simulations with uranium as target and/or the DD-generator as neutron source.

9 With the much appreciated help of Olaf Schumann, Fraunhofer INT, Euskirchen

10 Mass attenuation coefficient data from Hubbel and Seltzer [45]

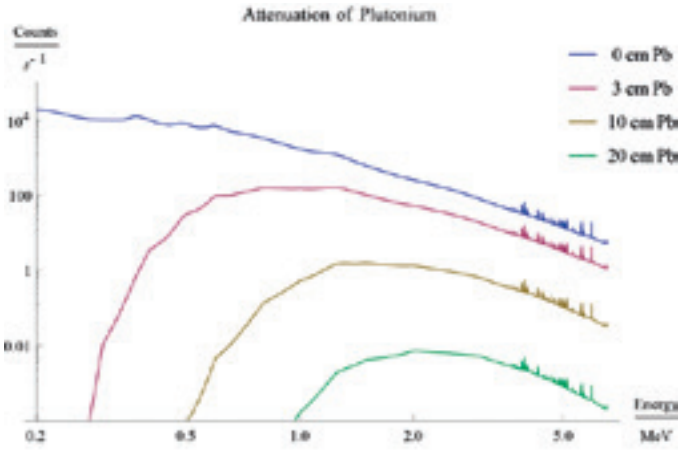

Figure 6: log–log Pu spectrum (95% Pu-235, 5% Pu-240, FRM-II, Figure 5), attenuated by 0-20 *cm* Pb.

5. Conclusion

Further measurements are necessary to complete the data base on neutron capture in uranium and plutonium. This applies particularly to fast neutron capture and the shift of the emitted gamma radiation to higher energies with higher incident neutron energies.

The estimates presented here indicate that (n,γ)-spectroscopy with a simple DD-generator set-up is not possible, neither for uranium as already reported by Chichester *et al.* [22], nor for plutonium. Even suppression of the major external background effects (fission and delayed fission gammas) would not allow the determination of the isotopic compositions.

It is shown that the identification of Pu-239 and Pu-240 is possible with reactor neutrons. It also looks promising to measure the isotopic vector of plutonium with thermalised neutrons from a DD-generator.

This does not apply to uranium. Further research is needed to assess the feasibility of determining the enrichment of uranium with neutron capture measurements.

Lead shielding poses an effective instrument in attenuating undesirable gamma-ray background without significant adverse mitigation of the (n,γ)-peaks between 33 and 6.5 *MeV*.

6. Outlook

The (n,γ)-measurement technique could expand current dismantlement verification techniques. It could solve the issue of an unknown shielding of the nuclear warhead or weapon pit in the container. Uncertainties could be reduced and therefore trust in the measurements and information barriers strengthened.

This measurement technique might also be useful in IAEA Safeguard applications and CBRN (Chemical, Biological, Radiological and Nuclear) defence. While active interrogation and the measurement of induced fission gammas might suffice to find hidden fissile material, it does not give information on the isotopic vector, although this information may be crucial.

In order to show the feasibility of the (n,γ)-technique, we are going to perform measurements with a research reactor and moderated DD-ENG neutrons. For CBRN defence, additional estimates with radioactive neutron sources such as americium-beryllium and californium-252 will be carried out.

7. Acknowledgements

The authors thank Martin B. Kalinowski for the initial idea for this project. It would not have been possible without him, Reinhard Lieberei, Götz Neuneck, Caren Hagner and Malte Göttsche. Further thanks go to Helmut Fischer, to Olaf Schumann, to Erik Buhmann and to Bradley Presentati for his help with the finer linguistic nuances.

This research is funded by the German foundation for peace research (DSF).

8. References

[1] Committee on International Security and Arms Control, National Research Council, *Monitoring Nuclear Weapons and Nuclear-Explosive Materials: An Assessment of Methods and Capabilities*, J. P. Holdren and S. Fetter, Eds. National Academy of Sciences, 2005. http://www.nap.edu/catalog.php?record_id=11265

[2] J. Carlson, J. Fuller, K. Hartigan, M. Dreicer, L. Duckworth, M. Göttsche, C. Hinderstein, S. Høibråten, D. Keir, D. B. Laird, M. Williamson, M. Bunn, A. Diakov, C. Hinderstein, R. Rajaraman, T. Renis, E. Rowan, J. Siegel, M. Smith, L. van Dassen, and T. Wood, *Innovating Verification: Verifying Baseline Declarations of Nuclear Warheads and Materials*, ser. Innovating Verification reports series. Nuclear Threat Initiative, July 2014. http://www.nti.org/analysis/reports/innovating-verification-verifying-baseline-declarations-nuclear-warheads-and-materials/

[3] M. Göttsche and G. Kirchner, "Measurement techniques for warhead authentication with attributes advantages and limitations," *Science & Global Security*, vol. 22, pp. 83–110, 2014. http://scienceandglobalsecurity.org/archive/2014/05/measurement_techniques_for_war.html

[4] J. T. Mihalczo, J. K. Mattingly, J. A. Mullens, and J. S. Neal, *NMIS With Gamma Spectrometry for Attributes of Pu and HEU, Explosives and Chemical Agents*, May 2002. http://www.osti.gov/scitech/servlets/purl/799512

[5] J. Church, D. Slaughter, S. Asztalos, P. Biltoft, M.-A. Descalle, J. Hall, T. Luu, D. Manatt, J. Mauger, E. Norman, D. Petersen, and S. Prussin, "Signals and

interferences in the nuclear car wash," *Nuclear Instruments and Methods in Physics Research*, vol. B 261, pp. 351–355, 2007.

[6] J. Hall, S. Asztalos, P. Biltoft, J. Church, M.-A. Descalle, T. Luu, D. Manatt, G. Mauger, E. Norman, D. Petersen, P. J., S. Prussin, and D. Slaughter, "The nuclear car wash: Neutron interrogation of cargo containers to detect hidden SNM," *Nuclear Instruments and Methods in Physics Research Section B: Beam Interactions with Materials and Atoms*, vol. 261, no. 1-2, pp. 337–340, August 2007. http://dx.doi.org/10.1016/j.nimb.2007.04.263

[7] A. Caffrey, J. Cole, R. Gehrke, and R. Greenwood, "Chemical warfare agent high explosive identification spectroscopy neutron induced gamma-rays," *IEEE Transactions on Nuclear Science*, vol. 39, no. 5, pp. 1422–1426, October 1992.

[8] E. H. Seabury and A. J. Caffrey, "Explosive detection and identification by PGNAA," Idaho National Engineering and Environmental Laboratory, Bechtel BWXT Idaho, LLC, Tech. Rep., November 2004.

[9] E. H. Seabury and A. J. Caffreys, "Explosives detection and identification by PGNAA," Idaho International Laboratory, Tech. Rep., April 2006. http://dx.doi.org/10.2172/911698

[10] T. R. Twomey, A. J. Caffrey, and D. L. Chichester, "Nondestructive identification of chemical warfare agents and explosives by neutron generator-driven PGNAA," Idaho National Laboratory, Idaho Falls, Idaho 83415 USA, Tech. Rep., 2007.

[11] G. A. Warren and R. S. Detwiler, "Nuclear resonance fluorescence for material verification in dismantlement," Pacific Northwest National Laboratory, 902 Battelle Blvd, MSIN J4-65, Richland, WA, 99352 USA, Tech. Rep., 2011.

[12] R. C. Runkle, D. L. Chichester, and S. J. Thompson, "Rattling nucleons: New developments in active interrogation of special nuclear material," *Nuclear Instruments and Methods in Physics Research Section A: Accelerators, Spectrometers, Detectors and Associated Equipment*, vol. 663, no. 1, pp. 75–95, January 2012. http://dx.doi.org/10.1016/j.nima.2011.09.052

[13] R. Chrien, J. Kopecky, H. Liou, O. Wasson, J. Garg, and M. Dritsa, "Distribution of radiative strength from neutron capture by Pu-239," *Nuclear Physics A*, vol. 436, no. 2, pp. 205 – 220, 1985. http://www.sciencedirect.com/science/article/pii/0375947485901964

[14] D. M. Drake, J. C. Hopkins, C. S. Young, and H. Condé, "Gamma-ray-production cross sections for fast neutron interactions with several elements," *Nuclear Science and Engineering*, vol. 40, no. 2, p. 294, 1970.

[15] M. A. Lone, R. A. Leavitt, and D. A. Harrison, "Prompt gamma rays from thermal-neutron capture," Atomic Energy of Canadas Limited Chalk River Nuclear Laboratories, Ontario, Canada, Tech. Rep., 1981.

[16] P. Matussek, W. Michaelis, C. Weitkamp, and H. Woda, "Studies of radiative neutron capture and delayed fission gamma-ray spectra from uranium and plutonium as a basis for new non-destructive safeguards techniques," in *Safeguards techniques: proceedings of a Symposium on progress in safeguards techniques / organized by the International Atomic Energy Agency and held in Karlsruhe, 6-10 July 1970*, vol. 2, no. IAEA-SM133/33, 1970, p. 113.

[17] P. Matussek, H. Ottmar, I. Piper, C. Weitkamp, and H. Woda, "Measurement of gamma-ray spectra from thermal neutron interaction with U235," in *Conference on Nuclear Structure Study with Neutrons*, 1972, pp. A42, 84.

[18] P. Matussek, H. Ottmar, C. Weitkamp, and H. Woda, "Study of Pu240 by thermal neutron capture," in *Conference on Nuclear Structure Study with Neutrons*, 1972, pp. A43, 86.

[19] H. Ottmar, P. Matussek, C. Weitkamp, and H. Woda, "Average width of E1 and M1 radiative transitions from neutron capture states in Pu-240," in *Conference on Nuclear Structure Study with Neutrons*, 1972, pp. A44, 88.

[20] C. Weitkamp, P. Matussek, and H. Ottmar, "Nondestructive nuclear fuel assay by neutron capture gamma-ray spectrometry," in *Neutron capture gamma-ray spectroscopy: proceedings of the Second International Symposium on Neutron Capture Gamma-Ray Spectroscopy and Related Topics*, Petten, The Netherlands, September 2-6 1974.

[21] G. Molnár, Z. Révay, and T. Belgya, "Non-destructive interrogation of uranium using PGAA," *Nuclear Instruments and Methods in Physics Research*, vol. 213, pp. 389–393, 2004.

[22] D. L. Chichester, E. H. Seabury, J. Wharton, and S. M. Watson, "INL neutron interrogation R&D: FY2010 MPACT end of year report," Office of Scientific and Technical Information, Tech. Rep., August 2010. http://www5vip.inl.gov/technicalpublications/documents/4680348.pdf

[23] Prompt Gamma-ray neutron Activation Analysis database (PGAA). (1999-2003) International Atomic Energy Agency (IAEA) Nuclear Data Service (NDS). https://www-nds.iaea.org/pgaa/

[24] Thermal Neutron Capture Gamma's database (CapGam). (2013, September) Brookhaven National Laboratory (BNL) National Nuclear Data Center (NNDC). http://www.nndc.bnl.gov/capgam/

[25] J. G. Fantidis, B. V. Dimitrios, P. Constantinos, and V. Nick, "Fast and thermal neutron radiographies based on a compact neutron generator," *Journal of Theoretical and Applied Physics*, vol. 6, no. 1, p. 20, 2012. http://dx.doi.org/10.1186/2251-7235-6-20

[26] J. Reijonen, K.-N. Leung, R. Firestone, J. English, D. Perry, A. Smith, F. Gicquel, M. Sun, H. Koivunoro, T.-P. Lou, B. Bandong, G. Garabedian, Z. Révay, L. Szentmiklosi, and G. Molnár, "First PGAA and NAA experimental results from a compact high intensity D-D neutron generator," *Nuclear Instruments and Methods in Physics Research*, vol. 522, pp. 598–602, 2004.

[27] J. Reijonen, "Compact neutron generators for medical, home land security, and planetary exploration," in *Proceedings of 2005 Particle Accelerator Conference, Knoxville, Tennessee*, 2005.

[28] P. Kudejova, L. Canella, R. Schulze, N. Warr, A. Türler, and J. Jolie, "Characterization of the new PGAA and PGAI facility at the research reactor FRM II," in *NRC7 - Seventh International Conference On Nuclear And Radiochemistry*, 2008.

[29] W. Petry, "Advanced neutron instrumentation at FRM-II," in *IGORR 9: Proceedings of the 9. meeting of the International Group On Research Reactors*, vol. IAEA Ref. Number 36019445, 2003, p. 346.

[30] *Advanced Lab Course in Physics at FRMII*, TU München, 2010.

[31] W. Petry. (2014) Advanced neutron instrumentation at FRM-II. Forschungs-Neutronenquelle Heinz Maier-Leibnitz (FRM II). http://www.frm2.tum.de/aktuelles/infos-und-downloads/misc0/advanced-neutron-instrumentation/

[32] Z. Révay, T. Belgya, Z. Kasztovszky, J. Weil, and G. Molnár, "Cold neutron PGAA facility at Budapest," *Nuclear Instruments and Methods in Physics Research*, vol. 213, pp. 385–388, 2004.

[33] Neutron-Induced Prompt gamma-ray Spectroscopy (NIPS) and Neutron Optics and Radiography for Material Analysis (NORMA). (2014) Budapest Neutron Centre. http://www.bnc.hu/?q=node/15

[34] Prompt Gamma Activation Analysis (PGAA). (2014) Budapest Neutron Centre. http://www.bnc.hu/?q=node/14

[35] G. L. Molnár, *Handbook of Prompt Gamma Activation Analysis with Neutron Beams*, G. L. Molnár, Ed., 2004.

[36] A. L. Nichols, D. L. Aldama, and M. Verpelli, "Handbook of nuclear data for safeguards: database extensions," International Atomic Energy Agency - Nuclear Data Section, Tech. Rep. IAEA INDC (NDS)-0534, August 2008.

[37] R. E. Hunter and L. Stewart, "Evaluated neutron-induced gamma-ray production cross sections for 239Pu and 240Pu," Los Alamos Scientific Laboratory, Tech. Rep. LA-4901, 1972.

[38] M. Chadwick, M. Herman, P. Obložinský, M. Dunn, Y. Danon, A. Kahler, D. Smith, B. Pritychenko, G. Arbanas, R. Arcilla, R. Brewer, D. Brown, R. Capote, A. Carlson, Y. Cho, H. Derrien, K. Guber, G. Hale, S. Hoblit, S. Holloway, T. Johnson, T. Kawano, B. Kiedrowski, H. Kim, S. Kunieda, N. Larson, L. Leal, J. Lestone, R. Little, E. McCutchan, R. MacFarlane, M. MacInnes, C. Mattoon, R. McKnight, S. Mughabghab, G. Nobre, G. Palmiotti, A. Palumbo, M. Pigni, V. Pronyaev, R. Sayer, A. Sonzogni, N. Summers, P. Talou, I. Thompson, A. Trkov, R. Vogt, S. van der Marck, A. Wallner, M. White, D. Wiarda, and P. Young, "ENDF/B-VII.1: Nuclear data for science and technology: Cross sections, covariances, fission product yields and decay data," *Nuclear Data Sheets*, vol. 112, no. 12, pp. 2887–2996, December 2011.

[39] V. V. Verbinski, H. Weber, and R. E. Sund, "Prompt gamma rays from 235U(n,f), 239Pu(n,f), and spontaneous fission of 252Cf," *Physical Review C*, vol. 7, no. 3, pp. 1173–1185, March 1973.

[40] A. Oberstedt, T. Belgya, R. Billnert, F.-J. Hambsch, Z. Kis, T. M. Perez, S. Oberstedt, L. Szentmiklosi, K. Takács, and M. Vidalid, "New prompt fission gamma-ray spectral data and its implication on present evaluated nuclear data files," in *Physics Procedia: Scientific Workshop on Nuclear Fission Dynamics and the Emission of Prompt Neutrons and Gamma Rays*, Biarritz, France, 28-30 November 2012.

[41] T. R. England and B. F. Rider, "Evaluation and compilation of fission product yields," Los Alamos National Laboratory, Tech. Rep., October 1993. http://ie.lbl.gov/fission/endf349.pdf

[42] R. Firestone. Table of radioactive isotopes. Lawrence Berkely National Laboratory. http://ie.lbl.gov/toi/radSearch.asp

[43] X.-. M. C. Team. (2003) MCNP - a general monte carlo n-particle transport code. Los Alamos National Laboratory. https://mcnp.lanl.gov/

[44] D. H. White, R. W. Hoff, H. G. Börner, K. Schreckenbach, F. Hoyler, G. Colvin, I. Ahmad, A. M. Friedman, and J. R. Erskine, "Nuclear structure of 241Pu from neutron-capture, (d,p)-, and (d,t)-reaction

measurements," *PHYSICAL REVIEW C*, vol. 57, no. 3, p. 1112, 1998.

[45] J. H. Hubbell and S. M. Seltzer. (1990) Tables of x-ray mass attenuation coefficients and mass energy-absorption coefficients from 1 kev to 20 mev for elements z = 1 to 92 and 48 additional substances of dosimetric interest. Radiation Physics Division, PML, NIST. http://www.nist.gov/pml/data/xraycoef/index.cfm

THE USE OF MEASUREMENT UNCERTAINTY IN NUCLEAR MATERIALS ACCOUNTANCY AND VERIFICATION

O. Alique; S. Vaccaro; J. Svedkauskaite

Nuclear Safeguards Directorate E, DG Energy, European Commission,
L-2920 Luxembourg, Luxembourg

Abstract:

EURATOM nuclear safeguards are based on the nuclear operators' accounting for and declaring of the amounts of nuclear materials in their possession, as well as on the European Commission verifying the correctness and completeness of such declarations by means of conformity assessment practices. Both the accountancy and the verification processes comprise the measurements of amounts and characteristics of nuclear materials. The uncertainties associated to these measurements play an important role in the reliability of the results of nuclear material accountancy and verification.

The document "JCGM 100:2008 Evaluation of measurement data – Guide to the expression of uncertainty in measurement" - issued jointly by the International Bureau of Weights and Measures (BIPM) and international organisations for metrology, standardisation and accreditation in chemistry, physics and electrotechnology - describes a universal, internally consistent, transparent and applicable method for the evaluation and expression of uncertainty in measurements.

This paper discusses different processes of nuclear materials accountancy and verification where measurement uncertainty plays a significant role. It also suggests the way measurement uncertainty could be used to enhance the reliability of the results of the nuclear materials accountancy and verification processes.

Keywords: measurement uncertainty, conformity assessment, verification

1. Euratom Nuclear Safeguards operating principle

The holders of nuclear materials in the European Union are subject to Euratom nuclear safeguards. The obligations for nuclear operators derived from nuclear safeguards include the implementation of a Nuclear Material Accountancy and Control (NMAC) system and the declaration of nuclear materials flows (monthly) and stocks (yearly). The European Commission verifies consequently the correctness and completeness of the declarations produced for nuclear materials flows and stocks by means of inspections. In a nutshell, Euratom nuclear safeguards are based on three sequential processes:

1. Accountancy and control of nuclear materials, performed by nuclear operators;
2. Declaration to the European Commission of flows and inventories of nuclear materials, performed by nuclear operators;
3. Verification of the correctness and completeness of these declarations by the European Commission.

Measurements and measurement uncertainties play a crucial role in the first and third processes. The role of measurement uncertainty and the way it is estimated and reported has been discussed on several occasions without reaching a clear agreement amongst the nuclear safeguards community. A deeper analysis can assist safeguards practitioners to understand the role of measurement uncertainty.

2. International standardisation of measurement uncertainties and application to Nuclear Safeguards

The metrology community has discussed for long in its attempt to find a harmonised way of reporting uncertainty. In 1977, recognizing the lack of international consensus on the expression of uncertainty in measurement, the world's highest authority in metrology, the 'Comité International des Poids et Mesures' (CIPM), requested the 'Bureau International des Poids et Mesures' (BIPM) to address the problem in conjunction with the national standards laboratories and to make a recommendation.

The BIPM prepared a detailed questionnaire covering the issues involved and distributed it to 32 national metrology laboratories known to have an interest in the subject (and, for information, to five international organizations). The BIPM then convened a meeting for the purpose of arriving at a uniform and generally acceptable procedure for the specification of uncertainty; it was attended by experts from 11 national standards laboratories. This Working Group on the Statement of Uncertainties developed Recommendation INC-1 (1980), Expression of Experimental Uncertainties [1]. The CIPM approved the Recommendation in 1981 and reaffirmed it in 1986.

The task of developing a detailed guide based on the Working Group Recommendation (which is a brief outline rather than a detailed prescription) was referred by the

CIPM to the International Organization for Standardization (ISO), since ISO could better reflect the needs arising from the broad interests of industry and commerce.

In 1995, the JCGM (Joint Committee for Guides in Metrology) formed by the BIPM and international organisations for metrology, standardisation and accreditation in chemistry, physics and electrotechnology, issued the first version of the Guide to the Expression of Uncertainty in Measurement (GUM). The GUM 2008 [2] was issued upon revision, with minor corrections, of the GUM 1995. Together with its supplements, this is the most recent international standard in the matter globally accepted and has been published by the International Organisation of Standardisation (ISO) as ISO/IEC Guide 98-2:2008.

It is important to note that not every actor of the nuclear safeguards community has incorporated to their practices the use of measurement uncertainties calculated according to the GUM Guide [2]:

- **Laboratories** providing measurement results to the nuclear inspectorates and nuclear operators' laboratories provide uncertainties calculated according to the GUM Guide [2].
- Measurements performed at **nuclear facilitie**s by plant staff do not always carry uncertainties calculated according to the GUM Guide [2]. Frequent examples are mass and volume measurements performed in the operations areas.
- Traditionally **nuclear inspectorates** have been using the classical statistical model of error for uncertainty calculation and for measurement data evaluation. The harmonized standard method for estimation and use of measurement uncertainty is not used by nuclear inspectorates 20 years after the first issue of the GUM guide.

3. Accountancy and control of nuclear materials

Nuclear operators account for and control all nuclear materials inside the Material Balance Areas (MBA) for which they are responsible. This process includes accounting for every amount of nuclear material entering or leaving the MBA and taking an inventory of the nuclear material held in the MBA once per year. When the nuclear material is in loose form, at any stage of the processes which take place in the MBA, measurements will play an important role in the accountancy process.

In this case the legislation in force, specifically Article 7 of the Commission Regulation (Euratom) 302/2005 of 8 February 2005, on the application of Euratom safeguards [3], obliges the measurement system used for accountancy purposes to be conform or equivalent in quality to the latest international standards. This legal requirement is often interpreted as the uncertainties of the nuclear operators' measurements to be equal or less than those expressed in the International Target Values (ITV) [4] issued by the IAEA (International Atomic Energy Agency). However, the ITVs are not standards with requirements on the quality of measurement systems. They uncertainties to be considered in judging the reliability of analytical techniques applied to industrial nuclear and fissile material subject to safeguards verification. They can be used by every actor in nuclear safeguards in method validation, conformity assessment and measurement performance evaluation.

There exist international standards that contain requirements about the quality of measurement systems. The most widely recognised standards are:

- ISO 17025:2005. General requirements for the competence of testing and calibration laboratories [5]
- ISO 10012:2003. Measurement management systems -- Requirements for measurement processes and measuring equipment.[6]

Both standards require that measurement methods are validated, and that measurement results are metrologically traceable. This condition requires the measurement results to be traceable to a unit of the International System of Units by an unbroken chain of calibrations, each one contributing to the final uncertainty of the result. It is therefore an implicit requirement that every measurement performed with nuclear materials accountancy purposes must be reported together with its associated uncertainty.

Other than the quality of the measurement systems, the European Commission imposes to nuclear operators keeping operating records. Regulation 302/2005 [3] stipulates in its article 8 that:

> "For each material balance area, the operating records shall include, where appropriate:
> […]
> (c) the data, including derived estimates of random and systematic errors, obtained from the calibration of tanks and instruments as well as from sampling and analysis;
> (d) the data resulting from quality control measures applied to the nuclear material accountancy system, including derived estimates of random and systematic errors;"

The expression *'estimates of random and systematic errors'* must be understood here as the combined standard uncertainty as defined in the GUM [2] and as additionally listed in the ITV [4]. It is important to note that no requirement exists for accompanying the measurement based declarations performed by the nuclear operators about nuclear materials with the associated uncertainties.

The same applies for the requirement of stating estimations of random and systematic errors as stated in Annex

I of the above mentioned Regulation 302/205 [3], with the purpose of declaring the Basic Technical Characteristics of the installation. This declaration must respond to a typical uncertainty obtained, so it must be interpreted as the maximum acceptable uncertainty for the nuclear operator.

The different measurements performed in nuclear materials accountancy can be grouped in two categories with respect to the uncertainty calculations required:

1. **Measurements performed in analytical laboratories**, which are in most of the cases metrologically traceable. These measurements are designed to obtain low uncertainties. Typically individual uncertainties are calculated for every measurement result, according to the GUM guide [2]. Titrations, mass spectrometry or calorimetry are good examples of this type of measurements.

2. **Measurements performed on industrial plants**. These measurements can be grouped as:
   a. Nuclear measurements. These measurements are designed to provide fast results without generating any waste and not destroying the sample analysed. The uncertainties obtained are normally bigger than those obtained in analytical laboratories. Often the full metrological traceability of these measurements is not ensured.
   b. Mass and volume measurements. When mass and volume measurements are performed in an industrial environment, an overall uncertainty associated with the instrument can be attributed to every measurement performed by that instrument, avoiding the necessity to perform uncertainty calculations for every measurement performed. This practice is only acceptable when three conditions are fulfilled:
      i. The overall uncertainty for the measurement instrument is recalculated after calibration;
      ii. Appropriate quality control is applied to the measurement device to ensure that last calibration is still valid;
      iii. The environmental conditions influencing the measurement are monitored and acceptance limits have been set-up in advance.

      It happens more often than one would expect that mass and volume measurements in industrial plants are not metrologically traceable, The most common reasons for this are the use of inappropriate standards for calibration or the incorrect uncertainty calculations.

Another important aspect of nuclear materials accountancy and control where measurement uncertainty plays an important role is the Material Balance Evaluation (MBE). MBE performed by nuclear operators consists in evaluating the difference between the results obtained in the accountancy books and the physical reality. This difference is named MUF (Material Unaccounted For). In installations that handle and measure materials in loose form (liquid, gas or powder), the MUF stemming from a physical inventory taking will never be zero. The potential causes of MUF are:

- Clerical mistakes
- Hidden inventories non accounted for
- Hidden loses non accounted for
- Legitimate measurement errors.

From these potential causes, only the last one is acceptable. In order to assess whether the MUF can be justified by legitimate measurement errors, it is compared with the parameter $\sigma_{MUF.}$ σ_{MUF} is the result of properly propagating all the uncertainties associated to the measurements that could explain the difference between accountancy books and physical reality. In order to perform a reliable assessment of MUF, the uncertainties propagated into σ_{MUF} must all be comparable and realistic. The method described in the GUM [2] provides uncertainty values that take into account all relevant factors and are comparable, transferrable (the uncertainty of a measurement result can be used in a consequent calculation of measurement uncertainty when the first measurement has an influence on the second) and auditable. Moreover, the combined standard uncertainty provided according to the GUM [2] can be characterized by standard deviations. This allows for statistical testing of MUF considering this parameter as a normally distributed variable.

4. Verification of the correctness and completeness of these declarations by the European Commission

The European Commission verifies the correctness and completeness of nuclear materials declarations provided by nuclear operators, following a series of conformity assessments. They are grouped according to their objectives as follows:

1. *First layer assessments*. This first group of conformity assessment activities serves as preparation for the physical verification of the nuclear materials declarations. They include the periodical verification of the Basic Technical Characteristics of the nuclear installations and the assessment of the correspondence between the nuclear materials declarations, accountancy records and operational records kept by nuclear operators. Further, the correctness in format and consistency of declarations provided to the European Commission is also checked. Finally, the quality of the measurement systems of the nuclear operators is evaluated.
   One basic activity performed to evaluate the quality of the nuclear operators' measurement systems is the

performance of independent measurements and comparison of the results obtained by the nuclear operators and the inspectorate. This assessment is performed according to the definition of metrological compatibility in the International Vocabulary of Metrology (VIM 2.47) [7]:

'Metrological compatibility of measurement results is a property of a set of measurement results for a specified measurand, such that the absolute value of the difference of any pair of measured quantity values from two different measurement results is smaller than some chosen multiple of the standard measurement uncertainty of that difference.

Metrological compatibility of measurement results replaces the traditional concept of 'staying within the error', as it represents the criterion for deciding whether two measurement results refer to the same measurand or not. If in a set of measurements of a measurand, thought to be constant, a measurement result is not compatible with the others, either the measurement was not correct (e.g. its measurement uncertainty was assessed as being too small) or the measured quantity changed between measurements.

Correlation between the measurements influences metrological compatibility of measurement results. If the measurements are completely uncorrelated, the standard measurement uncertainty of their difference is equal to the root mean square sum of their standard measurement uncertainties, while it is lower for positive covariance or higher for negative covariance.'

Hence, for fully independent measurements between the nuclear operator and nuclear inspector, the assessment on the compatibility is done according to the following formula:

$$\left| R_{op} - R_{ins} \right| \leq k \cdot \sqrt{u_{op}^2 + u_{ins}^2}$$

Where:

R_{op} is the measured value obtained by the nuclear operator,

R_{ins} is the measured value obtained by the inspectorate,

u_{op} is the combined standard uncertainty of the nuclear operator result,

u_{ins} is the combined standard uncertainty of the inspectorate result.

k is a constant to be chosen in function of the risk of false alarm. Typically, in nuclear safeguards assessments k equals three, which corresponds to a false alarm rate of 0.135 %

2. *Physical verification of nuclear materials*. This group includes physical verification techniques as identification, item counting, qualitative testing, quantitative testing, as well as verification of the results of containment and surveillance techniques.

Quantitative testing of nuclear materials with the purposes of physical verification implies the conformity assessment of a declaration with the support of a measurement result. This conformity assessment activity is different to the assessment of the nuclear operators' measurement system:

- The first difference originates from the property of nuclear material declarations not holding an associated uncertainty, contrary to measurement results provided by nuclear operators as operating records. Therefore, the conformity assessment for nuclear materials declarations cannot be supported by the concept of metrological compatibility.
- Another difference lies in the fact that nuclear materials declarations can refer to an item, or a batch of items, or a bulk amount of nuclear materials, so to support the conformity assessment in a measurement result often a sampling process takes place. Therefore, occasionally the sampling uncertainty will have a crucial importance in the conformity assessment of nuclear materials declarations.
- Another difference comes from declarations that could originate from estimations, calculations, or measurements not performed directly on the referred item or batch, but on the material while being in previous phases of the industrial process.
- Finally, there is a difference in the fact that often the inspectorate uses measurement techniques of lower accuracy than the techniques used by nuclear operators to produce their declarations, which influences strongly the conformity assessment process.

Therefore, for quantitative testing of nuclear materials with the purpose of physical verification, it is necessary to set a decision rule[1] to document the judgement of conformity based on a measured value and its uncertainty. There is extensive literature on how to set decision rules when the conformity assessment is based on the measurement of a property of the item to assess, and the conformity is expressed by tolerance limits in the form of intervals or thresholds. The decision rules are set in function of the risk that can be assumed of wrongly judging an item as conform and the risk of rejecting a conforming item.

Unfortunately, there is limited literature that refers to the use of measurement uncertainty for the assessment of nuclear materials declarations. There is a generally

1 From JGCM 106:2012 [8]
"Decision rule":
documented rule that describes how measurement uncertainty will be accounted for with regard to accepting or rejecting an item, given a specified requirement and the result of a measurement.

applied decision rule used in nuclear safeguards based on the measurement uncertainty obtained by the inspectorate. Acceptance is granted to the declaration if:

$$| D - R_{ins} | \leq k \cdot u_{ins}$$

Where:

D is the declared value for the assessed property of an item or batch of nuclear materials,

R_{ins} is the measured value by the nuclear inspectorate for the same property of the item/batch

u_{ins} is the combined standard uncertainty of the inspectorate result

k is a constant.

Typically, in nuclear safeguards assessments k has been assigned a fixed value equal to three. However, the risk that the inspectorate and the nuclear operator can assume of accepting a non-conform declaration or rejecting a conform declaration is not always the same. It depends on the type and amount of nuclear material measured, on the measurement method used, on the uncertainty obtained, on the possibilities to repeat the measurement and the cost of it, etc…

This is why, documented decision rules with clear risk assessments shall be applied by the inspectorates instead of using a fixed value for the constant k.

Two examples for a practical application are given. In cases of a. and b. the declaration by the nuclear operator refers to an item and it is based on indirect measurements, i.e. the measurement of the amounts and characteristics of the nuclear material contained in the item has not been performed on the item, but in previous stages of the industrial process having the considered item as a product. In both cases, the inspectorate will perform direct measurements on the considered item to assess the conformity of the nuclear operator's declaration:

a. The nuclear operator declares the mass of uranium contained in a fresh fuel element prepared for shipment in a fuel fabrication plant. In this case, the operator will declare the mass of uranium contained based on the measurements performed during the fabrication process, whereas the inspectorate performs a non-destructive measurement, by Active Neutron Coincidence Collar, directly on the fuel element with relative standard uncertainties going up to 11% of the measured value.
b. The nuclear operator declares the mass of plutonium oxide contained in cans produced in a reprocessing plant. The operator declares a mass value based on analysis performed during the chemical reprocessing process and weighing, while the inspectorate performs a non-destructive assay, by a combination of gamma spectroscopy and passive neutron coincidence counting, with relative standard uncertainties going up to 2%. Complementary to this, the nuclear inspectorate is branched to the weighing device of the nuclear operator, obtaining the weighing results and in addition assesses the quality of the nuclear operator's measurement system by means of destructive assay.

The cases a. and b. are totally different from the safeguards risk point of view regarding the amount and type of material, the cost of a second measurement or the consequences of a non-conform result. That is why the value of k should be used to adjust the risk assumed by the inspectorate of declaring conform a non-conform declaration and the risk assumed by the nuclear operator of getting non-conformity over a conform declaration.

3. *Material Balance Evaluation*. This is a group of activities that have the objective of gaining additional assurance on the correctness and completeness of the nuclear material declarations. The accountancy and physical verification processes are strongly based on measurements, therefore they are strongly influenced by measurement uncertainty. By assessing the declared MUF by nuclear operators, the nuclear inspectorate mitigates the risk of the nuclear safeguards conclusions drawn being erroneous due to inaccuracies in measurements.

   In order to assess the declared MUF by the nuclear operators, the inspectorate has to obtain a value for $\sigma_{MUF.}$ This can be properly done only by propagating the measurement uncertainties over the material balance period to evaluate. This information is not known to the inspectorate, and a recurrent practice is to estimate a figure for σ_{MUF} from other data such as uncertainties declared in the BTC (Basic Technical Characteristics) or using the ITVs. An alternative technique used is to estimate the measurement uncertainties from the statistical analysis of paired measured values and induction of uncertainty values from a set of estimators. Any of the above mentioned approaches result in an overestimation of the σ_{MUF} value, hence minimising the added value of this assessment. We strongly argue that it would be more reasonable to audit and validate all the components of the σ_{MUF} value performed by the nuclear operator and then use this value in the subsequent tests. For this reason, a realistic and auditable way of estimating uncertainties becomes very important for the benefit of nuclear safeguards conclusions.

   Another important assessment that takes place in the phase of Material Balance Evaluation is the assessment of shipper-receiver differences. When a shipper MBA declares a different value for the transferred nuclear material than the receiver MBA, the inspectorate must assess whether this difference is due only to legitimate measurement errors. To do that, the inspectorate will again base its decision on the concept of metrological

compatibility of measurements, by applying the following formula:

$$|R_{sh} - R_{re}| \leq k \cdot \sqrt{u_{sh}^2 + u_{re}^2}$$

Where,

R_{sh} is the measured value obtained by the nuclear operator shipping the nuclear material,

R_{re} is the measured value obtained by the nuclear operator receiving the nuclear material,

u_{sh} is the combined standard uncertainty of the result obtained by the nuclear operator shipping the nuclear material,

u_{re} is the combined standard uncertainty of the result obtained by the nuclear operator receiving the nuclear material.

k is a constant to be chosen in function of the risk of false alarm. Typically, in nuclear safeguards assessments k equals three.

The uncertainties used for this assessment have to be validated by the inspectorate.

Again the use of the constant k shall be optimised by the inspectorate as a function of the risks assumed by the nuclear operators and the inspectorate.

Conclusions

- Measurement uncertainties are an essential element in the nuclear material accountancy and control processes.
- The use of measurement uncertainties calculated according to the GUM Guide should be extended to all safeguards actors.
- Measurement uncertainties are involved in a number of conformity assessments leading to drawing nuclear safeguards conclusion, so they play a very important role in nuclear safeguards.
- Since these conformity assessments are based on the comparison of measurement results and their respective uncertainties, it is crucial for the reliability of the assessments to ensure the metrological traceability of the measurements and the compatibility of the measurement uncertainty calculations. The use of the most widely accepted methodology to estimate measurement uncertainties by nuclear operators and inspectorates becomes crucial to the reliability of the nuclear safeguards system.
- In order to optimize the use of measurement results and their associated uncertainties in nuclear safeguards, the inspectorates shall introduce the concept of risk in their decision rules for conformity assessment.

All the proposed improvements in the nuclear safeguards practices come at a cost. A cost-benefit evaluation must be performed beforehand. However, some of the requirements for measurement systems have already succesfully been implemented in several disciplines running from nuclear safety to industrial products trade showing an important rate of return [9]. It is calculated that for an industrialized country, measurements performed according to agreed metrology practices cost around 3% of GDP, returning around 9% of the GDP.

References

[1] KAARLS, R. (1981), *BIPM Proc.-Verb. Com. Int. Poids et Mesures* 49, A1-A12 (in French); Giacomo, P. (1981), *Metrologia* 17, 73 -74 (in English).

[2] JCGM 100:2008 GUM 1995 with minor corrections. Evaluation of measurement data — Guide to the expression of uncertainty in measurement. Joint Committee for Guides in Metrology, 2008.

[3] Commission Regulation (Euratom) 302/2005 of 8 February 2005 on the application of Euratom safeguards. Official Journal of the European Union 28/02/2005, L 54/1 - L 54/70.

[4] STR-368. International Target Values 2010 for Measurement Uncertainties in Safeguarding Nuclear Materials. IAEA. Vienna, November 2010.

[5] ISO 17025:2005. General requirements for the competence of testing and calibration laboratories

[6] ISO 10012:2003. Measurement management systems -- Requirements for measurement processes and measuring equipment.

[7] JCGM 200:2012. International vocabulary of metrology – Basic and general concepts and associated terms (VIM). 3rd edition. 2008 version with minor corrections. Joint Committee for Guides in Metrology. 2012

[8] JGCM 106:2012 Evaluation of measurement data – The role of measurement uncertainty in

conformity assessment. Joint Committee for Guides in Metrology. 2012

[9] The Assessment of the Economic Role of Measurements and Testing in Modern Society. Survey directed by Geoffrey Williams, Pembroke College, Oxford, 2002

Particle Swarm Imaging (PSIM) – A swarming algorithm for the reporting of robust, optimal measurement uncertainties

Dan Parvin, Sean Clarke
Cavendish Nuclear
Sellafield, Seascale, Cumbria, United Kingdom
E-mail: dan.parvin@cavendishnuclear.com, sean.clarke@cavendishnuclear.com

Abstract:

Particle Swarm Imaging (PSIM) overcomes some of the challenges associated with the accurate declaration of measurement uncertainties of radionuclide inventories within waste items when the distribution of activity is unknown. Implementation requires minimal equipment, making use of gamma-ray measurements taken from different locations around the waste item, using only a single electrically cooled HRGS gamma-ray detector for objects up to a UK ISO freight container in size.

The PSIM technique is a computational method that iteratively 'homes-in' on the true location of activity concentrations in waste items. PSIM differs from conventional assay techniques by allowing only viable solutions - that is those that could actually give rise to the measured data - to be considered. Thus PSIM avoids the drawback of conventional analyses, namely, the adoption of unrealistic assumptions about the activity distribution that inevitably leads to the declaration of pessimistic (and in some cases optimistic) activity estimates and uncertainties.

PSIM applies an optimisation technique based upon 'particle swarming' methods to determine a set of candidate solutions within a 'search space' defined by the interior volume of a waste item.

The positions and activities of the swarm are used in conjunction with a mathematical model to simulate the measurement response for the current swarm location. The swarm is iteratively updated (with modified positions and activities) until a match with sufficient quality is obtained between the simulated and actual measurement data. This process is repeated to build up a distribution of candidate solutions, which is subsequently analysed to calculate a measurement result and uncertainty along with a visual image of the activity distribution.

The application of 'swarming' computational methods to non-destructive assay (NDA) measurements is considered novel and this paper is intended to introduce the PSIM concept and provide examples of PSIM's ability to reduce the levels of pessimism inherent in reported uncertainties.

Keywords: PSIM, Imaging, Non-destructive assay

1. Introduction

One of the most significant contributions to measurement inaccuracy made by gamma based instrumentation on large waste items is the effect of non-uniform source distribution. Significant underestimation of activity can occur when the calibration assumes a uniform activity distribution and all the activity is actually present as a single point within the item (for example at the centre of a waste drum). In this case, the gamma-rays must pass through a significant amount of the internal matrix and therefore experience high levels of attenuation. Depending upon the size of the waste item and the density of the matrix, the underestimate may range from a few percent to several orders of magnitude. On a measurement by measurement basis these effects have to be evaluated and appropriately compensated for when reporting total measurement uncertainties, Ref. [1].

The drawback is that without any knowledge of the actual distribution of activity within a waste item, unrealistic assumptions about the activity distribution are often applied leading to the declaration of pessimistic (and in some cases optimistic) activity estimates and uncertainties.

2. Particle Swarm Imaging (PSIM)

To illustrate the concept of PSIM consider a measurement geometry comprising of an arbitrary volume (referred to as the 'search space') containing n point sources of activity, with each point source possessing an activity A_n. Consider the deployment of M detectors around the waste item (or alternatively M measurements using the same detector at M different positions) and let each individual point source have a detection efficiency with respect to each detector. The goal of the measurement is to determine the total activity within the search space. A schematic of the measurement arrangement is shown in Fig. 1.

Figure 1: Measurement geometry containing point sources of activity which are constrained to lie within a 3-dimensional 'search space' such as the interior volume of a drum or box, the surfaces of a wall, interior of a glovebox etc.

The count rates measured at each of the *M* measurement positions must be dependent upon the position and activity of each source within the search space. Representing the source distribution as a sequence of source activities at discrete locations (*x, y, z*), the measured count rates may be written

$$C_1 = A_1\varepsilon_{1,1} + A_2\varepsilon_{1,2} + \ldots A_n\varepsilon_{1,n}$$
$$\vdots$$
$$C_M = A_1\varepsilon_{M,1} + A_2\varepsilon_{M,2} + \ldots A_n\varepsilon_{M,n} \qquad \text{Eq. (1)}$$

where:

C_i = count rate measured at position = 1 to *M*
A_j = activity of source *j*
$\varepsilon_{i,j}(x, y, z)$ = detection efficiency of point sourceat measurement position

Although the number of point sources, activities and positions required to solve (Eq. 1) explicitly are not known, it is possible nevertheless to evaluate the 'quality' of the agreement between the count rates produced from any 'potential' distribution of activity within the search space and the actual count rates measured.

The PSIM approach initialises a 'swarm' of solutions within the search space. Representing the unknown point source activities and their positions as a vector **p** then the objective is to minimise

$$\text{minimise: } \sum_{i=1}^{M} \left[C_i - \hat{C}(\mathrm{p})_i \right]^2 \qquad \text{Eq. (2)}$$

where:

$\hat{C}(\mathrm{p})_i$ = count rates due to the activity within the search space at measurement position

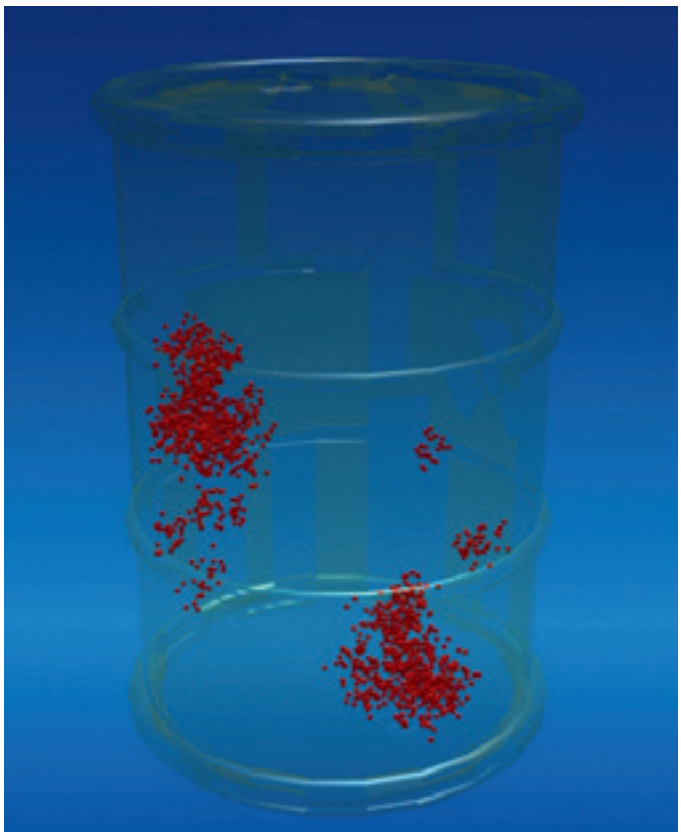

Figure 2: Example of PSIM image of the activity distribution within a 200 litre drum

The positions and activities of the swarm are used in conjunction with a mathematical model describing the measurement geometry to simulate the measurement response for the current swarm location. The swarm is iteratively updated (with modified positions and activities) until a match with sufficient quality is obtained between the simulated and actual measurement data i.e. until a solution to Eq. (2) is found. This process is repeated to build up a distribution of candidate solutions, which is subsequently analysed to calculate a measurement result and uncertainty along with a visual image of the activity distribution, a typical example of which is shown in Fig. 2.

The benefit of this approach is that only those solutions in the defined search space that could actually give rise to the measured data are considered. And this, in turn, facilitates more accurate quantification of total activity and activity distribution.

PSIM avoids the drawback of conventional analyses, namely, the adoption of unrealistic assumptions about the activity distribution that can lead to the declaration of pessimistic, or in many cases optimistic, activity estimates and uncertainties, Ref. [1].

2.1 Swarming Concept

Particle Swarming is a computational method that optimizes a problem by iteratively trying to improve a candidate solution with regard to a given measure of quality, see Eq.

(2). The particle swarming approach used by PSIM is a hybrid of the 'Particle Swarm Optimisation' or PSO approach originally attributed to Kennedy, Eberhart, Ref. [2] and 'Artificial Bee Colony Optimisation' or ABC attributed to D. Karaboga, B. Basturk, Ref. [3] and the 'Invasive Weed Optimization' or IWO algorithm developed by Mehrabian and Lucas [4].

The PSIM algorithm works by having a population (called a swarm) of candidate solutions (called particles). Each particle is assigned an activity value and position within the search space (for example the volume of a waste drum). The particles are moved around in the search space according to a few simple formulae. The movements of the particles are guided by their own best known position in the search space as well as the entire swarm's best known position. When improved positions are discovered these will then guide the movements of the swarm. The process is repeated until a match of sufficient quality is obtained with the measurement data.

Having established a good 'match' to the measurement data the swarm is allowed to evolve (either explore, expand or contract) seeking other candidate solutions that also produce a good 'match' to the measured data (exploitation). Over time the swarm effectively searches the entire search space (exploration) producing a distribution of solutions from which the final activity result and associated uncertainties are derived. The swarming pseudo - algorithm is shown in Fig. 3.

It is important to note that no assumption as to the physical size (number of particles) within the swarm is made. The swarm is able to concentrate or distribute the activity within the search space by adjusting its size as necessary throughout its lifetime.

Furthermore the approach does not seek a 'global' minimum (i.e. a single 'best' solution) as it not possible to find a unique solution to most measurement scenarios. In reality there are many solutions that will closely match the measurement data, all of which will be 'equally' valid.

However over the lifetime of the swarm, regions of 'preferred' space result, leading to regions where the solution density is higher. Regions of high solution density therefore correspond to the most likely position of the activity within the search space with the spread in the solutions representing a form of confidence interval space.

2.2 2.2. PSIM Software (Mathematical Model and Calibration)

The distribution of activity within the search space can be represented as a sequence of point sources at discrete locations, producing count rates described by (Eq. 1). To calculate the count rates at the measurement positions we require a user defined 'software' model that calculates the efficiencies for each point source of activity within the swarm. If the efficiencies are known then the count rates at the detector positions can be evaluated.

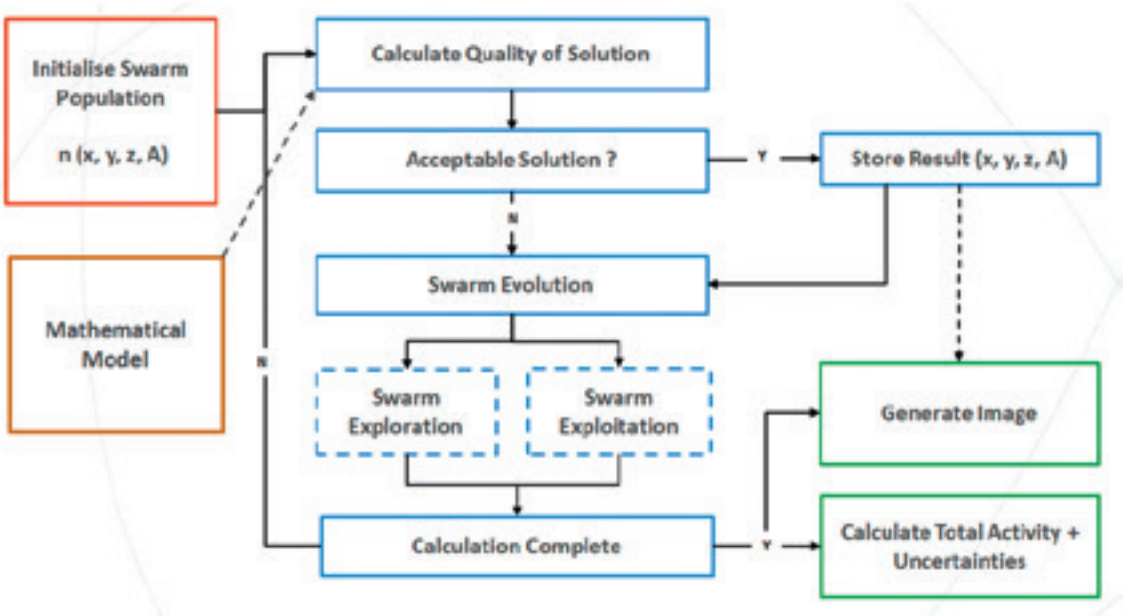

Figure 3: PSIM algorithm

The PSIM model is defined firstly by a series of quadric surfaces which define the measurement geometry. A quadric surface is represented by the following expression:

$$Ax^2 + By^2 + Cz^2 + Dxy + Exz + Fyz + Gx + Hy + Iz + J = 0 \quad \text{Eq.(3)}$$

where *A,..., J* are constants.

This notation allows the user to specify complex geometries including shapes that can be constructed from multiple planes, spheres, cylinders, cones etc. In addition to the surfaces that make up the measurement geometry it is necessary to define the cells within the geometry. Each cell is defined by a series of 'senses' with respect to each surface which uniquely defines the spatial extent of the cell volume within the measurement geometry. Each cell must be assigned a material density and mass attenuation coefficient appropriate to the gamma-ray of interest.

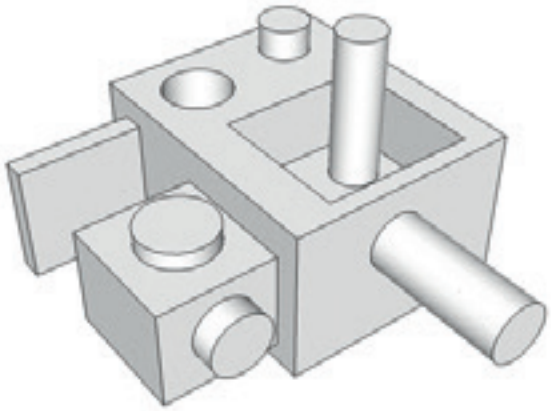

Figure 4: Complex geometries can be modelled by PSIM

The PSIM model does not use pre-defined 'template' geometries (as these will not always represent the true measurement geometry and configuration can be complex) providing the user with greater flexibility to specify more representative and complex geometries.

'Source' cells are identified within the PSIM model. Only these cells are permitted to contain sources of activity (an example of a 'source' cell would be the matrix within a drum or a vessel within a glovebox). This definition ensures that the swarm does not explore regions of the geometry within which no activity can exist. There is no restriction on the number of source cells allowing complex geometries to be considered (an example may be the measurement of multiple waste items within a room, a scenario which may be difficult to interpret using only pre-defined geometries due to the measurement cross-talk between individual objects and the measurement positions).

The PSIM model is completed by defining the locations at which the measurements were performed as well as the detector response. The measurement positions are simply defined by the central co-ordinates of the front face of the detector within the measurement geometry. The orientation of the detector with respect to the search space is defined by the normal vector perpendicular to the front surface of the detector. The detector response is pre-calibrated as a function of the incident gamma-ray energy. This detector calibration is the only model parameter that requires any pre-calibration prior to performing a measurement.

2.3 Percentile Uncertainty Reporting

The PSIM model is used to calculate the count rates at each measurement position for the current swarm position, and the fit 'quality' of the count rates is compared to the measured data. If the quality of the solution is 'acceptable' then the solution is archived (this then becomes a 'candidate' solution).

Before continuing with the PSIM analysis, the model can be perturbed (i.e. the cell densities, material types, efficiency of the detector, detector positions and measured count rates are all sampled) before the analysis resumes. Thus PSIM is able to incorporate the effects of uncertainty components associated with the model and measurement data into the final result.

Having established a good 'match' to the measurement data the swarm is allowed to evolve (either by exploration or exploitation) seeking other candidate solutions that also produce a good 'match' to the measured data. Over time the swarm effectively searches the entire search space producing many candidate solutions. The PSIM analysis is terminated once the required number of candidate solutions has been exceeded (a typical PSIM analysis will be configured for a total of 2000 - 3000 candidate solutions before a result is generated).

On completion of the analysis a frequency histogram is produced showing the distribution of the total activity (i.e. the sum of the activities of each point source or particle) for each candidate solution. It is from this histogram that the final activity result and associated uncertainties are derived – see Fig. 5.

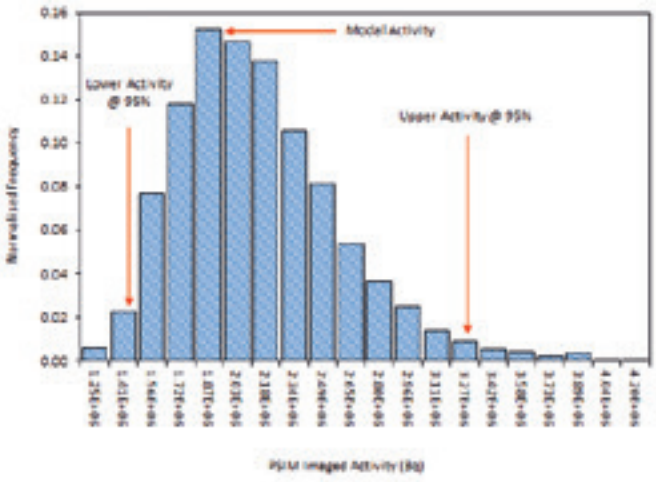

Figure 5: PSIM Imaged (total) activity frequency histogram

The activity results and uncertainties calculated by PSIM are based on a 'percentile' methodology. This method of confidence level reporting is ideally suited to PSIM because the set of activity solutions stored by PSIM are rarely normally distributed. In most cases the PSIM frequency histogram of solutions is skewed and contains important information that should be included when reporting robust measurement uncertainties.

To illustrate the percentile concept used in PSIM, consider Fig. 5, which shows a 'typical' normalised frequency histogram output by PSIM which has been constructed from a set of candidate solutions. A percentile is a measure used in statistics indicating the value below which a given percentage of observations in a group of observations (or PSIM solutions) fall. For example, the 20th percentile is the value below which 20% of the PSIM solutions may be found and the 90th percentile is the value above which 10% of the PSIM solutions would be found.

Suppose the histogram comprises 1000 different candidate solutions. After ranking the total activities from smallest to largest, let the values be denoted by (A_1, A_2,..., A_{1000}). If we choose to report uncertainties at the 95% confidence interval, then the minimum and maximum activity values would therefore be [A_{25}, A_{1975}] corresponding to the upper and lower 2.5% of solutions taken from each end of the distribution. Here A_{25} represents the lower activity value at 95% confidence and A_{1975} the upper activity value at 95% confidence (see both vertical lines shown in Fig. 5).

The PSIM 'best estimate' activity is usually reported as the modal value of the histogram, but other alternatives include the median or average value.

2.4. 'Hotspot' Imaging

This section presents examples of PSIM's ability to image the location of activity within a defined 3D search space; other examples are provided in Ref. [5]. This simulated example considers a 200 litre drum containing 2 x 1 MBq 'hotspots' of Cs-137 activity (the search space is defined as the interior volume of the drum consisting of concrete at a density of 1.2 g/cc). Two measurement scenarios are considered as shown in Fig. 6. The first considers 8 discrete measurements performed at the drum mid-height as shown in the left figure and the second a total of 8 discrete measurements taken at two different heights as shown in the right figure.

Fig. 7 shows a visual representation of the evolution of the swarm for Scenario #1. The bottom figure shows the final PSIM solution and the actual locations of the two hotspots of activity.

The lack of height information associated with Scenario #1 (i.e. all the measurement positions are at the same height) is reflected in the image shown in Figure 7, showing solutions extending along the full height of the drum.

This should be compared to the PSIM image result for Scenario #2 shown in Fig. 8. The addition of height information into the PSIM solution allows the two hotspot positions to be correctly resolved into the top and bottom regions of the drum.

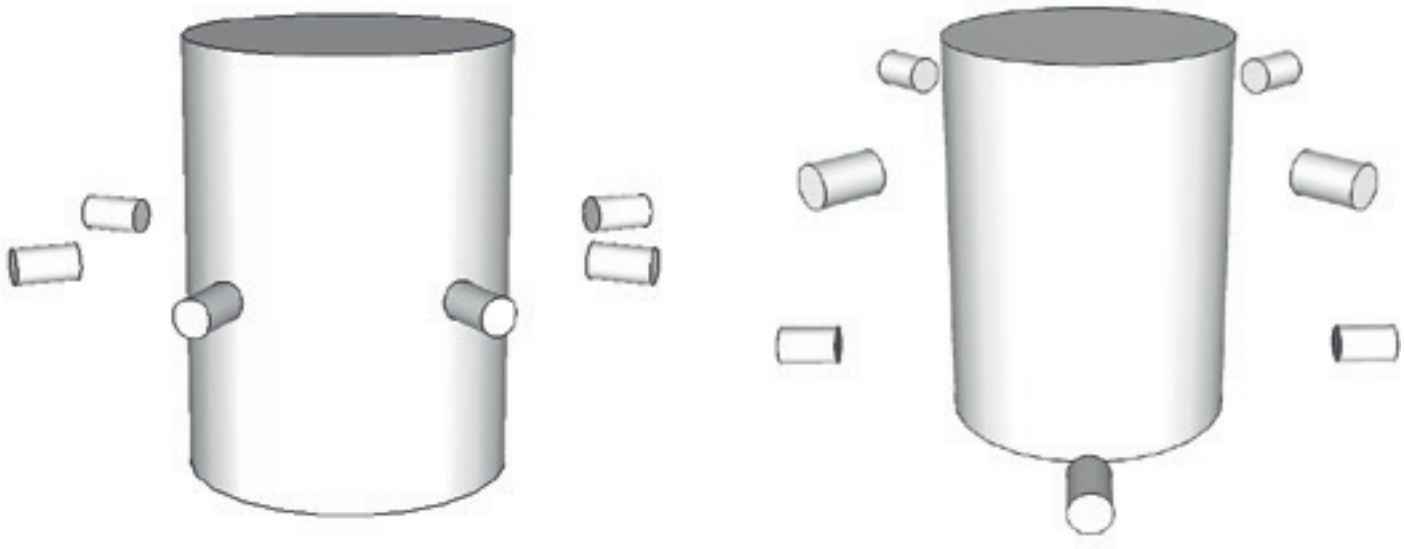

Figure 6: Detector deployments for PSIM imaging examples. Scenario #1 consists of 8 measurements at the drum mid-height (left) and Scenario #2 a total of 8 discrete measurements taken at two heights (right)

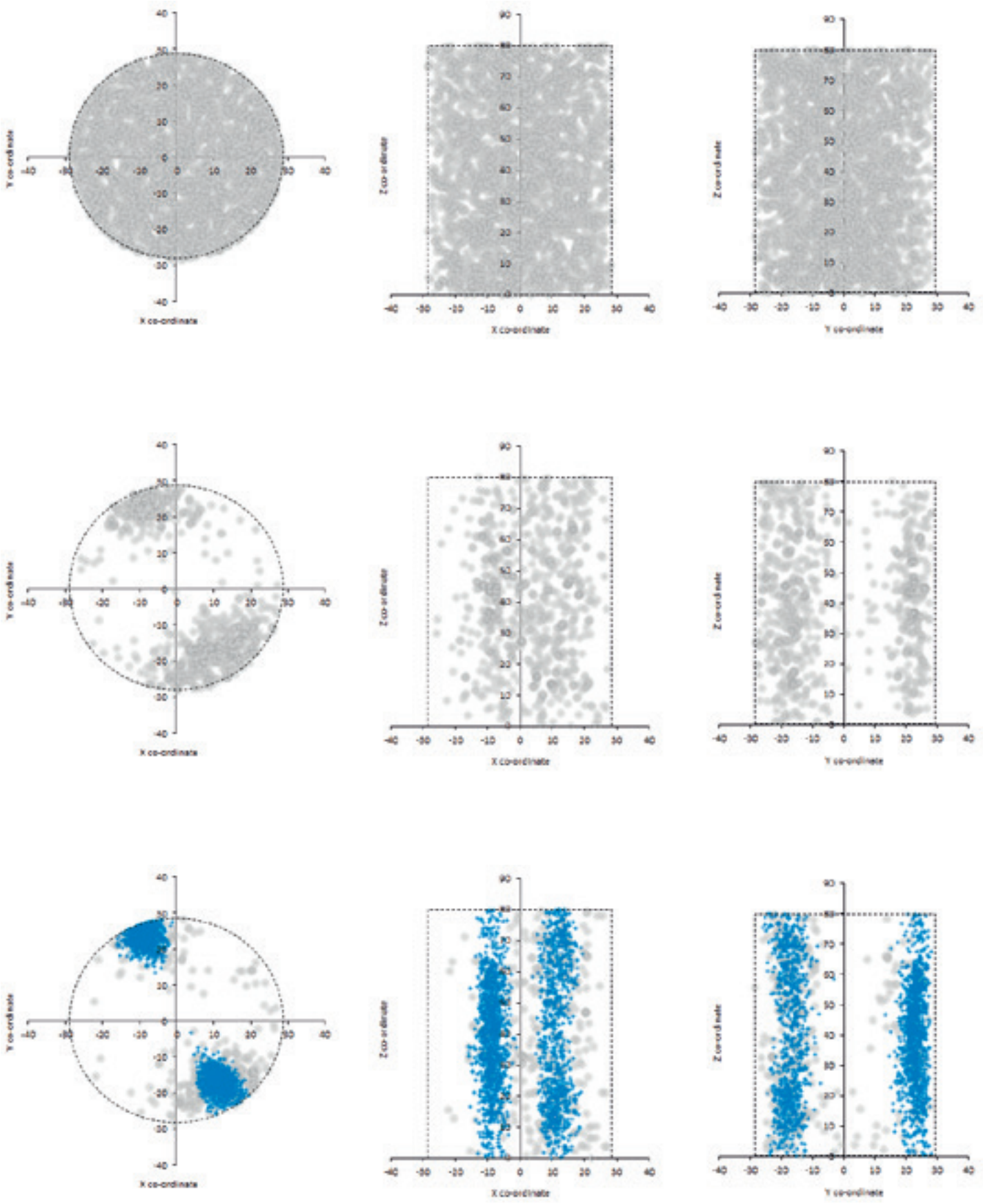

Figure 7: PSIM images for Scenario #1. The top figure shows the initial random swarm configuration. The middle figure shows the swarm after approximately 500 iterations. The bottom figure shows the final PSIM solution along with the actual location (red markers) of the two hotspots of activity within the drum. The data shown in blue represents locations within the drum contributing most to the overall 'quality' of the PSIM solution and represents therefore the most probable location of any activity within the drum.

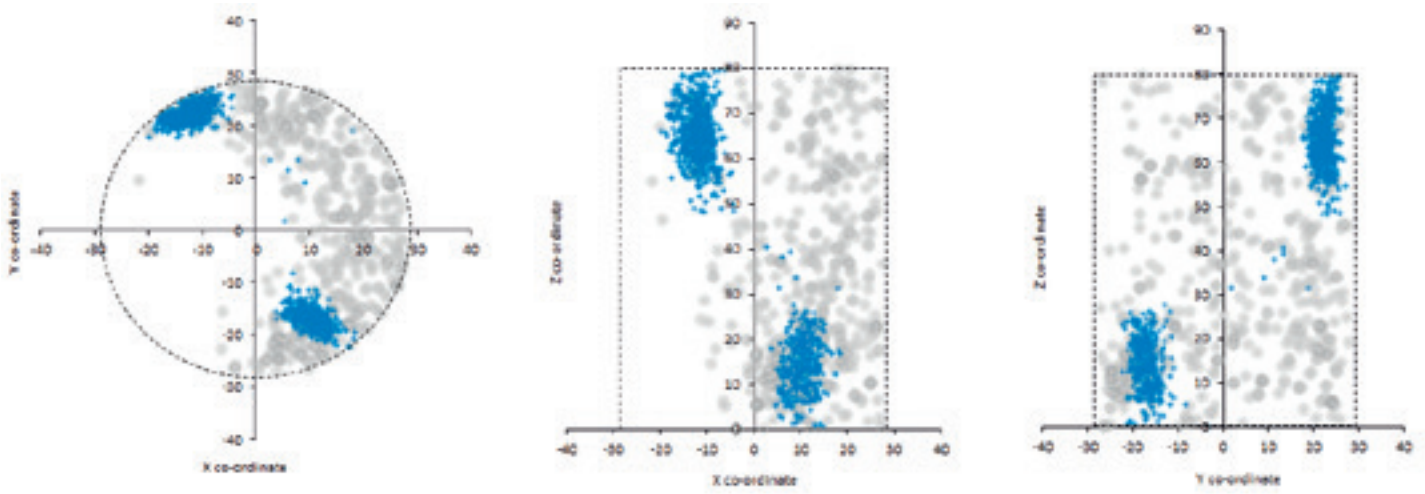

Figure 8: Final PSIM images for Scenario #2.

Fig. 9 shows the activity results returned by PSIM compared with those determined using more conventional analysis methods. In the conventional analysis method the calibration assumes the activity is 'uniformly' distributed throughout the drum volume, uses the sum of the count rates at each of the eight measurement positions, and the uncertainties are expressed at the 95% confidence intervals based on the assumption that any activity present has the potential to exist as a single point source located anywhere within the drum.

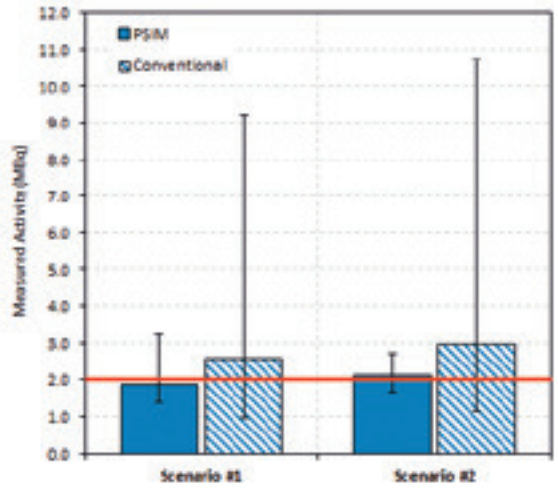

Figure 9: Comparison of PSIM and conventional analysis results for measurement Scenario #1 and Scenario #2 (note that the true activity within the drum is indicated by the solid red line and the uncertainties shown are at the 95% level of confidence generated using the percentile method described in Section 2.3)

In terms of accuracy, the best estimate PSIM value is closer to the known true value because it has imaged the actual location of the activity. In terms of uncertainty, PSIM only considers those solutions that could have given rise to the count rates at the measurement positions. Both these facilitate the quantification of total activity and uncertainty. The PSIM uncertainties are significantly smaller and the additional height information in Scenario #2 leads to a smaller uncertainty component than was the case for Scenario #1.

2.5. Dispersed Source Imaging

Waste items will not always contain discrete hotspots of activity, but rather multiple sources distributed in a random fashion throughout the waste volume. To compare the performance of PSIM in these circumstances against more conventional analysis methods a simulated trial was performed comparing the PSIM measurement uncertainties against those obtained using a conventional analysis approach.

The trial randomly located between 1 and 10 point sources within a 200 litre drum containing concrete having a bulk density of 1.2 g/cc. The measurement geometry used was that shown in Fig.6 (left). A total of 1,700 random trials were performed.

The conventional analysis is calibrated to assume the activity is 'uniformly' distributed throughout the drum volume, uses the sum of the count rates at each of the eight measurement positions, and the uncertainties are expressed at the 95% confidence intervals based on the assumption that any activity present has the potential to exist as a single point source located anywhere within the drum.

In contrast, the PSIM analysis makes no prior assumption as to the distribution of activity within the drum (i.e. no calibration is assumed prior to the measurement) and only required the generation of a model to reflect the measurement geometry.

Fig. 10 shows the results of the trial, comparing the uncertainties output by PSIM against those obtained from the conventional analysis approach described above. The uncertainty ratio shown equals the 95% upper uncertainty on the activity divided by the true activity within the drum. Thus ratio values greater than one would be expected in all cases. The PSIM uncertainty ratios have been sorted in order of increasing value and then plotted against the corresponding conventional value.

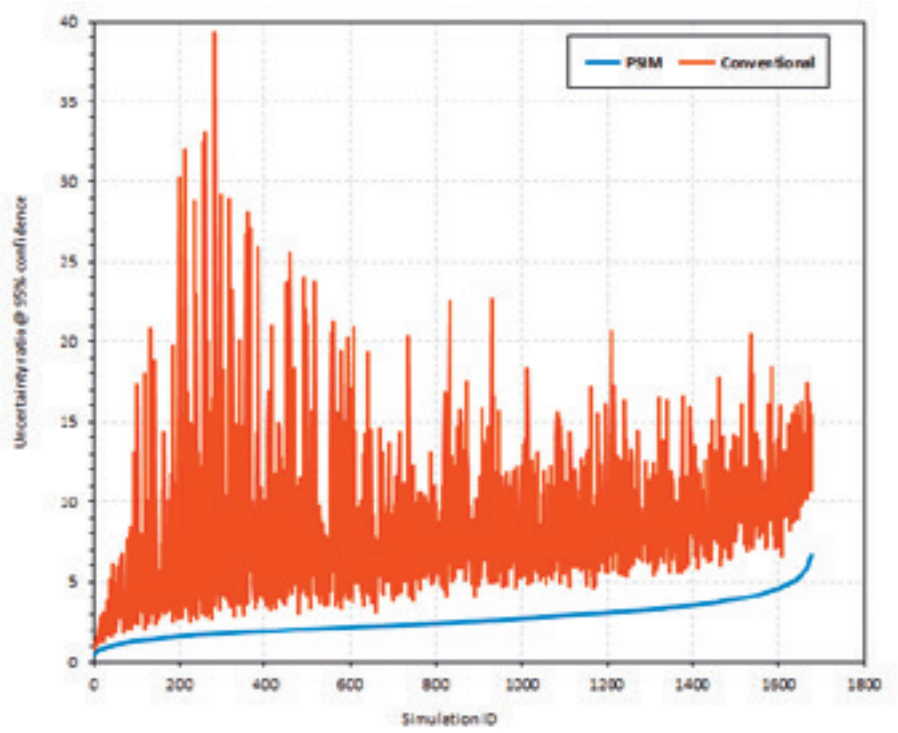

Figure 10: Comparison of PSIM and Conventional analysis methods. The uncertainty ratio shown equals the 95% upper uncertainty calculated using both analysis methods divided by the true activity within the drum.

The result of the trial demonstrates that the uncertainty ratios generated by PSIM are in every case less than those generated using the conventional analysis. For only a few cases is the uncertainty ratio less than unity and these represent 2.5% of the total trials performed and therefore entirely consistent with the confidence level of 95% chosen.

The PSIM uncertainties are on average approximately three times smaller (the average uncertainty ratio for the PSIM data being 2.6 compared to a value of 8.2 for the conventional analysis results).

3. PSIM Projects (United Kingdom)

PSIM has been used to perform measurements at nuclear facilities across the United Kingdom to confirm the suitability of waste to be consigned to LLWR and ILW and VLLW waste disposal and treatment facilities to support waste hierarchy re-categorisation. The PSIM technique has been used successfully for both characterisation and verification monitoring, including in-situ HRGS assay of a wide range of waste streams, waste item types and radionuclide species.

Recent projects include:

- VLLW bagged combustible wastes, for Sellafield / Environment Agency
- Legacy waste vault characterisation, for Sellafield
- Over 70 VLLW and LLW Isofreight containers, for LLWR / Sellafield / Environment Agency
- Drummed waste arising from low active drain operations, Sellafield
- Drummed wastes at other UK-wide nuclear sites such as Magnox Trawsfynydd, EDF Hunterston and EDF Heysham (ILW – containing concrete-shielding legacy wastes, VLLW and LA-LLW – containing asbestos and PPE, LLW – containing pond reactor and laundry waste, LLW – containing redundant plant and PPE)
- Multi-element bottles (MEBs) and other large metallic items prior to recycling at Studsvik.

Figure 11: PSIM measurements performed at various sites in the UK

4. Future Development – Neutron Swarm Imaging (NSIM)

PSIM is equally applicable to the assay of neutron emitting material such as plutonium (stored in waste drums, crates etc.) as well as monitoring and verification of material in process plant such as gloveboxes.

Despite the modelling required to determine the response of the swarm being more complex, the algorithm shown in Fig. 3 is readily adapted to neutron based measurements. In fact neutron based measurements benefit from producing both totals and reals (coincidence) count rates, therefore providing the swarm with more information for use in the optimisation process.

Fig. 12 shows the module mapping between PSIM and NSIM.

As well as imaging the location of neutron emitting material, methods are currently being developed for including both alpha (the ratio of (a, n) to spontaneous fission neutrons) and neutron multiplication as additional swarming variables in the solution eliminating the requirement to know or make assumptions for their values.

MCNP modelling is currently being used to test and validate the development of the NSIM algorithms. Fig. 13 shows a 3D visual of a glovebox containing three process vessels surrounded by 18 polythene moderated He-3 neutron detector modules.

Modelling has shown the capability of NSIM to 'image' the alpha value. This has been trialled using models based on the analytical definitions of the totals and reals count rates given in Ref. [6].

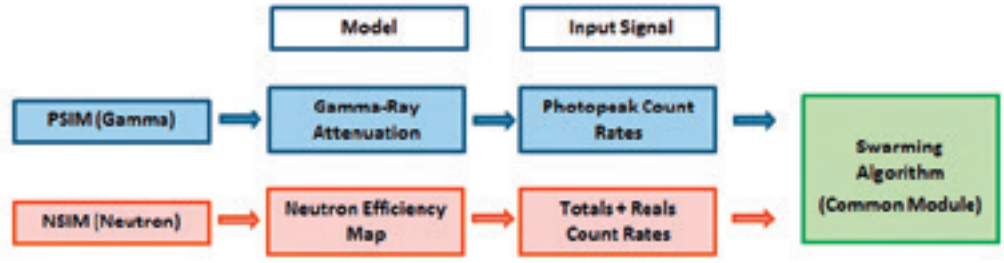

Figure 12: Module mapping between current PSIM algorithm and NSIM (Neutron Swarm Imaging)

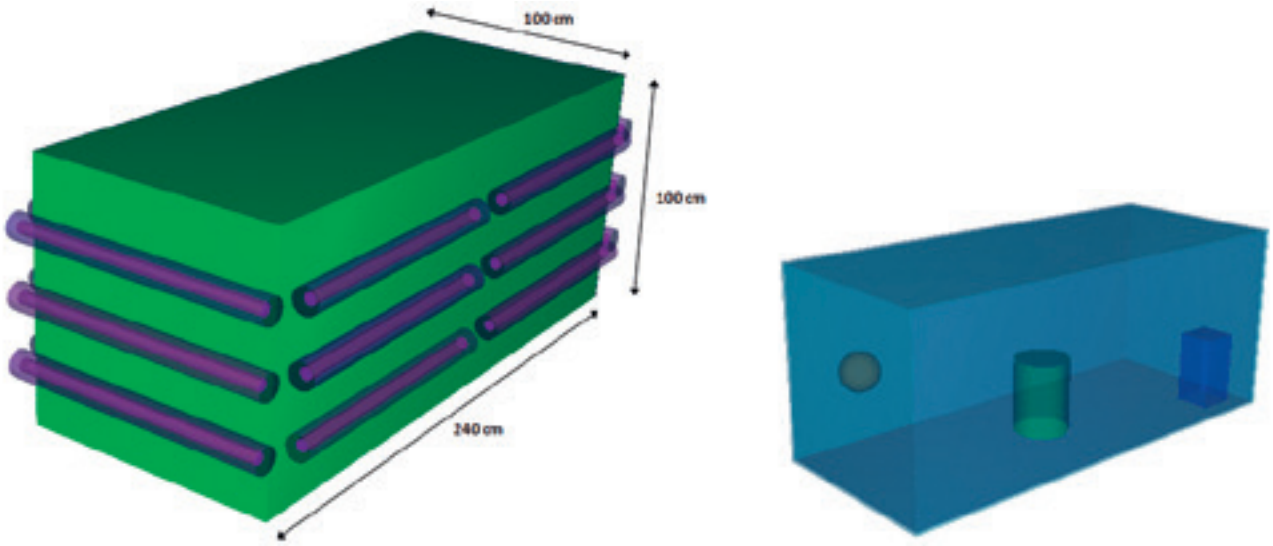

Figure 13: Example MCNP model used to validate the development of NSIM

Table 1 shows the results of a series of NSIM models based on the glovebox geometry shown in Fig. 13. For all three models a total of 500g Pu-240 effective mass was distributed throughout the three vessels and NSIM used to image the contents based on a measurement time of 60 minutes.

The 18 detector modules around the glovebox were grouped into 25 data channels (allowing NSIM to use 25 discrete count rates in the imaging process). Eighteen channels simulated the totals count rate on each detector, six data channels simulated the reals count rates (6 groups of three detectors) and a single data channel simulated the net reals rate for all 18 detectors.

For Model A, singles and doubles count rates were simulated based on an alpha value of 0.4. The alpha parameter was not included as a swarming variable (i.e. NSIM imaged the mass within the glovebox using the correct value of 0.4).

For Models B and C, the alpha value was included as a swarming variable for optimisation.

For Model B, singles and doubles count rates were simulated based on an alpha value of 0.4 and the NSIM value of alpha was constrained to lie between the values 0.2 and 10.

For Model C, singles and doubles count rates were simulated based on an alpha value of 5.0 and the NSIM value of alpha was constrained to lie between the values 0.2 and 100.

In all three cases NSIM yielded acceptable mass results (i.e. values exceeding the true mass of 500g Pu-240 effective) at the 65% and 95% levels of confidence. Furthermore, the calculated alpha values for Models B and C support the case for NSIMs capability to 'image' other variables other than position and mass.

An example of the NSIM fit to the modelled totals and reals count rates for Model A are shown in Fig. 14.

Parameter	Model A	Model B	Model C
Totals Count Rate (cps) [1]	6905.0 +/- 1.4		29593.0 +/- 2.9
Reals Count Rate (cps) [1]	31.7 +/- 1.6		31.7 +/- 7.0
'Best Estimate' Pu-240 equivalent mass (g)	497.4	502.6	388.4
Upper Pu-240 equivalent mass (g) @ 65% confidence	510.9	568.6	846.8
Upper Pu-240 equivalent mass (g) @ 95% confidence	526.0	598.8	968.4
Imaged 'alpha' value	N/A	0.39 +/- 0.14 (1s)	6.02 +/- 1.67 (1s)

[1] Equals the net count rate and 1s uncertainty for all 18 detector modules

Table 1: NSIM results for Models A, B and C

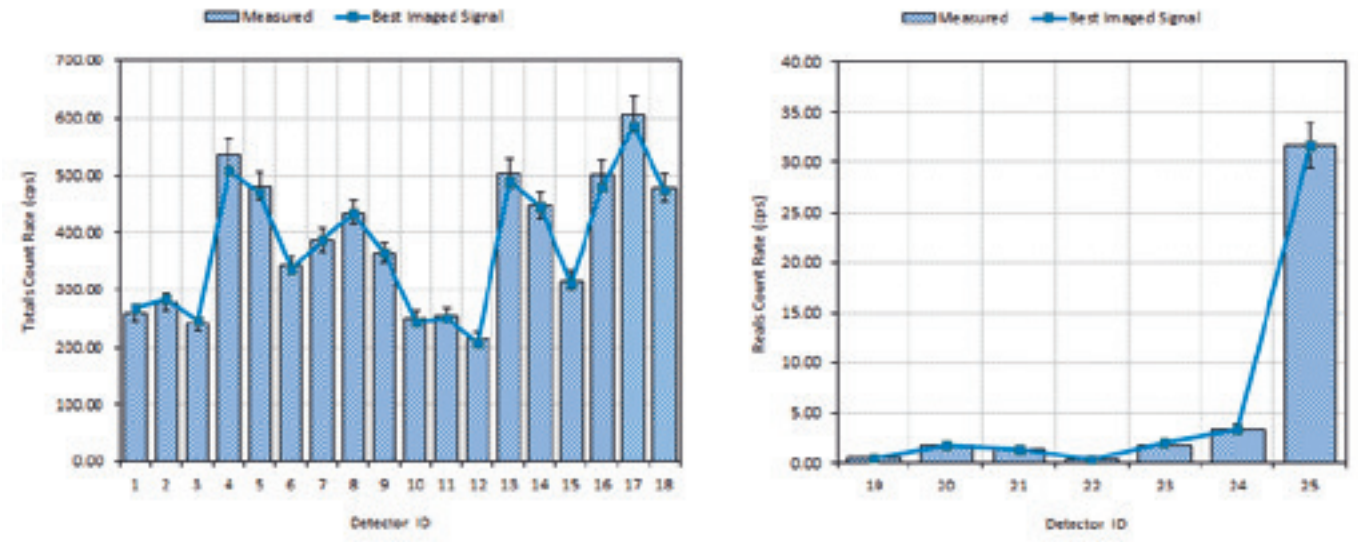

Figure 14: NSIM best 'fit' to the 25 data channels for Model A (Detector IDs 1- 18 representing the 18 'totals' count rates and IDs 19 – 25 the 7 'reals' count rates) used in the imaging (uncertainties shown at 1s).

Similar to the examples of gamma-ray imaging shown earlier, the 3D schematic shown in Fig.15 is an example of NSIM imaging the neutron emitting material in the three process vessels as well as, in the case shown, material located on the floor of the glovebox.

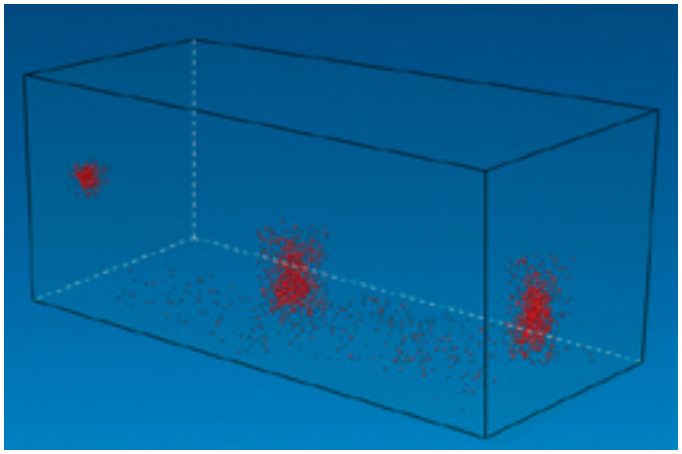

Figure 15: Example of NSIM imaging in process vessels and the glovebox floor (see Fig. 13)

NSIM is in the initial stages of development. The results are promising and the intention is to perform extended modelling trials using more complex models to develop and assess the potential limitations and performance as well as experimental trials using representative neutron standards to support its validation.

5. Summary

Particle Swarm Imaging (PSIM) is an innovative approach for performing gamma-ray assay.

PSIM overcomes some of the challenges associated with the accurate declaration of measurement uncertainties of radionuclide inventories within waste items when the distribution of activity is unknown. Implementation requires minimal equipment, making use of gamma-ray measurements taken from different locations around the waste item.

PSIM avoids the drawback of some conventional analysis methods, namely, the adoption of unrealistic assumptions about the activity distribution that inevitably lead to the declaration of pessimistic (and in some cases optimistic) activity estimates and uncertainties.

NSIM is being developed for the assay of neutron emitting material such as plutonium (stored in waste drums, crates etc.) as well as monitoring and verification of material in process plant such as gloveboxes.

The application of computational 'swarming' techniques to NDA measurements is considered novel. Other fields of NDA measurements and safeguards applications may benefit from a similar approach where other alternative optimisation strategies are being applied.

6. References

[1] D. Tattam, L. Keightly, "Radiometric Non-Destructive Assay", NPL Measurement Good Practice Guide No. 34, ISSN 1368-6550, 2012.

[2] J. Kennedy, R. Eberhart, (1995), "Particle Swarm Optimization", Proceedings of IEEE International Conference on Neural Networks. IV. pp. 1942–1948.

[3] D. Karaboga, B. Basturk, "A Powerful and Efficient Algorithm for Numerical Function Optimization: Artificial Bee Colony (ABC) Algorithm", Journal of Global Optimization, Volume 39, Issue 3, pp: 459–471, Springer Netherlands, 2007.

[4] A. R. Mehrabian, C. Lucas, (2006) “A novel numerical optimization algorithm inspired from weed colonization”, Ecological Informatics, Vol.1, pp 355-366.

[5] D. Parvin, “Particle Swarm Imaging (PSIM) - Innovative Gamma-Ray Assay”, 132497, WM2013 Conference, February 24 – 28, 2013, Phoenix, Arizona USA.

[6] N. Ensslin, W. C. Harker, M. S. Krick, D. G. Langner, M. M. Pickrell, J. E. Stewart, “Application Guide to Multiplicity Counting”, LA-13422-M, Safeguards Science and Technology Group, Los Alamos National Laboratory, Los Alamos, New Mexico, September 1998.

Monitoring Nuclear Facilities Using Satellite Imagery and Associated Remote Sensing Techniques

Marc Lafitte (marc.lafitte@satcen.europa.eu),
Jean-Philippe Robin (jean-philippe.robin@satcen.europa.eu),
European Union Satellite Centre, Apdo de Correos 511, E-28850 Torrejon de Ardoz, Madrid, SPAIN

Abstract

The mission of the European Union Satellite Centre (SatCen) is "to support the decision making and actions of the European Union in the field of the CFSP and in particular the CSDP, including European Union crisis management missions and operations, by providing, at the request of the Council or the European Union High Representative, products and services resulting from the exploitation of relevant space assets and collateral data, including satellite and aerial imagery, and related services" [1].

The SatCen Non-Proliferation Team, part of the SatCen Operations Division, is responsible for the analysis of installations that are involved, or could be involved, in the preparation or acquisition of capabilities intended to divert the production of nuclear material for military purposes and, in particular, regarding the spread of Weapons of Mass destruction and their means of delivery [2].

For the last four decades, satellite imagery and associated remote sensing and geospatial techniques have increasingly expanded their capabilities. The unprecedented Very High Resolution (VHR) data currently available, the improved spectral capabilities, the increasing number of sensors and ever increasing computing capacity, has opened up a wide range of new perspectives for remote sensing applications. Concurrently, the availability of open source information (OSINF), has increased exponentially through the medium of the internet.

This range of new capabilities for sensors and associated remote sensing techniques have strengthened the SatCen analysis capabilities for the monitoring of suspected proliferation installations for the detection of undeclared nuclear facilities, processes and activities. The combination of these remote sensing techniques, imagery analysis, open source investigation and their integration into Geographic Information Systems (GIS), undoubtedly improve the efficiency and comprehensive analysis capability provided by the SatCen to the EU stake-holders.

The following document aims at reviewing the benefits of the suite of sensors and associated remote sensing capabilities afforded with regards to the monitoring of nuclear facilities.

1. Introduction

The number and capabilities of space-based electromagnetic sensors has increased dramatically over the last four decades. Meanwhile, the huge leaps in computing power, associated technology and communications has strongly supported the development of a wide range of applications utilising satellite imagery. Currently, almost any part of the earth can easily be imaged in High (HR) or even Very High Resolution (VHR) through web applications. However, remote sensing techniques based mainly on the three pillars commonly called spatial, spectral and temporal resolution remains a specialist domain.

This paper aims to review the potential techniques based on electromagnetic measurements acquired from space-borne platforms to support EU decision makers regarding Non-Proliferation of weapons of mass destruction issues dealing mainly with material diverted from the nuclear fuel cycle.

The nuclear fuel cycle is the set of industrial processes which make use of nuclear materials in the production of electricity.

Most of these processes can be scrutinised and assessed using remote sensing techniques based on the analysis of satellite imagery [3].

Remote sensing is the art and science of obtaining useful information about an object or area acquired by a device that is not in contact with the object, area or phenomenon under investigation [4].

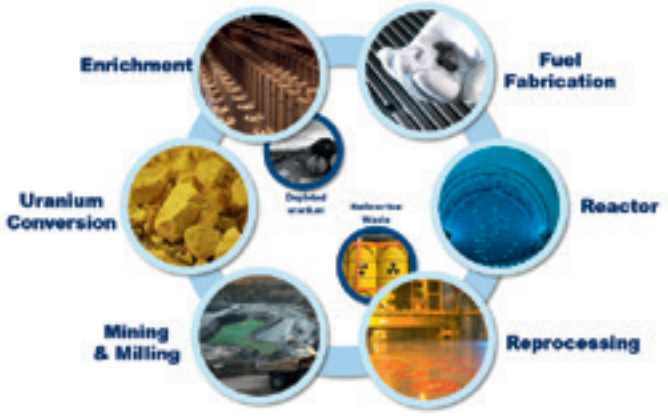

The first civilian remote-sensing sensor based on a space-borne platform launched on 23 Jul 1972, known as Landsat-1 (originally named ERTS-A -Earth Resources Technology Satellite) supplied satellite imagery with a ground sample distance (GSD) of 80 metres. [5].

However, military programs such as CORONA, the first US military satellite-based reconnaissance program, were already operating from August 1960 until May 1972.

Over the last decade, Hollywood movies have highlighted, and most of the time overstated, the abilities of satellite imagery.

Satellite imagery and associated remote sensing techniques are applied and analysed by humans. By nature this analysis is driven by a range of motivational and emotional factors which undoubtedly influence the processing of visual stimuli.

Our eyes do not send images to our brains. The images are constructed in our brain based on the very simple signals sent from our eyes. We only "see" after the brain has interpreted what was sent by the eyes. The human brain forms images based on pattern recognition learned from an early age.

2. The Sensors

Nowadays, more than 160 earth-observation satellites are commercially available worldwide [6].

Of the wide range of sensors available, the selection of the most suitable and efficient sensor is the key issue in order to broaden remote sensing techniques and to strengthen the analysis.

2.1 Space-based EO Sensors

Space-based sensors and in particular Electro-Optical (EO) sensors may be categorised by GSD capacity (Spatial resolution), electromagnetic capabilities (Spectral resolution) or revisit frequency abilities (Temporal resolution).

- Spatial Resolution is "a measure of the finest detail distinguishable in an image". The most commonly used descriptive terms for spatial resolution is the ground sample distance (GSD). It is commonly agreed on the following scale of spatial resolution
  - Low Resolution: larger than 30 m
  - Medium Resolution: 2 - 30 m
  - High Resolution: under 2 m
  - Very High Resolution: sub-metre
- The Spectral Resolution of the sensor is based on the number of bands, their location on the electromagnetic spectrum and how narrow the bands are. Spectral resolution is commonly applied to EO sensors, optical and infrared, which measure reflected or radiated energy. Panchromatic sensors acquire data from a single broad region of visible light, and sometimes also from the adjacent near-infrared of the electromagnetic spectrum. Multispectral sensors are capable of acquiring simultaneously from 3 to 10 wider bands while hyperspectral instruments can capture hundreds of narrow bands.
- The Temporal Resolution specifies the revisit frequency of a satellite sensor for a given location. It is commonly agreed on the following scale:
  - High temporal resolution: < 24 hours - 3 days
  - Medium temporal resolution: 4 - 16 days
  - Low temporal resolution: > 16 days

High temporal resolution is significantly enhanced by the capability of on-board sensors to point both along and across the satellite track, providing a revisit capability of 1 to 3.5 days, depending on latitude. A constellation of satellites can also considerably shorten the revisit period.

2.2 Space-based SAR Systems

The Synthetic Aperture Radar (SAR) is an active and coherent sensor working in the microwave domain of the electromagnetic (EM) spectrum. It collects the backscatter signal of an electromagnetic wave. This electromagnetic wave is characterized by two fundamental properties: amplitude and phase.

- The amplitude is a function of backscattered energy displayed as intensity ($I = A^2$) and can be considered as the "visual" part of the information. The behaviour of the backscattered electromagnetic energy depends on the interaction between the electromagnetic wave and the physical and dielectric properties of the target; the roughness and the moisture. Some materials such as metal have a high reflective quality while other such as grass have a poor capacity to reflect incidental energy.
- The phase is a property of a periodic phenomenon which is the fraction of one complete sine wave cycle (from $-\pi$ to $+\pi$) corresponding to the wavelength. It is a key element for the estimation of displacement (sensor-to-target distance) and thus used for interferometric measurement. The analysis of differences between phases of reflected radiation is called interferometry. There are two main possible sources of phase shift: vertical (terrain altitude) and horizontal (terrain motion).

The processing of the backscatter signal collected by the multiple antenna locations which form the synthetic antenna aperture allows the formation of a matrix of pixels in two dimensions: range and azimuth (cross range).

Space-borne SAR sensors use L, C or X-band and most of them are able to emit and receive with various polarizations (multi-polarization). These bands provide different spatial resolution and moreover a range of capabilities regarding ground and foliage penetration.

On 17 July 1991, the first Earth-observing SAR platform, the European Remote Sensing satellite (ERS) was placed into orbit. Since 03 April 2014, Sentinel-1A operates in the C-band and provides Copernicus, the European Programme for the establishment of a European capacity for Earth Observation, with SAR imagery/data at medium resolution [7].

3. Remote Sensing & Image Analysis

3.1 Analysis of Multi-Spectral Imagery

Despite a low spatial resolution, the Terra (Aster) and Landsat series are particularly useful space-borne sensors for multi-spectral analysis. The capability to simultaneously collect radiation from multiple narrow wavelength bands, in particular the reflected infrared (including near infrared "NIR" and shortwave infrared "SWIR") of the electromagnetic spectrum, enhances the ability to discriminate and characterise a wide range of natural elements which, by nature, have different spectral reflectance signatures.

This technique is particularly useful for the characterisation of soils by the discrimination of various minerals (eg. Uranium mines) or the classification of a range of vegetation/crops.

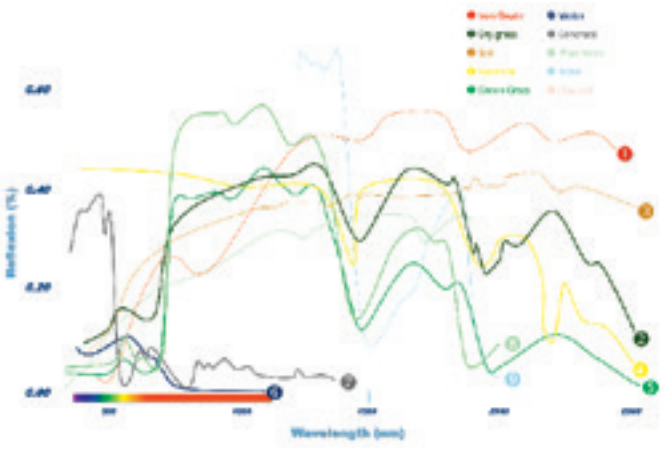

Amongst other wavelength bands, most high-resolution multi-spectral sensors provide at least one spectral band in the NIR, relevant for the analysis of vegetation stress or diseases by using NDVI techniques.

To a further extent, NIR bands are also frequently used to highlight moisture or vegetation growing on the roof of workshops, a main indicator for a derelict status.

WorldView-2 provides high-resolution 8-band multispectral imagery of which [8]:

- Red-Edge spectral band (705-745 nm) improves the accuracy and sensitivity of NDVI and plant studies. It can also enhance the discrimination between healthy vegetation, and those impacted by disease.

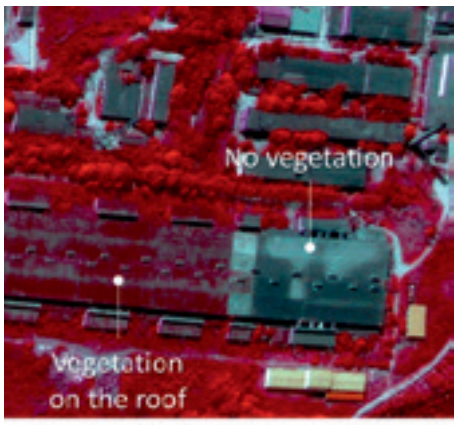

- Coastal Blue band (400-450 nm) strengthens the capabilities for "bathymetric" measurements. In addition, the absorption of this wavelength by chlorophyll in healthy plants may improve vegetation analysis.
- Yellow (585-625 nm) band enhances vegetation classification capabilities.

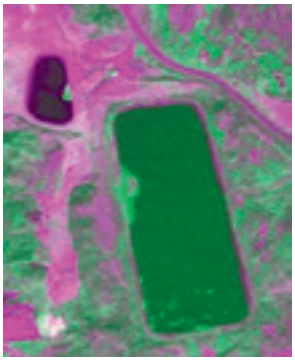

These spectral bands can also be very useful in determining the density and/or turbidity analysis of liquid ponds as well as demonstrating vegetation stress caused by toxic gas release or fire.

3.2 Use of Thermal data

The infrared (IR) wavelengths of the spectrum, lie between 1µm and 14µm and can be further broken down into two sub-domains respectively: the reflected infrared (1µm to 2.5µm) and the thermal infrared, also called TIR (3µm and 14µm). Due to atmospheric absorption windows, TIR is generally measured over two wavelength extents: 3µm - 5µm and 8 µm to 12 µm.

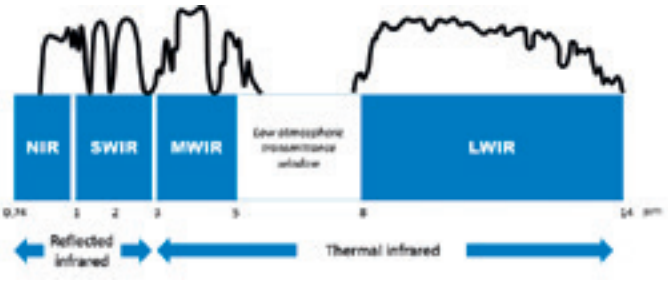

Terra (Aster) and Landsat series (Landsat 7 and 8) space-borne sensors acquire low spatial resolution (respectively 100 m, 60 m and 120 m GSD) temperature data between 8 µm and 12 µm.

In remote sensing, the radiance measured (radiant temperature) by thermal radiometers in the TIR are firstly

converted into Digital Numbers (DNs) and subsequently to degrees Kelvin (Kinetic heat). The derived estimated surface temperature map is a significant asset for the analysis and assessment of various processes within the nuclear fuel cycle.

KOMPSAT-3A (Arirang 3A), successfully launched on 26 Mar 2015, hosting among other sensors an Infrared Imaging System (IIS) operating over the 3 μm - 5 μm wavelength region at high spatial (5m GSD) and thermal resolution [9]. Until now this type of imagery has not been commercially available. It will provide the community with a tremendous improvement in capability, in particular for the detection and monitoring of local processes where, for example, heat/steam is generated/inducted.

The use of the longer wavelengths of the infrared domain avoids anomalies from solar reflection and also therefore allows for the use of imagery collected by night.

3.3 Processing and Analysis of SAR Data

Synthetic Aperture Radar (SAR) is a coherent system. SAR images comprises of complex data which contains both amplitude and phase information.

A series of specific techniques are commonly used by SatCen image analysts to extract information from SAR data.

The analysis of single SAR data requires a lot of experience and a good understanding of SAR geometry regarding phenomenon such as layover, foreshortening, shadowing and texture. The visualisation (display) of the full range of SAR dynamic data is one of the main challenges. The SatCen routinely uses coloured dynamic look-up tables (LUT) and in particular the rainbow colour display. This coloured image enhances the analysis of high reflected radiation as well as features which do not reflect any, or very poor, radiation.

The Amplitude Change Detection (ACD) technique consists of comparing at least two examples of SAR data acquired using similar orbit and frequency parameters on different dates. The amplitude data is co-registered before being respectively assigned to the corresponding colour channel (Red, Green and Blue). Thus, changes appear according to the colour synthesis model defined.

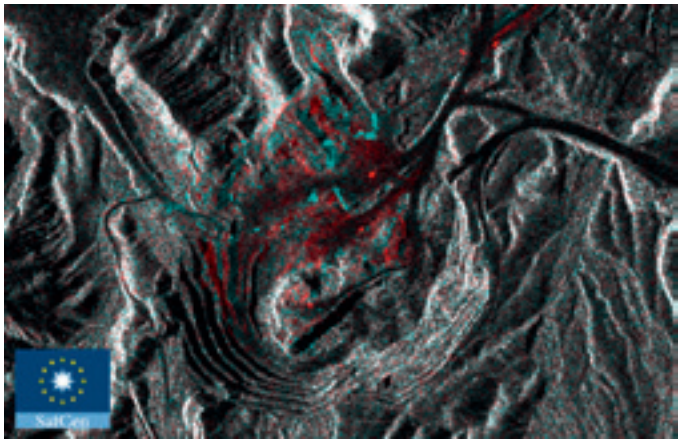

The monitoring of nuclear-related nocturnal activity is one of the main application of amplitude SAR data at the SatCen.

However, the analysis derived solely from SAR amplitude imagery can only provide assumptions and therefore requires confirmation by electro-optical analysis.

One of the main advantage of SAR system is of being independent of atmospheric and sunlight condition. Moreover, SAR signal have a high level of phase coherence [11]. Therefore when two or more examples of SAR data have been collected along identical orbits with similar acquisition parameters, commonly known as interferometric acquisition conditions, a coherence map derived from the processing of a SAR interferometric pair can be generated. The Coherence Change Detection (CCD) techniques highlight coherence losses mainly due to structural changes between the two acquisition dates. It is particularly relevant for the monitoring and the activity assessment of large uranium mines.

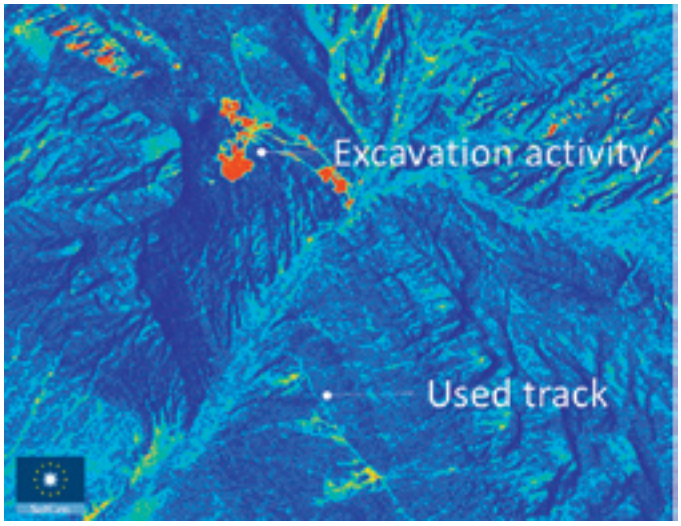

The Multi-Temporal Coherence product combines the two previous techniques. It consists of the combination of two multi-temporal amplitude images and the corresponding computed coherence image. Each image is assigned to one of the colour channels (Red, Green and Blue). The MTC image highlights changes between two states of a target which appeared unchanged by ACD analysis. This technique is particularly relevant when surveying large storage areas (UO2 or UF6 casks) and often use to complement the CCD technique.

Ground-surface deformation phenomena induced by underground development may be detected using a Synthetic Aperture Radar differential interferometry subsidence

map. Subsequent interferograms, formed by patterns of interference between the phase components of two SAR data acquired from the same orbit with slightly different incidence angle and at different times, provides high-density spatial mapping of ground-surface displacements. Under ideal conditions, it is possible to resolve changes in elevation in the order of a few millimetres.

Amongst the differential interferometric techniques [10], the permanent or persistent scatterer interferometry (PSI) [12] may provide evidence of tunnelling or ongoing underground activity. However, the amount of SAR data required for input to process and produce an accurate and reliable subsidence map, as well as the timeline for the acquisition of the required dataset, means that this technique is not very well suited for time sensitive operational usage. In addition, natural changes due to vegetation or seasonal variation will denigrate the relevant results. Thus, differential multipass Synthetic Aperture Radar Interferometry (DInSAR) is a technique useful for accurately detecting and estimating the ground displacement or land deformation. In this case, the phases of less SAR data (3 to 5), acquired from slightly different orbit configurations at different times, are combined in order to exploit the phase shift of the signals and compute a surface displacement map.

From the range of space borne SAR platforms available, the Italian COSMO-SkyMed constellation provides the SatCen with the most relevant advanced SAR capabilities, particularly regarding the high revisit frequency which allows relevant interferometry products [13].

3.4 Analysis of Multi-Temporal data (Monitoring/survey)

The accuracy of the assessment of a nuclear facility using remote sensing is based mainly on the capability to detect nuclear facilities at the earliest stage of construction. The foundations of the various constructions, the network of underground utility ducts, the internal layout and structure of the main buildings are crucial for the analysis of the facility.

Subsequently, the monitoring of a nuclear facility is driven mainly by the revisit capability commonly referred to as temporal resolution and the availability of the sensor.

Once the facility is operating, the analysis of the status of the facility from satellite imagery relies on indirect indicators of activity such as vapour plumes, efflux, liquid output, cooling fan rotation, vehicle activity, maintenance activity, damage, etc.

As an example, the analysis of snow covered imagery may reveal human activity, vehicle tracks, heat, etc.

The low solar incidence during the winter period provides extended shadows which can significantly enhance the analysis of vertical features.

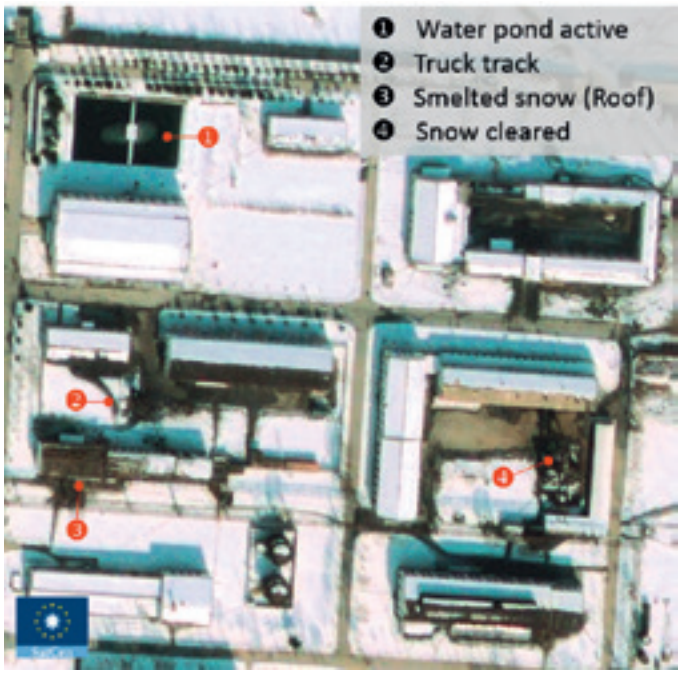

The monitoring of infrastructure and the analysis of changes can be visually strengthened by the processing of anaglyph views formed from two satellite images taken with slightly different angles. The image acquired with the larger incidence is assigned to the red-colour channel while the other imagery is allocated to the two remaining colour channels. This combination will create the illusion of relief and can be seen using bi-coloured lens glasses commonly RED/GREEN or RED/BLUE.

Monitoring data sets including heterogeneous sensor, viewing angle and season, can also be used to create 3D modelling [14]. The 3D models derived from satellite imagery provide the analyst with a more realistic contextual view of specific features.

3.5 Use of Digital Elevation Model (DEM)

An accurate Digital Elevation Model (DEM) can be obtained from the processing of an interferometric data pair as well as from an optical stereo-pair and can be used for the 3D rendering of an optical satellite imagery. This product provides the image analyst with an enriched contextual insight

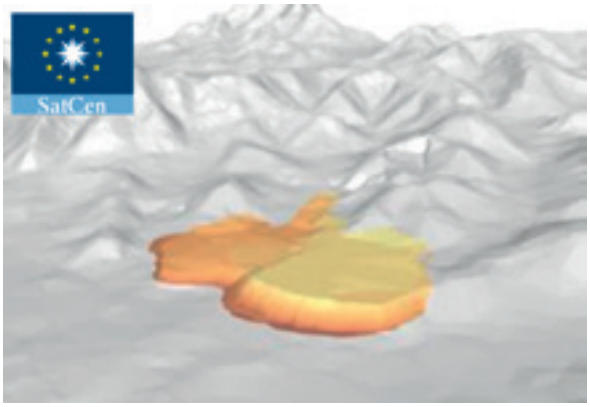

and a more realistic and natural perspective of the area of interest (AOI).

Furthermore, the difference between two DEMs may also be used to estimate volume variation, in particular in assessing spoil from underground extraction over a specific time period.

3.6 Open Source

Open Source Information (OSINF) includes any piece of information which can be obtained legally and ethically from public sources.

The amount of information or data available has grown exponentially over the last decade and new techniques are required nowadays in order to investigate the tremendous volume of data and be able to extract only the useful and relevant pieces of information.

Data Mining is a process which consists of analytical tools capable of exploring and analysing data from varying perspectives by investigating correlations or patterns amongst predefined key values.

As an example, the report which followed the visit to the Yongbyon Nuclear Complex on 12 Nov 2010 by Standford University experts provided, amongst other pieces of information, a detailed description of the “Uranium Enrichment Workshop” layout. The “transcription” of this textual depiction into a 3D model, based on satellite imagery along with knowledge of the current techniques for enrichment has provided the SatCen with a far greater understanding of the facility [15].

However, the reliability of open source information is an issue and all sources must be cross-checked and/or verified to become effective. Open source information which is knowingly biased, falsified or perverted is called deception. Over the recent years, the spread of false, edited or mocked-up pictures and imagery has become commonplace. Something as simple as the manipulation of the acquisition date (or time) of one satellite image may cause an entirely inaccurate assessment. In addition, the falsification of imagery is also widely used to serve propaganda or doctrine dissemination purposes.

The SatCen dedicates significant effort when using satellite imagery and open source information, in order to corroborate and verify reliability and accuracy across the whole range of data used.

4. Conclusion and Way Ahead

The significant number of earth observation satellites placed into orbit for the last two decades, and the ensuing deterrence of steady overhead surveying, has not refrained the ambition of some states to develop or pursue undeclared or illicit nuclear programmes.

Although satellite imagery and subsequent remote sensing techniques will never supply all the relevant information required for the assessment of nuclear facilities, and moreover of undeclared facilities, the number of space-borne platforms, the progress in sensor techniques and the development of a range of applications described in this paper should contribute profoundly to a more comprehensive analysis.

The synthesis of the range of information acquired over various part of the electromagnetic spectrum, as well as the synergy of the remote sensing proficient techniques including Geospatial Information Systems (GIS) strengthen the SatCen’s capabilities while assessing potential proliferation facilities. Subsequently this is of benefit to the EU stakeholders by providing reliable arguments and evidence.

The development of remote sensing techniques and in particular emerging novel space-borne sensors will most likely offer new favourable perspectives.

The space borne platforms delivering High-Definition video sequences (Up to 90 seconds) already commercially available, will very soon provide multiple intra-daily acquisitions capabilities (eg. SkyBox constellation) while in the upcoming years (2025+) high resolution (HR) imagery from geostationary platform would improve (ESA study) scrutinize potential. In addition, medium-resolution (MR) hyperspectral sensors such as EnMAP (Environmental Mapping and Analysis Program), planned for 2018 and capable of collecting hundreds of narrow bands from 420 nm to 2450 nm with a spatial resolution of 30 m, will provide the community with an unprecedented capability to detect specific gases released during the different steps of the nuclear fuel cycle and also to distinguish a large collection of materials.

Finally, innovative technology such as Big Data will be needed to investigate the huge amounts of data for the extraction of valuable and relevant information (http://big-project.eu).

References

[1] Council Decision 2014/401/CFSP of 26 June 2014 on the European Union Satellite Centre and repealing Joint Action 2001/555/CFSP on the establishment of a European Union Satellite Centre

[2] European Council strategy against proliferation of Weapons of Mass Destruction - 15708/03 EU - 10 Dec 2013

[3] "From the mining of uranium to the disposal of nuclear waste" - IAEA

[4] Remote Sensing and Image Interpretation - Lillesand and kiefer, 1979

[5] http://landsat.usgs.gov

[6] Union of Concerned Scientists (UCS) "UCS Satellite Database" - http://www.ucsusa.org/

[7] SENTINEL-1 ESA's Radar Observatory Mission for GMES Operational Services - SP-1322/1 - March 2012

[8] WorldView-2 data sheet, Sep 2014- https://www.digitalglobe.com/

[9] AIM-Space Cryocooler Programs M. Mai, I. Rühlich, A. Schreiter, S. Zehner

[10] InSAR Principles: Guidelines for SAR Interferometry Processing and Interpretation – ESA, Feb 2007

[11] Robust techniques for coherent change detection using CSK images – A. Bouaraba, D. Closson and al., 2012

[12] Permanent scatterers in SAR interferometry. – A. Ferretti and al. - 2001

[13] The COSMO-skymed very high resolution SAR satellites constellation for Earth observation and its applications in support of monitoring activities - L. Pietranera,F. Britti - e-GEOS, Rome, Italy

[14] www.sketchup.com

[15] A Return Trip to North Korea's Yongbyon Nuclear Complex - Siegfried S. Hecker - Center for International Security and Cooperation - Stanford University, 20 Nov 2010

Modelling Seismic-Signal Propagation at a Salt Dome for Safeguards Monitoring

Jürgen Altmann

Experimentelle Physik III, Technische Universität Dortmund,
44221 Dortmund, Germany

Abstract:

The potential of seismic methods for detecting undeclared activities in/near an underground repository is an area of high interest for the German Support Programme to the IAEA. An experimental and theoretical focus is on salt since this is the best-investigated potential repository medium in Germany. After measurements of seismic and acoustic signals from various mining activities in a salt dome 2010 - 2012 the follow-on project is dealing with modelling of the propagation of seismic signals from relevant sources to potential sensor positions. Model structures resembling a part of the salt dome and meshes covering it were constructed by "sweeping" a two-dimensional cross section through the third dimension. For the seismic parameters of the various strata typical values were used; attenuation was modelled by quality factors constant with frequency. The three-dimensional propagation was computed by the program SpecFEM3D on the LiDO computer cluster of TU Dortmund. The source was put at the centre of the potential repository or at potential access pathways from above or the side. To simulate blasts a seismic-moment step function was used, picking and other sources were modelled by force impulses. Seismic signals were gained at many positions, underground and at the surface. The signals did not differ much if the sweeping method was varied. For the repetitive sources blasts and picking the single-pulse signals were superposed with appropriate delays. By fitting model amplitudes to measured ones preliminary assessments of source strengths were done. For intrusion detection more sensors were used, but those too close to the potential repository were not considered. The signal strength decreased roughly in proportion to the inverse squared distance. If a threshold is given, a detection range can be estimated that in turn would allow conclusions on the required spacing and number of the sensors.

Keywords: final repository, salt, seismic monitoring, seismic modelling

1. Introduction

Without reprocessing spent nuclear fuel contains plutonium, thus such material should remain under IAEA safeguards even after emplacement in an underground final repository. This presents a new challenge for monitoring; geophysical techniques and methods have been proposed for this task [e.g. 1-5]. During operation, the creation of undeclared cavities needs to be detected, and those parts of the mine already filled with refuse have to be kept under surveillance for undeclared re-opening. After the emplacement phase, when drifts and shafts will have been closed, and the above-ground parts of the final repository will have been cleared for other uses, the IAEA needs the capability of long-term monitoring for covert access to the repository.

One potential technique is seismic sensing. Mining and other underground operations produce vibration directly as well as via acoustic noise. Seismic excitation propagates through the ambient medium and can thus be used to detect activities at a distance. The main question with seismic monitoring is whether signals from undeclared activities can be separated from signals from other sources and from background noise. In the operational phase of the repository most noise stems from the normal activity (mining, transport, filling, etc.), and sensors can be deployed at many sites in the mine. After closure, no sensors and cables can remain in the repository [e.g. 5: 22]; in this phase sensors

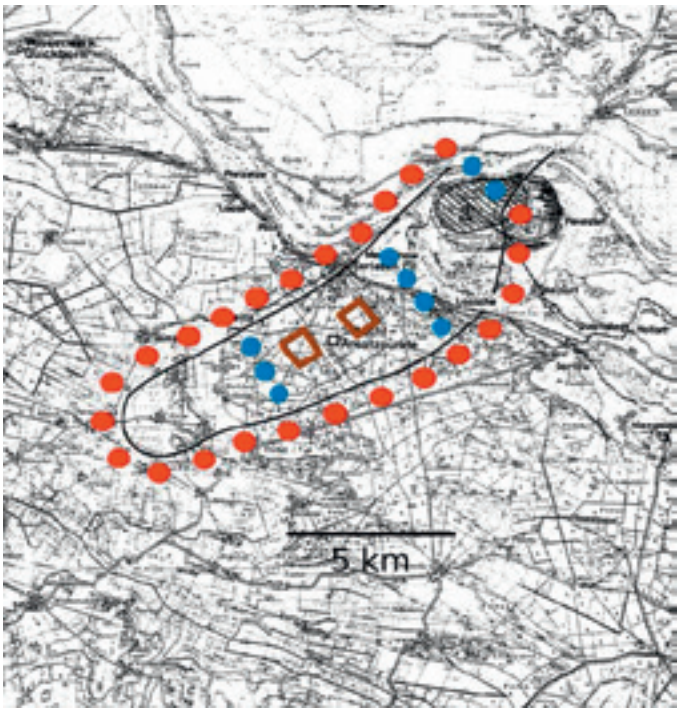

Figure 1: Notional possibilities for placement of seismic sensors after a possible emplacement phase in Gorleben, avoiding the planned repository volume at around 900 m depth (brown/light-grey quadrangles) in the salt-dome centre. Blue/light-grey dots: in the salt dome, red/dark-grey dots: surrounding it. Additional positions could be underground hundreds of metres above the repository, and possibly at the surface. (Based on BfS map)

need to be located at some distance, but still underground in order to reduce seismic background, produced by traffic, industry, agriculture and weather at the surface.

The German Support Programme to the IAEA has since many years taken an interest in seismic monitoring for final-repository safeguards. One potential repository site in Germany is the Gorleben salt dome (Figure 1); it was explored for its usability since 1986 under contract to the Federal Office for Radiation Protection (BfS). Following the new German Site Selection Act (Standortauswahlgesetz) of 2013, exploration has been stopped, but in the new search for an optimum repository medium and site, Gorleben remains an option.

Should this site be selected, the repository would be built at around 900 m depth in the centre of the salt dome (Figure 2). To detect undeclared activities in the vicinity, mainly new excavation, a monitoring system would use a sensor "fence" around the repository (Figure 1), with sensors and cables at safe distances from the backfilled and sealed shafts and tunnels. While sensors at the surface could contribute, they would suffer from relatively strong background noise from natural as well as artificial sources. For higher detection sensitivity most sensors would be deployed underground, at several hundred metres depth, laterally around the repository, outside and inside of the salt dome. In addition, underground positions above the repository, at shallower depth, could be used.

In order to gain information on the properties of seismic signals from mining activities, a dedicated measurement project had been carried out 2010-2012 at Gorleben, tasked by the German Support Programme to the IAEA [6, 7]. Many sources were measured with seismic and acoustic sensors deployed at various positions in the exploratory mine and at the surface. However, underground positions outside of the mine or even outside of the salt dome, as they would be used for seismic monitoring, could not be covered.

To find out the actual strengths and other properties of the signals from mining activities at such positions, measurements are needed, but these require expensive drilling that could be done only at very few test sites. As a prior step, a modelling project was done from August 2012 to June 2015, again tasked by the German Support Programme to the IAEA. This article presents the most important results, more detail will be given in a JOPAG report.

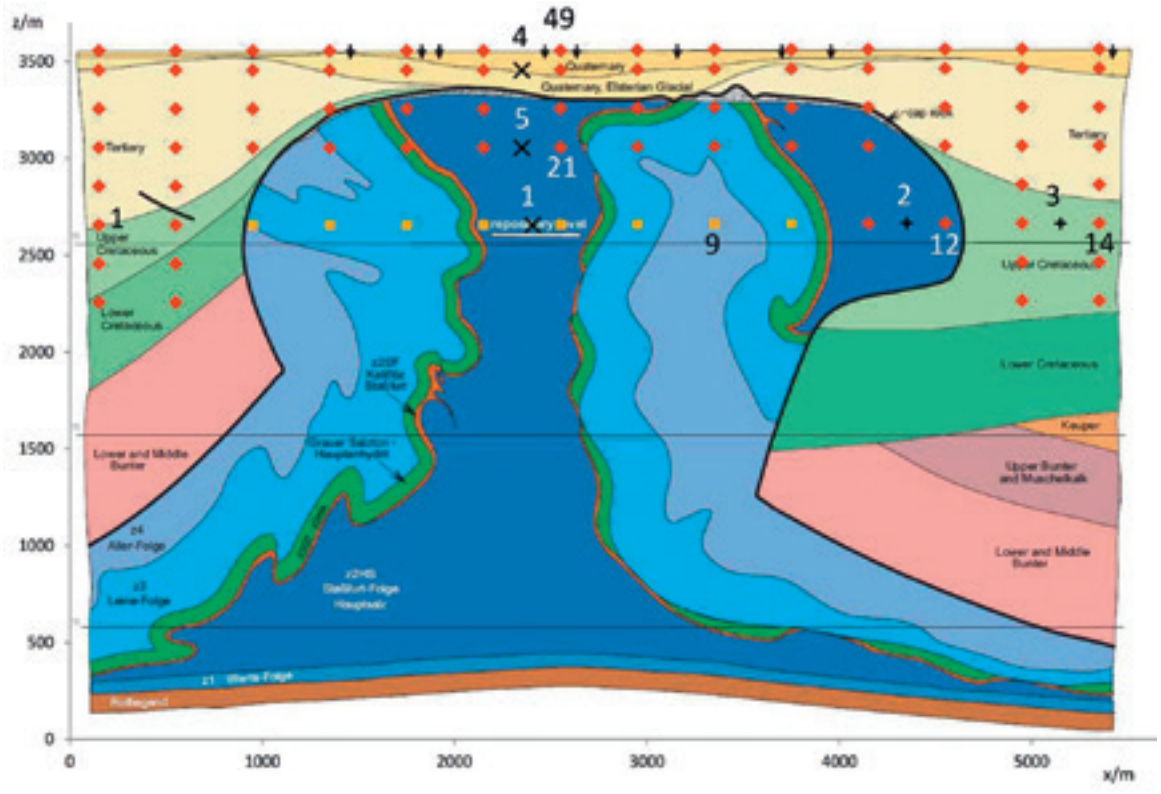

Figure 2: Simplified geological cross section in NW-SE direction through the salt dome. A possible repository level at about 930 m depth is indicated. The x and z axes of the chosen co-ordinate system are shown, the y axis points into the section plane. The section measures 5.52 km in the x and 3.57 km in the z direction, respectively. x is roughly south-east. Shown is the centre plane at y = -500 m. Source positions are indicated (x Positions 1, 4, 5 in this plane, + Positions 2, 3 projections from y = -200 m). Red dots denote the sensor positions, numbers 1, 9, 12, 14, 21 and 49 are indicated. To not mask the positions at 100 m depth, the ones at 150 m are not shown, including Position 35. Yellow squares denote the sensor positions at 900 m depth that are too close to the potential repository. Whether the corresponding positions at 500 m depth could be used is questionable. The same sensor arrangement is used in the parallel planes at y = -900 m, -700 m, -300 m and -100 m. To prevent too small mesh elements, the z2SF layer was removed and some valleys in the cap rock were smoothed. (Based on Figure 36 in [11], used by permission.)

2. Modelling programs

Because the salt dome and its surroundings have a complicated structure, numerical computations were needed. For this the spectral-finite-element code called SpecFEM was used, it has been developed for numerical simulation of seismic-wave propagation in heterogeneous and anisotropic media [e.g. 8, 9]. This open-source program [10] is widely used in the seismological community. It is very efficient, with boundary conditions included. Attenuation can be incorporated by quality factors constant with frequency.

After a two- or three-dimensional structure was set up e.g. in AutoCAD, it was transferred as an ACIS file to the commercial program Trelis (formerly CUBIT) [11] which was then used to produce a mesh of quadrilaterals or hexahedra, respectively, to assign seismic properties to the partial volumes and to combine those belonging to the same geological stratum to blocks. Several programs, part of the SpecFEM2D or SpecFEM3D packages, then separated the geometry into parts, one for each processing node to be used, and built the respective data-base files of mesh nodes and the associated seismic properties.

While two-dimensional propagation was run on a single Linux PC with a 4-core CPU, three-dimensional computations were done on mostly 340, sometimes 256 or fewer processors of the LiDO computing cluster of Technische Universität Dortmund [12]. The processing time depended on the number of mesh elements and the modelling duration, of course. Running the model for 2 seconds on 340 processors for 100,000 time steps of 0.02 ms required around 1 hour in case of about 420,000 elements (intended mesh-element size 40 m) and around 40 hours (close to the limit of 48 h with such a number of processors) with 5.5 million elements (intended size 15 m) (see also Table 1 below).

3. Model structures, meshing

For realistic simulations of seismic propagation, in principle knowledge of the full three-dimensional structure of the underground would be needed, at a resolution comparable to the size of the mesh elements, on the order of 10 m. However, this information was not available throughout the salt dome – the data that were provided by the Bundesanstalt für Geowissenschaften und Rohstoffe (BGR, Hannover) comprise several horizontal and vertical planes only [see e.g. 13]. As a consequence it was decided to proceed from the simplified geological cross section of the salt dome and its surroundings shown in Figure 2, and extend it along the salt-dome axis (y) direction. The cross section was converted to an AutoCAD file describing the boundaries of the 16 media involved. To avoid too small elements, one thin and curled layer had to be removed and one media boundary had to be smoothed somewhat.

A first three-dimensional structure was built by joining the 15 remaining media of the cleaned cross section to four: base rock, salt, adjoining rock and overlying rock. This was then swept orthogonally, in the -y direction, by 1.0 km (Figure 3). A better approximation to reality was to keep the 15 media and sweep the full structure along the same orthogonal vector of the same length. This kept the different structures in the salt as well as in the adjoining rock that – even though the differences in wave speeds and densities are small – give rise to reflection. But this structure shows identical x-z cross sections at all y co-ordinates, and the media boundary surfaces are flat in y direction. As a consequence, specular reflection could occur over relatively large media-boundary areas.

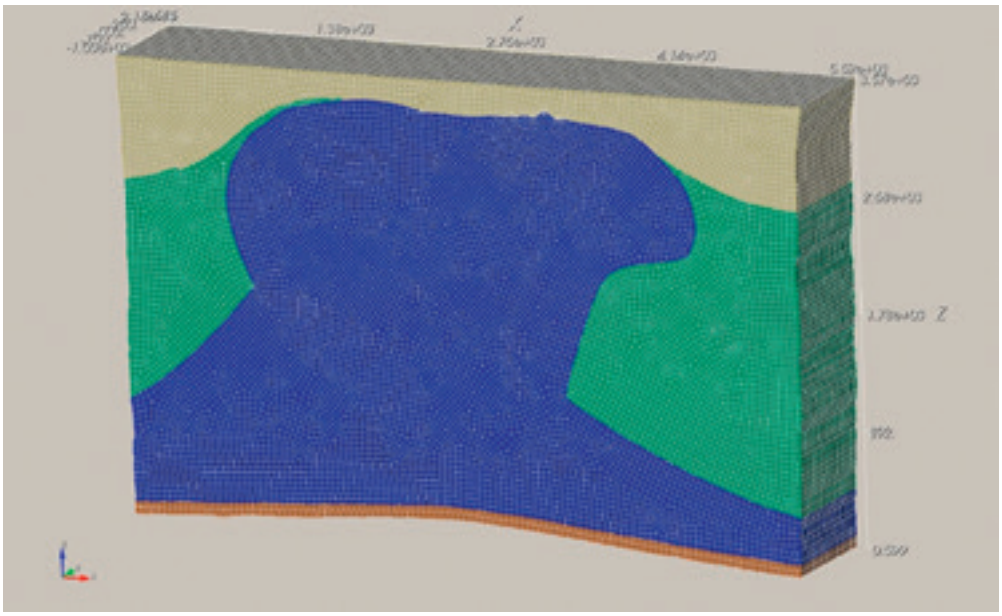

Figure 3: Three-dimensional underground model where the strata of Figure 2 have been united to form four partial blocks and the result has been swept in -y direction by 1.0 km, here with a mesh of 40 m intended element size.

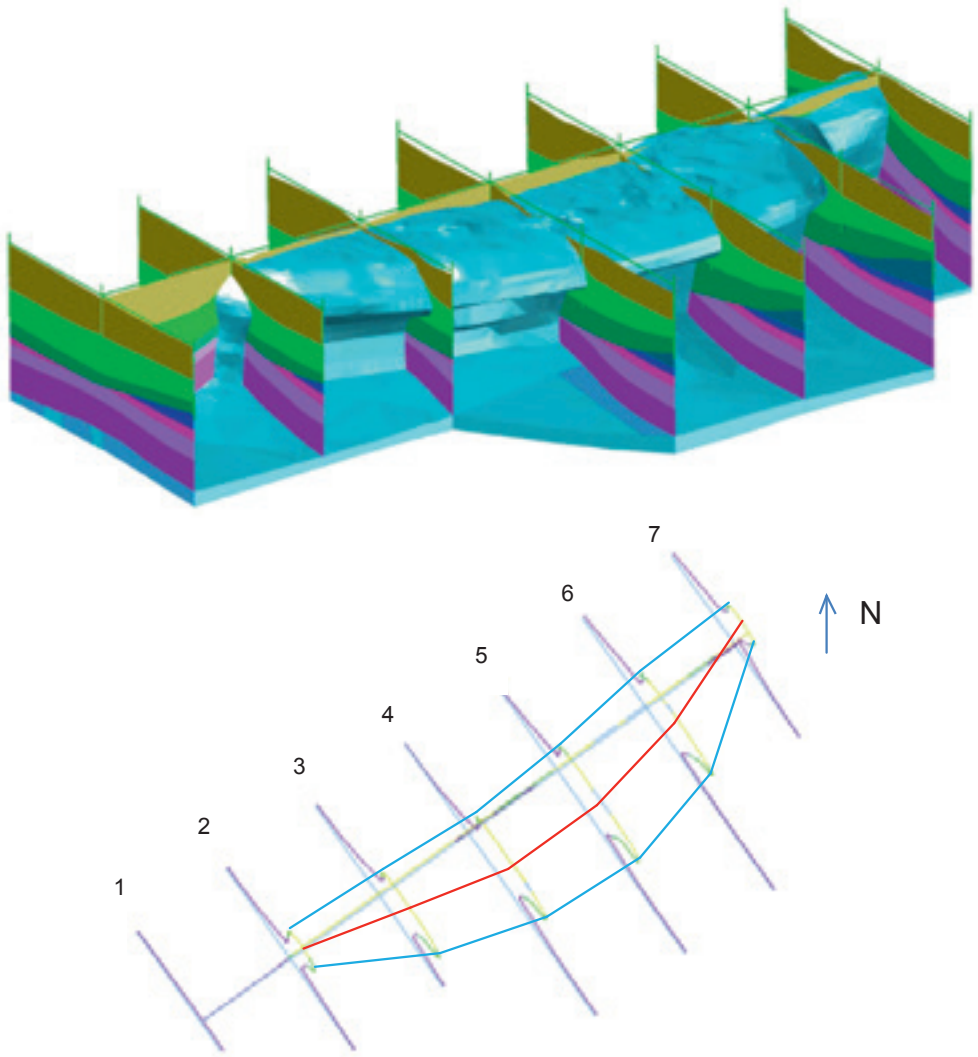

Figure 4: Salt-dome hull and adjoining layers.
Top: View of the salt-dome hull, looking roughly north, and the surrounding layers in various sections.
Bottom: Vertical sections through the outer salt-dome surface, seen nearly from vertically above. The cross section of Figure 2 is close to Section 5, the exploratory mine is between Sections 4 and 5. The extent of the salt-dome bulge is marked, the red line connects the respective centre points. Along these points a spline was constructed to guide the sweeping of the two-dimensional cross section that started at Section 5 and went to Section 2.
(Produced from BGR data)

To achieve curved boundary surfaces that better represent the actual salt-dome shape, the two-dimensional cross section was swept along a three-dimensional spline that went through the centre points of seven sections through the salt dome (Figure 4). Unfortunately, the form and size could not be changed during the sweeping. To limit the number of mesh elements, the resulting structure of 9 km length was cut to 1 km length (Figure 5).

Meshing by the Trelis program was done first in two dimensions, applied to the media surfaces at Section 5. This was then extended towards the respective surfaces on the opposing margin of the model. One has to define an intended mesh-element size; the program then adapts the shape and size of the mesh elements so that the elements fit to the media boundaries. Table 1 shows the resulting number of elements if the intended size is varied between 40 and 10 m, for the three structures: 4- and 15-media models, swept along an orthogonal vector, and 15-media model, swept along the spline. It is evident that the actual element size varies significantly as the mesh accommodates the shapes of the various media boundaries. Similarly the distances between the so-called Gauss-Lobatto-Legendre (GLL) points (there are 5^3 GLL points in each mesh element), where the various properties are to be computed,[8] vary markedly.

After a mesh was built its quality was assessed, using the distribution of characteristics such as skew and shape. For an acceptable mesh, the former should be below 0.8, and the latter above 0.2 for (nearly) all mesh elements [10, 11]. This was fulfilled strictly for 15 m intended size and below, but for 20 m and 40 m the share of elements with worse characteristics was very low.

The last row of Table 1 gives the approximate run time for 1 second of model time using 340 processors and a 0.02 ms time step. Because about 2 s of model time are

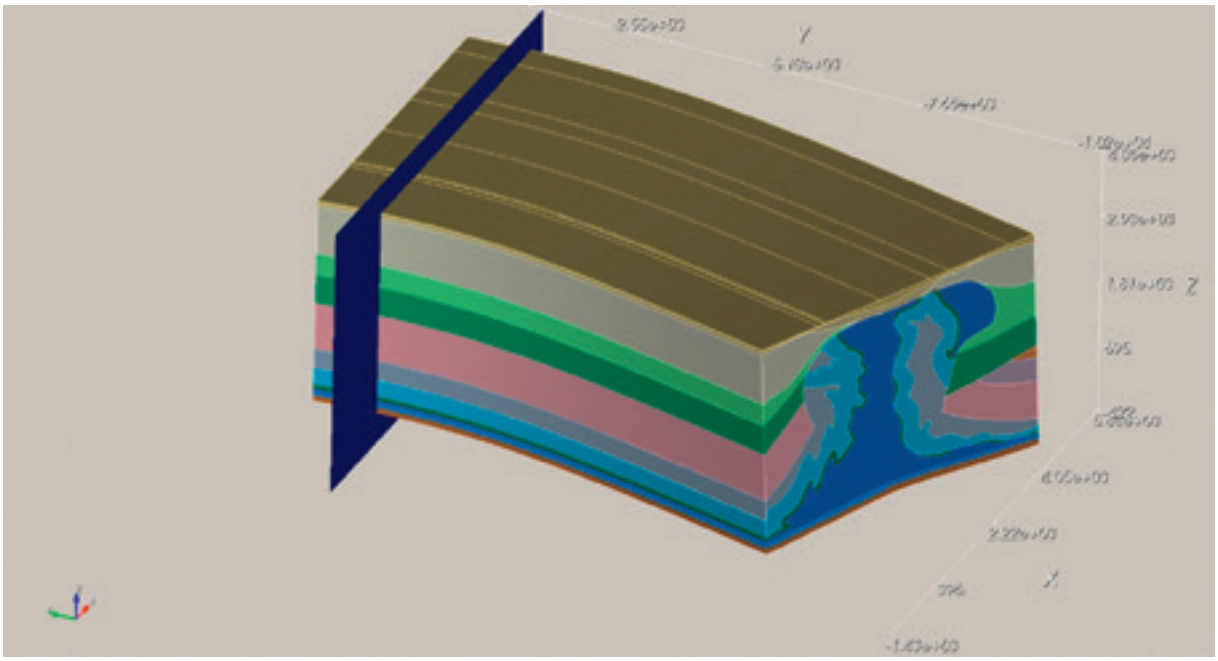

Figure 5: Result of sweeping the 15-media cross section of Figure 2 (with the modifications) along the three-dimensional spline from Section 5 at y = 0 m to Section 2. The structure was then cut at y = -1000 m and only the part left of the cut plane retained.

Intended mesh-element size / m	40	20	15	10
No. elements with 4 media, vector sweep	$0.320 \cdot 10^6$	$2.39 \cdot 10^6$	$5.50 \cdot 10^6$	$16.5 \cdot 10^6$
No. elements with 15 media, vector sweep	$0.415 \cdot 10^6$	$2.40 \cdot 10^6$	$5.49 \cdot 10^6$	$18.2 \cdot 10^6$
No. elements with 15 media, spline sweep	$0.419 \cdot 10^6$	$2.39 \cdot 10^6$	$5.47 \cdot 10^6$	$18.4 \cdot 10^6$
Minimum element size / m, 15 media, vector sweep	2.1	2.1	2.1	2.6
Maximum element size / m, 15 media, vector sweep	84.3	52.4	38.1	30.1
Min. GLL point distance / m, 15 media, vector sweep	0.36	0.36	0.36	0.45
Max. GLL point distance / m, 15 media, vector sweep	27.6	17.2	12.5	9.8
Approximate run time per s / h	0.4	6	19	100

Table 1: Properties of the meshes for the three models with various intended element sizes: numbers of mesh elements (hexahedra), minimum and maximum element sizes, minimum and maximum distance between the Gauss-Lobatto-Legendre (GLL) points in the elements (the latter two for the 15-media orthogonal-vector sweep, the others are very similar), and approximate run time per second of model time using 340 processors with 0.02 ms time step.

needed mostly, 10 m intended size with around 200 hours computation time, far above the maximum of 48 h with a few hundred processors, is excluded. But 15 m fits, so this intended size was used mostly.

The time step was chosen as 0.02 ms for most runs. This is about half the threshold acceptable using a stability criterion. As source time functions for a force pulse a quasi-Dirac function was used, and an explosion was modelled by a quasi-Heaviside function for the seismic moment. To suppress spurious higher-frequency contributions from these short-duration excitations while maintaining separation of individual arrivals, the seismic signals were convolved with a Gaussian function of nominal half duration 5 or 10 ms, equivalent to 250 or 500 time steps.

Constant-quality attenuation is implemented in SpecFEM3D by normally three standard linear solids. The highest characteristic frequency is derived from the longest propagation time between neighbouring GLL points. This was 32 Hz with 15 m intended mesh-element size, whereas the source time function convolved with 5 or 10 ms half duration has a spectrum to above 100 Hz. Whether this mismatch produces errors in the attenuation needs to be investigated. Simply reducing the mesh-element size would reduce the GLL-point distance, but would run against the computing-time limit.

Because the seismic excitation is computed at all points for every time step, recording it at many positions does not increase the computation time, only the memory and disk space for the result files. Thus 56 sensors were put in five x-z planes each, at y = -500 m (the plane of the source), -900 m, -700 m, -300 m and -100 m. For the detection runs, additional sensors were used and some positions were discarded (see Section 5.3 and Figure 2).

4. Visualisation in two dimensions

For testing and better visualisation a few model runs were done in two dimensions with the program SpecFEM2D, just using the modified cross section. Here the geometric expansion in a homogeneous volume reduces the seismic amplitude with distance r in proportion to $r^{-0.5}$ whereas in three dimensions it is with r^{-1}. Figure 6 shows snapshots of wave propagation every 0.1 s after an explosion was ignited at the usual source position. The same parameters were used for the 15 media as in the three-dimensional case (Table 3), only here in addition to shear attenuation some bulk attenuation was included, with $Q_\kappa = 2\ Q_\mu$ for all media.

In Figure 6 the grey values indicate the P-wave velocities, the red colour in the wave fronts is linked to the seismic velocity. Various effects can be seen, most relevant are reflection and transmission at the salt-dome boundaries with strong velocity contrast and at the free surface, but they occur also between different salt layers with a small velocity difference. Also visible is conversion from P to S waves and vice versa. Pictures such as these can be used to assign wave arrivals at a certain sensor position to the respective propagation paths.

5. Results – three-dimensional propagation

5.1 Comparison of the three underground models

Runs using a force pulse in –z direction were done with the three model structures produced from the two-dimensional cross section: the four-media orthogonal-vector sweep, the 15-media orthogonal vector sweep, and the 15-media spline sweep. Figure 7 shows the vertical component of seismic velocity for selected sensors at the depth of the source, 900 m, in the y = -500 m plane of the source. Proceeding from Sensor 9 at 944 m from the source to the farthest Sensor 14 at the model margin one can follow the dominant S-(transversal-)wave excitation as it arrives with increasing delay. The expected arrival times from the partial distances and corresponding S-wave speeds are marked “S” in the salt and “SS” after transmission to the adjoining rock, they fit very well. Figure 8 presents the vertical seismic velocity at the sensors near-vertically above the source, from 500 m depth via 150 m depth to the surface. Due to the vertical excitation here the P (longitudinal) wave is dominant; its expected arrivals are marked “P”, and “PP” after transmission to the overlying rock.

The major difference between the three structures is that at some sensors at the source depth the four-media

No.	Medium	ρ /(kg/m³)	v_P /(m/s)	v_S /(m/s)	Q_κ	Q_μ
1	Rotliegend	2,650	4,850	2,800	9,999	125
2	Surrounding rock	2,400	3,500	1,850	9,999	50
3	Overlying rock	2,000	1,750	1,000	9,999	20
4	Salt	2,200	4,400	2,600	9,999	50

Table 2: Seismic properties of the underground model of four different media as shown in Figure 3. Given are the density ρ, the P-wave velocity v_P, the S-wave velocity v_S, the bulk quality Q_κ (9,999 means no bulk attenuation) and the shear quality Q_μ.

No.	Medium	ρ /(kg/m³)	v_P /(m/s)	v_S /(m/s)	Q_κ	Q_μ
1	z4	2,200	4,400	2,700	9,999	125
2	Upper Bunter/Muschelkalk	2,600	4,350	2,500	9,999	50
3	Cap Rock	2,550	3,750	2,200	9,999	125
4	z3GT/HA	2,200	4,000	2,650	9,999	125
5	Lower Cretaceous	2,350	3,000	1,400	9,999	50
6	z3	2,200	4,400	2,700	9,999	125
7	Tertiary	2,100	2,100	1,200	9,999	20
8	z2HS	2,200	4,400	2,600	9,999	125
9	Upper Cretaceous	2,400	3,500	1,850	9,999	50
10	Keuper	2,500	3,300	1,700	9,999	50
11	Lower/Middle Bunter	2,650	4,300	2,500	9,999	50
12	Rotliegend	2,650	4,850	2,800	9,999	125
13	z1	2,200	4,600	2,650	9,999	125
14	Quaternary Elsterian glacial	2,000	1,750	1,000	9,999	20
15	Quaternary	2,000	1,750	1,000	9,999	20

Table 3: Seismic properties in the 15-media model. For the media see Figure 2. Given are the density ρ, the P-wave velocity v_P, the S-wave velocity v_S, the bulk quality Q_κ and the shear quality Q_μ. In order to have only shear attenuation, the Q_κ values were set to fictitious 9,999. Zechstein strata: z1 Werra Formation; z2 Stassfurt Formation (HS: main salt, SF: Kaliflöz); z3 Leine Formation (GT/HA Grauer Salzton/ Hauptanhydrit), z4 Aller Formation.

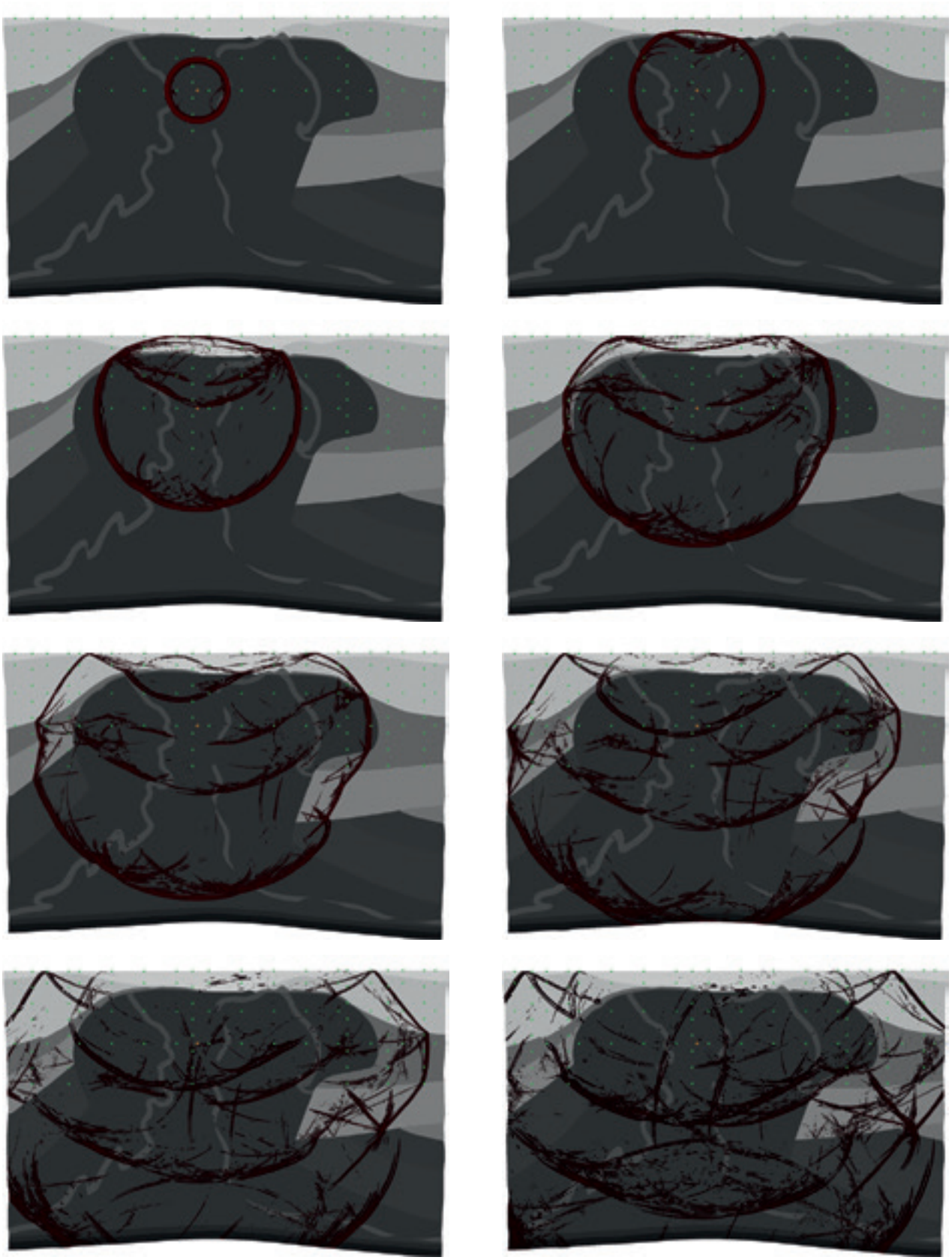

Figure 6: Snapshots of wave propagation every 0.1 s from an explosion (yellow dot) at 900 m depth, from 0.1 s to 0.8 s. Shown is the absolute magnitude of the seismic velocity, indicated by red colour, with some logarithmic distortion to make smaller values better visible. The grey value follows the P-wave velocity, from 1750 m/s at the surface to 4850 m/s in the base rock at about 3,300 m depth. The green dots denote sensor positions.

arrivals are somewhat later. This can be understood because the S-wave speed in the united salt body is the one of the main salt z2HS whereas in the 15-media model the wave additionally propagates through layers z2GT/HA, z3 and z4 with slightly higher S-wave velocities. But the general appearance and amplitudes are similar for all three models. Concerning the 15-media structures, the differences between the orthogonal-vector sweep and the spline sweep are relatively small. Similar behaviour was observed at the other sensor positions analysed.

5.2 Single and repetitive signals

Two types of repetitive signals were modelled: a sequence of blast shots and picking. The four-media model was used here, with 40 m intended mesh-element size and a time step of 0.05 ms. In the convolution a Gaussian function with an equivalent half duration of 5.0 ms was used. Many single-pulse signals were superposed with time delays and in numbers similar to the ones observed in the measurements. As examples the signals at Sensors 7 and 13 (at the source depth of 900 m, 144 m and 2544 m, respectively, from the source in x direction), and at Sensors 21 and 49 (near-vertically above the source at 500 m depth and the surface, respectively, the x co-ordinate of both is 144 m higher than the one of the source) are shown.

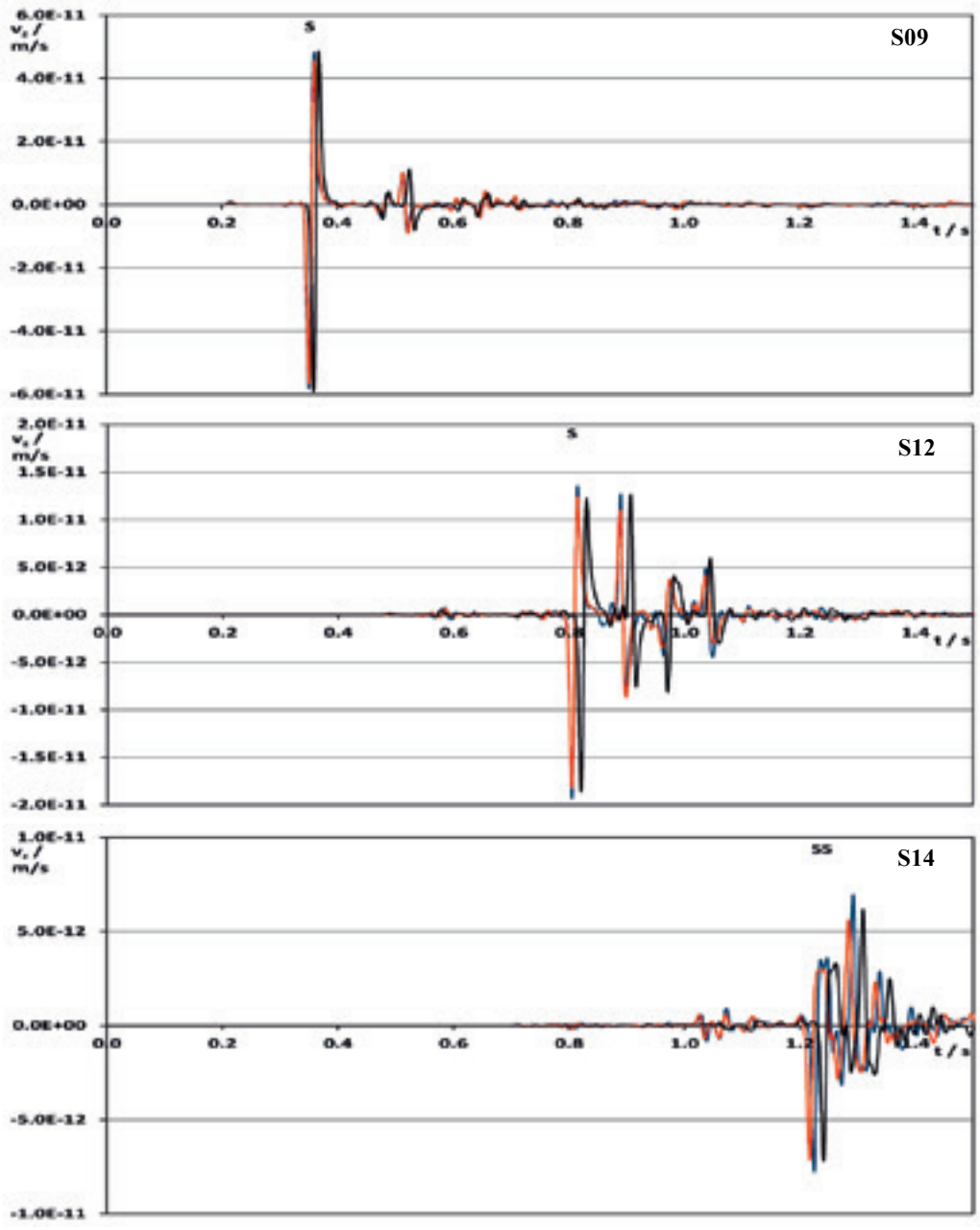

Figure 7: Vertical component of seismic velocity at various x co-ordinates in the source plane (y = -500 m) at the source depth (900 m) after a force pulse in -z (down) direction. Sensors and source distances in x direction, from the top: 9, 944 m; 12, 2144 m; 14, 2944 m. Black: 4 media, orthogonal sweep; blue: 15 media, orthogonal sweep; red: 15 media, spline sweep. The S- and SS-wave arrivals are marked.

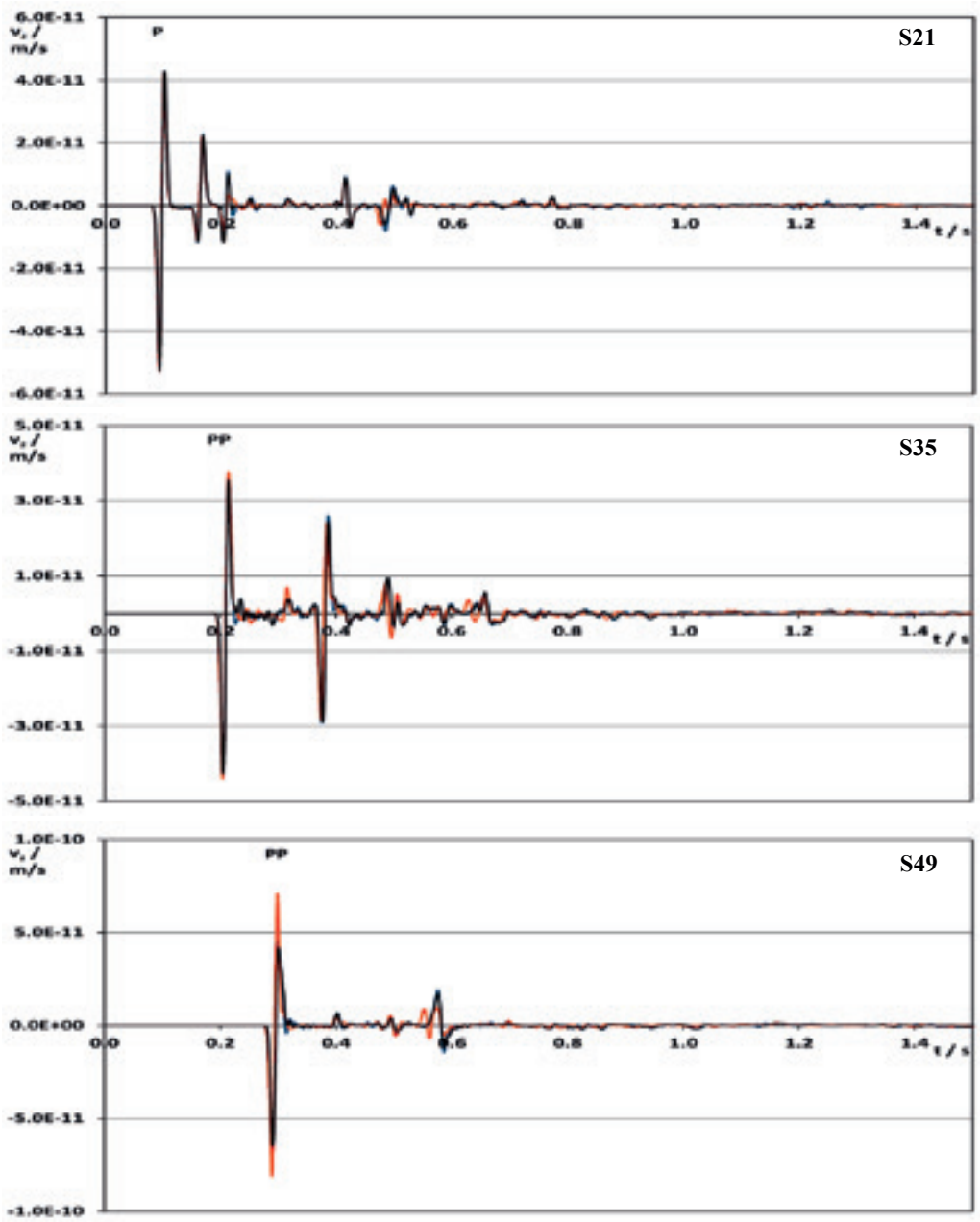

Figure 8: Vertical component of seismic velocity at various x co-ordinates in the source plane (y = -500 m), near-vertically above the source (at depth 900 m) after a force pulse in -z (down) direction. Sensors and source depths, from the top: 21, 500 m; 35, 150 m; 49, 0 m. Black: 4 media, orthogonal sweep; blue: 15 media, orthogonal sweep; red: 15 media, spline sweep. The P- and PP-wave arrivals are marked.

Blast shots: When a tunnel was to be extended by five more metres, usually about 11 shots were done with 0.25 s spacing, igniting groups of charges in the different drill holes. The shots were modelled by a spherically symmetric point source, that is the seismic-moment tensor had equal values in the three main-diagonal elements and zero in the other components. The value was chosen as 1 Nm. Figure 9 shows the single-shot signals at the left and the 11 superposed ones with 0.25 s spacing at the right. Since an explosion excites nearly exclusively P waves, for the sensors lying in horizontal direction from the source the x component of seismic velocity is shown, for the ones near vertically above the source the z component is presented. The z component at Sensors 7 and 13 as well as the x component at Sensors 21 and 49 are very small. The y component is essentially zero for sensors in the y = -500 m plane of the source, but it gets significant in the other planes where the P wave has a slant projection in the x-y plane. At many positions the duration of the one-shot signals is shorter than the repetition period, thus not much mutual overlap exists and the superposed signals look similar to simple repetitions, with similar amplitudes and spectra.

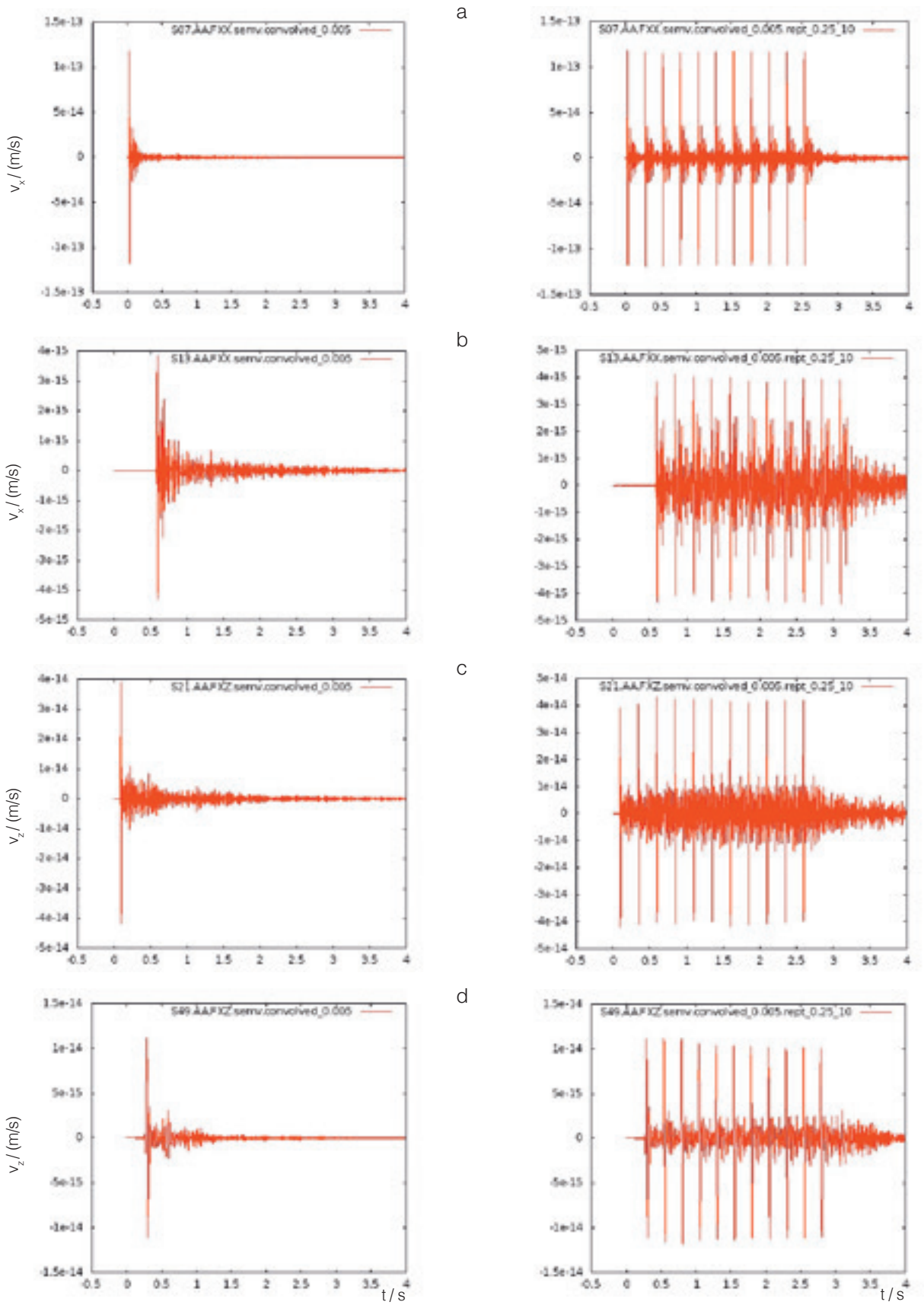

Figure 9: Model signals (seismic velocity) at various sensor positions from a single explosion (left) and an 11-shot blast with 0.25 s spacing (right) in the main salt at 900 m depth.
a) x component at Sensor 7 (900 m depth, 144 m from the source in x direction);
b) x component at Sensor 13 (900 m depth, 2544 m from the source in x direction, just outside the salt);
c) z component at Sensor 21 (500 m depth, x co-ordinate 144 m higher than the source);
d) z component at Sensor 49 (at the surface, x co-ordinate 144 m higher than the source).

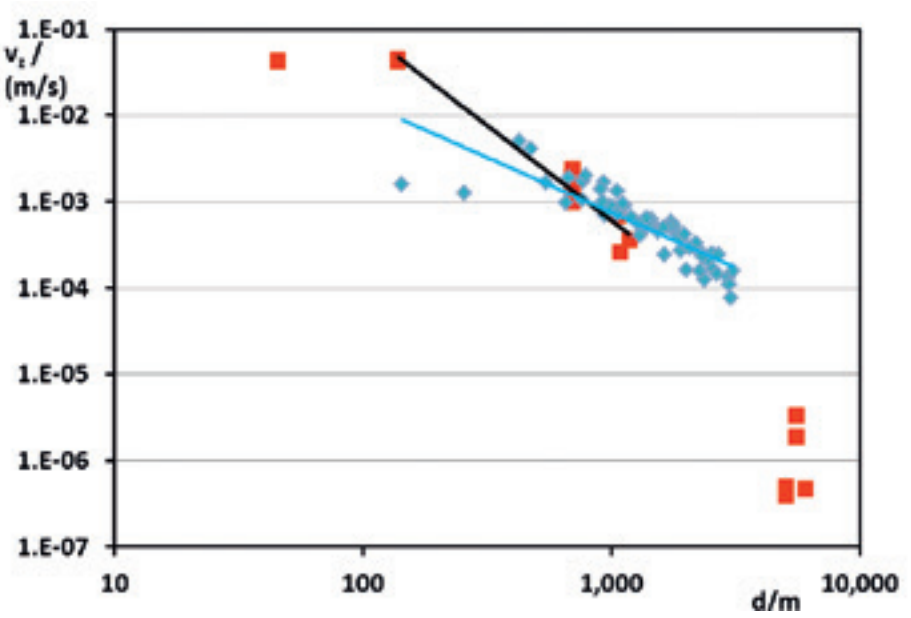

Figure 10: Peak-to-peak value of vertical seismic velocity versus distance. Red squares: measured from blast shots at 840 m depth; blue diamonds: model computation from an 11-shot blast at 900 m depth, multiplied by $6{\cdot}10^{10}$ to fit to the measured data at several 100 m distance. Measured values and trend as in [6]: Fig. 67; distances excluded from trend: 44 m (the sensor is in the seismic shadow of a drift), 5-6 km (much lower recording bandwidth). Power-law exponents are -2.2 for the measured data and -1.3 for the model ones.

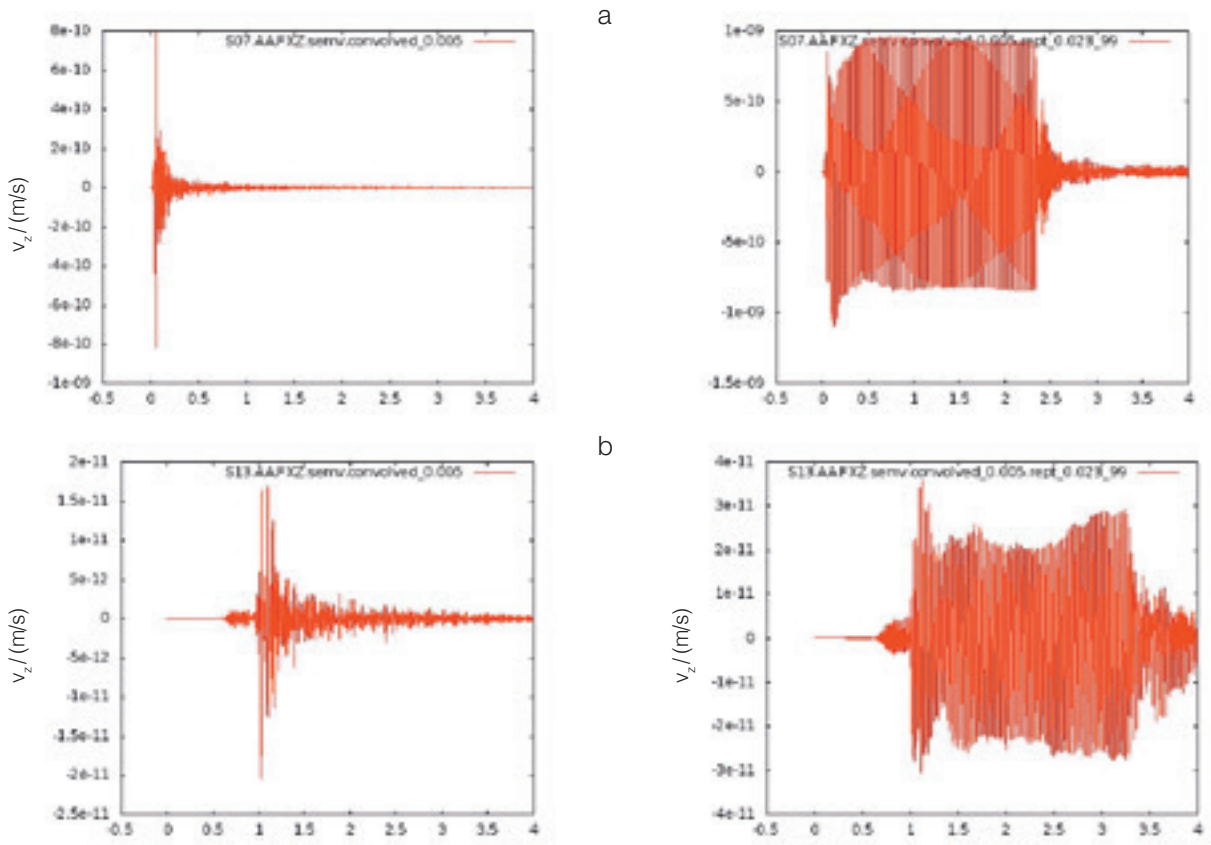

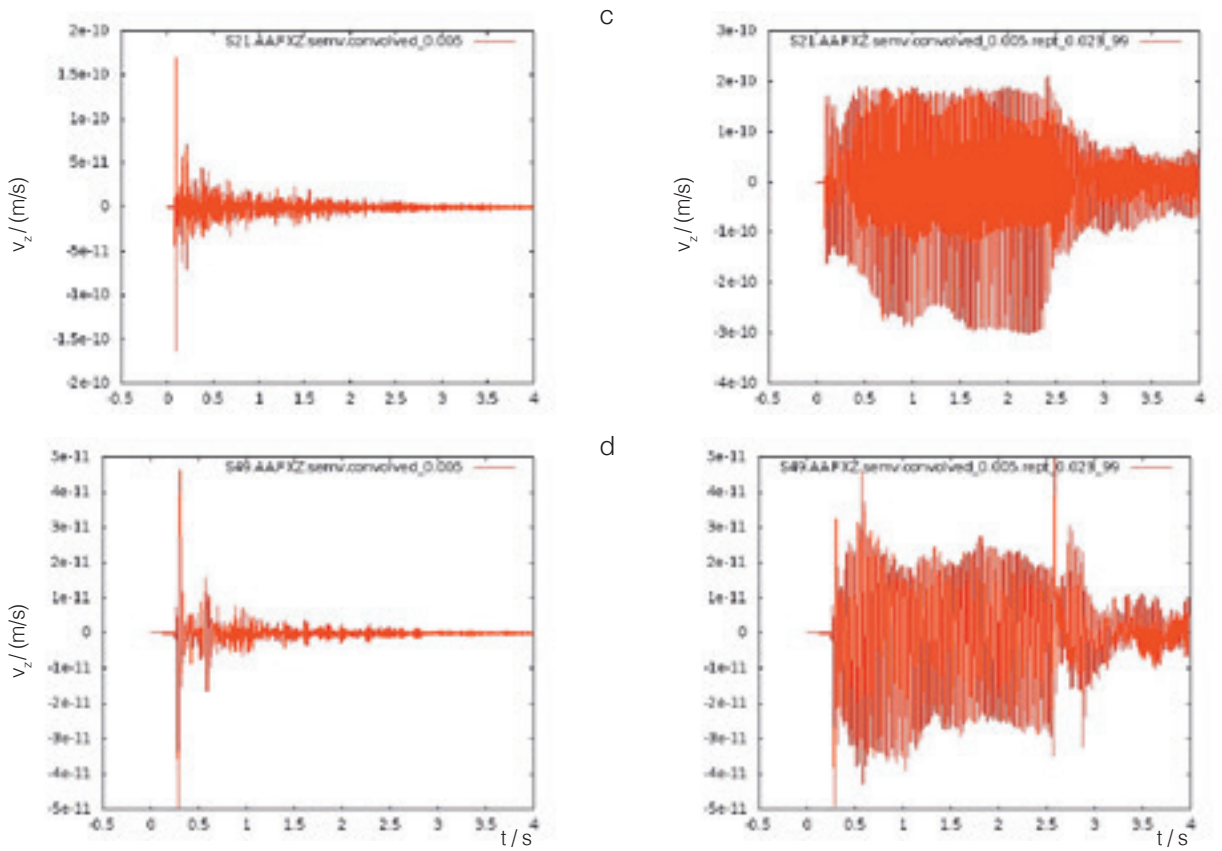

Figure 11: Model signals (seismic velocity) at various sensor positions from a single force pulse in -z direction (left) and a sequence of 100 such picking blows with 23 ms spacing (right) in the main salt at 900 m depth.
a) z component at Sensor 7 (900 m depth, 144 m from the source in x direction);
b) z component at Sensor 13 (900 m depth, 2544 m from the source in x direction, just outside the salt);
c) z component at Sensor 21 (500 m depth, x co-ordinate 144 m higher than the source);
d) z component at Sensor 49 (at the surface, x co-ordinate 144 m higher than the source);

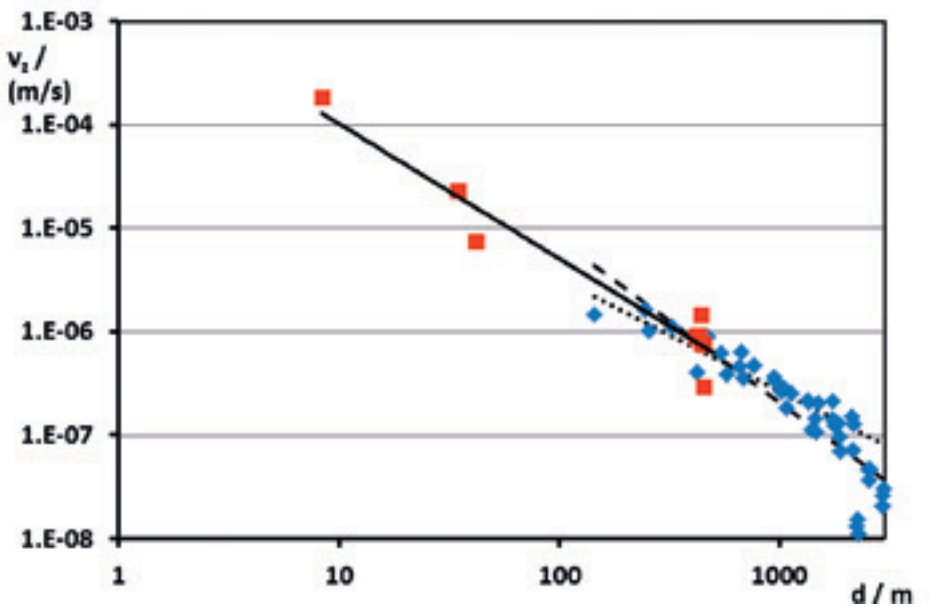

Figure 12: Measured peak-to-peak values for picking (red squares) with power-law trend line (solid), and model results from 100 blows with 23 ms spacing, multiplied by 700 (blue diamonds). Power-law exponents are -1.3 for the measured data and -1.6 for the model data using all positions (dashed) and -1.1 for the positions in the salt dome only (dotted).

To compare the absolute amplitudes with the measured ones, Figure 10 shows the peak-to-peak values of seismic velocity of the model signals at all 56 sensor positions shown in Figure 2 (the y = -500 m plane of the source) versus geometric distance, in double-logarithmic scale. The best-fit power-law trend line has an exponent of -1.3. In order to fit the model values to the measured ones at several 100 m distance, the former had to be multiplied by $6 \cdot 10^{10}$.

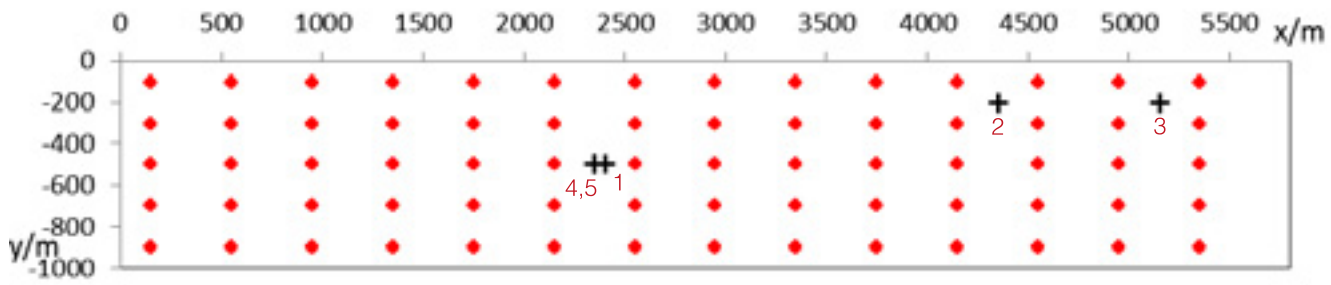

Figure 13: Sensor (dots) and source (+ signs) positions projected into the x-y plane, different x and y scales. The salt dome extends in x direction from about 900 m to about 4700 m, see Figure 2. A repository could cover a projected area extending over less than 1 km in x direction but several km in y direction, beyond the 1-km extent of the model, Source 1 is at its centre at 900 m depth, source Positions 4 and 5 are nearly vertically above at depth 150 m and 500 m, respectively. Positions 2 and 3 are at 900 m depth. At depths below 500 m the sensors closer than about 1 km to the repository centre are not considered.

This means that – with the chosen moment-step equivalent-triangle half duration of 0.25 ms and the convolution half duration of 5.0 ms – the seismic moment is around 10^{11} Nm. Whether this is the correct order of magnitude for a momentary release of the mechanical energy of several kilograms of explosive, that is several megajoules, needs to be investigated.

Picking: The hand-held electrohydraulic pick hammer is used for a few seconds at a time. To model a single chisel blow a Gaussian force pulse of 1 N with equivalent half duration of 0.163 ms, applied in the -z direction, was assumed. The measurements had shown that the repetition frequency of the pick-hammer chisel is 44 Hz. Thus 100 single-pulse signals were superposed with 23 ms spacing. Here the single-signal duration is shorter than the repetition period, thus considerable overlap and significant variation of the envelope shape results. Figure 11 shows the single signals at the selected sensor positions at the left, and the superposed ones at the right. Because the force was vertical, the z component is shown for all four sensors; it has to be noted that in the horizontal direction (to Sensors 7 and 13) the main excitation travels as an S (transversal) wave whereas in the (near-)vertical direction (to Sensors 21 and 49) the seismic motion is mainly vertical, that is in the form of a P (longitudinal) wave. The x and y components are markedly smaller. Because the next single-blow signal is added to the preceding one when the latter still has significant amplitude, the superposed signal was found to be stronger than the single one by up to a factor 3.

Figure 12 shows the peak-to-peak values of vertical seismic velocity from the model (all 5*14 sensors at the source depth in the planes at y = -900 m, -700 m, -500 m, -300 m and -100 m) and from the measurements versus geometric distance, again in double-logarithmic scale. Depending on whether the positions outside of the salt dome are included or not, the power-law trend line has an exponent of -1.6 or -1.1, the exponent for the measured data is -1.3. To fit the model values to the measured ones at several 100 m distance, the former had to be multiplied by $7{\cdot}10^{2}$, corresponding to an integrated model force of around 700 N with the source half duration of 0.163 ms and the convolution one of 5.0 ms. Whether this is plausible for a picking chisel releasing about 25 J energy needs to be investigated.

5.3 Signal strengths from intrusion attempts

There are two general methods of approaching the repository.

1. Vertically from above, for example by driving a new shaft.

2. Fom the side, going underground at considerable distance and for example excavating a new tunnel.

The first would mainly be detected by an area sensor network near the surface. The second would be covered by deeper underground sensors around the repository. Using a simple amplitude criterion. the maximum distance between neighbouring sensors depends on the detection sensitivity, the decrease of the signal strength with distance, the background noise and the required signal-to-noise ratio for detection. However, most of this is not known at present. To approach an answer to these questions, model calculations were done with five different source positions along the two principal pathways: at depths 150 m and 500 m above the centre (which is at 900 m), at this centre, and at 900 m depth near the outer margin of the model volume (Figure 13). 200 additional sensor positions were used to cover depths from 100 m to 1300 m with 200 m spacing. To keep the safety distance of about 500 m from the repository margin, from 700 m to 1300 m depth the closer positions were not computed or excluded from consideration (see Figure 2). The standard single force pulse of 1 N in downward (-z) direction was assumed. In order to keep the computation time limited, in the meshing the intended element size was increased from 15 m to 20 m, retaining the time step of 0.02 ms. The computed signals were convolved with a Gaussian function of nominal half duration 5 ms.

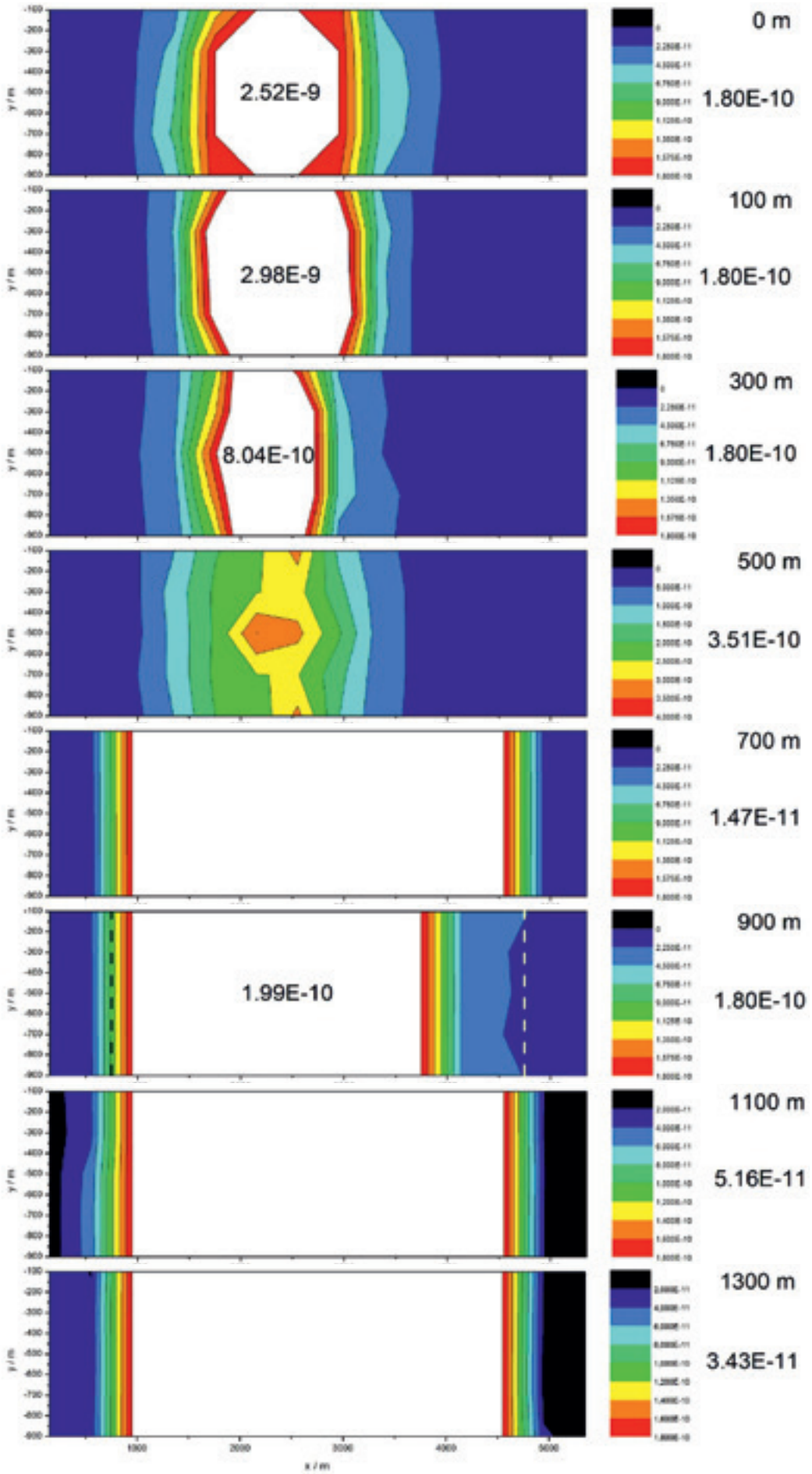

Figure 14: Peak-to-peak values of vertical velocity at different depths (right), source 4 at (2350/-500/150) m.

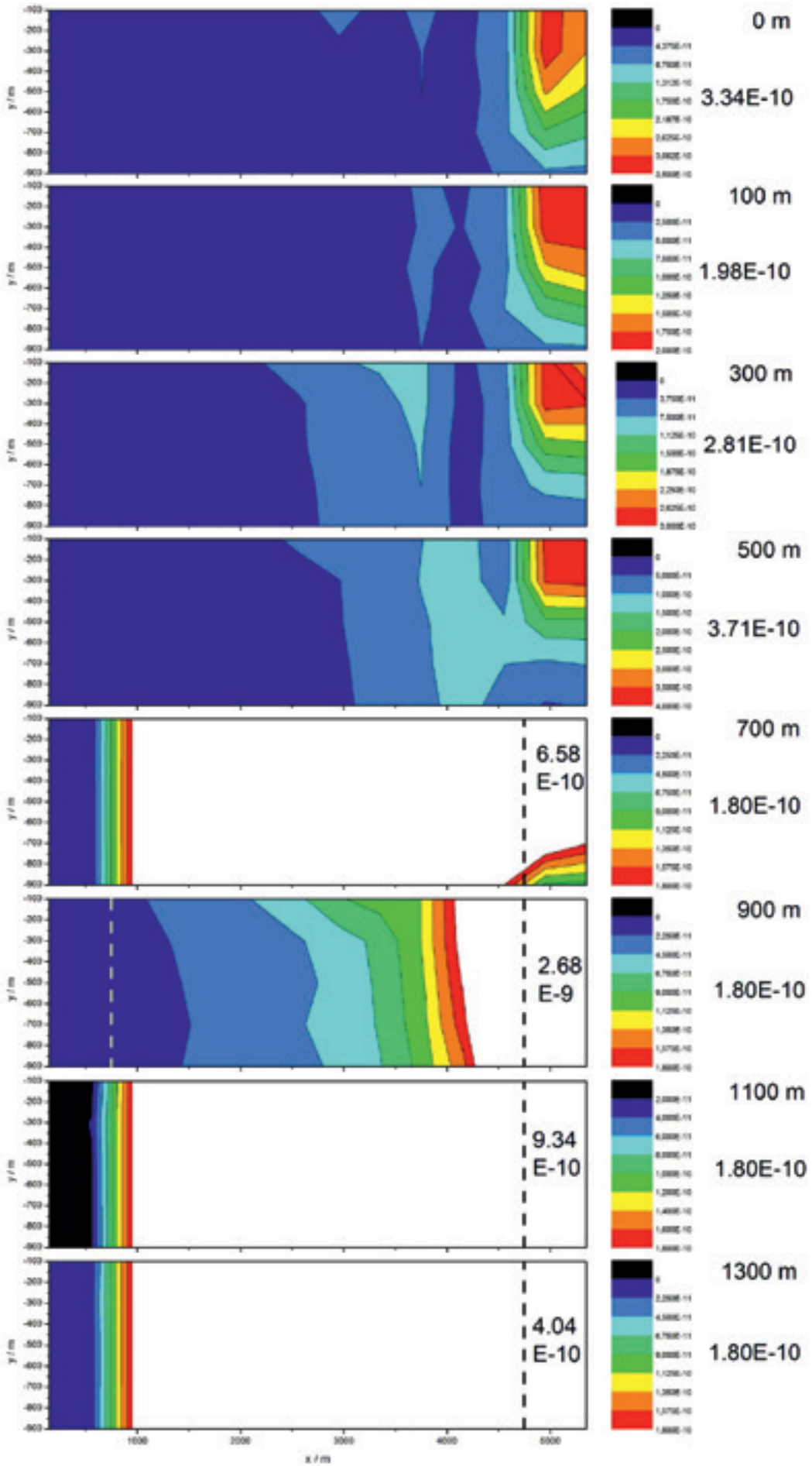

Figure 15: Peak-to-peak values of vertical velocity at different depths (right), source 3 at (5150/-200/900) m.

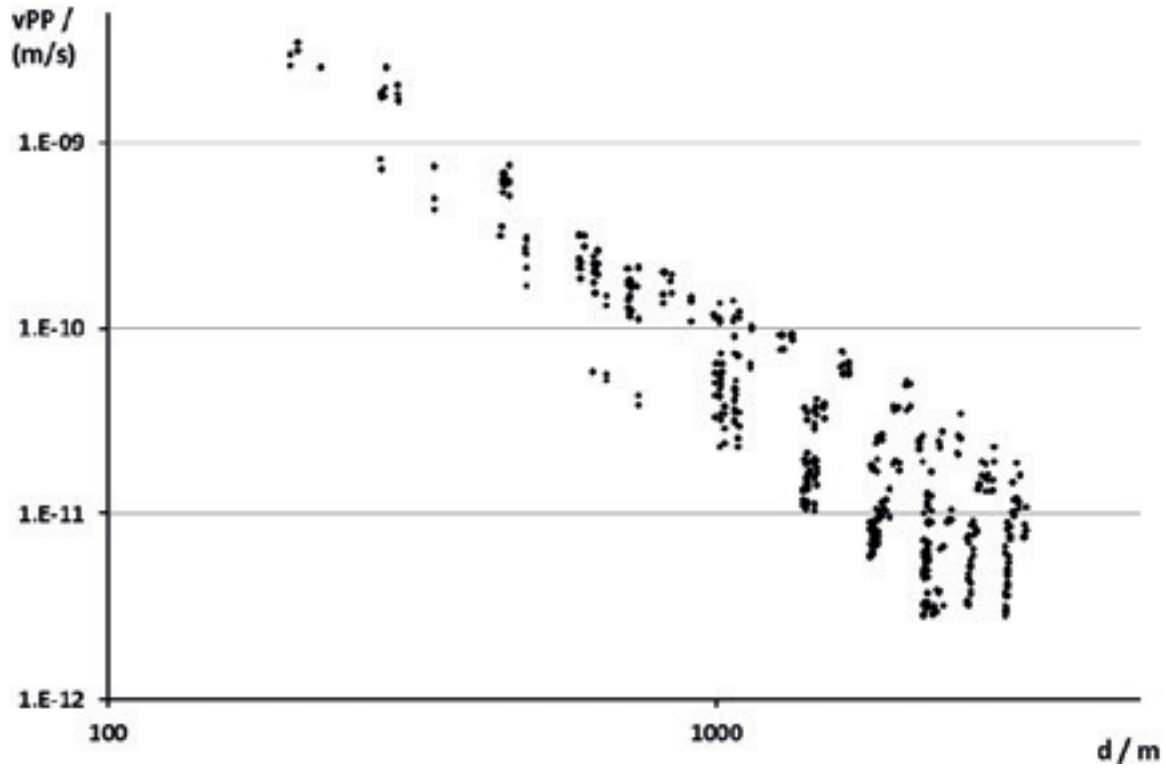

Figure 16: Peak-to-peak values of vertical seismic velocity versus geometric distance, source Position 4 (150 m depth, nearly vertically above the assumed repository centre).

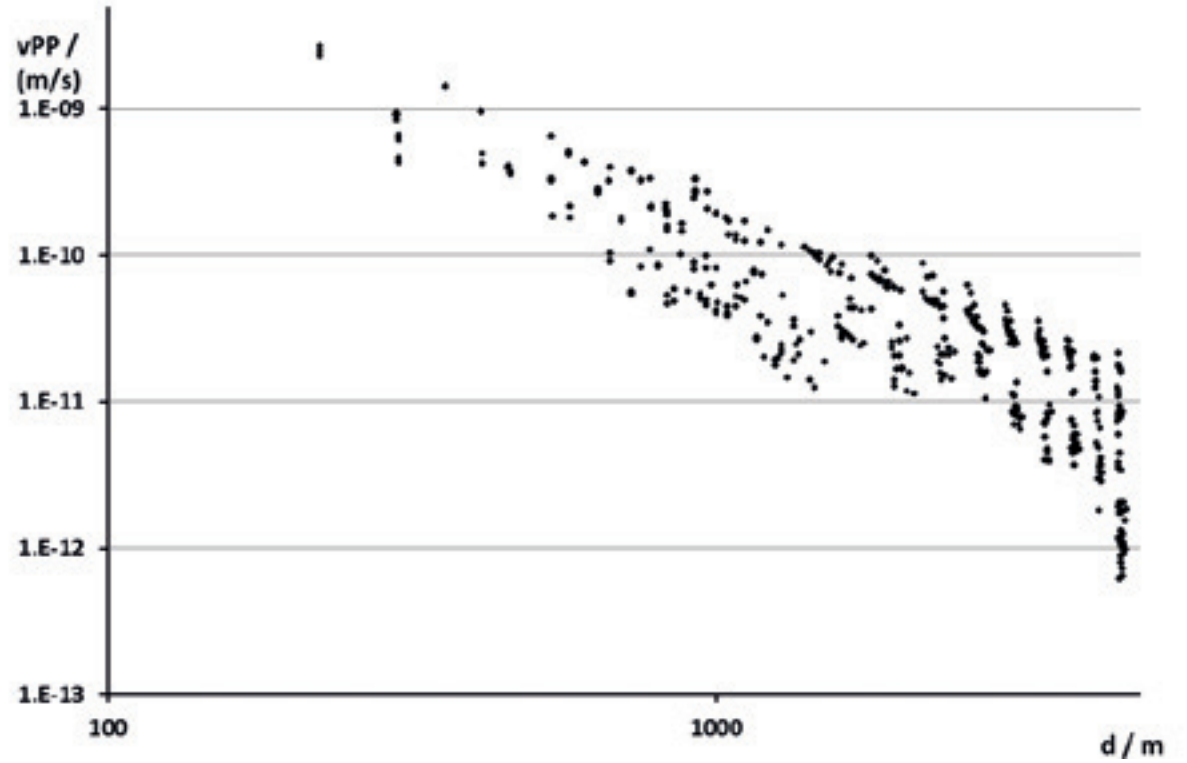

Figure 17: Peak-to-peak values of vertical seismic velocity versus geometric distance, source at Position 3 (900 m depth, near the model x-y corner).

For each sensor the maximum peak-to-peak values of vertical seismic velocity were determined. As examples, two-dimensional contour colour plots of these values are shown in Figure 14 for Source Position 4 at 150 m depth, nearly vertically above the centre, and in Figure 15 for Source Position 3 at 900 m depth, close to the model corner. The captions give the co-ordinates (x, y, depth). In these figures the sensor values at depths from 0 m to 1300 m are shown, with the depth given at the right.[1] The colour scale, shown beside the contour plots, extends to the maximum value at the respective sensor depth, these values are shown at the right except where they are extraordinarily high or low:

1. To roughly achieve an absolute assignment of colour with absolute value, for high maxima the scale is limited to a value of $1.8 \cdot 10^{-10}$ m/s (typical at around 800 m distance from the source). The region of higher values is shown in white. The maximum value is given in the white area, the value at the right is the maximum for the colour scale.

2. If the maximum at some depth is below $1.8 \cdot 10^{-10}$ m/s, the colour scale is extended to this value.

At depths 700 m, 1100 m and 1300 m where there are sensors only at the left and right margins of the model (x = 150 m and 550 m and x = 4950 m and 5350 m, respectively, see Figure 2) no values exist in between, also here a white region is shown.[2] At depth 900 m two more sensor positions are included at the right-hand side (x = 4150 m and 4550 m). The values from 500 m depth are shown in full but being only 400 m above the repository the central positions should probably not be used.

The decrease of the signal strength with increasing source-sensor distance is shown quantitatively, in double-logarithmic scale, in the corresponding Figure 16 for Position 4 and Figure 17 for Position 3. (Similar behaviour occurs at the other source positions.) Here the sensor positions at depth 900 m, too close to the repository, are included. With the given force value and pulse duration, the resulting seismic velocity is on the order of 10^{-9} m/s at several hundred metres distance, decreasing to 10^{-11} m/s at 1 km and 10^{-12} m/s at 5 km. The values show scatter of one order of magnitude. Power-law fits give exponents of distance r of -2.1 and -2.3; the deviations from the theoretical r-1 dependence in a homogeneous volume can be caused by the effects of (curved) boundaries, the angle between the force and the propagation direction, and – for larger distances – by attenuation.

These figures allow a rough estimate of the peak-to-peak value of seismic velocity from a source at a given distance, or of the detection range if a detection threshold is given. Of course for both the values have to be scaled according to the actual value and time course of the force.

Because actual force strengths and time functions of mining activities that would be used for undeclared access as well as the background at the various potential monitoring positions are not known, and because a threshold for the required signal-to-noise ratio cannot yet be defined, exact quantitative statements on the detection range for certain activities cannot be made at the present stage. For the time being one should rather rely on the evaluation of the earlier measurements (Altmann/Kühnicke 2013, Altmann 2013a).

The approach to determine the required sensor number is explained in an illustrative example. If the detection range is 1 km and one demands that penetrating a sensor fence should be detected at two positions at least, neighbouring sensors should have a spacing of 1 km. Assuming a repository of 1.5 km horizontal extent at about 1 km depth, demanding a distance of 1.5 km from the centre, a circle or square around it would have a length of 10 or 12 km, requiring 10 or 12 sensors. Deployed at about 500 m depth one such arrangement would suffice to detect penetrations from the side at depths from 0 m to 1.5 km. To cover the projected surface area 3 sensors would be needed in each dimension, in total 9. Because at the surface the background would be higher, these sensors should rather be deployed at some depth, say 100 m. In this scenario thus about 10 sensors would be deployed in shallower boreholes and about 10 in deeper ones.

5.4 Additional observations

Assignment of events: Many signals contain several smaller events. They come about by reflection and transmission at media boundaries. When the wave does not impinge orthogonally, continuity conditions effect conversion from P to S waves and vice versa. In case of a second boundary – for instance the salt-dome top and the surface – various waves with mixed histories can occur, for example PPP, PPS, PSP etc. If the partial path lengths in the different media are known well, the expected arrival times can be found precisely, allowing unique assignment at least for the simpler events, but for some mixed histories the arrival times are too similar for differentiation.

Comparison of excitation by directed force and by explosion: In test runs of an explosion and a horizontal force pulse – for propagation in x direction both produce mainly P waves – the x components of seismic velocity at the corresponding Sensors 7 to 14 were very similar, except for much lower amplitudes in the case of the explosion. Figure 18 shows the peak-to-peak values, determined as the difference between the maximum and the minimum values over the full time for each signal; these extreme values

[1] Note that due to reflection of waves from below, at the surface (depth 0 m) the values are doubled.

[2] Note that due to the method of achieving a white region in Origin 7 at the margins of the empty area artefacts occur where interpolated values are above the actual maximum shown at the right.

occur at the respective main events. The ratio between the values from the force pulse of 1 N and an explosion of 1 Nm seismic moment (half durations by convolution in both cases 10 ms) has a mean of $4.4 \cdot 10^3$. This issue needs further investigation.

Transmission from salt to surrounding media: Whereas reflection and transmission of a seismic wave at a media boundary are normally very complex, in case of orthogonal incidence of a plane wave on a plane boundary the respective coefficients can be described simply in terms of the impedances $Z_i = v_i \rho_i$, where v_i is the relevant (P- or S-) wave speed and ρ_i, is the density in medium i. The reflection and transmission coefficients are

$$R = \frac{Z_2 - Z_1}{Z_2 + Z_1}, \quad T = \frac{2Z_1}{Z_2 + Z_1}.$$

For monitoring a final repository in a salt dome most sensors would be positioned outside of the salt (Figure 1). Thus the transmission from the salt to the adjoining and overlying layers is relevant. For a rough check of this transmission results from the 15-media orthogonal-vector sweep were used. The signal strength at a position just inside the salt was compared with the one at the neighbouring position just outside it, corrected for distance r assuming an r^{-1} dependence. For P waves propagating in x direction the peak-to-peak values of the x components of seismic velocity at Sensors 12 and 13 are used, for vertical propagation this concerns the z components at Sensors 21 and 35. The resulting ratios of peak-to-peak velocities are compared with the expected transmission ratios in Table 4, the impedances were gained by multiplying the P-wave speed and density entries of the respective media in Table 3. There is good agreement, the fact that the incidence is not exactly perpendicular and that the wave fronts and boundaries are curved does not seem to produce a strong deviation. This means that sensors outside of the salt dome should have generally similar detection capabilities as ones inside the salt dome. Only when attenuation becomes stronger, such as with the low quality values in the overlying sediment at higher frequencies, detectability is expected to deteriorate.

6. Conclusion and Outlook

Considerable effort was spent to achieve a model structure that resembles the reality to some extent from a simplified two-dimensional cross section. The three structures investigated showed some differences in the seismic signals, but these seem small enough to not be relevant from the perspective of monitoring and detecting activities where the exact time of arrival or small-scale events are of little importance. But since the 15-media spline-sweep model is closer to reality, it should be used in future investigations, as long as additional methods of improving the fidelity of the model, such as scaling and morphing while sweeping, are not available. A full three-dimensional description of the real structure will probably remain unattainable.

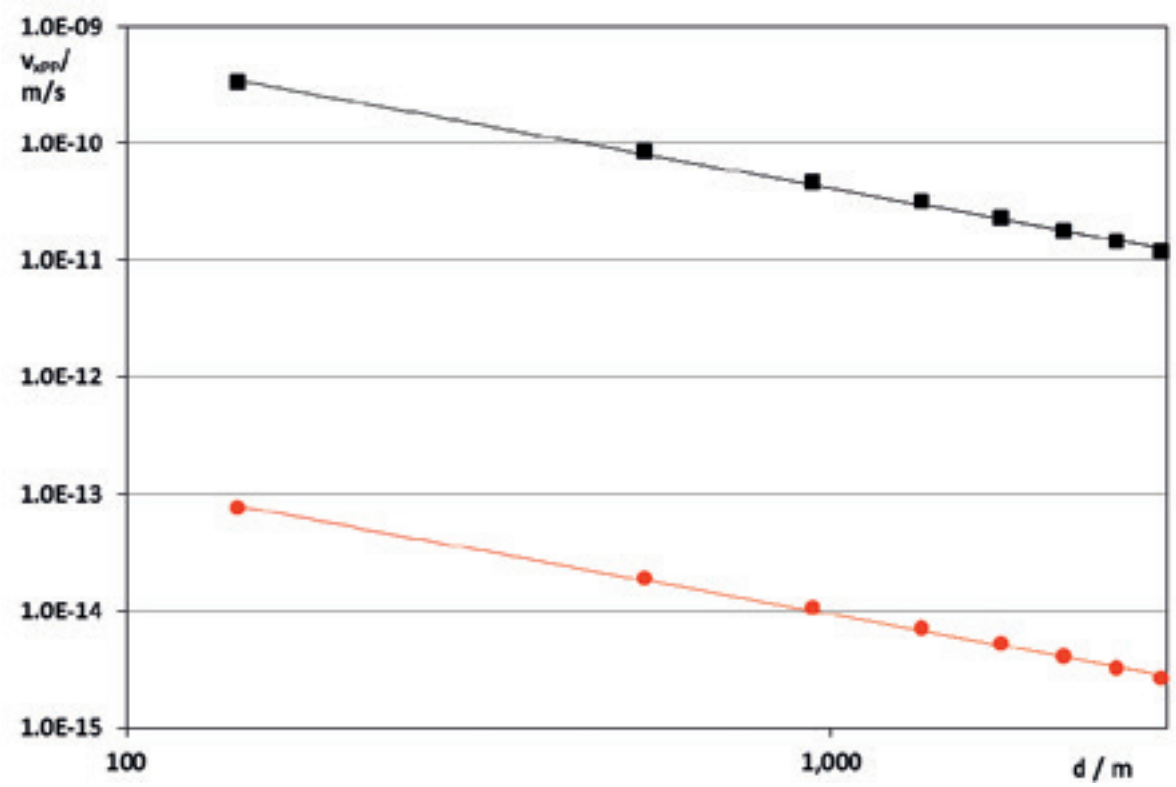

Figure 18: Peak-to-peak value of the x component of seismic velocity versus distance along the horizontal line from the source in x direction (Sensors 7 to 14). Signals were computed with the 15-media structure, spline sweep, with 0.02 ms time step, and then convolved with a Gauss function of 10 ms half duration. Black squares: force of 1 N in x direction, red dots: explosion with 1 Nm seismic moment. Power-law trend lines are indicated, their exponent (slope in double-logarithmic scale) is -1.1 for both sets.

The complex inner structure of the salt dome, with for example inner boundaries intersecting the axis direction, is not represented in the model. Also, broken-up and mixed layers at the salt-dome margins could give rise to multiple scattering, reducing the transmission from salt to the surrounding rock. This issue needs further investigation.

Signals from the repetitive sources blasting and picking showed generally similar behaviour to the one seen with measurements. Since the force time function of the real sources was not known, it could not be input into the model. To achieve signal strengths at various distances that were comparable to the measured ones, model signals had to be multiplied by considerable factors. This is some form of calibration, but the frequency range in the model is a few hundred hertz whereas the measurements contain frequencies up to a few kilohertz. Also here further study is required.

With source positions as they would be used for access to the potential repository from above or from the side, signals were computed at many more sensor positions, however excluding those that would be too close to the repository. The strengths decreased roughly in proportion to the inverse squared distance, with scatter covering an order of magnitude. Thus for a given detection threshold – in a simple detection scheme – the range could be estimated. But to define such a threshold one needs to know the background – another factor that is not yet known.

To get closer to reliable statements about the required sensor spacing and number, a few issues remain to be investigated. This concerns above all the question of absolute amplitudes, next the seismic background at various potential depths.

Given the relatively strong transmission through the salt dome and across its boundaries to the adjacent rock, already now it seems that the outlook for the utility of seismic monitoring for safeguarding an underground final repository in salt is generally good.

Acknowledgements

I want to thank the Bundesanstalt für Geowissenschaften und Rohstoffe (BGR, Hannover) for providing figures and for allowing the use of their data of the salt-dome surroundings, and the firm bicad (Hannover) for actually providing them, including reactions to several requests. Thanks go to Wolfgang Friederich who heads the Chair of Geophysics, Ruhr-Universität Bochum, and to Andreas Schuck of GGL Geophysik und Geotechnik Leipzig, for valuable advice. I am grateful to Marcel Paffrath, student at the Chair of Geophysics, Ruhr-Universität Bochum, for his work in producing three-dimensional structures from the two-dimensional section. Further I thank Lasse Lambrecht, PhD student at the Chair of Geophysics, for tips in case of program problems. Particular thanks go to the LiDO team at Technische Universität Dortmund; these colleagues gave invaluable advice on the use of the computer cluster, including providing scripts.

This work was funded under task JNT C1611 of the German Support Programme to the IAEA.

Sensor	Medium	Z / kg/(m² s)	R	T	v_{PP} ratio	Distance-corrected
S12	z2HS	$5.72 \cdot 10^6$				
S13	Upper Cretaceous	$4.44 \cdot 10^6$	-0.071	1.071	0.81	0.96
S21	z2HS	$5.72 \cdot 10^6$				
S35	Quaternary/Elsterian	$2.00 \cdot 10^6$	-0.469	1.469	0.83	1.50

Table 4: Impedances Z for P waves at sensors on both sides of a media boundary, ensuing (amplitude) reflection (R) and transmission (T) coefficients, and ratio of the peak-to-peak velocities v_{PP} in x (S12, S13) and z (S21, S35) directions, respectively, plus this ratio corrected for source-sensor distance.

References

[1] Peterson, P.F., Long-term safeguards for plutonium in geologic repositories, *Science & Global Security* **6** (1), 1-29, 1996.

[2] Peterson, P.F., Issues for Detecting Undeclared Post-Closure Excavation at Geologic Repositories, *Science and Global Security*, **9** (1), 1-39, 1999.

[3] International Atomic Energy Agency, *Safeguards for the Final Disposal of Spent Fuel in Geological Repositories*, STR-312, Vienna: IAEA, 1998.

[4] International Atomic Energy Agency, *Monitoring of Geological Repositories for High Level Radioactive Waste*, IAEA-TECDOC-1208, Vienna: IAEA, April 2001; http://www-pub.iaea.org/mtcd/publications/pdf/te_1208_web.pdf.

[5] International Atomic Energy Agency, *Technological Implications of International Safeguards for Geological Disposal of Spent Fuel and Radioactive Waste*, IAEA Nuclear Energy Series No. NW-T-1.21, Vienna: IAEA, 2010, http://www-pub.iaea.org/MTCD/publications/PDF/Pub1414_web.pdf.

[6] Altmann, J., Kühnicke, H.; *Acoustic and Seismic Measurements for the Detection of Undeclared Activities at Geological Repositories – Results from the Gorleben Exploratory Mine*, JOPAG/11.13-PRG-404; Joint Programme on the Technical Development and Further Improvement of IAEA Safeguards between the Government of the Federal Republic of Germany and the International Atomic Energy Agency, Nov. 2013.

[7] Altmann, J.; Seismic Monitoring of an Underground Repository in Salt – Results of the Measurements at the Gorleben Exploratory Mine; *ESARDA Bulletin* no. 50, 61-78, Dec. 2013.

[8] Komatitsch, D., Vilotte, J.P.; The spectral-element method: an efficient tool to simulate the seismic response of two-dimensional and three-dimensional geological structures; *Bull. Seismol. Soc. Am.* 88 (2), 368-392, 1998.

[9] Komatitsch. D., Tromp, J.; Introduction to the spectral-element method for three-dimensional seismic wave propagation; *Geophys. J. Int.*, 139, 806-822, 1999.

[10] Computational Infrastructure for Geodynamics (CIG), Princeton University (USA), CNRS and University of Marseille (France), ETH Zürich (Switzerland); *SPECFEM 3D Cartesian User Manual*, Version 2.1; Sept. 30, 2013, via https://geodynamics.org/cig/software/specfem3d (20 Jan. 2014).

[10] csimsoft; *Trelis — Advanced Meshing Software*; http://www.csimsoft.com/ (29 April 2015). Threshold 0.2 for the shape parameter: warning in the program.

[11] O. Bornemann et al.; *Description of the Gorleben Site Part 3 – Results of the Geological Surface and Underground Exploration of the Salt Formation*, Hannover: BGR, 2008 (via http://www.bgr.bund.de/DE/Themen/Endlagerung/Aktuelles/2011_04_20_aktuelles_gorleben_engl_Part1bis3.html (29 April 2015) (German version: O. Bornemann et al.; *Standortbeschreibung Gorleben Teil 3 – Ergebnisse der über- und untertägigen Erkundung des Salinars*; Geologisches Jahrbuch C73; Hannover/Stuttgart: BGR/Schweizerbart, 2008).

[12] *LiDO – Der Linux-HPC-Cluster an der Technischen Universität Dortmund*; http://www.itmc.tu-dortmund.de/dienste/hochleistungsrechnen/lido.html (29 April 2015).

[13] Bundesanstalt für Geowissenschaften und Rohstoffe (BGR); *Erkundung des Salzstockes Gorleben*; http://www.bgr.bund.de/DE/Themen/Endlagerung/Projekte/Endlagerstandorte/laufend/ Erkundung_Salzstock_Gorleben.html?nn=1550704 (29 April 2015).

Safeguards Indexing Method for the Regulatory Assessment of Safeguards Culture at Nuclear Facilities

Zsolt Stefánka, Hedvig Éva Nagy, Árpád Vincze
Hungarian Atomic Energy Authority
P.O.B.: 676, H-1539, Budapest, Hungary
E-mail: stefanka@haea.gov.hu

Abstract:

The Hungarian Atomic Energy Authority (HAEA) has just introduced a safeguards indexing method for evaluation the safeguards culture at Hungarian nuclear facilities. The main goal of this indexing method is to provide a useful tool for the regulatory body to evaluate the safeguards culture at nuclear facilities. The evaluated parameters are e.g. educational requirement for safeguards staff, quality of safeguards reporting for IAEA and EC, results of safeguards inspections etc. Input of the method is for the one hand the outcome of the comprehensive domestic safeguards verification system consisting of regular comprehensive SSAC verifications of the facilities. The main goals of the comprehensive verification system are: (i) to assess the facilities safeguards system compliance with the relevant national legislation and recommendations, (ii) to assess the activities of the facility aimed at maintaining and further developing its safeguards system and (iii) to revise validity of data and information previously provided by the facility subject to safeguards licensing procedures. On the other hand the annual report of the nuclear facilities also supports the safeguards indexing method, which is a good indicator of the present and future effectiveness of the facility level safeguards system and the level of safeguards culture.

Keywords: safeguards culture assessment, safeguards indexing method, national safeguards system, comprehensive domestic safeguards verification system, SSAC

1. Introduction

The effectiveness and efficiency of a State System of Accountancy and Control (SSAC) greatly depends on how the management in the nuclear facilities is committed to the non-proliferation objectives of the country.

In Hungary safeguards licensing procedures are obligatory to possess nuclear material, launch any activity related thereto, launch any modification important to safeguards, transport nuclear materials, as well as to terminate safeguards requirements in case of terminating nuclear activities. In addition to it, facilities are obliged to maintain a facility level nuclear material accountancy system and create the required conditions for international, regional and national verification activities. It is, however, essential that the above obligations be integral parts of a coherent facility management policy.

Based on very promising experiences in the field of nuclear safety, the Hungarian SSAC has introduced a comprehensive domestic safeguards verification system consisting of regular comprehensive SSAC verifications in the whole lifetime of the facilities [1,2].

The structure, preparation, conduction, documentation and initial experiences of the comprehensive safeguards verification system is introduced below.

Additionally, HAEA has just introduced a safeguards indexing method for evaluation of the safeguards culture at Hungarian nuclear facilities. The main goal of the indexing method and the evaluated parameters are also shown in the paper.

2. The comprehensive domestic safeguards verification system (CDSVS)

The introduction of the comprehensive domestic safeguards verification system (CDSVS) by the Hungarian SSAC started with laying down the procedure of the CDSVS in the Hungarian Atomic Energy Authority's (HAEA) Quality Assurance System. The QA procedure for the CDSVS was approved by the General Deputy Director General of the HAEA. Carrying out CDSV falls into the competence of the Department of Nuclear Security, Non-proliferation and Emergency Management of the HAEA (hereinafter referred to as the Safeguards Department).

2.1 Goal of the CDSVS

The main goal for the CDSVS was defined as follows: to review whether the facility level safeguards system of the organization is ran in compliance with the relevant legal instruments and recommendations in force. To reach this goal two tools are to be applied:

a) to review all the safeguards relevant procedures of the organization. In this review the focus is to check whether procedures for fulfilling the obligations are regulated by internal documentations (e.G. Instructions, procedures) and to find practical examples for the procedures by the competent staff.

b) To assess the activities of the organization in view of whether it ensures sustainability and improvement of the safeguards system in all levels of organisation, with special regards to the commitment on management level.

During the last four years the Safeguards Department of the HAEA conducted comprehensive verification inspection in every Hungarian nuclear facility on annual basis, e.g. in 2011 at the Modular Vault Dry Storage (MVDS) of the Spent Fuel Assemblies, in 2012 at the Paks Nuclear Power Plant, in 2013 at the Training Reactor at the Budapest University of Technology and Economics and in 2014 at the Budapest Research Reactor. Verification of the management systems (highest management and safeguards division management) as well as safeguards relevant areas as operation and maintenance, accountancy and data provision were selected for verification.

2.2 Verification levels

2.2.1 'Level – A' verification

As the primary goal of the verification is to assess the commitment of the highest management, verification 'Level A' was assigned to the top management of the organisation. 'Level – A' verification was planned to assess the commitments of the managers in the field of safeguards and the guarantees provided by the management to enable the organization to meet its safeguards obligations.

A list of issues in 6 themes was provided in advance for the management to help preparation for the on site inspection. Issues were grouped into ten themes. Short description of the issues:

1) External influence (e.g. dependence of meeting their safeguards obligation on political changes, Technical Support Organizations (TSOs); public acceptance of their mission, safeguards in their external communication; possible responses of the organization in case of negative effects.)

2) Objectives and strategies (objectives of non-proliferation relevance, consultation process in drafting strategies, possible future plans on any changes in this field)

3) Management functions and their review (selection criteria in the management, evaluation of proper and improper safeguards related decisions, competences, etc.)

4) Allocation of resources (corporate procurement and/or restructuring with non-proliferation and safeguards aspects)

5) Human resource management (reduction of staff - giving priority to safeguards staff; vacancy and fluctuation in safeguards staff; promotion, reward system for safeguards staff, etc.)

6) Training (professional training possibilities for the safeguards staff, safeguards training for the staff in general, etc.)

7) Knowledge management (ensuring continuity of safeguards staff, communication channels for safeguards knowledge, etc.)

8) Regulation (regulation work processes in view with safeguards obligations, inclusion of safeguards aspects in revision of documents, etc.)

9) Organization culture (evaluation of the performance safeguards related tasks on individuals' appraisal or on organization's level, who performs the appraisal of the individual in the safeguards unit, etc.)

10) Communication (channels of information from external source to the safeguards staff and vice-versa.)

2.2.2 'Level – B verification'

'Level - B' was assigned to different safeguards related fields with the following subdivision:

B1 – Safeguards division (analyses of the safeguards division structure, its relation with the highest managements, scope of competences; educational background and professional training of the safeguards staff; adequate human resource for the related tasks, etc.)

B2 – Operation and maintenance (availability, authentication and maintenance of the measurement equipment to support the accountancy, measures to ensure safe and secure operation of the safeguards containment and surveillance systems, utilization of the organization's own operational experience as well as safeguards experience and research and development activities of other organizations; procedures established to enable national and international inspections, e.g. ground pass systems, safeguards duty system with telephone contact availability, etc.

B3 – Accountancy and data provision (internal procedures regulating the nuclear material accountancy and safeguards related data provision system, operation and reliability of the computer based accountancy system, etc.)

2.3 Schedule of the verification

The CDSV is carried out along the following schedule:

1.) Preparatory phase (review and processing of the related internal documents of the organization)

2.) On site inspection

3.) Assessment

2.3.1 The preparatory phase

The preparatory phase is a very important part of the verification. The Safeguards Department held an initial

meeting to prepare the verification. At this meeting goals of the CDSVS and levels of verification were explained to the representatives of the facilities. Participants of the meeting agreed on collecting the internal documents regulating the tasks of the organization and allocating the responsibilities within the units of the organization. It was agreed that these documents would be provided for the HAEA well in advance of the meeting to enable the staff's preparation for the verification. Potential participants on the on-site inspection both from the HAEA and the facilities were discussed but not finalized.

In the preparatory phase representatives of HAEA for the on-site inspections will study the internal documents of the facilities and finalize the list of issues on the areas assigned to them.

2.3.2 The on-site inspection phase

The on-site inspection is planned to be conducted according to the following agenda:

– Kick-off meeting – information on the goal and areas of inspection, and the methods to be applied
– Inspections to be conducted
  - with participants identified in advance
  - based on list of issues for revision (While level – A issues were handed over in advance, list of issues for the level – B areas will be used for the on-site inspection only)
  - detailed records on answers and other observations will be prepared by the inspectors
– Closing meeting – A preliminary evaluation will be given. There will an opportunity for the licensee to argue the preliminary evaluation results.

2.3.3 Assessment phase and corrective actions

After the on-site inspection, the HAEA will finalize the report on the inspection and send it to the facilities for comments. The report focused on identifying best practices and deficiencies, if any, and clearly state the authorities positions on how to make corrective actions. The facilities shall comment on the main findings and formulate its position on the HAEA's conclusions and recommendations. Moreover, facilities shall identify the means and timeframe of the corrective actions to be performed. Taking the response and proposal from facilities full into account, the HAEA will issue a regulatory resolution on the corrective actions to be taken and determine deadlines for each. In addition the HAEA will establish the next review program of the CDSVS focusing on those areas where corrective actions were identified.

3. The Safeguards Performance Assessment Index for evaluation the safeguards culture

The Safeguards Performance Assessment Index (SPAI) for nuclear facilities has been developed by the Hungarian Atomic Energy Authority for the facilitation of the periodical comprehensive regulatory review of the performance of the operators' safeguards system. The parameters included into SPAI were selected on the basis of objectivity, availability and operability.

The SPAI is designed to be compatible with the system that was developed for the safety performance assessment of the facilities, therefore the comprehensive assessment of the facilities including safety, security and safeguards will be possible in the future.

Definitions:

- Safeguards Assessment Index (Index): a particular value determined by one or several characteristics of the performance of the facility's safeguards system.
- Safeguards Characteristics (Characteristics): A classification value based on quantitative data determined by the individual rule of assessment.
- For the assessment of safeguards characteristics, four rates are defined, as follows:
- **Acceptable:** A safeguards characteristic is acceptable if the authority finds the level of performance such that no corrective actions are required. A safeguards characteristic marked with green colour indicates compliance with all of the relevant regulatory requirements. This rating may show a good practice as well where the facility is proactive and shares a good practice leading to efficient performance without any regulatory requirements.
- **Alarming:** A safeguards characteristic is alarming if there is a slight deviation from the desired value within the regulatory permissible set of values. Though only minor mistakes but no serious issues exist yet, characteristics falling into the yellow zone may need improvement. The licensee shall be instructed to set up a plan of actions to make the necessary improvements. As a response to the plan of actions the regulatory body sends a written notice to the licensee calling for the implementation of the plan of actions. Execution of the required actions are to be checked in the course of regulatory inspections.
- **Not acceptable:** It means that the safeguards characteristic is not acceptable. Rating in the red zone refers to a non-compliance, however, only characteristics covered by regulations may be qualified as red. If a safeguards characteristic has been assessed as red, an explanation is required on what occurred, exact time and date when the non-compliance occurred, its consequences and measures taken by the regulatory authority. The licensee

is obliged to set up a plan of actions which will be then sent back by the regulatory body in the form of a regulatory notice, including additional measures considered to be important by the regulatory body. Execution of the required actions shall be checked in the course of regulatory inspection.

- **Not known:** The system of safeguards index is the same for all nuclear facilities. It may occur, however, that certain characteristics of the index are not relevant for every licensee. In this case characteristics not relevant for the facility are marked white.
- Margins for a four-grade zone will be individually determined for the different characteristics. In case of several characteristics determined for a Safeguards Assessment Index, the index gets the same rating as its characteristic with the worst assessment among all.

3.1 Areas of the assessment

The areas assessed by SPAI for nuclear facilities covers the three major parts of the facility safeguards system, (i) safeguards organisation; (ii) operation of the safeguards system; (iii) safeguards licensing procedures. In the following section the assessment indexes, characteristics and evaluation criteria for the above mentioned three assessment areas are introduced.

3.1.1 Safeguards organisation

An effective safeguards organization needs the sufficient number of staff who are able to substitute each other's place and who have appropriate knowledge on nuclear safeguards. Based on this the HAEA defined two indexes: a) The number of staff and b) Training.

These assessment indexes are described with two characteristics in detail: a) The number of staff, substitution which is a quantitative characteristic of the safeguards organization (number of staff, order of substitution within the safeguards organization, ensuring preparedness outside working hours) and b) The requirements for competence of safeguards officer which is a qualitative characteristic of safeguards organization (quality of training for the new staff and to maintain the safeguards knowledge, its frequency, education background, etc.).

Evaluation of the quantitative characteristic of the safeguards organization

Rule of quantification: Ratio of the number of safeguards relevant tasks and the available number of qualified staff. Quantitative assessment of the safeguards organization is made based on the number of the tasks performed by the safeguards staff. Safeguards tasks performed within the given period of time are summed and the number of safeguards relevant tasks (inspections, reports, licensing procedures) incumbent for one person within the given period of time is checked.

Comments: The value is based on good practice. The preceding four years (2009-2012) were evaluated for an acceptable level of operation of safeguards organizations and the average results of the four years were considered as appropriate. Classification values were defined accordingly.

Evaluation of the quantitative characteristic of the safeguards organization

Rule of quantification: Relative percentage of compliance of the staff with the required trainings.

Comments: The required qualification and trainings should always be satisfied.

3.1.2 Operation of the safeguards system

The safeguards system includes nuclear material accounting system that produce the accounting data at facilities; administrative controls (such as collection and submittal of BTC) and the results, experience and follow up actions of inspections. These are described with the following indexes: a) Nuclear material accountancy system (reports), b) Information provision system (BTC, Additional Protocol), c) Conclusions of the inspections. All of these assessment indexes are defined with the help of different characteristics. The index of the Nuclear material accountancy system is evaluated by the characteristics of the i) Correctness of reports sent (error lines, correction lines) and ii) On time delivery of reports (late lines). Similar method was used to evaluate the index of Information provision system (R&D, site description, waste). The two applied characteristics are the i) Correctness and completeness of information submitted (requirements for additional data, corrections, etc.) and the ii) On time delivery of information, declaration. The third index which feature the operation of the safeguards system is the Experience of inspections. This is described with the characteristics as the i) Conditions provided for inspections (ground pass, access to nuclear material, clear spent fuel pond water, etc) and ii) Non-compliance discovered in course of inspections (discrepancies, anomalies).

Evaluation of the Nuclear material accountancy system

i. Correctness of accountancy data transmitted

   Rule of quantification: Relative percentage correct and inadequate reports

ii. On time delivery of reports

   Rule of quantification: Relative percentage of accountancy reports sent on time and those sent beyond the time limit

   Comments: The index is marked with the colour of the characteristic assessed as the worst. If a report is not transmitted on time, time-limit of the accountancy report is be marked as yellow, and in this case the indicator of the accountancy system cannot be better than yellow.

Evaluation of the Information provision system (R&D, site description, waste)

i. Correctness and completeness of information submitted (Provision of information)

   Rule of quantification: Relative percentage of information submitted in compliance and those in non-compliance

   *Comment*s: Provision of information subject to Additional Protocol are analysed

ii. On time delivery of information, declaration

   Rule of quantification: Relative percentage of declarations sent on time and those sent beyond the time limit

   Comments: Provision of information subject to Additional Protocol is checked. The index is marked with the colour of the character assessed as the worst. If any of the information is not transmitted on time, time-limit of the information provision is be marked as yellow, and in this case the indicator of the information provision system cannot be better than yellow.

Evaluation of the Experience of inspections

i. Facilitating inspections

   Rule of quantification: Relative percentage of inspections where all the conditions necessary for an inspection were provided for and of those that lacked one or some of the conditions.

   Comment: Conclusions of the inspections are drawn based on the evaluation of the inspection reports

ii. Non-compliance found in course of the inspections

   Rule of quantification: Relative percentage of inspections where no anomaly was found and inspections where anomalies were experienced by the inspector.

   Comments: Conclusions of the inspections are drawn on the evaluation of the inspection reports

3.1.3 Safeguards licensing procedures

The Hungarian SSAC contains four types of safeguard licenses. A first safeguards license issued by the HAEA is necessary to possess nuclear material and launch any activity related thereto.

A safeguards modification license is required to launch any important safeguards relevant modification.

For the transport of nuclear materials not requiring export-import license according to separate regulation to and from the territory of the Republic of Hungary a safeguards transport license is necessary.

A safeguards termination license is issued for the termination of safeguards requirements subsequent to termination of nuclear activities.

To evaluate the safeguards licensing procedures from the site of the licensee we use two assessment indexes: a) the Regulatory measures/resolutions and b) Meeting regulatory deadlines. These indexes are mostly the same as the characteristics which we use for evaluation: i) Regulatory measures (execution of regulatory measures, requests for additional information by the regulatory authority to make the licensing documentation complete, licensing applications refused by the regulatory authority) ii) Deadlines (meeting the regulatory time-limits).

Evaluation of the Execution of measures requested by the regulatory body

Rule of quantification: Content and administrative compliance of safeguards relevant applications with legal requirements. Ratio of applications in compliance and those in no-compliance with the requirements.

Comments: The value is based on good practice. The preceding four years (2009-2012) were evaluated for acceptable level of operation of safeguards organizations and the average results of the four years were considered as appropriate. Classification values were defined accordingly.

Evaluation of the Deadlines

Rule of quantification: Meeting the time limits defined by relevant regulations or the regulatory authority for the safeguards licensing applications (e.g. first safeguards licence, requests to complete licensing documentation, etc.) Ratio of documents submitted within and beyond the required time-limits.

Comments: The value is based on good practice. The preceding four years (2009-2012) were evaluated for acceptable level of operation of safeguards organizations and the average results of the four years were considered as appropriate. Classification values were defined accordingly.

4. Conclusion

The new comprehensive domestic safeguards verification system was introduced in 2011. Based on the experiences collected during the four years period it can be concluded that the new program has reached the following objectives:

- The management became more aware of its safeguards obligation. 'Level – A' list of issues helps the management to analyse the set of documents of the facility, from the organization's strategy documents to the low level internal documents. Safeguards related scope of competence needs to be assessed from the top management level to the safeguards officers' level.
- Review all the safeguards relevant procedures of the organization helps to disclose the possible gaps in the

regulation of the procedures or in the scope of competence.

- The need for sustainability of the safeguards system and to improve in performance at all levels within the organization will clearly be highlighted through the whole verification process.

The nuclear safeguards indexing method was designed using the experience collected from the nuclear safety indexing method, therefore using both methods an integrated assessment can be carried out. Moreover, the developed nuclear safeguards indexing method helps the authority to assess the safeguards culture at the specific site.

In this way improving the nuclear safeguards culture in the organization is expected to get the same importance as nuclear safety and security culture.

5. References

[1] E. SZÖLLÖSI, G. RÁCZ, Zs. STEFANKA, Á. VINCZE, K. HORVÁTH
Assessing and Promoting the Level of Safeguards Culture in Hungarian Nuclear Facilities, 2011 33rd ESARDA Annual Meeting, Budapest

[2] Assessing and Promoting the Level of Safeguards Culture in Hungarian Nuclear Facilities
Zsolt Stefánka, Árpád Vincze. IAEA Safeguards Symposium 2014, Vienna

Potential Causes of Significant Inventory Differences at Bulk Handling Facilities and the Importance of Inventory Difference Action Levels

Alan Homer, Brendan O'Hagan

Nuclear Materials Accountancy & Safeguards Department
Sellafield Limited, Seascale
Cumbria, CA20 1PG, United Kingdom
E-mail: alan.homer@sellafieldsites.com

Abstract:

Accountancy for nuclear material can be split into two categories. Firstly, where possible, accountancy should be in terms of items that can be transferred as discrete packages and their contents fixed at the time of their creation. All items must remain accounted for at all times, and a single missing item is considered significant. Secondly, where nuclear material is unconstrained, for example in a reprocessing plant where it can change form, there is an uncertainty that relates to the amount of material present in any location. Cumulatively, these uncertainties can be summed and provide a context for any estimate of material in a process. Any apparent loss or gain between what has been physically measured within a facility during its physical inventory take and what is reported within its nuclear material accounts is known as an inventory difference. The cumulative measurement uncertainties can be used to set an action level for the inventory difference so that if an inventory difference is observed outside of such action levels, the difference is classified as significant and an investigation to find the root cause(s) is required. The purpose of this paper is to explore the potential causes of significant inventory differences and to provide a framework within which an inventory difference investigation can be carried out.

Keywords: inventory difference; action levels; uncertainty; measurement; investigation

1. Introduction

Accountancy for nuclear material falls into two categories. Firstly, where possible, accountancy is in terms of 'items', that can be transferred as discrete packages. Their contents are fixed at the time the discrete package is created. Generally, items are recognised in terms of being containers that can be counted, for example a uranium drum, a plutonium can, or a transport flask. The safeguards criteria for areas where the nuclear material contents are only in the form of items is uncomplicated. Items are counted into and out of the area and all items must be accounted for. A single missing item is considered significant. Similarly, if an item was tampered with and the tampering was detected through containment and/or surveillance measures then this would also be a significant incident.

Where nuclear material is unconstrained, for example as part of a process within a reprocessing facility, then there is an uncertainty in any measure that relates to the amount of nuclear material present. Cumulatively these uncertainties can be summed and can provide a context for any estimate of material in the process. In summary, the aim is to know how much nuclear material is present by measurement and the level of confidence in that measurement by analysis of the uncertainty so as to demonstrate that the area is in control and to detect losses or diversion of nuclear material.

The difference between what is physically measured within a facility at a physical inventory take (PIT) and the amount of nuclear material declared within its nuclear material accountancy system is known as the inventory difference (ID). The uncertainty of measurement in the ID, σ_{ID}, defines what is known as the inventory difference action level (IDAL). Typically the IDAL is quoted at the k equals 3 confidence level (99.73% confidence), i.e. 3 σ_{ID}.

2. The Basic Units

For the remainder of this discussion, everything will be viewed in terms of quantity and proportion:

- Quantity is usually either volume or mass, however it can be the result of a more complicated indirect measurement system e.g. mass is equal to volume multiplied by density in plutonium nitrate (PuN) liquor transfers.
- Proportion is the concentration of a particular accountable nuclear material contained within an amount of some other substance e.g. the amount of plutonium in plutonium dioxide (PuO_2) powder.

Whether the nuclear material in question is an inventory item or the amount of nuclear material being transferred into or out of an area (a transaction), the nuclear material quantity is calculated in the same way, nuclear material is equal to quantity multiplied by proportion. For example, if a uranium trioxide (UO_3) drum contains 800 kg of UO_3, and its uranium assay is 88% (a proportion of 0.88), then 88% of the material in the drum is uranium, 704 kg.

3. What is Inventory Difference?

A minimum of once per calendar year (and at intervals of not greater than 14 months), each material balance area (MBA) will shut down normal operations, move its nuclear material into an area where it can be measured and verified, and perform a PIT. During the period since the previous PIT, the nuclear material accountants will have maintained a book account (BA) where

Book **A**ccount = **O**pening Physical **I**nventory + **R**eceipts – **S**hipments (Eq. 1)

where the opening physical inventory (OI) is the amount of nuclear material in the MBA at the time of the previous PIT, and receipts (R) and shipments (S) are the amounts of nuclear material moved into and out of the MBA since the previous PIT. The results of the PIT (the closing physical inventory, CI) are then compared with the book account. Theoretically these values should be identical, however in practice they usually differ producing an ID where:

ID = CI – BA

= CI – (OI + R – S). (Eq. 2)

If there were no uncertainties involved with this process i.e. all measurements were exact, then the ID should be zero because everything would add up as expected. However, an observed non-zero ID will commonly occur because it is not possible to measure all material exactly. The root cause of an ID can be due to many factors, some of which are examined later in this paper.

4. What is an Inventory Difference Action Level and why do we need it?

As nothing can be measured exactly, there are uncertainties associated with each measurement of inventory, receipts, and shipments. These uncertainties can be combined to calculate the total uncertainty on the ID, σ_{ID} (using Eq. 2). If the measured ID falls within the bounds given by the overall measurement uncertainty, usually $\pm 3\sigma_{ID}$, then the data support a theory that the apparent difference is due to measurement uncertainty rather than a true difference. The IDAL is the maximum acceptable ID based on measurement uncertainty. If the ID is outside of these bounds then the difference must be investigated.

It is important that all measurement uncertainties for inventory, receipts, and shipments are technically justified. This means that the uncertainties are underpinned with calibration data or reviewed technical papers justifying the parameters used. International Target Values (ITVs) [1] (which incorporate both random and systematic uncertainties) are primarily used as targets but can be used as a starting point for estimating uncertainties. The IDAL is required to ensure the plant is in control, and, in the event of loss of control, to start an investigation to determine the cause.

5. Who Needs an Inventory Difference Action Level?

Process facilities have nuclear material that is unconstrained (i.e. not confined to discrete containers), as the material is in a constant state of flux between holding vessels, with the material often undergoing a change in form. The measurement uncertainty then accumulates with each measurement which makes up the receipts, shipments, and inventories. This can lead to an ID and hence an IDAL is required in these facilities.

Storage facilities do not need an IDAL since the material is constrained in containers such as drums and cans. There is however a need to count the containers to ensure none are missing. Exact knowledge of the number of containers does not imply exact knowledge of their contents. When the containers are put into the storage facility, the amount of material in each container is recorded in the inventory. Each container will have its own uncertainty which leads to a global uncertainty for the store. Take for example a PuO_2 storage can which consists of an inner can, a polyethylene bag and an outer can. The amount of nuclear material in the can is the gross mass minus the tare masses of the two cans and the bag making up the overall package. If the polyethylene bag masses were systematically being reported incorrectly, then the amount of nuclear material claimed to be in the store would be incorrect even though it can be confirmed that what went into the store is still in the store.

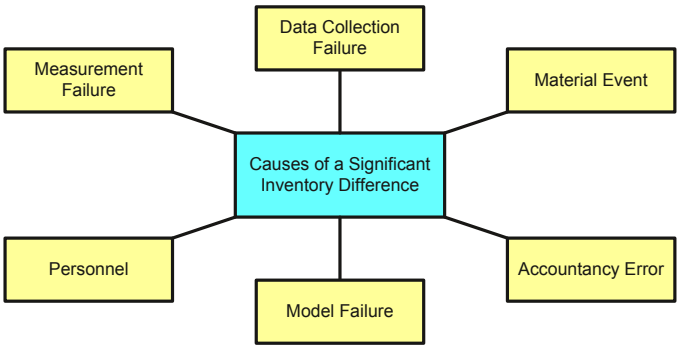

Figure 1: A diagram illustrating the main reasons why an inventory difference may arise.

The storage area would not register an ID because the item count and the product can gross masses would be correct, but the issuing MBA would show a consistent ID as the shipments would be systematically biased. This type of problem is difficult to identify and the exact nature of the problem may only become truly apparent if the store and its contents are re-measured.

6. Causes of Inventory Difference

This work categorizes the main reasons why a significant ID may occur into six areas, shown diagrammatically in figure 1. It is not sufficient to identify a single cause without considering all contributory factors. Figure 2 shows that there are significant links that should be considered and it is worth noting that many of them lead back to the "personnel" category. These interconnections and the finer details are discussed throughout the remainder of this paper. If learning from experience is to have any meaning then it is important that all linking parts are examined.

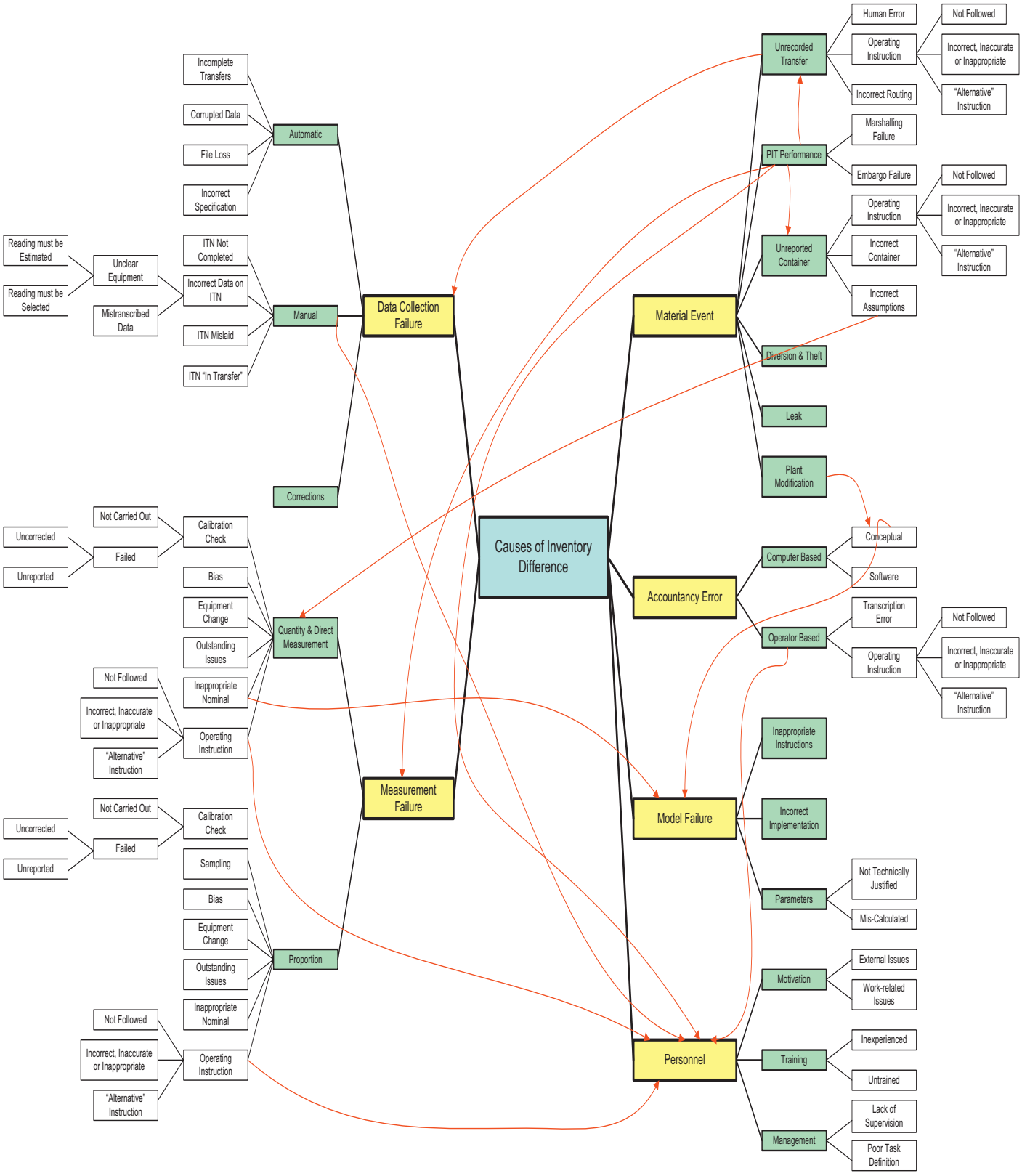

Figure 2: A diagram to illustrate potential causes of significant inventory difference and some of their various inter-dependencies.

When a potentially true non-zero ID is identified (i.e. an ID falls outside of the bounds of a calculated IDAL) an investigation must take place to explain what has happened within the associated material balance period (the period between two consecutive PITs). At Sellafield, the following framework for an investigation has been developed. The first phase of any ID investigation focuses on three main areas:

- Has there been a nuclear material event?
- Has there been a data collection failure?
- Has there been a failure of the nuclear materials accountancy model.

These questions will be considered in more detail in sections 6.1 – 6.3. If any of the questions are answered in the affirmative then they should be addressed immediately, the ID recalculated and if the issue is not resolved, the investigation should move into a second phase which is discussed in more detail in sections 6.4 – 6.6.

The second phase of the investigation focuses on whether or not there been a measurement failure, an accountancy error, or if there are any personnel issues with people involved. Generally, the most common cause of a significant ID is related to measurement as particularly for flows, small errors can accumulate over a long campaign into very substantial amounts. It should also be remembered that, although measurement issues can also be associated with inventory measurements, these would apply to both opening and closing inventories and therefore the error would be associated with the difference between opening and closing values. Given that, under most circumstances, the facility should be minimising its inventory and/or ensuring nuclear material is in a measurable form and location to minimise any process hold up, the status of a facility at PIT is usually fairly constant and this difference between opening and closing inventories is not usually that large.

6.1 Nuclear Material Event

Of all of the potential causes of a significant ID, a nuclear material event is the most crucial. The underlying premise of a nuclear material event is that nuclear material is not where it is expected to be.

6.1.1 Diversion and Theft

From a safeguards perspective the worst scenario is that nuclear material has been diverted or stolen. Good practice is that any investigation should start from a position of no diversion or theft has occurred. It is essential to inform the security department as soon as there is thought to be an apparent breach of IDAL. This allows the security department to perform any preliminary investigations they see necessary and feedback their findings to provide assurance to the nuclear material custodian / controller, and through them to other stakeholders.

6.1.2 Nuclear Material Leak

The nuclear material custodian / controller should arrange for those with direct oversight of the various areas within an MBA to perform a visual check of plant areas. Where a direct visual check is not possible, assurance should be sought through indirect measures such as sump checks, neutron monitor alarms etc. looking for any unusual readings or behaviours. Checks for material leaks should also include the possibility that key measurement points have been bypassed.

6.1.3 PIT Performance

When a PIT is performed, best practice informs that all movements should be halted in an area. In practice however, movements are often still required between a PIT and physical inventory verification (PIV). All such moves should be recorded and provided to the safeguards inspectorates before the PIV is initiated. Failure to correctly record moves or lack of communication between the facility, the nuclear material custodian / controller and the nuclear materials accountancy and safeguards (NMAS) department can easily lead to nuclear material being mislaid or double counted, its location being recorded incorrectly, and general confusion surrounding nuclear material control. Long term trending of ID performance also allows detection of potential process bias.

6.1.4 Unrecorded Transfer and/or Unreported Container

An unrecorded transfer would tend to be caused by a procedural breakdown when a nuclear material move takes place with no paperwork generated, paperwork going astray, or a failure in an automated transfer system. An unreported container could be described similarly but in actuality would include finds[1] of nuclear material. The nuclear material status of a facility is recorded on a list of inventory items (LII) and the nuclear material custodian / controller must ensure that there is a direct correlation between the LII and the facilities physical layout. For example, it can be easy to overlook a sweepings container in a glovebox if it is normally present and empty. Similarly, the assumption that a hopper is empty is open to challenge if no physical assessment has been made and / or the location is unverifiable. Consideration must also be given to possible material hold up in process pipes, filters etc.

6.1.5 Facility Modification

Nuclear materials accountancy is based on a shared model with the actual facility. The nuclear material custodian / controller is responsible for the control of nuclear material in their area and therefore must inform the NMAS department of any modifications to the facility. There is also a regulatory obligation to inform the safeguards

[1] A “find” is unforeseen nuclear material which is found in a material balance area.

inspectorates in a timely manner to ensure they can verify such modifications. If there is disconnect between the facility model and the nuclear materials accountancy system then transfers could be lost and nuclear material stored in inventory locations missed.

6.2 Data Collection Failure

The premise of data collection failure is that the nuclear material is where it should be but there has been a process failure in collecting the data.

6.2.1 Manual Failure

Data is always recorded in some manner and failure to complete, process and record the data is not necessarily easy to detect. Such failures may only be identified through a check within the facility for missing or extra inventory items against the LII. Mislaid or in-transfer documentation is easier to identify if documents used for nuclear materials accountancy purposes have a sequence number which can be checked. The latter should become clear to the NMAS department when performing a check of documentation received. At this time the NMAS department should also perform a quality check of the data received to identify transcription errors e.g. wrong decimal places recorded or figures incorrectly transposed.

6.2.2 Automatic Failure

The initial testing and commissioning of automatic data transfer should be sufficient to give confidence in a systems performance, however, if a facility suffers an unexpected outage it is possible for errors to occur. Data may be lost or incorrect shutdown and restart procedures can give rise to file corruption or loss. Care must always be taken in the event of a power failure or unplanned shutdown to ensure that there is no effect on data transfer.

6.2.3 Corrections

All corrections made to nuclear materials accountancy documentation should be countersigned and be fully traceable. Similarly, where changes are made in the nuclear materials accountancy system, they should be logged, with an explanation to allow traceability in the event of an investigation.

6.3 Model Failure

The premise of a model failure is that measurements have been made correctly and the nuclear material is correctly located, but the interpretation of that data is inappropriate in some way. The nuclear material custodian / controller should commence an investigation utilizing both facility technical support and NMAS department as early as possible within the investigation. Such an investigation will effectively undertake a qualitative check on the nuclear materials accountancy model.

6.3.1 Inappropriate Assumptions

When a measurement is made there are almost always some associated assumptions. For example, it is a reasonable assumption that the surface of a liquid is flat in a large vessel though not when estimating a level of a receptacle with a narrow diameter. Similarly, a container holding powder is unlikely to have a level surface where material has recently been dispensed. Also, powder in a vessel will typically compact when left to settle, resulting in the density being different at the top and bottom causing sampling issues. The nuclear materials accountancy model must reflect physical reality as accurately as possible. Shipper–receiver differences must also be considered. If any differences are not measured appropriately then the receiving facility is at risk of absorbing any difference initiating at the issuing facility into its own ID.

6.3.2 Incorrect Implementation

Generally, testing of software or spreadsheets which manipulate data should have been sufficiently detailed to ensure that the process exactly replicates manual calculation. It is possible, nonetheless, to generate incorrect data, especially if the implementer of the system and the user do not share a common set of assumptions. Equally important here is a review of the IDAL calculation itself because failure to capture all relevant details or incorrect estimations of associated uncertainties (both random and systematic) can lead to an ID uncertainty that is artificially small or large and consequently an IDAL that is simply unattainable or unrealistic.

6.3.3 Model Parameters

Where data manipulation takes place that involves the use of parameters (e.g. the inclusion of a dilution factor in a calculation to account for a steam ejection pump transfer) then these parameters should be supported by a technical justification. Any that do not have an associated technical justification should be flagged for consideration.

6.4 Measurement Failure

The premise of measurement failure is that the nuclear material is where it should be but there has been an error in measuring the quantity or proportion of the material. Before investigating beyond that expected from our understanding of metrology, the probability of contribution of every measurement to an ID, whether that be a material flow or inventory location, should be considered. By producing a list of all flows and inventory locations, a simple rule to prioritise areas of interest could be to assign the observed ID to each flow and inventory location and ask the question, what would it take to generate an ID of that magnitude from that specific flow or inventory point and what are the implications?

Such analysis should identify the most probable areas where measurement failure could produce or impact on ID and therefore provide some focus for the investigation. This does not mean that smaller effects should be ignored, in fact small bias effects can have significant effects in plants with high throughput and where identified they should still be corrected, but the most appropriate areas of concern should be targeted first.

6.4.1 Quantity and Direct Measurement

In general the first thought with quantity measures should be to analyse the routine verification activities of the measurement system. With weighing systems this should be relatively straightforward, with traceable evidence that the system has been recently calibrated and routine checks between calibrations have been performed to ensure the system is working as expected. With large vessels, and in general volumetric calibration, it may be extremely difficult to recalibrate after initial commissioning. The best option may be an inter-tank transfer comparison with other tanks in the processing stream.

Additional issues may occur where non-destructive analysis (NDA) equipment shares a joint function with safety and nuclear materials accountancy. Measurements generated for safety reasons can be deliberately biased to incorporate a 'worst-case' scenario for criticality purposes. Where such readings are used for nuclear materials accountancy without reference to a 'best estimate', these biases can accumulate. For example, PCM packets with an absolute plutonium content of less than half a gram should generate a zero accountancy value but the measurement system may typically record accountable quantities for safety purposes. It does not take many packets over a material balance campaign to generate a 1 kg ID.

6.4.2 Proportion

Where analysis for assay, concentration, or density takes place then it is important to confirm that no changes in the measurement process or equipment have occurred as these can affect both ID and IDAL. It is essential that samples taken are representative and that they are homogenous. Where possible, some repeat analysis for large bulk samples is useful confirmation as is the use of alternative procedures to ensure consistency and negligible bias. A small bias is expected and is a fundamental limitation of nuclear materials accountancy.

6.5 Accountancy Errors

6.5.1 Computer-Based Errors

Computer based errors fall broadly into two areas, the first being conceptual issues. If there has been a plant modification, or change to a measurement process, does the accountancy system reflect physical reality? If not, there is a fundamental failure of the accountancy model and these changes can propagate errors throughout the accountancy system which could potentially result in material being unaccounted for, double counted or in the case where incorrect parameters are set in the underlying nuclear materials accountancy system code, incorrect data.

The second issue relates to the actual software itself which computes the nuclear material accountancy records. Where software is upgraded or operating systems are changed, robust testing of the accountancy system is required to ensure there are no bugs in the system. This is especially important when dealing with legacy accountancy systems which may have limited technical support and the expertise is not available to support transfer of the systems.

6.5.2 Operator-Based Errors

Ideally all nuclear materials accountancy systems would utilize automatic data capture and an operator or nuclear materials accountant would be responsible for peer-review and data verification. In many cases, especially with older plants, manual data entry by both plant operators and nuclear materials accountants is still required. An obvious error trap with manual data entry is transcription errors which can be difficult to recognise and correct. Therefore, a robust peer-checking process is essential.

The importance of clear, robust operating instructions must also be emphasized. Where operating instructions are not followed, are incomplete, inaccurate, inappropriate or there are multiple instructions for the same task, mistakes are likely to occur. Such issues also result in a lack of transparency, consistency and accuracy which is necessary for good nuclear materials accountancy.

6.6 Personnel

People work within systems and if those systems are properly constructed, supervised, and appropriate training provided, then mistakes are less likely to happen. However, there always remains the 'human factor' meaning errors cannot be totally eliminated. To mitigate the propagation of repeatable errors it is good practice to undertake regular debriefs and post job reviews to ensure any LFE is captured.

A key personnel issue worth considering in an investigation is motivational issues. Are the individuals involved focussed on the task at hand? Has enough time been allocated to the operators for completing the PIT and the nuclear materials accountants for producing the relevant reports to the required quality? Secondly, are the individuals involved with the PIT, suitably qualified and experienced. Mistakes can happen with both inexperienced and experienced personnel and it is key that all people involved with nuclear materials accountancy are aware of and maintain an awareness of their responsibilities and the

impact that their actions may have. Finally, from a management perspective adequate supervision must be ensured to drive a high standard of plant condition at the time of the PIT, accountancy data is kept up to date and people involved have clear task definition.

7. Conclusions

The conclusions of this paper are as follows:

- In item accountancy areas of a facility, an IDAL is not required. A single missing item is considered significant, and an investigation required.
- In process areas of a facility, where material is changing form and measurements are being made, an IDAL is required. All measurements have an uncertainty and it is the cumulative sum of these uncertainties for all receipts into an area, shipments out of an area and for inventory measurements at a physical inventory take which determine the IDAL.
- An IDAL will change from one material balance period to the next as it depends on plant throughput and the amount of inventory change between successive physical inventory takes.
- If an ID falls outside of the bounds of a technically justified IDAL then an investigation should be performed.
- There are many potential causes of ID and this paper categorizes them into six key areas:
    1. Material Event
    2. Data Collection Failure
    3. Accountancy Error
    4. Measurement Failure
    5. Model Failure
    6. Personnel Issues
- Many causes of ID are interlinked and identifying the root causes of an ID is a complex task which must be fully examined. If a potential contributing cause to an ID is identified early in an investigation, it should still be completed in its entirety to ensure all contributing factors are captured.

8. Privacy regulations and protection of personal data

The author agrees that submission of this work automatically authorises ESARDA to publish the work in whole or in part in all ESARDA publications – the bulletin, meeting proceedings, and on the website.

The author declares that this work is original and not a violation or infringement of any existing copyright.

9. References

[1] International Atomic Energy Agency, *International Target Values 2010 for Measurement Uncertainties in Safeguarding Nuclear Materials*, STR-368, Vienna, November 2010.

Nuclear Forensics Technologies in Japan

N. Shinohara, Y. Kimura, A. Okubo and H. Tomikawa

Japan Atomic Energy Agency
Tokai, Ibaraki 319-1195, Japan
E-mail: shinohara.nobuo@jaea.go.jp

Abstract:

Nuclear forensics is the analysis of intercepted illicit nuclear or radioactive material and any associated material to provide evidence for nuclear attribution by determining origin, history, transit routes and purpose involving such material. Nuclear forensics activities include sampling of the illicit material, analysis of the samples and evaluation of the attribution by comparing the analysed data with database or numerical simulation. Because the nuclear forensics methodologies provide hints of the origin of the nuclear materials used in illegal dealings or nuclear terrorism, it contributes to identify and indict offenders, hence to enhance deterrent effect against such terrorism. Worldwide network on nuclear forensics can lead to strengthening global nuclear security regime.

In the ESARDA Symposium 2015, the results of research and development of fundamental nuclear forensics technologies performed in Japan Atomic Energy Agency during the term of 2011-2013 were reported, namely (1) technique to analyse isotopic composition of nuclear material, (2) technique to identify the impurities contained in the material, (3) technique to determine the age of the purified material by measuring the isotopic ratio of daughter thorium to parent uranium, (4) technique to make image data by observing particle shapes with electron microscope, and (5) prototype nuclear forensics library for comparison of the analysed data with database in order to evaluate its evidence such as origin and history. Japan's capability on nuclear forensics and effective international cooperation are also mentioned for contribution to the international nuclear forensics community.

Keywords: nuclear forensics; impurity; isotopic composition; age determination; database

1. Introduction

International incidents of illicit trafficking in nuclear and other radioactive materials are increasing from the 1990's according to IAEA database [1]. Domestic technologies against such illicit trafficking of nuclear material and radioactive substances must be established for supporting criminal investigation and prosecution for security and maintenance of public peace even in Japan. When illicit trafficking of nuclear material happens in a third-country in future, there is possibility that the nuclear material is suspected to be stolen in Japan because we have various nuclear facilities and multiplex nuclear materials. Japan's own technology for nuclear forensics (NF) should be retained in order to keep reliance of our nuclear activities.

Japan Atomic Energy Agency (JAEA) has engaged in research and development activities of NF for strengthening nuclear security in accordance with Japan's national statement at the Washington Nuclear Security Summit in 2010 [2]. The JAEA has developed analytical methods for measurement of isotopic abundance and impurity in nuclear material in order to identify its source and determine the point of its origin and routes of transit. Joint researches with the US national laboratories have been implemented in the fields of uranium age dating measurements, characterization of nuclear fuel for forensics purposes, and establishment of a proto-type national NF library. In this paper, capabilities of the NF technologies in Japan are presented for the purpose of sharing our experience with international NF community.

2. Development of nuclear forensics technologies

The JAEA has developed the fundamental technologies for NF from 2011 to 2013, namely (1) technique to analyse isotopic composition of nuclear material, (2) technique to identify the impurities contained in the material, (3) technique to determine the age of the purified material by measuring the isotopic ratio of daughter thorium to parent uranium, (4) technique to make image data by observing particle shapes with electron microscope, and (5) prototype nuclear forensics library for comparison of the analysed data with database in order to evaluate its evidence such as origin and history.

2.1 Isotopic composition of nuclear material

Isotopic abundances of nuclear material can be measured by means of Thermal Ionization Mass Spectrometry. A mass dependent bias observed in this analytical technique was previously corrected by measuring well characterized standards. Total evaporation (TE) is, however, an excellent analysis technique for the measurement of uranium isotopic ratios, where highly precise and accurate data can be obtained because the mass dependent bias is

Uranium Isotopic Standards	Atom Percent			
	^{234}U	^{235}U	^{236}U	^{238}U
NBL U500 Certified Value	0.5181±0.0008	49.696±0.050	0.0755±0.0003	49.711±0.050
Our Measured Value	0.5187±0.0001	49.703±0.004	0.0760±0.0001	49.703±0.007
NBL U050 Certified Value	0.0279±0.0001	5.010±0.005	0.0480±0.0002	94.915±0.005
Our Measured Value	0.0279±0.0001	5.011±0.001	0.0482±0.0001	94.913±0.001

Table 1: Isotopic abundances of uranium standards of CRM U500 and U050.

neglected [3]. This TE technique has been demonstrated for isotope ratio measurements of uranium using well characterized Certified Reference Materials (CRMs) of U500 and U050 from New Brunswick Laboratory (NBL). The certified values and our results are shown in Table 1. It is concluded that the TE technique is applicable to the NF analysis of illicit nuclear materials. The TE technique has been applied to the analyses of several kinds of uranium (yellow cake, ammonium diuranate (ADU), UO_2, UO_3, U_3O_8) possessed in JAEA. The measured data was stored in database of our NF library.

2.2 Impurities contained in nuclear material

Contents of impurity elements are quite different among the samples, because the points of their origins and routes of transit are varied. Information on the impurities of nuclear materials is useful for the purpose of NF investigation. Impurity analysis was then examined by ion exchange separation and mass spectrometry. Procedure for impurity analysis was accomplished by using extraction chromatography and inductively coupled plasma-mass spectrometry (ICP-MS) measurement. A result is shown in Table 2, where 53 elements can be analysed within one week by our method.

Element	Minimum Limit of Determination by ICP-MS (mg/g of sample)	Element	Minimum Limit of Determination by ICP-MS (mg/g of sample)
Li	3	Sn	3
Be	1	Sb	1
Ca	500	Te	10
Sc	0.3	Cs	0.5
Ti	15	Ba	3
V	1	La	0.2
Cr	5	Ce	0.3
Mn	4	Pr	0.1
Fe	100	Nd	0.5
Co	1	Sm	1
Ni	3	Eu	0.2
Cu	2	Gd	0.4
Zn	15	Tb	0.2
Ga	2	Dy	0.3
Ge	10	Ho	0.1
As	4	Er	0.2
Se	100	Tm	0.2
Rb	1	Yb	0.2
Sr	1	Lu	0.2
Y	0.2	Hf	0.4
Nb	2	W	0.5
Mo	2	Re	0.5
Ru	1	Ir	0.2
Rh	0.5	Tl	1
Ag	1	Pb	2
Cd	3	Bi	1
In	0.5		

Table 2: Analysable elements and their limits of determination in impurity analysis.

2.3 Age determination of uranium

The age of nuclear material is also essential information to identify the source of the material, especially for knowing the date when the material was produced or purified [4]. The ^{234}U-^{230}Th chronometer is widely applied to NF, because the radioactive decay of ^{234}U provides a chronometer. The age *t* of the uranium can be calculated using equation (1):

$$t = \frac{1}{\lambda_{234U} - \lambda_{230Th}} * ln\left[1 + \frac{R(\lambda_{234U} - \lambda_{230Th})}{\lambda_{234U}}\right] \qquad (1)$$

where *R* is measured $^{230}Th/^{234}U$ atom ratio and l_x is the decay constant of isotope X.

Procedure for age determination of uranium by ion-exchange purification and mass spectrometry has been developed in JAEA. We conducted procedure exchange and inter-laboratory comparison exercise on uranium age dating between US national laboratories (LANL and LLNL) and JAEA, where the same NBL standard materials of CRM U050 were independently analysed [5]. The analysis of age determination on the uranium oxide standard was performed and the date of its purification can be estimated as shown in Table 3.

Laboratory	Determined Model Date	Uncertainty (days)
LANL	23-June-1956	310
LLNL	1-March-1957	160
JAEA	4-August-1957	220

Table 3: Results of age determination for the NBL standard material of CRM U050. Records from the production of U050 indicate that it was removed from the enrichment cascade on October 4, 1957 and was purified between October 7 and November 7, 1957.

2.4 Particle analysis by electron microscope

Visual inspection of a sample can give useful information as an NF evidence. Scanning electron microscopy (SEM) displays an image or map of the sample. Figure 1 shows an example of particle image observed by SEM. Backscattered electrons carry information about average atomic number of the area and can detect spatially resolved phases of chemical composition. For the NF analysis, we have installed a transmission electron microscopy (TEM). The energetic electron beam of TEM transmits through an ultra-thin sample and can image extremely fine structure more than SEM in spite of tight restrictions on sample thickness. Transmitted electrons can undergo diffraction effects to determine crystal phases in the material.

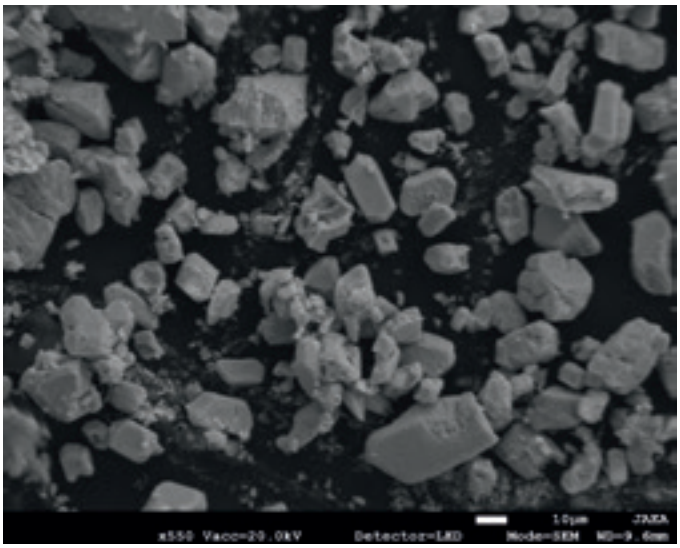

Fig. 1: Particle image of uranium (ADU) observed by SEM.

2.5 NF library

A prototype national nuclear forensics library (NNFL) was constructed based on the data related to nuclear materials and other radioactive materials. The data gathering on the nuclear materials possessed in JAEA has been continued. The JAEA participated in the first international table top exercise of NNFL "Galaxy Serpent," held by the International Technical Working Group (ITWG) as a part of our NNFL development project [6]. Figure 2 shows an isotope correlation plot in order to evaluate the seizure. The seized material strongly associated with the PWR-2 reactor as seen in this figure. The present prototype system will be transferred to the future national responsible authority as a real NNFL which will support the nuclear security activities in Japan.

3. Recent activities to enhance the NF technologies at JAEA

Under the fundamental technologies of NF mentioned above, the JAEA has started a next project for enhancement of functionality of the NF technologies from 2014, which are (a) improvement of the library, (b) new technology of particle analysis by TEM, (c) database construction, (d) development of new age determination, and (e) further international cooperation.

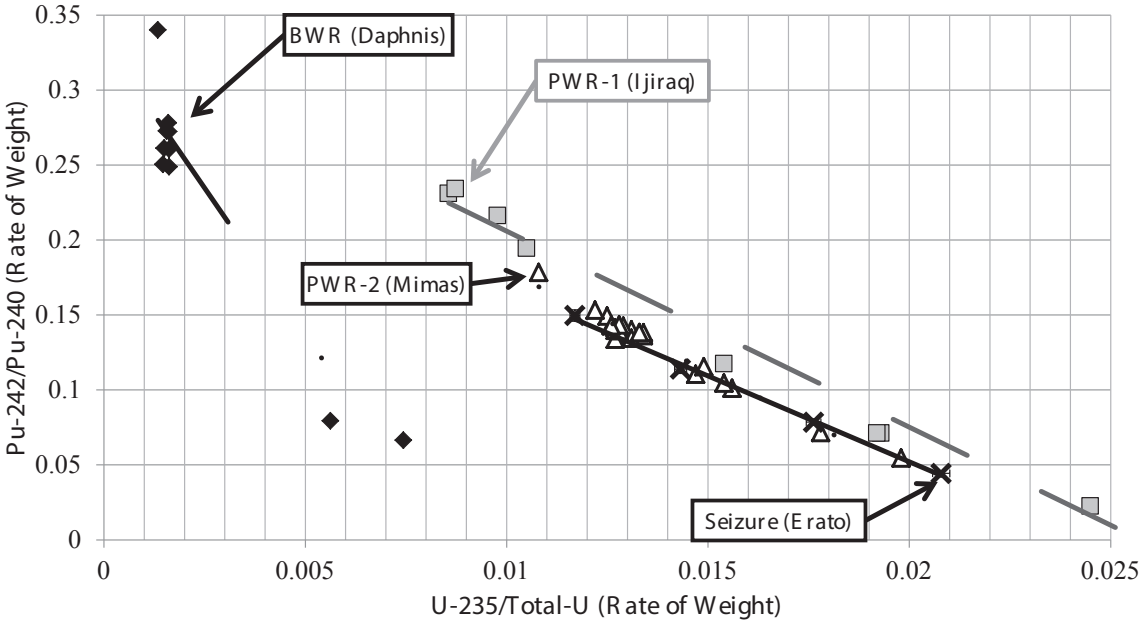

Fig. 2: Isotope correlation plot of $^{235}U/^{Total}U$ vs. $^{242}Pu/^{240}Pu$ for international table top exercise of NNFL "Galaxy Serpent." Daphnis, Ijiraq, Mimas and Erato are the nicknames of the exercise.

3.1 Improvement of the NF library

In order to attribute the belonging of nuclear material to a datum from huge NF database by evaluating its analysed data, a multivariate analysis tool for seizure analysis is being developed together with image evaluation tool for microscope images. Knowledge accumulation system for such NF analysis is important for serial evaluation methodologies which deal with conditions for survey, data items, applied procedure, evaluation of results, and all performed records. According to the knowledge accumulation system, it is possible to carry out reliable and rapid attribution analysis which is independent of evaluator's ability.

3.2 JAEA database

A prototype system of NNFL deals with the data of nuclear and other radioactive materials that the JAEA has possessed in the past research activities. Basic data handling system for nuclear material database (NMDB) was already installed in our NNFL. Data compiling on the JAEA NMDB has been now continued. In the next step of the NNFL project, it is planned to develop a prototype of radioactive materials database (RMDB), which will contain the radioisotopes in medical and industrial usage and the radioactive waste produced in nuclear facilities. An integrated NNFL will consist of the combination of NMDB and RMDB complementally.

3.3 Particle analysis by TEM

Fine feature of nuclear material like crystal structure can be observed by using TEM. Such particle analysis is useful to obtain new NF signature, because fine structure of uranium oxide depends on its sintering temperature. For the purpose of particle analysis by TEM, observation method is now investigated by making very thin (less than 100 nm) specimen with focuses ion beam (FIB). Diffraction contrast image to observe crystal defect and damage, electron diffraction image to analyse crystal structure, and high-resolution transmission image to understand grain boundary become important evidences for NF. Electron energy-loss spectroscopy (EELS) installed in TEM is also available to analyse the elements and their bonding states.

3.4 New age determination

Age dating to elucidate the final purification date of uranium is important subject on NF analysis. The parent/daughter pair of ^{234}U-^{230}Th established in the field of geochemical science has been applied for nuclear forensics. If the uranium has not been fully separated or purified, the chronometer misleads incorrect information about the age. To avoid this systematic error, it is recommended to measure various parent/daughter ratios. The parent/daughter pair of ^{235}U-^{231}Pa is our next subject for age dating.

3.5 International cooperation

Exchange of the newest NF information through international cooperation is useful for each State, because the NF activity has a global side of criminal investigation. The JAEA implements joint researches with US and EC/JRC for forensics purposes. The Integrated Support Center for Nuclear Nonproliferation and Nuclear Security (ISCN) under the JAEA has been providing training courses to support domestic and international capacity building for regulators, mainly from Asian countries in cooperation with the IAEA. The IAEA Regional Training Course on Introduction to Nuclear Forensics was hosted by the ISCN in May 2012 and received total 24 participants from ten Asian countries. The ISCN will promote International Training Course on Practical Introduction to Nuclear Forensics in February 2016.

4. Nuclear forensics capabilities in Japan

In view of the importance of nuclear security and international impetus to construction of NF regime, the pertinent agencies in Japan must cooperate with one another. It is necessary to organize Japan's own system for NF by establishing a national NF laboratory and collaborating with traditional forensics. We must "improve capabilities to search for, confiscate, and establish safe control over unlawfully held nuclear or other radioactive materials and substances or devices using them," as mentioned in the Statement of Principles committed to the participants in the Global Initiative to Combat Nuclear Terrorism (GICNT)

The NF laboratory consists of analytical and storage facilities for seizure materials and NNFL. The laboratory should have ability to secure the reliabilities of evidence analysis techniques, guarantee of quality to the results analysed as evidence, database and its comparison with evidence. Because the JAEA has developed the fundamental technologies for NF as mentioned above, it is possible for us to take charge of the analysis for nuclear materials as a work of NF laboratory. In the NF analysis of seizure and the database construction of NNFL, the judicial reliability of the data is required on the basis of standardization of the analytical scheme and inter-laboratory round-robin exercises. We should enhance our analytical skills for the sake of international progress of the nuclear security.

5. Conclusion

The JAEA has developed fundamental and reliable technologies for NF (Nuclear Forensics) and is now measuring actual uranium samples to populate a NF database. A prototype system of NNFL (National Nuclear Forensics Library) is constructed on the basis of international cooperation. The pertinent agencies in Japan must cooperate with one another to organize Japan's own system for NF by establishing a national NF laboratory. The laboratory should have the reliabilities of evidence analysis techniques, guaranteed quality of the evidence, and database and its comparison with evidence. Another important subject of ours is domestic and international capacity building of nuclear security, especially for Asian countries, in cooperation with IAEA, GICNT and ITWG.

6. Acknowledgements

The authors would like to express our gratitude to Mr. N. Toda, Mr. Y. Funatake, Mr. O. Kataoka, and Mr. T. Matsumoto for their support and advice regarding this study. The work presented in this paper has been supported by the Ministry of Education, Culture, Sports, Science, and Technology (MEXT) of Japan.

7. References

[1] IAEA; *IAEA Incident and Trafficking Database (ITDB) 2014 Fact Sheet*; http://www-ns.iaea.org/ downloads/security/itdb-fact-sheet.pdf.

[2] Nuclear Security Summit 2014; *National Progress Report Japan*; http://www.mofa.go.jp/dns/ n_s_ne/ page18e_000059.html; Hague; 2014.

[3] Fiedler R; *Total evaporation measurements: experience with multi-collector instruments and a thermal ionization quadrupole mass spectrometer*; Int. J. Mass Spectrom. Ion Processes; 146; 91-97; 1995.

[4] Mayer K, Wallenius M, Varga Z; *Nuclear forensic science: correlating measurable material parameters to the history of nuclear material*, Chem. Rev.; 113; 884–900; 2013.

[5] Steiner R, Kinman W.S, Williams R, Gaffney A, Schorzman K, Pointurier F, Hubert A, Magara M, Okubo A; ^{230}Th - ^{234}U *Thorium Radiochronometry Method Comparison: A Tri-Lateral Round-Robin Exercise*; International Conference on Advances in Nuclear Forensics; IAEA; Vienna; IAEA-CN-218-54; 2014.

[6] Kimura Y, Shinohara N, Funatake Y; *Lessons Learned from the International Table Top Exercise of National Nuclear Forensics Library at JAEA*; Journal of Nuclear Material and Management; 42.4; 2014; p 4-11.

Application of the GIF PR&PP methodology to a commercial fast reactor system for a preliminary analysis of PR scenarios

Fabiana Rossi
University of Bologna, Laboratories of Nuclear Technologies at Montecuccolino
Via dei Colli 16, Bologna 40136 (BO) Italy
E-mail: fabiana.rossi@unibo.it

Abstract:

The Generation IV International Forum (GIF) Proliferation Resistance and Physical Protection (PR&PP) Working Group has developed a methodology for the PR&PP evaluation of the next generation Nuclear Energy Systems (NESs). Following the methodology proposed by the working group, applicable to assessing the proliferation resistance of an NES and its individual elements, the main objective of this work is to apply the methodology to show an example of how its results could be used by designers to improve the PR of the system. In this study, the reactor site of a hypothetical and commercial sodium-cooled fast neutron nuclear reactor system (SFR) was used as the target NES for the application of the methodology. The design of this SFR is based on the layout of the Japanese Sodium Fast Reactor (JSFR) with a safeguards design based on the safeguards approach of the Japanese prototype fast breeder reactor Monju. The methodology is applied to all the PR scenarios described in the methodology: diversion, misuse and breakout. The methodology was first applied to the SFR to check if this system meets the target of PR as described in the GIF goal; secondly, a comparison between the SFR and a light water reactor (LWR) with an open fuel cycle was performed to evaluate if and how it would be possible to improve the PR&PP of the SFR. The LWR layout is based on the European Pressurized Water Reactor. The comparison was implemented according to the following example development target: achieving proliferation resistance to material diversion similar or superior to domestic and international advanced LWR. Three main actions were performed: implement the evaluation methodology based on its assumptions; characterize the PR&PP for the nuclear energy system applying the methodology to the SFR; and identify recommendations for system designers through comparing the SFR with the LWR.

Keywords: PR&PP; proliferation resistance; Safeguards-by-Design; sodium fast reactor; light water reactor

1. Introduction

Proliferation resistance (PR) is "that characteristic of an NES that impedes the diversion or undeclared production of nuclear material or misuse of technology by the Host State seeking to acquire nuclear weapons or other nuclear explosive devices" [1].

The Generation IV International Forum has developed a methodological approach for the assessment of Generation IV nuclear energy systems for proliferation resistance and physical protection robustness that is applicable to the evaluation of nuclear systems from the early development stages throughout the full life cycle [2].

The PR technology goal for Generation IV NESs can be expressed as: "a Generation IV NES is to be the least desirable route to proliferation by hindering the diversion of nuclear material from the system and hindering the misuse of the NES and its technology in the production of nuclear weapons or other nuclear explosive devices" [3].

A similar goal could be also found in some development targets. In general, a development target describes the requirements for the future energy system in ensuring safety, reduction of environmental burden, economic competitiveness, efficient utilization of resources, and enhancement of nuclear non-proliferation. As an example, the Japanese development target, described in the Japanese Fast Reactor Cycle Technology Development Project (FaCT Project), says that a Fast Breeder Reactor (FBR) cycle system can be internationally accepted by achieving proliferation resistance to material diversion and facility misuse similar or superior to domestic and international advanced LWR cycle and next generation nuclear system [4].

Consistent with these development targets, it was decided to choose an LWR based on the design of the European Pressurized Reactor (EPR) with a once-through fuel cycle as a comparison.

Following the methodology proposed by the PR&PP Working Group and focusing on PR scenarios at the reactor site, the main objective of this work is to show an example of how to use results from the application of the PR&PP evaluation methodology to address both the GIF goal and the generic development target. The following actions were performed to achieve this objective:

1. Implement the evaluation methodology based on the study's assumptions (see Table 1);
2. Characterize the PR&PP for the nuclear energy system applying the methodology to a commercial hypothetical SFR;
3. Compare the study system, SFR, with the reference system, LWR.

Following this analysis, recommendations for system designers were identified.

Description	Assumption
SFR layout	Based on the JSFR
SFR safeguards system	Based on the Japanese prototype Monju
LWR layout	Based on the EPR
LWR safeguards system	Based on the LWR common practice
Development target	PR similar or superior to advanced LWR
State capability	Based on Japan's situation; participant of the International Community

Table 1: Assumptions under the study.

2. Description of the Sodium Fast Reactor

The hypothetical commercial SFR is a sodium-cooled loop-type fast breeder reactor fueled with mixed oxide (MOX) with thermal and electric outputs of 3.57 GWth and 1.5 GWe, respectively. This system consists of a reactor vessel (RV) containing the core fuel assemblies, blanket fuel assemblies, control rods and other structures; a primary and secondary circuit of two loops each; one circulating pump for each primary circuit loop integrated within the Intermediate Heat Exchanger (IHX); one IHX for each loop; one Steam Generator (SG) for each secondary circuit loop composed of an Evaporator (EV) and a Superheater (SH).

The core of the SFR is composed of 288 inner core fuel subassemblies, 274 outer core fuel subassemblies, 96 radial blanket subassemblies and 57 control rods. The target for the maximum breeding ratio of the SFR is 1.1 to 1.2. The high breeding core with breeding ratio of 1.2 is achieved by changing of fuel specifications with the same fuel assembly (FA) size as the low breeding core and the same core layout. In the high breeding core, the core height is 75 cm and the pin length is 2,690 mm like that of the low breeding core, while the number of fuel pins per fuel assembly is 315, in order to avoid an increase in the linear heat rate. Figure 1 shows the cross section of the reference configuration; Table 2 and Table 3 summarize the core and fuel specifications and the plutonium isotopic composition [5,6].

Other relevant information for the analysis is the path of the nuclear material (e.g. fuel assembly) once it enters the facility. In this study, the focus is the reactor site that is characterized by the following system elements: the reactor building and its auxiliary building, the interim storage pool and the diesel building. These are the facilities inside the SFR containing nuclear material, equipment or processes that could be attractive for proliferation or theft and/or sabotage. In our hypothesis, there is no reprocessing plant inside the reactor site, so it would be important to consider all the shipments between the plant and external facilities. Spent fuel will be moved after two years from the spent fuel storage pool inside the auxiliary building to the interim storage pool outside the reactor building where it will remain until its final shipment to the reprocessing plant or permanent storage.

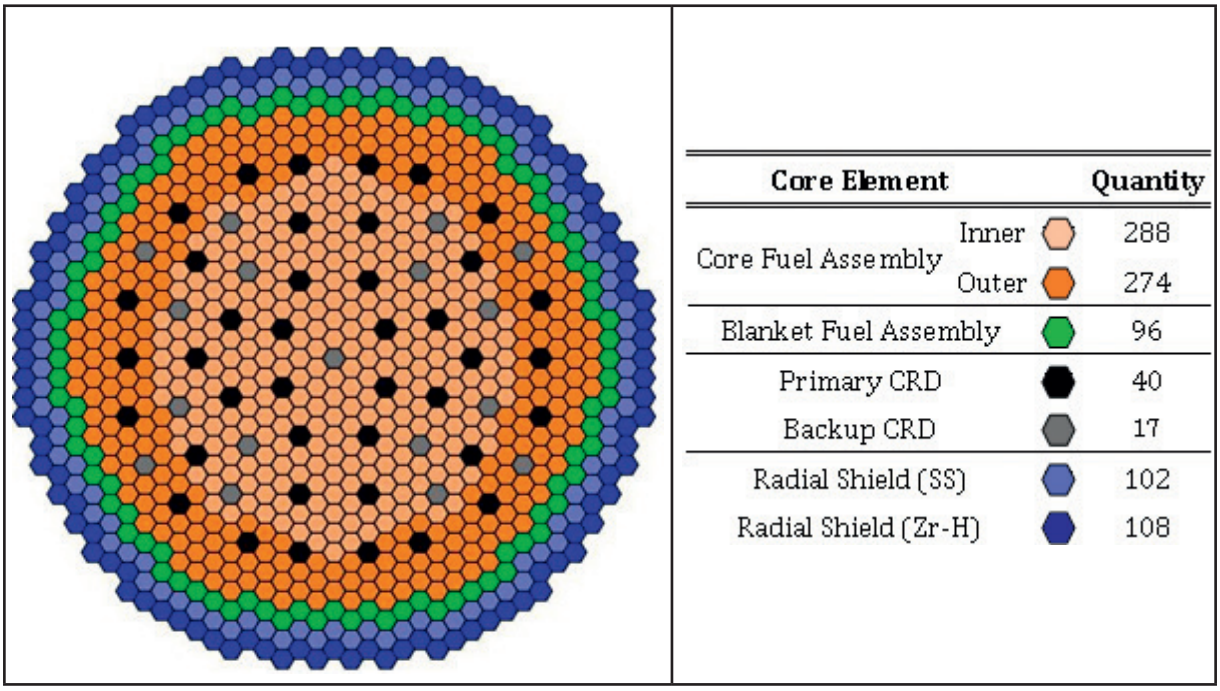

Figure 1: Scheme of the SFR core [7].

Specification	Low breeding	High breeding
Fuel type	MOX	
Core height [cm]	100	75
Axial blanket length (upper / lower) [cm]	40 (20 / 20)	90 (40 / 50)
Number of pins per FA	255	315
Fuel pin diameter [mm]	10.4	9.3
Fuel pin length [mm]	2960	
Fuel assembly pitch [mm]	206	

Table 2: SFR Core and fuel specification of the SFR.

Plutonium Isotopic Composition [wt%]	238	1.7
	239	55.9
	240	30.5
	241	3.4
	242	3.3
Pu-Fissile Enrichment [%]	Inner	21.9
	Outer	24.3

Table 3: SFR Plutonium isotopic composition and Pu-fissile enrichment in fresh fuel.

3. Description of the safeguards approach for the SFR

For the safeguards approach for the SFR, the prototype Monju safeguards approach was taken as reference that was developed in the context of an INFCIRC/153-type comprehensive safeguards agreement concluded between Japan and the International Atomic Energy Agency (IAEA) [8].

The international safeguards objective is the timely detection of the possible diversion of the plutonium-bearing transuranic (TRU)-fuel. The goal quantity for detection is 1 significant quantity (SQ) in the form of TRU-fuel, fuel rods, or portions thereof. The timeliness goal for detecting the possible diversion depends on whether the plutonium is in un-irradiated fresh or irradiated spent fuel. In the former case, the timeliness goal is one month, while, in the latter case, the timeliness goal is three months. The former essentially dictates the need for monthly inspections by the IAEA inspectors, but possible variances from these frequencies may be applied.

The traditional safeguards approach applied to all MOX or TRU-fuel reactors includes:

– Defined Material Balance Areas (MBAs) for nuclear material accounting;
– Defined Key Measurement Points (KMPs) for measuring the flow and inventory of nuclear material;
– Defined Strategic Points for containment and surveillance and other verification measures;
– Nuclear Material Accountancy, via review of operating records and state reports;
– A Physical Inventory Taking (PIT) - typically a “shutdown” inventory taking that involves measuring of all nuclear material within MBA and verified during the Annual Physical Inventory Verification (PIV);
– Verification of domestic and international transfers of nuclear material;
– Verification of facility design information;
– Verification of the operator’s measurement system.

Additional features were provided in this case to ensure robust safeguarding of the TRU-fuel, including:

– Advanced multiple containment and surveillance systems, consisting of several kinds of sensors, gamma detectors, neutron detectors, and surveillance cameras. The digital data from these systems are reviewed by a super-fast image processing review system to detect changes in the areas under surveillance, in a semi-automated manner.
– Continuous, unattended custom-designed non-destructive assay (NDA) systems to monitor the movement of TRU fuel in the facility and to determine by interpreting the gamma and neutron radiation if the fuel is a non-fuel dummy, fresh TRU-fuel, depleted uranium (DU) blanket fuel, or spent TRU fuel.

Figure 2 shows the material balance area covering the reactor building (MBA XS01), while Figure 3 shows the scheme of the fuel handling system.

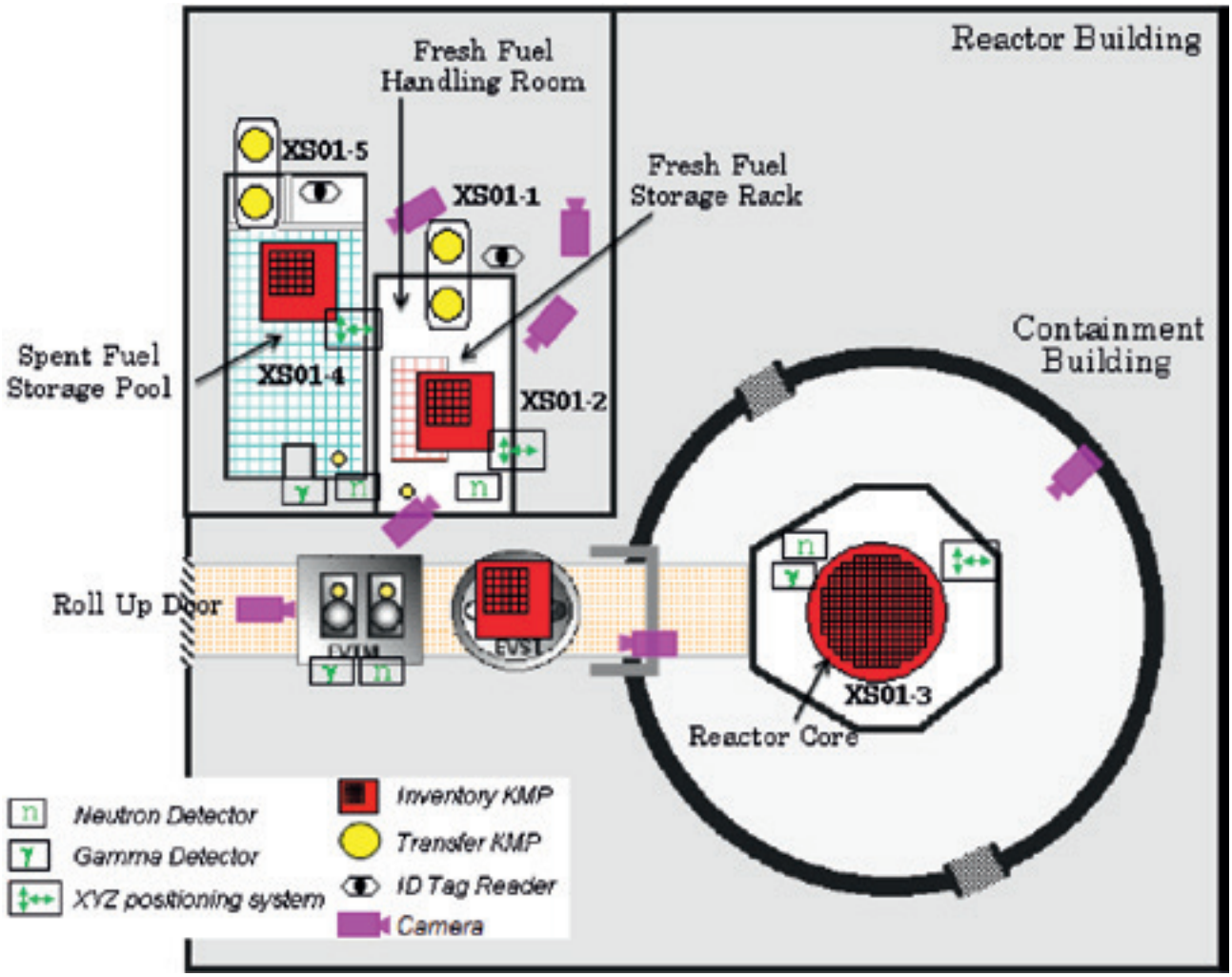

Figure 2: Detail of the MBA XS01 for the SFR reactor. Adapted from [9]

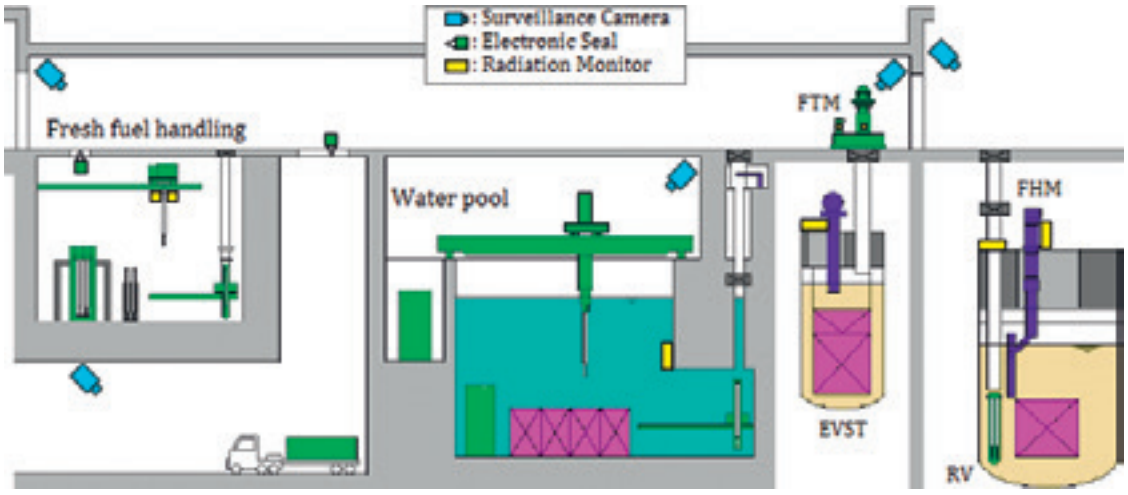

Figure 3: SFR fuel handling system. Adapted from [10]

4. Description of the PR&PP Methodology

The PR&PP methodology has been developed in the framework of the Generation IV International Forum. This methodology can assess both the proliferation resistance and the physical protection robustness of a nuclear facility.

The challenges to the NES are the threats posed by potential proliferant States and by sub-national adversaries. The technical and institutional characteristics of the Generation IV systems are used to evaluate the response of the system and determine its resistance to proliferation threats and robustness against sabotage and terrorism threats. The outcomes of the system response are expressed in terms of PR&PP measures and assessed.

The first step of the methodology is the threat definition that describes the *challenges* that the system may face and includes characteristics of both the actor and the actor's strategy.

When threats have been sufficiently detailed for the particular evaluation, analysts assess *system response*, which has four components:

1. System Element Identification.
2. Target Identification and Categorization.
3. Pathway Identification and Refinement.
4. Estimation of Measures.

More details about these steps could be found in the PR&PP methodology documents [2].

The measures relative to PR used in this study are listed below as presented in the PR&PP methodology document [2] and the relative metrics are summarized in Table 4 [2], where the higher values mean more effort for the proliferator. In the PR&PP methodology document, the Detection Resources Efficiency (DE) measure is also discussed. It is presented as the efficiency in the use of staffing, equipment, and funding to apply international safeguards to the NES. That measure is not discussed in detailed in this study due to lack of information, but only generic consideration in relation to the Detection Probability measure value is presented.

– Proliferation Technical Difficulty (TD) is "the inherent difficulty, arising from the need for technical sophistication and materials handling capabilities, required to overcome the multiple barriers to proliferation".
– Proliferation Cost (PC) is "the economic and staffing investment required to overcome the multiple technical barriers to proliferation, including the use of existing or new facilities".
– Proliferation Time (PT) is "the minimum time required to overcome the multiple barriers to proliferation".
– Fissile Material Type (MT) is "a categorization of material based on the degree to which its characteristics affect its utility for use in nuclear explosives".
– Detection Probability (DP) is "the cumulative probability of detecting a proliferation segment or pathway".

5. Evaluation of SFR

5.1 Challenges

Possible threats to the system can be both concealed and overt diversion of material, both concealed and overt misuse of the facility, or the use of a clandestine facility alone.

The sets of PR representative pathways identified and analyzed in this study are:

– Concealed diversion of material;
– Concealed misuse of the facility;
– Breakout and overt diversion of material and misuse of the facility.

The threat description includes also the description of the actor and its capabilities. In particular, considered as an actor is a Host State with capabilities of an industrial nation with nuclear competence such as the operation of a Nuclear Power Plant (NPP), with reprocessing plants but no enrichment. The objective to reach is the acquisition of at least 1 SQ.

For an easier assessment of the system, two different MBAs are identified: MBA XS01 covering the fresh fuel handling system, the reactor building and the spent fuel pool (Figure 2); and MBA XS02 covering the interim storage pool. The MBA XS01 is the scope of this study.

Measures and metrics	Metric scales bins (median)	Proliferation resistance qualitative description
Proliferation Technical Difficulty (TD) Metric: Probability of segment or pathway failure from inherent technical difficulty considering threat capabilities **Detection Probability (DP)** Metric: Probability that safeguards will detect the execution of a diversion or misuse segment or pathway	0-5% (2%)	Very Low
	5-25% (10%)	Low
	25-75% (50%)	Medium
	75-95% (90%)	High
	95-100% (98%)	Very High
Proliferation Cost (PC) Metric: Fraction of national military budget required to execute the proliferation segment or pathway, amortized on an annual basis over the Proliferation Time	0-5% (2%)	Very Low
	5-25% (10%)	Low
	25-75% (50%)	Medium
	75-100% (90%)	High
	>100% (>100%)	Very High
Proliferation Time (PT) Metric: Total time to complete segment or pathway, starting with the first action taken to initiate the pathway	0-3 mo (2 mo)	Very Low
	3 mo-1 yr (8 mo)	Low
	1-10 yr (5 yr)	Medium
	10-30 yr (20 yr)	High
	>30 yr (>30 yr)	Very High
Fissile Material Type (MT) Metric: Dimensionless ranked categories HEU*, WG-Pu*, RG-Pu*, DB-Pu*, LEU*	HEU	Very Low
	WG-Pu	Low
	RG-Pu	Medium
	DB-Pu	High
	LEU	Very High

* HEU = high-enriched uranium, nominally 95% 235U; WG-Pu = weapons-grade plutonium, nominally 94% fissile Pu isotopes; RG-Pu = reactor-grade plutonium, nominally 70% fissile Pu isotopes; DB-Pu = deep burn plutonium, nominally 43% fissile Pu isotopes; LEU = low-enriched uranium, nominally 5% 235U.

Table 4: Metrics and evaluation scales used in the analysis for PR [2].

5.2 System response

5.2.1 System element identification

In this step, the identification of the system elements that are relevant for the threats considered must be defined. Figure 2 and Figure 3 are schematic representations of the facility considering the transfers of nuclear material and the places where the material will be stored.

5.2.2 Target identification and categorization

Diversion

The target analysis considered the different types of nuclear material in each system element, their locations, and their configurations. The possible diversion targets are presented in Table 5.

Misuse

Misuse threats, different from diversion threats that deal specifically with the removal of materials already in the system, use the facility to produce or process weapons-useable materials that are outside of safeguards, possibly to avoid detection through accountancy and other safeguards measures.

There are many ways in which NPPs could contribute to a Host State's weapons aspirations, but the most significant one is to use them for the covert production or processing of weapons-useable material. The success of any misuse activity depends on the capabilities and objectives of the Host State. For this study, it is assumed that the Host State will attempt to minimize disruption of normal facility operations during misuse of the facility. It must be noted that in this study the fabrication and reprocessing facilities are outside the NES, however, they must be taken into account when considering the entire fuel cycle for an NES.

Breakout

"Breakout does not exist unto itself but "as a 'strategy modifier': ultimately every successful proliferant state necessarily breaks out if/when it decides to use or announce possession of a nuclear weapon. The nature of the breakout determines much of the nature of the threat (both the time available to the proliferant state – before and after breakout, and ultimately the complexity of weapon)" [11]. The interesting aspect of breakout is the scenario,

Diversion points	Target ID	Target Description	Target Material Character	Potential Diversion Containers	Container Transition	Process	Safeguards
XS01-1	T5	Cask of MOX fuel bundles	Fresh MOX	Casks	Parking area	Storage	Cameras Inventory
	T6	MOX fuel bundle(s)	Fresh MOX	Casks	Transit in the FF handling room	Unloading	Cameras Inventory
XS01-2	T6	Individual FF bundle(s) in fuel storage rack	Fresh MOX	Cask/other containers	Transit from XS01-1	Storage in fuel rack	Cameras Inventory
XS01-4	T7	Individual SF bundle(s) in fuel storage rack	Irradiated MOX	Cask/other containers	Transit from XS01-5	Storage in fuel rack	Cameras Inventory Neutron det. Gamma det.
	T8	Individual irradiated blanket bundle(s) in fuel storage rack	Irradiated ^{238}U	Cask/other containers	Transit from XS01-5	Storage in fuel rack	Cameras Inventory Neutron det. Gamma det.
XS01-5	T9	Cask of MOX fuel bundles	Irradiated MOX	Casks	Parking area	Storage	Cameras Inventory
	T7	MOX fuel bundle(s)	Irradiated MOX	Casks	Transit in the shipping station	Loading	Cameras Inventory

Table 5: Possible diversion targets present in MBA XS01.

diversion and/or misuse "that minimizes the time from breakout to weapons readiness, which is a subset of the PT measure. The goal of analysing the breakout scenario is therefore to complement the concealed misuse/diversion scenarios by exploring the minimum post-breakout time to weapons readiness" [11].

Several strategies of breakout are possible. "The strategy chosen by a proliferant state will affect both the time available and potential complexity for proliferation activities" [11].

For this study, only the "immediate absolute" and the delayed intended" breakout scenarios were considered [11] (see Figure 4), taking into account that the safeguards measures would be not applicable after the breakout declaration, while it was considered that the Host State would continue acting under the safety regulations regime. The choice of the immediate absolute strategy and the delayed intended strategy is connected with the main advantages for the Host State: for the first strategy, in fact, the overall proliferation time is the minimum one; while for the second strategy, the proliferation time during the overt program could be minimal and this could affect the response time.

Even if the breakout scenarios are based on diversion and misuse, some extra considerations are needed. Here it was considered that activities of reprocessing would be performed at the legal reprocessing plant present in the Host State. In particular, a small Plutonium and Uranium Recovery by Extraction (PUREX) type reprocessing plant was considered. Due to the fact that two different types of PUREX plants are available, the co-conversion and the co-extraction, they will be both discussed. The difference between these two types of plants can be summarized as follows: in the co-extraction plants, U and Pu are always together in the process so extra activities based on pH are needed for the extraction of Pu itself; using the co-conversion type, instead, U will be added to Pu after its extraction.

5.2.2. Pathway identification

Diversion

Even if several diversion strategies could be identified such as the replacement of a full cask with an empty cask during the transportation into / out of MBA XS01, or the replacement of fresh or spent fuel or blanket assemblies with dummy ones, for the scope of this study, the following scenario was used in the evaluation: dummy fuel assemblies present in the spent fuel pool, resulting from a loading trial, are used to substitute at least one irradiated blanket from the spent fuel pool. The camera may not need to be compromised, but the ID reader or its data must be falsified. Casks are prepared for shipping and sent to the concealed processing facility.

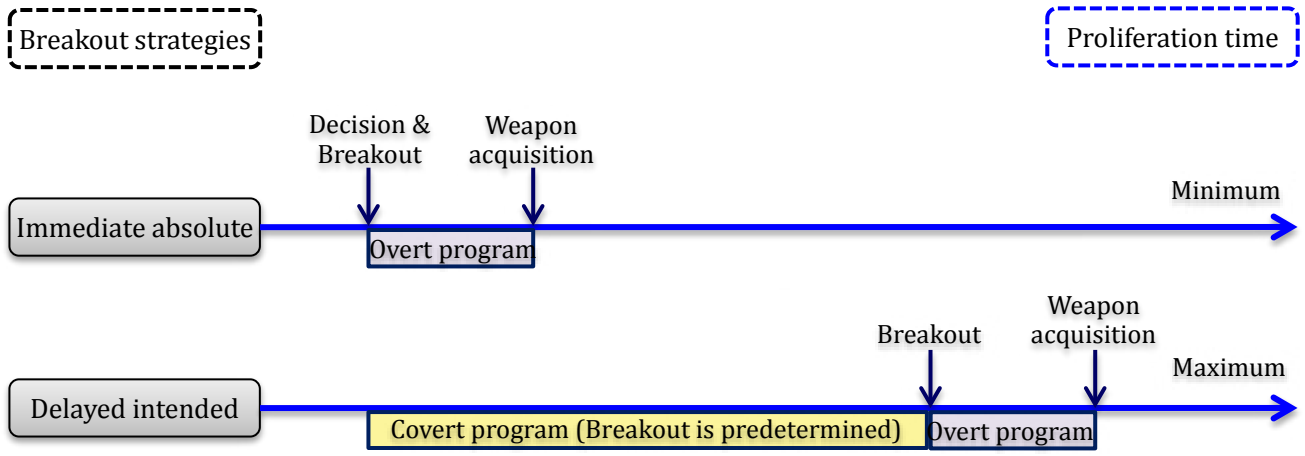

Figure 4: Qualitative description of breakout strategies used in this study. Adapted from [11].

Misuse

For the misuse scenario, instead, the irradiation for the unreported plutonium production can occur mainly inside the core even if in a different location (inner or outer core, or blanket position). It was assumed that the Host State will acquire DU or reprocessed uranium (RU) outside the facility as a normal operation and have some capability of storage for fresh fuel. The Host State will then prepare the target pins outside the NES. In particular, it will substitute two fuel assemblies in the outer ring of the core with two assemblies like the blanket type. To reach an SQ they must be irradiated for one fuel cycle.

Breakout

For the breakout strategies described in Figure 4, the following scenarios are considered.

For the immediate breakout, the overt diversion of irradiated blanket assemblies was assumed.

For the delayed intended strategy, the covert diversion of irradiated blanket assemblies, until the preparation and the shipment to the reprocessing plant, and the subsequent overt program concerning the reprocessing and the Pu extraction was chosen.

5.2.35.2.2. Estimation of measures

The proliferation resistance measures have been evaluated according to the analysts' judgment, together with the reference documents for the methodology.

A generic proliferation strategy can be divided into the following segments:

- Acquisition: activities carried out to acquire nuclear material in any form.
- Processing: activities carried out to convert the nuclear material obtained in the acquisition stage into material ready for use in a nuclear weapon.
- Fabrication: activities carried out to manufacture and assemble a nuclear explosive device.

Table 6 gives an example of measures estimation for the acquisition and the processing activities in the case of diversion scenario.

The fabrication segment has not been taken into account because it requires specific classified information about the design of nuclear explosives.

From Table 7 to Table 9, the summary results of evaluation are presented and represented by colours in the corresponding bins.

Measure	Evaluation basis	Value	Assumptions
TD	Reprocessing will be the dominant segment. The State already has reprocessing plants like PUREX: it has the knowledge and the technology needed. A laser must be used to shear the wrapper tube, but this fact was considered to not increase the TD.	LOW (5-25%)	Difficulties for device falsification and weapon's assembly are not considered. Device falsification will be quite easy. Difficulty for weapon's assembly might be not so high due to the MT.
PC	The Japanese military budget is about $5x10^{12}$ yen (about $4x10^{10}$ euro). Comparing $1.2x10^{11}$ yen to $5x10^{12}$ yen is about 2.4%. Of course, for a clandestine facility the budget will be even lower.	VERY LOW (0-5%)	The same budget associated with the construction of a full scale plant for reprocessing experiments (RETF) in Japan was taken as a reference: $1.2x10^{11}$ yen (about $1x10^{9}$ euro).
MT	Weapons Grade Pu	LOW (WG-Pu)	
DP	The 1st detection point is the camera at the pool during the replacement of blanket fuel (BF). Also seals are placed on the shipping door ⇒ the detection probability is increased.	HIGH (75-95%)	We based our description on the Monju safeguards approach
PT	Prepare a small clandestine reprocessing laboratory (dominant segment): cutting machine, dissolution tank, mixer settler for extraction, nitrogen gas & TBP (2 weeks). Falsify camera and ID reader (not applicable). Remove irradiated BF from the pool and replace it with dummy element in the pool (1 h/BF). Prepare the shipment (1 day/BF). Shipment to the clandestine reprocessing plant (1 day/BF). Separation of Pu (dominant segment) includes retrieving assemblies from the casks, storing them in the pool (1 day/2 FA), disassembly to pins, cutting, dissolution and extraction (16 days/BF).	VERY LOW (0-3 months) Total time is ≃ 33 days	State has a reprocessing facility ⇒ it has hot cell, but needs to install all other equipment for a pin by pin separation process. Without this, the PT will be at least 1 year (Medium). Dummy elements are present in the pool. Cask exists in the hall next to the pool. It was considered that shearing the wrapper tube takes more time for the cutting phase compared with the LWR case, but the extraction process is faster even if the Pu content makes a smaller batch size compared with the LWR case.

Table 6: Measure evaluations for diversion scenario.

	VL	L	M	H	VH
MT					
	HEU	WG-Pu	RG-Pu	DB-Pu	LEU
PT					
	0 - 3 mo	3 mo - 1 yr	1 -10 yr	10 - 30 yr	> 30 yr
DP					
	0 - 5 %	5 - 25 %	25 - 75 %	75 - 95 %	95 - 100 %
TD					
	0 - 5 %	5 - 25 %	25 - 75 %	75 - 95 %	95 - 100 %
PC					
	0 - 5 %	5 - 25 %	25 - 75 %	75 - 100 %	> 100 %

Table 7: Binned measure values for diversion pathway. (VL: very low, L: low, M: medium, H: high, VH: very high)

	VL	L	M	H	VH
MT					
	HEU	WG-Pu	RG-Pu	DB-Pu	LEU
PT					
	0 - 3 mo	3 mo - 1 yr	1 -10 yr	10 - 30 yr	> 30 yr
DP					
	0 - 5 %	5 - 25 %	25 - 75 %	75 - 95 %	95 - 100 %
TD					
	0 - 5 %	5 - 25 %	25 - 75 %	75 - 95 %	95 - 100 %
PC					
	0 - 5 %	5 - 25 %	25 - 75 %	75 - 100 %	> 100 %

Table 8: Binned measure values for misuse pathway.

	VL	L	M	H	VH
PT					
	0 - 3 mo	3 mo - 1 yr	1 -10 yr	10 - 30 yr	> 30 yr
DP					
	0 - 5 %	5 - 25 %	25 - 75 %	75 - 95 %	95 - 100 %

Table 9: Binned measure values for breakout strategy. Orange and purple refer to the immediate absolute and delayed intended strategy respectively; measures not shown are the same as the previous pathways.

6. Discussion

6.1 GIF goal

The GIF Goal for the Generation IV nuclear energy systems says that a GEN-IV NES is to be the least desirable route to proliferation by hindering the diversion of nuclear material from the system and hindering the misuse of the NES and its technology in the production of nuclear weapons or other nuclear explosive devices.

To see if the system analysed satisfies the GIF Goal, it is important to set, for each measure, the limit for unacceptable proliferation risk. In particular, each State needs to decide under which level a system can be considered adequately proliferation resistant. It means that these limits are strongly dependent on the State background, and because each State may need to set its own levels, there is not a unique solution Once the limits are set, it is important to compare the results obtained with the evaluation of the system: when a measure is below the limit, it means that possible ways to upgrade the measures need to be identified.

In Table 10 and Table 11, an example of these limits compared to the SFR system for both diversion and misuse scenarios is shown.

To set the limits, the following conditions are set:

– For MT, the limit is set to be at least medium considering the material's suitability for an explosive device;
– For PT, the limit is set to low considering that IAEA inspection frequency for the systems analysed is every 3 months;
– For DP and TD, the limits are set with probability of at least 50%;
– For PC, the limit is set to be at least medium considering an acceptable reduction of the military budget.

It must be remembered that the limits for unacceptable proliferation risk are strongly dependent on the State background so even with the same values obtained by the evaluation methodology, the following comparison and suggestions could be different depending on how the limits are set up.

A possibility for setting up limits could be forming a working team of both policy makers and system designers.

In our example, comparing these limits with the evaluation results for the SFR system, it is possible to see that for the diversion scenario, the only measure above the limit is the DP, while, for the misuse scenario, the Proliferation Time is also above the limit.

Considering now the breakout scenario based on the diversion pathway of the SFR, we need to set different conditions depending on the type of strategy: immediate absolute or delayed intended. In Table 12, the comparison between the limits and the SFR system for the delayed intended strategy is presented.

For the breakout scenario, only the Proliferation Time and the Detection Probability are subject to change and, in particular, for the immediate absolute strategy, the Detection Probability has no meaning because the State has

already declared its intention to break out. Under these conditions and because in the diversion scenario, with the present limits, the only measure that is in the acceptable region is the Detection Probability, it means that in the case of the immediate absolute strategy, there are no measures that are over the set limits because the Proliferation Time still remains in the very low bin.

According to the findings of the diversion scenario, since the measures on which designers can act are mainly the Material Type and the Detection Probability, in the case of the immediate absolute strategy, a key role is played by the response time after the State declaration of breakout. If this time is lower than the Proliferation Time, limiting actions can be done effectively. However, the response time could be affected by some State characteristics such as its transparency and international framework.

For the delayed intended, instead, the Detection Probability has meaning only during the covert program but, following the evaluation results, the bin of interest is from medium to high. It means that, according to the situation, the results could be at the borderline with the set limit. Also the Proliferation Time, presented here as the total time for both the covert and overt programs, still remains in the very low bin and is, therefore, under the acceptable limit. However, different from the immediate absolute strategy, here it is also important to consider the Proliferation Time before and after the declaration of breakout. In this situation, in fact, if the State actions are not detected during the covert program, the response time after the declaration is even shorter than the previous case. As already underlined, this is one of the big advantages for the State in choosing the delayed intended strategy.

	VL	L	M	H	VH
MT					
	HEU	WG-Pu	RG-Pu	DB-Pu	LEU
PT					
	0 - 3 mo	3 mo - 1 yr	1 -10 yr	10 - 30 yr	> 30 yr
DP					
	0 - 5 %	5 - 25 %	25 - 75 %	75 - 95 %	95 - 100 %
TD					
	0 - 5 %	5 - 25 %	25 - 75 %	75 - 95 %	95 - 100 %
PC					
	0 - 5 %	5 - 25 %	25 - 75 %	75 - 100 %	> 100 %

Table 10: Example of SFR diversion results for the GIF goal: red is the unacceptable area, green is the acceptable area, yellow is SFR results.

	VL	L	M	H	VH
MT					
	HEU	WG-Pu	RG-Pu	DB-Pu	LEU
PT					
	0 - 3 mo	3 mo - 1 yr	1 -10 yr	10 - 30 yr	> 30 yr
DP					
	0 - 5 %	5 - 25 %	25 - 75 %	75 - 95 %	95 - 100 %
TD					
	0 - 5 %	5 - 25 %	25 - 75 %	75 - 95 %	95 - 100 %
PC					
	0 - 5 %	5 - 25 %	25 - 75 %	75 - 100 %	> 100 %

Table 11: Example of SFR misuse results for the GIF goal: red is the unacceptable area, green is the acceptable area, yellow is SFR results.

	VL	L	M	H	VH
MT					
	HEU	WG-Pu	RG-Pu	DB-Pu	LEU
PT					
	0 - 3 mo	3 mo - 1 yr	1 -10 yr	10 - 30 yr	> 30 yr
DP					
	0 - 5 %	5 - 25 %	25 - 75 %	75 - 95 %	95 - 100 %
TD					
	0 - 5 %	5 - 25 %	25 - 75 %	75 - 95 %	95 - 100 %
PC					
	0 - 5 %	5 - 25 %	25 - 75 %	75 - 100 %	> 100 %

Table 12: Example of SFR breakout results for the GIF goal: red is the unacceptable area, green is the acceptable area, yellow is SFR results and the purple one is the SFR result for only the delayed intended strategy.

6.2 Development target

The development target considered in this study is an FBR system that can be internationally accepted by achieving proliferation resistance to material diversion and facility misuse similar or superior to the domestic and international advanced LWR cycle and next generation nuclear system.

To satisfy this target, the results from the evaluation of SFR, must be compared with the results obtained for a LWR system.

For the LWR, the diversion scenario is assumed to be the following: Dummy fuel assemblies present in the spent fuel pool (resulting from the loading trial) are used to substitute at least two LWR spent fuel assemblies. The camera may not need to be compromised, but the ID reader or its data must be falsified. Casks are prepared for shipping and sent to the concealed processing facility.

In Table 13, the comparison between SFR and LWR is shown.

Looking at this comparison, when an SFR measure is below the LWR measure, it would be important to identify the possible ways to upgrade it. It must be underlined that one of the assumptions made for the Host State capabilities was that it is an industrial nation with nuclear capabilities: not only an operating plant for energy production, but also reprocessing plants for both LWR and SFR fuels. This is a very strong assumption and means a very high capability of the Host State and it is reflected in a low PT value. Because the State already has the knowledge and the plants, it could very easily and quickly assemble a clandestine extraction site. The State can use the hot cell present in the reprocessing plant and the only equipment needed for the clandestine laboratory are the cutting machine, the dissolution tank, the mixer and the acids for extraction. On the other hand, without these capabilities, the proliferation time will be enhanced to medium because the construction time would require at least 1 year.

Another important point to underline is found inside the technical difficulty measure. In fact, at least three different types of difficulties were analysed during the discussion: the surveillance equipment falsification, the Pu extraction process and the weapons assembly difficulties. Only the intrinsic difficulties of the Pu extraction process were considered in the evaluation process. It was assumed that the surveillance equipment falsification could be done easily, but the weapon construction is strongly connected with the material type and maybe some tests must be conducted after the weapons assembly. It means that this parameter can enhance both the TD and the PT in scenarios with MT between medium and very high.

The last important point to underline is found inside the DP measure. The DP, in fact, can be linked to instruments (camera, detector, seal, etc.) or inspection activities. In this second case, the time needed to perform the verification is a key parameter that must be considered.

Considering now the misuse scenario, for the LWR it is assumed that the Host State will acquire LEU outside the facility as a normal operation and store this fresh fuel. The Host State will then prepare the target pins outside the NES. In particular, it will substitute two control rods for each FA with LEU material and irradiate them for one fuel cycle. To reach an SQ, the same procedure must be repeated three times. The comparison between SFR and LWR is shown in Table 14.

Again, the Host State has nuclear capabilities that include the reprocessing plants for both LWR and FBR fuels and this influenced the value of TD.

	VL	L	M	H	VH
MT					
	HEU	WG-Pu	RG-Pu	DB-Pu	LEU
PT					
	0 - 3 mo	3 mo - 1 yr	1 -10 yr	10 - 30 yr	> 30 yr
DP					
	0 - 5 %	5 - 25 %	25 - 75 %	75 - 95 %	95 - 100 %
TD					
	0 - 5 %	5 - 25 %	25 - 75 %	75 - 95 %	95 - 100 %
PC					
	0 - 5 %	5 - 25 %	25 - 75 %	75 - 100 %	> 100 %

Table 13: Comparison of binned measure values for diversion pathways: blue is for the LWR and yellow is for the SFR.

	VL	L	M	H	VH
MT					
	HEU	WG-Pu	RG-Pu	DB-Pu	LEU
PT					
	0 - 3 mo	3 mo - 1 yr	1 -10 yr	10 - 30 yr	> 30 yr
DP					
	0 - 5 %	5 - 25 %	25 - 75 %	75 - 95 %	95 - 100 %
TD					
	0 - 5 %	5 - 25 %	25 - 75 %	75 - 95 %	95 - 100 %
PC					
	0 - 5 %	5 - 25 %	25 - 75 %	75 - 100 %	> 100 %

Table 14: Comparison of binned measure values for misuse pathways.

Another important aspect to take into account for the determination of TD is the influence that the insertion of targets inside the reactor core can produce on the neutron flux and reactivity and, consequentially, on the reactor operations. It must be remembered that one of the extra assumptions made for the misuse scenario was that the Host State wants to minimize disruption of normal facility operations. During the evaluation process, it was considered that the targets insertion will not affect neutronics. However, this can be considered quite true for the SFR case where the target is inserted in the core outer ring (in proximity of the blanket area) and substituted for one of the fuel elements, while for LWR, where more fuel elements are introduced in the reactor core using the control rod (CR) space, a most careful evaluation must be done. In this case, the TD might be enhanced.

Moreover, the importance of the value reached in the MT measure must be emphasized. Because the main objective for the misuse scenario is to produce at least one SQ of weapons-useable material, the LWR case would be less attractive since the material quality still remains RG-Pu even using an ad-hoc target. This result can be explained considering that the material used in the case of LWR is LEU: the only way to obtain a MT better than RG-Pu is to reach a BU less than 5-10 gigawatt days per metric ton of uranium (GWd/MTU), but it implies that the target must be in the reactor less than 1 cycle (18 months) and it will increase the value of DP and influence negatively the reactor operations due to the need to repeatedly shut down. On the other hand, the choice of using LEU is made because we want to focus only on the reactor site. If the Host State will use natural uranium (NU), the MT quality will be

	VL	L	M	H	VH
MT					
	HEU	WG-Pu	RG-Pu	DB-Pu	LEU
PT					
	0 - 3 mo	3 mo - 1 yr	1 -10 yr	10 - 30 yr	> 30 yr
TD					
	0 - 5 %	5 - 25 %	25 - 75 %	75 - 95 %	95 - 100 %
PC					
	0 - 5 %	5 - 25 %	25 - 75 %	75 - 100 %	> 100 %

Table 15: Comparison of binned measure values for breakout pathways under the immediate absolute strategy: blue is for the LWR and yellow is for the SFR.

increased but it will imply that the Host State needs to introduce this material surreptitiously into its boundary, which is out of the scope of this study.

The last point to underline is the difference in the value of the DP measure. For the LWR, the first assumption made during the evaluation process was that there are no detection measures checking the replacement of control rods. In this case, the detection probability for misuse will be Very Low. To enhance this value, application of the Additional Protocol will be required. An example proposed during the evaluation process for future study is the introduction of detection monitors at the fabrication facility. However, looking back at the configuration of MBA XE01, it is possible to see that some detection monitors are present in the transfer channel. Due to the fact that the only route to bring out the CRs from the reactor core is towards this channel, if the detection limit is sufficient to distinguish between fuel rods and activated materials, the DP can be enhanced to High.

Also for the SFR case study, relative to the DP measure, two different possibilities were examined during the evaluation discussion: the target materials sent to the clandestine facility or to the legal facility. The assumption under these two possibilities is that the irradiated targets for the misuse will be shipped out of the reactor with the normal shipment. The presence of radiation monitors in the reactor site will be enough only if the assemblies are diverted before the shipment. For the following analysis and the scope of this study, only the possibility of using the clandestine reprocessing plant will be taken into account In this case, the detection probability is considered to be Very High because at the legal reprocessing facility two empty elements will be found during inspection. This value is obtained considering that the assemblies will arrive at the reprocessing facility before the completion of the pathway. In the other case, this check will be not effective.

Considering now the breakout scenario, the immediate absolute strategy for LWR is the overt diversion scenario of spent fuel assemblies: the spent fuel assemblies in the spent fuel pool will be shipped to the legal reprocessing plant where they will be reprocessed to extract Pu. This material will be used for weapons fabrication. The comparison is shown in Table 15.

The delayed intended strategy, instead, is assumed to be the covert misuse of the reactor for the production of Pu and the overt reprocessing and Pu extraction. To obtain a better quality of material, the Host State will acquire LEU outside the facility and irradiate the fuel assemblies as a normal operation. However, the irradiation time will be lower than for normal operations (about 54 days). The comparison is shown in Table 16.

In the immediate absolute strategy it is easy to notice that, due to the fact that the Detection Probability is not available for this case, the only remaining difference between the LWR and the SFR is the Material Type. However, it must be remembered that the design can increase the value of MT avoiding the use of blanket, but this decision must be done in accordance with the State energy policy.

It is different, however, for the situation of the delayed intended. In this case, while the scenario for the SFR is still based on the diversion cases, the scenario assumed for the LWR is based on the misuse pathway to obtain a better quality of material. The irradiation time for this case is reduced from 1 cycle to about 2 months and under this condition it is possible to reach weapons grade plutonium even with a light water reactor. Using these pathways, there is no difference in the Material Type between the SFR and the LWR, but there still remains some difference in the Proliferation Time and the Detection Probability. However, the PT is different only in relation to the number of FAs that are needed to be treated in the LWR to reach 1 SQ. Even if it is

	VL	L	M	H	VH
MT					
	HEU	WG-Pu	RG-Pu	DB-Pu	LEU
PT					
	0 - 3 mo	3 mo - 1 yr	1 -10 yr	10 - 30 yr	> 30 yr
DP					
	0 - 5 %	5 - 25 %	25 - 75 %	75 - 95 %	95 - 100 %
TD					
	0 - 5 %	5 - 25 %	25 - 75 %	75 - 95 %	95 - 100 %
PC					
	0 - 5 %	5 - 25 %	25 - 75 %	75 - 100 %	> 100 %

Table 16: Comparison of binned measure values for breakout pathways under the delayed intended strategy: blue is for the LWR and yellow is for the SFR. The dotted cell in PT refers to the case of more than 6 FAs.

better to investigate the number of FAs to be treated to reach 1SQ, the PT measure can be analysed as a fixed term plus a variable one. The fixed amount of time is connected with the irradiation time inside the reactor, while the variable term is linked with the time needed for the shipment and for the Pu extraction and purification. This last time is strongly linked with the number of FAs to be treated. Using a parametric analysis, if the number of FAs is below six, the PT still remains in the very low bin without any appreciable difference from the case of the SFR. However, if the number of FAs is equal to or exceeds six, the PT measure for the LWR is moved from the very low to the low bin. In a first approximation, with the availability of data of abnormal Pu production of a 400 MWe light water reactor and considering a scale factor of 4 for a commercial LWR with a power of 1600 MWe, the production of Pu could be considered to be about 6.4 kg of Pu per ton of U. Using this value, the number of FAs needed could be estimated to be three, meaning that the PT measure for the LWR still remains in the very low bin, not any different than the SFR case. Moreover, the same condition regarding the response time is still available for these cases.

The last point regarding a possible difference between the case of the SFR and the LWR is the Detection Probability. In the case of the LWR, the shutdown of the NPP after about two months and the consequent shipment of fuel outside the facility is not a normal operation so the probability of being detected is high. Instead, for the SFR, the presence of the extra seal on the shipping door is no more effective because it is assumed that the State will wait until the regularly scheduled shipment from the facility to the reprocessing plant. As underlined during the evaluation process, this is an important result and the designer could work on it by creating more layers of safeguards for the detection of diversion.

7. Recommendations for designers

For both the GIF goal and the development target results, in the case of the Host State as actor, the application of the methodology shows that the measures Proliferation Time, Technical Difficulty, and Proliferation Cost are more strongly dependent on the State's background than on the type of NES considered. This is reflected by the fact that the value of these measures for both the LWR and the SFR is the same. That means that designers cannot directly act on this measure to enhance its value, but it is responsibility of the State itself.

The measure Fissile Material Type is instead an important point for the SFR. Designers can act directly on this measure in different ways. For example, they can increase its value by avoiding the use of blanket or changing the type of core material and its composition and configuration, but this decision must be done in accordance with the State energy policy. Moreover, it is possible that for some scenarios this measure reaches the same value, so before taking any decision a complete study of scenario and pathways must be performed. In any case, in an indirect way, to compensate for the Fissile Material Type measure, system designers can act on other measures such as the Detection Probability. This measure is strongly connected with the safeguards approach used, so designers can increase its value adding different safeguards layers.

For the last measure, Proliferation Time, the methodology shows that it is strongly connected to the reprocessing activities and depends more on the State's capabilities. There is a small difference between the LWR and SFR cases, but this is not relevant for the methodology and the comparison; it is mainly caused by the different number of fuel assemblies needed to obtain 1 SQ in the two systems.

8. Conclusions

The PR&PP methodology was applied at the reactor site of a hypothetical commercial SFR focusing on three PR scenarios to address both the GIF goal and the development target. It has been shown that the results coming from the evaluation could be used for both the comparison of the target system with the limits of unacceptable risk of proliferation and with another system such as an LWR. In particular, the comparison shows clearly which are the measures and the parameters that could be used by the system designers to improve the study system. From the case considered in the study, for example, it could be seen that the measures on which designers can mainly act are the material type and the detection probability and, indirectly, the proliferation time. The technical difficulty and the cost, instead, considering the reactor site only, are mainly influenced by the State's capabilities. Changing, for example, the material type could affect the technical difficulty of the reprocessing activities.

9. Acknowledgements

The author thanks Dr. Inoue (now Radionuclide Officer at The Comprehensive Nuclear-Test-Ban Treaty Organization) and Ms. Kawakubo of the Japan Atomic Energy Agency (JAEA) for technical assistance; Ms. Heinberg, Mr. Hiyama, Mr. Hori and Mr. Tomikawa for technical support during the evaluation phase for the application of the PR&PP methodology.

10. References

[1] Como II, *IAEA STR-332*, December 2002

[2] Proliferation Resistance and Physical Protection Evaluation Methodology Working Group of the Generation IV International Forum, *Evaluation Methodology for Proliferation Resistance and Physical Protection of Generation IV Nuclear Energy Systems, Revision 6*, September 15, 2011.

[3] R. Nishimura, R. Bari, P. Peterson, J. Roglans-Ribas and D. Kalenchuk, *Development of a methodology to assess proliferation resistance and physical protection for Generation IV systems*, Americas Nuclear Energy Symposium, Miami, FL (US), 2004.

[4] R. Nakai, *Current status of fast reactor cycle technology development (FaCT) project in Japan*, Advanced Nuclear System Research and Development Directorate - JAEA, 2007.

[5] M. Ogura, Y. Okubo, T. Ito, M. Toda, S. Kobayashi, S. Ohki, T. Okubo, T. Mizuno and S. Kotake, *Conceptual design study of JSFR (1) - Overview and Core Concept*, International Conference on Fast Reactors and Related Fuel Cycles (FR09), Kyoto, 2009.

[6] M. Etoh, Y. Kamishima, S. Okamura, O. Watanabe, K. Ohyama, K. Negishi, S. Kotake, Y. Sakamoto and H. Kamide, "Conceptual design study of JSFR (2) - Reactor System," in International Conference on Fast Reactors and Related Fuel Cycles (FR09), Kyoto, 2009.

[7] T. Takeda, W. E. G. van Rooijen, K. Yamaguchi, M. Uno, Y. Arita and H. Mochizuki, "Study on Detailed Calculation and Experiment Methods of Neutronics, Fuel Materials, and Thermal Hydraulics for a Commercial Type Japanese Sodium-Cooled Fast Reactor," *Science and Technology of Nuclear Installations,* vol. 2012, no. Article ID 351809, 2012

[8] E. Umebayashi, Y. Yamaguchi, M. Matsuguchi, S. Usami, S. Yoshimoto and S. Yatsu, *Safeguards in Prototype Fast Breeder Reactor Monju*, International Conference on Fast Reactors and Related Fuel Cycles: Safe Technologies and Sustainable Scenarios, Paris, 2013.

[9] P. C. Durst, I. Therios, R. Bean, A. Dougan, B. Boyer, R. L. Wallace, M. H. Ehinger, D. N. Kovacic and K. Tolk, "Advanced Safeguards Approaches For New Fast Reactors," Pacific Northwest National Laboratory, Richland, WA (US), 2007.

[10] K. Aoto, S. Kotake, N. Uto, T. Ito and M. Toda, *JSFR Design Study and R&D Progress in the FaCT Project*, in International Conference on Fast Reactors and Related Fuel Cycles (FR09), Kyoto, 2009.

[11] Proliferation Resistance and Physical Protection Evaluation Methodology Working Group, *PR&PP Evaluation: ESFR Full System Case Study Final Report*, October 2009.

Reflected-Point-Reactor Kinetics Model for Neutron Coincidence Counting: Comments on the Equation for the Leakage Self-Multiplication

S Croft[1], A Favalli[2], D Hauck[2], D Henzlova[2], V Henzl[2], RD McElroy, Jr.[1], and PA Santi[2]

[1]Safeguards & Security Technology
Nuclear Security and Isotope Technology Division
One Bethel Valley Road, PO Box 2008, MS-6166, Oak Ridge, TN 37831-6166, USA.
[2]Safeguards Science & Technology Group (NEN-1)
Non-proliferation and Nuclear Engineering Division
Los Alamos National Laboratory, MS E540, Los Alamos, NM 87545, USA.

Abstract

Passive neutron correlation counting is widely used, for example by international inspection agencies, for the non-destructive assay of spontaneously fissile nuclear materials for nuclear safeguards. The mass of special nuclear material present in an item is usually estimated from the observed neutron counting rates by using equations based on mathematically describing the object as an isolated multiplying point-like source. Calibration using representative physical standards can often adequately compensate for this theoretical oversimplification through the introduction and use of effective-interpretational-model-parameters meaning that useful assay results are obtained. In this work we extend the point-model treatment by including a simple reflector around the fissioning material. Specifically we show how the leakage self-multiplication equation mathematically connects the traditional bare source and the reflected source cases. In doing so we explicitly demonstrate that although the presence of a simple reflector changes the leakage self-multiplication the traditional bare-item point model multiplicity equations retain the same mathematical form. Making and explaining this connection is important because it helps to explain and justify the practical success and use of the traditional point-model equations even when the assumptions used to generate the key functional dependences are violated. We are not aware that this point has been recognized previously.

Key words: neutron coincidence counting; autocorrelation counting; neutron multiplicity counting; point-model; nuclear safeguards; neutron measurements; neutron transport.

1. Introduction

The interpretation of neutron multiplicity counting data (singles, doubles, and triples) in terms of item parameters (effective spontaneous fission mass, relative (α,n)-to-spontaneous fission neutron production, and leakage self-multiplication) is usually done within the framework of a one-energy neutron-group point-source reactor kinetics model [1]. Within this model it is natural to ask how the observables are changed when a multiplying item is surrounded by a simple neutron reflector. One example of a reflector would be the containers used to store bulk plutonium oxide product. We shall work with the coupled equations describing the neutron number in the item and in the reflector and show how the leakage self-multiplication factor connects the bare and reflected cases.

2. Approach, based on neutron balance (Integral approach)

Here we shall build our approach on the general model introduced by Spriggs et al [2] for reflected nuclear reactors and adopt the definitions and notations for convenience. These authors deduced probability relationships to calculate the coupling parameters between the reactor core and reflector, and they used them to derive the effective multiplication of the system, core and reflector, in terms of the multiplication factor of the core, and the average probability of a neutron to leak to a core and the average probability of a neutron to leak from a reflector to the core.

First we recap some definitions, following Spriggs et al [2]:

f_{ca}, f_{ci}, f_{cr} are the average probabilities that a neutron can be absorbed in the core, can leak to infinity, or can leak from core to reflector, respectively. The sum of these probabilities must be unity because they comprise all possibilities for each neutron, therefore:

$$f_{ca} + f_{ci} + f_{cr} = 1 \qquad (1)$$

f_{ra}, f_{ri}, f_{rc} are the average probabilities that a neutron can be absorbed in the reflector, can leak to infinity, or can leak from the reflector to the core, respectively. Again the sum of these probabilities must be unity, so that:

$$f_{ra} + f_{ri} + f_{rc} = 1 \qquad (2)$$

It is worth underlining here that f_{xy} represents "the average probability of a particular outcome on each neutron through a given region" [2], and not the instantaneous values that can change according to if, for example, a neutron is born close to the edge of the core/reflector or of the core/void.

The next step is to calculate neutron balance in the entire system, i.e. the core and reflector together. There are just four outcomes for each neutron. We can therefore write the sum of probabilities as follows:

$$P_{ca} + P_{ci} + P_{ra} + P_{ri} = 1 \qquad (3)$$

where

P_{ca} is the fraction of the neutrons absorbed in the core;

P_{ci} is the fraction of the neutrons leaked from the core to infinity;

P_{ra} is the fraction of the neutrons absorbed in the reflector;

P_{ri} is the fraction of neutrons leaked from the reflector to infinity;

Defining:

$$f = f_{cr} f_{rc} \qquad (4)$$

The following equations can be obtained based on average neutron balance:

$$P_{ca} = \frac{f_{ca}}{1-f} \qquad (5)$$

$$P_{ci} = \frac{f_{ci}}{1-f} \qquad (6)$$

$$P_{ra} = \frac{f_{cr} f_{ra}}{1-f} \qquad (7)$$

$$P_{ri} = \frac{f_{cr} f_{ri}}{1-f} \qquad (8)$$

By defining the *effective multiplication factor* of the system (core + reflector), k_{eff}, as the number of neutrons produced per neutron lost (either absorbed or leaked); and the *multiplication factor of the core region*, k_c, as the number of neutrons produced in the core per neutron lost from the core, using the relationship previously introduced, Spriggs and coworkers derived the following equation:

$$k_{eff} = \frac{k_c}{1-f} \qquad (9)$$

This is the key equation we need to connect the assay of a bare source and the assay of the same source surrounded by a reflector. To appreciate this, recall that for a subcritical system, the total multiplication M can be defined as [1]:

$$M = 1 + k_{eff} + k_{eff}^2 + k_{eff}^3 + \ldots = 1/(1-k_{eff}), \text{ with } k_{eff} < 1 \qquad (10)$$

So, multiplication of the system (core + reflector) is given by the following relationship:

$$M_{eff} = \frac{1}{1-k_{eff}} \qquad (11)$$

For the core, by the following relationship also holds:

$$M_c = \frac{1}{1-k_c} \qquad (12)$$

By substitution of expressions (11) and (12) into equation (9),the following new relationship is obtained:

$$M_{eff} = \frac{M_c (1-f)}{1 - M_c f} \qquad (13)$$

It is evident from (13) that M_{eff} with the M_c are connected by the reflector parameter *f*. When *f* approaches zero the M_{eff} approaches M_c as expected. As *f* increases, i.e. the effectiveness of the reflector is increasing, then M_{eff} also increases as a consequence.

In the context of the present discussion we are concerned with the coupled system comprising the source and reflector, and we are interested in the leakage self-multiplication because we are concerned with counting those neutrons that emerge from the item into an external detector, so, introducing P_L as the probability of leakage for the system, the leakage self-multiplication we are after may be written as follows [1]:

$$M_{L,eff} = P_L M_{eff} \qquad (14)$$

P_L is calculated as the sum of P_{ci} and P_{ri}, the two events that leak neutrons out of the system making them available to be counted, and thus the following equation follows:

$$P_L = P_{ci} + P_{ri} = \frac{f_{ci}}{1-f} + \frac{f_{cr} f_{ri}}{1-f} \qquad (15)$$

Substituting (13) and (15) into (14), the new equation for leakage self-multiplication, which now also accounts for absorption and reflection by the reflector, is obtained:

$$M_{L,eff} = P_L \frac{M_c (1-f)}{1 - M_c f} = (f_{ci} + f_{cr} f_{ri}) \frac{M_c}{1 - M_c f} = (f_{ci} + f_{cr} f_{ri}) \frac{M_c}{1 - M_c f_{cr} f_{rc}} \qquad (16)$$

If the reflector is not present ($f_{cr}=f_{ri}=f_{rc}=0$) expression (16) reduces to the familiar isolated point-model formula reported in Croft et al [1].

For a given item measured under reflected configuration we now clearly see from expression (16) that the situation may still be described using a single leakage self-multiplication parameter so that the familiar results of the isolated (bare or unreflected) point-model in describing the neutron counting rates (singles, doubles and triples) still apply. In other words, by introducing the reflector we have shown that it is not necessary to introduce any extra parameters into the mathematical description which would otherwise need to be determined by the experiment. This is important because we usually already have an underdetermined problem [3]. The leakage self-multiplication parameter defined by Equation(16) describes the behavior of the special nuclear material item (the multiplying core in the present terminology) in

its particular reflecting environment. It cannot be reduced to the total or to the leakage self-multiplication of the core in free space without additional information about the reflector which in general will not be known but neither is it of interest in a routine mass quantification determination based on inverting the standard point-model equations. This is simply a realization of the general principle that reactivity is not a intrinsic property of an object but depends on the environment in which the object resides.

Discussion

Despite the obvious apparent short comings of the point-model kinetics equations is worth remembering that interpretation of experimentally obtained neutron counting rates is presently performed almost exclusively in terms of this framework [4]. The results of the present paper are not going to inspire a measurement practice revolution because current practice is adequate and well established for many practical needs and nor have we introduced significant additional realism or fidelity into the theoretical framework. For instance we are still implicitly assuming that all of the temporal behavior associated with multiplication happens on a time scale which is much faster than the average lifetime of neutrons which enter the external detector (the so called prompt fission or superfission assumption). However, from a teaching and applications perspective what we have explained and consequently justified is the use of the traditional point-model equations to the seemingly more complex problem of a reflected object when one might imagine a reflected model with extra parameters might be needed.

A quality measurement also depends on many other factors outside the scope of our present narrow discussion, including other types of non-ideal behavior which take place in real detector systems which must be manage by design or compensated for. Prominent amongst these are deadtime losses, amplifier baseline recovery, and the use of measured detector parameters such as gate utilization factors [5]. However, we note that in the field of safeguards considerable advances have been made in recent years in the application of Monte Carlo transport methods to the modeling and simulation of neutron coincidence and multiplicity counters. Noteworthy in this regard was the development by Abhold and Baker [6] of MCNP-REN (Monte Carlo N-Particle – Random Exponentially Distributed Neutron Source) that provided a means to directly simulate coincidence and multiplicity counting. The ideas in MCNP-REN have been carried forward and the functionality extended in MCNPX through, for example, the convenience of coincidence tallies [7]. The MCNP-PoliMi code [8], with origins in the Polytechnic of Milan (which explains the name) and the University of Michigan, also provide a flexible tool for extracting correlated particle information from simulated neutron counting experiments. These tools remove the necessity to use reactor point model equations to either predict performance or to interpret (invert or solve) measured rates. Although the potential to use Monte Carlo simulations in the solution step has attractions, especially where acceptable knowledge may be available to help constrain the solution space (recall we generally have more unknown model parameters than measured rates and so the inversion step is underdetermined), because The Monte Carlo technique can incorporate the full richness of spatial, energy and temporal behaviors (in the case of thermally coupled moderating reflectors spectral changes and time dynamic, things we have ignored in the treatment above, will certainly come into play), but, at the time of writing this possibility has not be explored with the vigor one might expect. The predominant method of analysis for neutron correlation count data remains exploitation of the point-model equations. It is because of this that our present contribution remains relevant.

Conclusion

Drawing on the reflected point reactor work of Spriggs et al [2] we have shown that, in the traditional framework of the one neutron-energy-group point-model, the action of a simple reflector can be accounted for using an appropriate numerical value of the leakage self-multiplication. Most importantly the presence of a reflector does not alter the structure of the traditional isolated point-model equations which can be solved in the familiar way. That is to say just one effective parameter, which may be treated as an unknown parameter in the inversion step, is needed to describe the leakage self-multiplication processes even when a reflector is added. The usual expressions used in neutron multiplicity counting for the singles, doubles, and triples rate therefore still apply. The consequence is that with a simple (without energy change) reflector the assay values for mass will remain valid although the numerical values for the apparent leakage self-multiplication will change. This result, made explicit here for the first time, explains why encapsulation does not need to be treated in the traditional analysis approach unless it is because there is a significant associated efficiency correction required. Our conclusions are consistent with the well-known fact that the multiplication (or reactivity) of an item is a property of the item and the surroundings, not of the item alone. Our expression (16), which we believe to be new, also explains why conceptually additional encapsulation may be considered to be either part of the measurement item or part of the external detector. This property of the theoretical analysis is important in the teaching and calibration of correlated neutron counting methods.

Looking to the future we envision a movement away from the point-model equations. Algebraic extensions can contribute to this advance, but as noted in the discussion Monte Carlo methods such as MCNP-REN, MCNPX, and MCNP-PoliMi offer the possibility of representing the item, its environment, the detector and its response characteristics in far greater detail and with far greater fidelity.

Acknowledgements

We acknowledge the US Department of Energy National Nuclear security Administration (NNSA) Office of Nonproliferation and International Security for supporting this work. We are also appreciative of insightful comments by anonymous reviewers that served to sharpen our discussion.

References

[1] Croft S., Favalli A., Hauck D.K., Henzlova D., and Santi P.A. Feynman variance-to-mean in the context of passive neutron coincidence counting, Nucl. Instrum. and Meths. in Phys. Res A686 (2012)136-144.

[2] Spriggs, G.D., Busch, R.D.,Williams, J.G. Two-region kinetic model for reflected reactors. Ann. Nucl. Energy 24 (3)(1997)205–250.

[3] Pázsit, I., Enqvist A., and Lénárd, P. A note on the multiplicity expressions in nuclear safeguards, Nucl. Instrum. and Meths. in Phys. Res A603 (2009)541-544.

[4] Ensslin, N., Harker, W.C., Krick M.S., Langner, D.G., Pickrell, M.M., and Stewart J.E., Application guide to neutron multiplicity counting, Los Alamos National Laboratory Report LA-UR-98-4090.

[5] Ensslin, N. Principles of neutron coincidence counting, Chapter 16 In: D Reilly, N Ensslin, H Smith, Jr, and S. Kreiner (Eds), Passive Nondestructive assay of nuclear materials, US Nuclear Regulatory Commission report NUREG/CR-5550 (March, 1991), ISBN 0-16-032724-5. Also known as Los Alamos National Laboratory report LA-UR-90-732.

[6] Abhold M.E. and Baker, M.C. MCNP-REN: a Monte Carlo tool for neutron detector design, Nucl. Instrum. and Meths. in Phys. Res A485 (2002)576-584.

[7] Swinhoe, M.T. and Hendricks, J.S. Calculation of the performance of ^{3}He alternative detectors with MCNPX, Advancements in Nuclear Instrumentation Measurement Methods and their Applications (ANIMMA), 2011 2nd International Conference on,vol., no., pp.1,6, 6-9 June 2011. doi: 10.1109/ANIMMA.2011.6172919.

[8] Pozzi S.A., Clarke, S.D., Walsh, W.J., Miller, E.C, Dolan, J.L., Flaska, M., Wieger, B.M., Enqvist, A., Padovani, E., Mattingly, J.K., Chichester, D.L., and Peerani, P. MCNPX-PoliMi for nuclear nonproliferation applications, Nucl. Instrum. and Meths. in Phys. Res A694 (2012)119-125.

Workshop on He-3 alternatives for safeguards applications

Carlos Carrapico, Bent Pedersen, Vittorio Forcina, Paolo Peerani, Francesca Rosas, Arturs Rozite, Hamid Tagziria, Georgios Takoudis, Alice Tomanin

European Commission, Joint Research Centre (JRC), Institute for Transuranium Elements (ITU),
Nuclear Security Unit, Via Enrico Fermi 2749, 21027 Ispra (VA), Italy
E-mail: paolo.peerani@jrc.ec.europa.eu

Abstract:

On 13-17 October 2014, the Joint Research Centre (JRC) hosted the second of two workshops on helium-3 (He-3) alternative materials and technologies for safeguards applications, under the U.S. Department of Energy/National Nuclear Security Administration (DOE/NNSA)-Euratom Action Sheet 47, at the JRC Ispra Site.

The recent Ispra workshop served as a direct follow-up to the Los Alamos workshop. Participants provided updates on several of the technologies discussed in 2013. In particular, workshop participants evaluated the applicability of the He-3 alternative technologies to a pre-established list of use cases and identify any capability gaps. In addition, the workshop included discussions of implementation strategies for advancing the prototype technologies to commercially deployable systems. The workshop included a demonstration of some of these technologies. Moreover, a field trial has been held on the margins of this workshop to provide a head-to-head comparison of various He-3 alternative prototypes for nuclear fuel verification.

Keywords: NDA; neutron counting; He3 shortage; neutron detection

1. Introduction

On 13-17 October 2014, the Joint Research Centre (JRC) hosted the second of two workshops on helium-3 (He-3) alternative materials and technologies for safeguards applications, under the U.S. Department of Energy/National Nuclear Security Administration (DOE/NNSA)-Euratom Action Sheet 47, at the JRC Ispra Site.

The International Atomic Energy Agency (IAEA) and regional safeguards inspectorates rely heavily on neutron assay techniques, and in particular, on coincidence counters for the verification of declared nuclear materials under safeguards and for monitoring purposes. The reliability, safety, ease of use, gamma-ray insensitivity, and high intrinsic detection efficiency of He-3 based detectors made it an ideal detector material. However, an anticipated shortage of He-3 led to efforts to develop and field neutron detectors that make use of alternative materials.

From 22-24 March 2011, the IAEA held an international meeting to address the question of possible replacement technologies for He-3 based neutron detectors. This was followed by a workshop at Los Alamos National Laboratory in June 2013, which provided an in-depth review of selected international efforts to develop and deploy technologies designed to serve as viable, near-term alternatives to He-3 based systems for international safeguards applications. Participants included experts from U.S. national laboratories and Universities, Euratom, JRC, Japan Atomic Energy Agency (JAEA), and the IAEA.

The recent Ispra workshop served as a direct follow-up to the Los Alamos workshop. Participants provided updates on several of the technologies discussed in 2013. In particular, workshop participants evaluated the applicability of the He-3 alternative technologies to a pre-established list of use cases and identify any capability gaps. In addition, the workshop included discussions of implementation strategies for advancing the prototype technologies to commercially deployable

systems. The workshop included a demonstration of some of these technologies. Moreover, a field trial has been held on the margins of this workshop to provide a head-to-head comparison of various He-3 alternative prototypes for nuclear fuel verification.

2. Inter-comparison benchmark

In the margins of the “Workshop on He-3 alternatives for Safeguards applications”, JRC hosted an inter-comparison benchmark that took place in the PERLA laboratory at the JRC facilities of Ispra on the two days before the workshop (October 13th-14th, 2014).

The scope of the benchmark was to compare the performances of few prototypes of neutron counters based on alternative technologies among them and compared to those of ordinary He-3 devices ordinarily used by IAEA and Euratom for safeguards inspections.

Six prototypes were tested and compared to three reference He-3 instruments corresponding to three different usage cases, as described in table 1. During the benchmark each developer operated his own instrument, whereas JRC staff operated the reference instruments.

Usage cases	Reference ^{3}He instrument	Alternative prototypes	Developer
Passive coincidence counting in Pu-bearing cans	HLNCC	ABUNCL with B-coated tubes	GERS
		HLNCC with straw Boron tubes	PTI
		Well counter with Li6-ZnS blades	Symetrica
Active coincidence counting for fresh fuel elements	UNCL	Liquid scintillator neutron coincidence collar	IAEA
Neutron monitors	UNCL slab	Parallel plate B slab counter	LANL
		Stilbene scintillator	UMICH

Table 1: Prototypes tested in the benchmark

2.1 Short description of the prototypes

2.1.1 ABUNCL with B-coated tubes

The ABUNCL was initially developed by General Electric Reuter Stokes as a collar for active measurement of fuel elements and as such had been demonstrated at the Los Alamos workshop in 2013. The prototype tested in Ispra was a modification of the original collar that transformed the ABUNCL into a well counter by adding a fourth detecting side (see figure 1). The counter is equipped with 72 10B-lined proportional tubes.

2.1.2 HLNCC with straw Boron tubes

The straw HLNCC has been developed by PTI. It consists of 804 straws (narrow diameter 10B-lined proportional tubes) embedded in a structure have roughly the same dimensions (cavity, height and footprint) of a standard HLNCC (figure 2).

2.1.3 Well counter with Li6-ZnS blades

This prototype was developed by Symetrica in collaboration with JRC. It was only a partial prototype equipped with 8 blades out of the 32 foreseen in the final instrument (see figure 3). Each blade consists in a sandwich of PVT wavelength shifter coated with ZnS scintillator for charged particles doped with 6Li acting as neutron converter.

2.1.4 Liquid scintillator neutron coincidence collar

This collar was developed by IAEA in collaboration with JRC and Hybrid Instruments and consists in 3 slabs, each containing 4 cubic liquid scintillators; the fourth slab can host the interrogation AmLi source like in a common UNCL.

2.1.5 Parallel plate slab counter

This is a neutron slab based on boron-lined parallel plate technology; the same as in the HLNB prototype demonstrated in Los Alamos in 2013. This slab prototype has been particularly targeted for challenging conditions like high count rates and gamma fields. The demo was particularly intended to show the fast signal processing electronics.

2.1.6 Stilbene scintillator

The University of Michigan provided a couple of stilbene detectors with pulse shape discrimination capability.

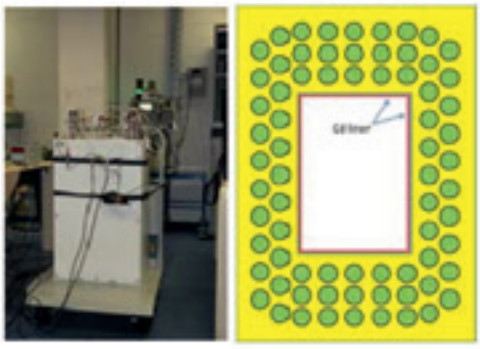

Figure 1: ABUNCL with B-coated tubes (picture and cross section)

Figure 2: Straw HLNCC

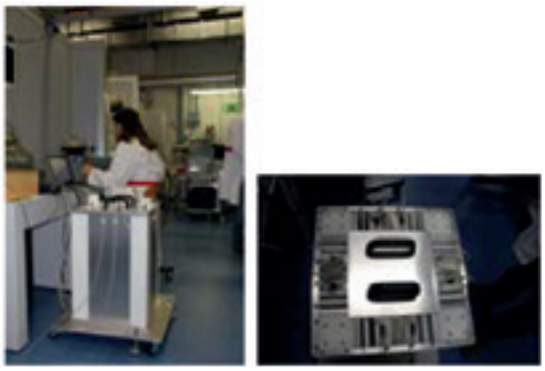

Figure 3: Well counter with Li6-ZnS blades (side and top views)

Figure 4: Liquid Scintillator NCC

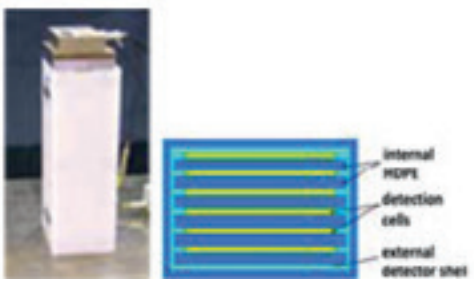

Figure 5: Parallel plate slab (picture and cross section)

Figure 6: Stilbene scintillator

2.2 Testing procedures

The purpose of the benchmark was to demonstrate the performance of alternative 3He systems against safeguards relevant parameters and perform benchmarking of these systems against available reference 3He-based systems. The key component of this activity involved side-by-side comparative measurements of a range of available SNM samples in the 3He-based systems and their proposed alternatives. The actual procedures have been slightly different for the three usage cases.

2.2.1 HLNCC-types

The main benchmarking parameters were:

– HV plateau and gamma sensitivity: the plateau was measured in the presence of a 252Cf and gamma-ray sources (with dose rates of operational interest) to establish the optimum HV setting for benchmarking measurements and efficiency evaluation.
– Efficiency: using available well-characterized 252Cf source and the optimum HV setting determined in step 1 the neutron detection efficiency was measured and compared with the reference 3He-based system.
– Figure of Merit: the die-away was measured and then the FOM was computed as FOM = ε / sqrt(τ) and compared to the reference 3He-based system.
– Gamma sensitivity: the gamma influence was assessed by measuring a strong gamma source in absence and presence of a reference 252Cf source.
– Statistical uncertainty: side-by-side measurements were performed using the available SNM samples in the alternative and reference 3He-based system and the statistical uncertainty was compared.

2.2.2 UNCL-types

The main benchmarking parameters were:

– Efficiency: using available well-characterized 252Cf source the neutron detection efficiency was measured and compared with the reference 3He-based system.
– GARR: the gamma rejection was estimated by adding a strong gamma source to the reference 252Cf source.
– Statistical uncertainty: side-by-side measurements were performed mimicking passive and active fuel measurements in the alternative and reference 3He-based system and the statistical uncertainty was compared.

Due to the unavailability of a real fuel element the operating conditions were simulated by placing a 252Cf source in the cavity providing a fission rate comparable to that expected in presence of a fuel element. Three types of measurements have been simulated:

– Passive measurement (with weak 252Cf source in the cavity reproducing the spontaneous fission rate from U-238)
– Active measurement in thermal mode (with AmLi in the lateral slab and a strong 252Cf source in the cavity reproducing the induced fission rate in U-235 in thermal mode: ratio AmLi/Cf = 10:1)
– Active measurement in fast mode (with AmLi in the lateral slab and a weak 252Cf source in the cavity reproducing the induced fission rate in U-235 in fast mode: ratio AmLi/Cf = 100:1)

2.2.3 Monitor-types

The main benchmarking parameters were:

– Efficiency: using available well-characterized 252Cf source the neutron detection efficiency was measured and compared with the reference 3He-based system.
– Gamma sensitivity: the gamma influence was assessed by measuring a strong gamma source in absence and presence of a reference 252Cf source.

In addition for the parallel plate using list-mode data acquisition, the performance of the parallel-plate detector with fast amplifier was demonstrated and compared with standard PDT amplifier.

2.3 Benchmark results

We report hereby the main results obtained during the benchmark.

2.3.1 HLNCC-types

The major detection characteristics are reported in table 2, whereas table 3 gives the performance with respect to gamma sensitivity and table 4 the statistical uncertainty for measurements of MOX samples.

The results can be quickly summarized as follows:

– The PTI system has a slightly lower efficiency than the 3He HLNCC, but compensated by a much shorter die-away. As a combination of the two it gives a slightly better FOM, whose effect is confirmed by the lower statistical uncertainty in the Pu sample measurement. Moreover it has better gamma rejection.
– The partial Symetrica system has half of the efficiency of the HLNCC and a longer die away, but we should recall that the prototype contains only one quarter of the expected blades (8 out of 32); Monte Carlo extrapolations have estimated that a full system would have and efficiency of 25%, a die away of 31 μs and a FOM of 4.6 (60% better than HLNCC). Gamma sensitivity is comparable with HLNCC.
– The GERS system has inferior performances than HLNCC both in term of efficiency and die-away. Also in this case it has to be reminded that the demonstrator was a modification of the collar prototype, so it was not optimized in terms of geometry.

Parameters	^{3}He-based HLNCC	GERS-NCC	^{6}Li/ZnS based HLNCC	B-straw HLNCC
Efficiency [%]	16.50	10.20	8.90	13.56
Die-away time [μs]	43.30	65.40	55.90	26.00
FOM ($\varepsilon/\sqrt{\tau}$)	2.51	1.26	1.19	2.66

Table 2: Detection characteristics of HLNCC prototypes

Source type	^{3}He-based HLNCC		GERS-NCC		^{6}Li/ZnS based HLNCC		B-straw HLNCC	
	Singles [s^{-1}]	Doubles [s^{-1}]	Singles [s^{-1}]	Doubles [s^{-1}]	Singles [s^{-1}]	Doubles [s^{-1}]	Singles [s^{-1}]	Doubles [s^{-1}]
^{137}Cs (3.7 MBq)	40.3	0.008	11.4	0.013	0.7	0.000	4.9	0.003
^{137}Cs + ^{252}Cf	1196.6	218.003	1888.6	178.779	-	93.830	-	-
^{252}Cf (7000 n/s)	1194.1	215.991	1893.9	183.927	-	92.610	-	-

Table 3: Gamma sensitivity results of HLNCC prototypes

	^{3}He-based HLNCC	GERS-NCC	^{6}Li/ZnS based HLNCC	B-straw HLNCC
MOX1 (168 g Pu)				
Measurement time [s]	600	600	600	600
Doubles [s^{-1}]	1088.95	315.81	165.33	770.76
σ	8.71	3.74	4.39	4.19
Relative precision [%]	0.80	1.18	2.66	0.54
MOX2 (191 g Pu)				
Measurement time [s]	600	600	NA	NA
Doubles [s^{-1}]	1242.54	357.43		
σ	9.94	4.99		
Relative precision [%]	0.80	1.40		

Table 4: Statistical uncertainty on Pu sample measurements of HLNCC prototypes

2.3.2 UNCL-types

The results are reported in table 5. From the data we can conclude that the LS-NCC has the potential to provide better performances of UNCL, especially for measurements in fast mode (used mostly for Gd-loaded fuel elements).

2.3.3 Monitor-types

By nature slab monitors are scalable, so the efficiency has to be compared either as intrinsic efficiency (neutron detected per neutron hitting the surface of the detector) or the absolute efficiencies should be normalized per unit surface or covered solid angle. In the case of the systems demonstrated during the benchmark, the main purpose was not necessarily to provide a direct comparison of performance with He-3 detectors.

For the University of Michigan the goal was to demonstrate the capabilities of novel plastic scintillators (in particular stilbene) as dual-particle detector with satisfactory gamma/neutron distinction by pulse shape discrimination. Figure 8 shows for instance the gamma sensitivity result: the neutron detection in presence of a strong gamma source was unaffected up to a dose rate of 30 μSv/h.

For the parallel plate slab the main purpose was to demonstrate the high-count rate performances. Unfortunately the response of the Boron module was affected by noise on one of the amplifiers that has somehow degraded the performance of the detector during the benchmark.

3. Conclusions from the workshop

The workshop was attended by 45 participants coming from several research centres in Europe, United States and Japan, industry and inspectorates (IAEA and Euratom). 25 presentations were delivered in the three technical sessions (general concepts / Li- and B-based alternatives / scintillation technologies), followed by a demonstration of the prototypes and concluded by a round table discussion table to which all participants contributed. The discussion was structured in four consecutive topics; for each topic an expert was invited to present a short statement that was supposed to trigger the discussion involving the entire audience. The four topics were:

– Technical challenges
– Standardized best practices for testing instruments
– Use cases and technology gap
– Implementation and path forward

a) Technical challenges (facilitator S. Croft)

In the introductory statement the facilitator has evidenced three major areas for research:

– the need to further develop the fundamental theory of coincidence and multiplicity counting,
– simulation tools for the alternative technologies
– availability of experimental facilities and round robin exercises

Safeguards parameters	^{3}He-based HLNCC	LS-NCC
Efficiency - singles (S) [%]	10.01	9.54
Efficiency - doubles (D) [%]	3.23	3.43
GARR = S/(S+γ)	< 1.0e-8	8.4e-4
D - passive mode (252Cf only)	61.55±0.87%	67.30±0.50%
D – active thermal mode (AmLi+^{252}Cf 10:1)	64.78±2.05%	68.98±0.49%
D – active fast mode (AmLi+252Cf 100:1)	4.07±9.77%	4.77±1.87%

Table 5: Comparison of results for UNCL and LS-NCC

Concerning Monte Carlo simulation, the current tools work very well for He-3 counters, but require improvements to properly model the physics of the novel technologies. Modelling of boron or lithium based detectors would require a complete charged particle transport, whereas organic scintillators need modelling of a complex process including light emission/transport/collection and computation of pulse shape/height distributions.

The use of spectroscopy could bring some advantages, but this needs to be first investigated and assessed.

There would not probably be a fit-all-purposes solution, but we should seek for matching technologies to specific applications.

In some cases a change from the classical way of working could be needed; the traditional way of measuring coincidences through the shift register logics could be replaced by other way of processing raw data, in particular for fast neutron detectors. In this view list mode data collection and analysis can open to a wider spectrum of possibilities in data processing.

The use of fast neutron detectors (organic scintillators) would get a remarkable boost from developments in the data acquisition electronics: for instance, the capability to perform pulse shape analysis in real time and/or wave form digitalization.

The lifetime of the new technologies has still to be demonstrated.

Finally it was identified the need of bringing the appropriate competence from different disciplines to the NDA field.

b) Standardized Best Practices for Testing (facilitator R. Kouzes)

The first fundamental question is: there are no standards for safeguards: do we need them? The safeguards "market" is relatively small and restricted and maybe do not justify the effort of developing standards.

Then, as a consequence, the next question follows: can best practices replace standards and how? The answer is probably yes, but this would in any case require an intensive review of testing campaigns and the publication of agreed testing methods/protocols.

The organization of benchmarks can be challenging, mostly from a logistic point of view. Benchmarks can be performed both as inter-comparisons (among different technologies) and versus real material and have to be targeted to end-user goals.

The expected performance should be driven by the end-user needs; for instance the International Target Values (ITV) of IAEA are useful for some applications, but are not fully comprehensive and are in any case determined by experience on past performances.

c) Use Cases and Technology Gaps (facilitator B. McElroy)

A provoking statement: since He-3 solves everything and it is not going to disappear totally in the short term, new technologies might find a place to only specific applications. Developers should aim to identify and target where their technology fits and where it can provide viable solution for replacement or even for improving the current situation. For instance attended/unattended applications might be tackled with different perspectives.

– Use cases where current equipment is not fully satisfactory and where R&D should be focused can include:
– fresh fuel with poisons
– fresh fuel with heterogeneity
– partial defect in spent fuel
– encapsulation/final repository safeguards

d) Implementation and path forward (facilitator T.H. Lee)

Here the facilitator has listed some of the issues considered of main relevance:

– Optimize the use of He-3 (e.g. deploying hybrid B10+ tubes and modular detector assemblies)
– Replacement of He-3 by B-10 or other alternatives for less challenging applications and where efficiency is not an issue (e.g. gross counting)
– Still relying on He-3 for demanding applications (e.g. multiplicity counting)
– active interrogation applications: fast neutron systems (organic or noble gas scintillators)
– additional information from gamma/neutron detectors (multi-particle coincidences)

Other properties of replacement technologies according to IAEA requirements are:

– modeling possibility (required)
– simple physical swap (desired)
– compatibility with existing electronics (strongly desired)

Finally the requirements for future systems should take into account:

– field deployable (weight, cost, stability,…)
– user friendliness
– authorization process through evaluation vs existing systems

Proliferation Resistance and Material Type considerations within the Collaborative Project for a European Sodium Fast Reactor

Guido Renda, Fatih Alim[1] and Giacomo G.M. Cojazzi
Institute for Transuranium Elements, Nuclear Security Unit (Ispra)
Joint Research Centre, European Commission
Via E. Fermi, Ispra 21027 (VA) Italy
E-mail: guido.renda@jrc.ec.europa.eu

Abstract:

The collaborative project for a European Sodium Fast Reactor (CP-ESFR) is an international project where 25 European partners developed Research & Development solutions and concepts for a European sodium fast reactor. The project was funded by the 7th European Union Framework Programme and covered topics such as the reactor architectures and components, the fuel, the fuel element and the fuel cycle, and the safety concepts. Within sub-project 3, dedicated to safety, a task addressed proliferation resistance considerations. The Generation IV International Forum (GIF) Proliferation Resistance & Physical Protection (PR&PP) Evaluation Methodology has been selected as the general framework for this work, complemented by punctual aspects of the IAEA-INPRO Proliferation Resistance methodology and other literature studies - in particular for material type characterization. The activity has been carried out taking the GIF PR&PP Evaluation Methodology and its Addendum as the general guideline for identifying potential nuclear material diversion targets. The targets proliferation attractiveness has been analyzed in terms of the suitability of the targets' nuclear material as the basis for its use in nuclear explosives. To this aim the PR&PP Fissile Material Type measure was supplemented by other literature studies, whose related metrics have been applied to the nuclear material items present in the considered core alternatives. This paper will firstly summarize the main ESFR design aspects relevant for PR following the structure of the GIF PR&PP White Paper template. An analysis on proliferation targets is then discussed, with emphasis on their characterization from a nuclear material point of view. Finally, a high-level ESFR PR analysis according to the four main proliferation strategies identified by the GIF PR&PP Evaluation Methodology (concealed diversion, concealed misuse, breakout, clandestine production in clandestine facilities) is presented.

Keywords: proliferation resistance; sodium fast reactors; PR&PP.

1. Introduction

The collaborative project on the sodium fast reactor (CP-ESFR) [1] is an international project where 25 European partners developed R&D solutions for a European Sodium Fast Reactor concept [2, 3]. The project was funded by the 7th European Union Framework Programme [4] and foresaw several sub-projects (SP) covering topics such as the fuel, the fuel element and the fuel cycle (SP2), the safety concept options and Proliferation Resistance & Physical Protection (PR&PP) (SP3), the innovative reactor architecture, components and balance of plant (SP4), education and training (SP5) [5]. Within sub-project 3, dedicated to the system's safety concepts, a specific task led by JRC-ITU, with contributions of AREVA, EdF and ENEA addressed proliferation resistance issues [6].

The aim of this task was to propose an approach to evaluate the level of protection of a given nuclear power plant (NPP) design with respect to nuclear proliferation. Before doing applied studies, an approach was to be defined to take into account the methods and the parameters used to evaluate the proliferation resistance aspects of interest. This had to integrate the contributions of the Generation IV International Forum (GIF) Proliferation Resistance & Physical Protection working group (PR&PP WG) activities [7, 8], as well as the activities on proliferation resistance (PR) carried out within the International Project on Innovative Nuclear Reactors and Fuel Cycles (INPRO) of IAEA [9]. In order to collect the system's PR relevant information, the structure of the GIF PR&PP study on the Generation IV systems [10] has been chosen, and by following it a reflection on the system's possible response to the GIF proliferation strategies (concealed diversion, concealed misuse, breakout and replication of technology on clandestine sites) has been performed in a qualitative way.

Since a full PR analysis for the entire system was beyond the scope of this task, the high level reflections made following [10] helped in identifying the diversion strategy as the most interesting one to investigate further. The focus was therefore put on a more detailed analysis of the impact of the core alternatives under consideration on a potential diversion strategy. The study identified the potential diversion targets, the potential diversion points for each target and performed an analysis of the attractiveness of

[1] Currently at Division of Nuclear Safeguards and Security, Department of Nuclear Safety, Turkish Atomic Energy Authority, Ankara, Turkey.

the available targets for a potential proliferant State. This activity has been carried out taking the GIF Proliferation Resistance and Physical Protection Evaluation Methodology (GIF PR&PP EM) [7] and its Addendum [8] as the general guideline for identifying targets and potential diversion points. The diversion targets' proliferation attractiveness has been analyzed in terms of the suitability of the targets' nuclear material as the basis for being used in nuclear explosives. Since the PR&PP Fissile Material Type measure was felt too coarse for a thorough investigation, other literature studies and their related metrics have been applied [9, 11, 12, 13] to the nuclear material items present in the considered core alternatives [6, 14].

This paper will firstly summarize the GIF PR&PP evaluation methodology [7] and the structure of the study on the PR&PP features of the six GEN IV systems carried out by the GIF PR&PP working group with the six System Steering Committees of the Generation IV International Forum [10] (section 2). Section 3 highlights the main ESFR design aspects relevant to PR and section 4 identifies the main system elements and PR targets along the lines of [7]. Section 5 presents a material type analysis of selected core options considered by the collaborative project, aimed at understanding the possible impact of the considered core design variations on the system's attractiveness from a diversion strategy point of view. Finally, along the lines of [15], section 6 presents some high level considerations on the proliferation resistance of the CP-ESFR system with respect to the main proliferation strategies considered by the PR&PP Evaluation Methodology.

2. The GIF PR&PP Evaluation Methodology and the Study on the Six Generation IV systems

The Generation IV International Forum defines proliferation resistance as "that characteristic of an NES that impedes the diversion or undeclared production of nuclear material or misuse of technology by the Host State seeking to acquire nuclear weapons or other nuclear explosive devices"[7].

The GIF PR&PP working group developed a PR&PP evaluation methodology, whose framework is illustrated in Figure 1.

According to the PR&PP methodology the proliferation strategies to be considered for the threat posed by a host state actor are 1) *Concealed diversion,* 2) *Concealed production of nuclear material,* 3) *Breakout* and 4) *Production in clandestine facilities*. Threats of non-state actors are addressed in the context of physical protection and will not be further considered here. The PR part of the methodology foresees an acquisition pathway analysis to evaluate the system' response to potential proliferation challenges. The acquisition pathways are analyzed via the quantification of six PR measures [7]:

- "Proliferation Technical Difficulty – The inherent difficulty, arising from the need for technical sophistication and materials handling capabilities, required to overcome the multiple barriers to proliferation;
- Proliferation Cost – The economic and staffing investment required to overcome the multiple technical barriers to proliferation, including the use of existing or new facilities;
- Proliferation Time – The minimum time required to overcome the multiple barriers to proliferation (i.e., the total time planned by the Host State for the project);
- Fissile Material Type – A categorization of material based on the degree to which its characteristics affect its utility for use in nuclear explosives.
- Detection Probability – The cumulative probability of detecting a proliferation segment or pathway;
- Detection Resource Efficiency – The efficiency in the use of staffing, equipment, and funding to apply international safeguards to the NES."[2]

In 2011 The Generation IV Proliferation Resistance and Physical Protection Evaluation Methodology Working Group and the six System Steering Committees of the Generation IV International Forum published a joint report illustrating the main PR and PP features of the six Generation IV conceptual designs (gas-cooled fast reactor – GFR -, very-high-temperature reactor – VHTR -, supercritical-water-cooled reactor – SCWR -, sodium-cooled fast reactor – SFR -, lead-cooled fast reactor – LFR -, molten salt reactor – MSR -), together with a number of common cross-cutting issues [10].

The report was the outcome of a joint effort of the above-mentioned groups, implying a close collaboration via workshops and the compilation of a PR&PP White Paper template for each of the six designs. The structure of the White Paper template aims to capture the relevant pieces of information needed for a PR&PP analysis – PR&PP relevant design description and PR&PP considerations - in a structured way, and foresees the following steps [10]:

1. Overview of Technology
2. Overview of Fuel Cycle(s)
3. PR&PP Relevant System Elements and Potential Adversary Targets
4. Proliferation Resistance Considerations Incorporated into Design
5. Physical Protection Considerations Incorporated into Design

[2] [7], p. xiii.

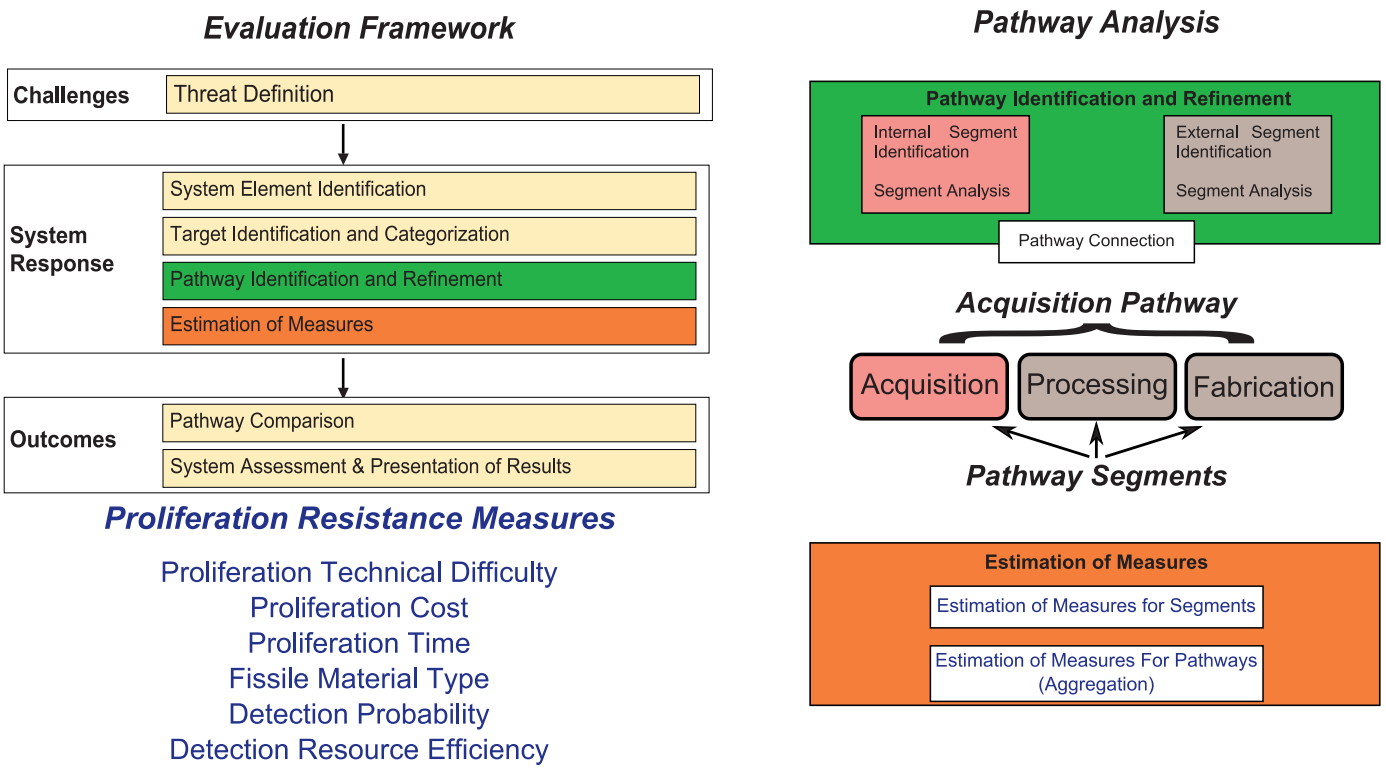

Figure 1: The GIF PR&PP methodology framework. Adapted from [7].

For steps 3 (PR&PP Relevant System Elements and Potential Adversary Targets), 4 (Proliferation Resistance Considerations Incorporated into Design) and 5 (Physical Protection Considerations Incorporated into Design), the activity foresees the application of elements of the PR&PP Evaluation Methodology.

A full PR evaluation of the systems design was beyond the scope of the CP-ESFR project, and the approach used in [10] was felt as the most appropriate to conduct a CP-ESRF PR analysis. The GIF PR&PP methodology framework has been used to decompose the system into system elements and to identify and characterize potential nuclear material diversion targets. These targets where then analyzed in terms of their nuclear material attractiveness to a potential proliferation programme. Finally, high-level considerations on the four PR proliferation strategies considered by [7] were made.

3. Aspects of the ESFR design relevant to proliferation resistance (Overview of Technology)

Two concepts of 1500 MWe reactors called “working horses” have been proposed in the context of CP-ESFR: a pool and a loop design. For both designs, two reference core options have been considered: one with U and Pu oxide fuel and the other with U and Pu carbide fuel. For both carbide and oxide cores, the inner and outer fuel regions have different Pu mass content [16]. The reactor architectures (pool and loop) and the reference cores of the oxide and carbide fuel options are shown in Figure 2. A comparison of the ‘working horses’ main characteristics with respect to the sodium fast reactor designs considered in the GIF sodium fast reactor study [10] is reported in Table 1.

The systems could be used for minor actinide (MA) management, either in homogeneous or heterogeneous mode [17]. Several core options were explored [17]: here one homogeneous (HOM4) and one heterogeneous (HET2) option will be considered. Homogeneous MA management basically consists in replacing part of the uranium in the fresh fuel elements with minor actinides (4% MA content – HOM4 option), while heterogeneous MA management considers adding to the reference oxide core a radial blanket ring of blanket assemblies (BAs), composed of depleted UO_2 and MA. The HET2 core option therefore foresees the same fresh FA of the reference core plus radial blanket assemblies made of 80% depleted UO_2 and 20% MA. The project partners investigated the possibility to perform MA management only within the oxide core type.

Table 2 presents the main characteristics of the ESFR fresh reference fuel assemblies, Table 3 reports the plutonium isotopic composition of the fresh fuel assemblies - containing plutonium coming from spent LWR reprocessed fuel -, and Table 4 illustrates the MA composition of the fresh fuel assemblies in the case of MA management (HOM4, and HET2 configurations).

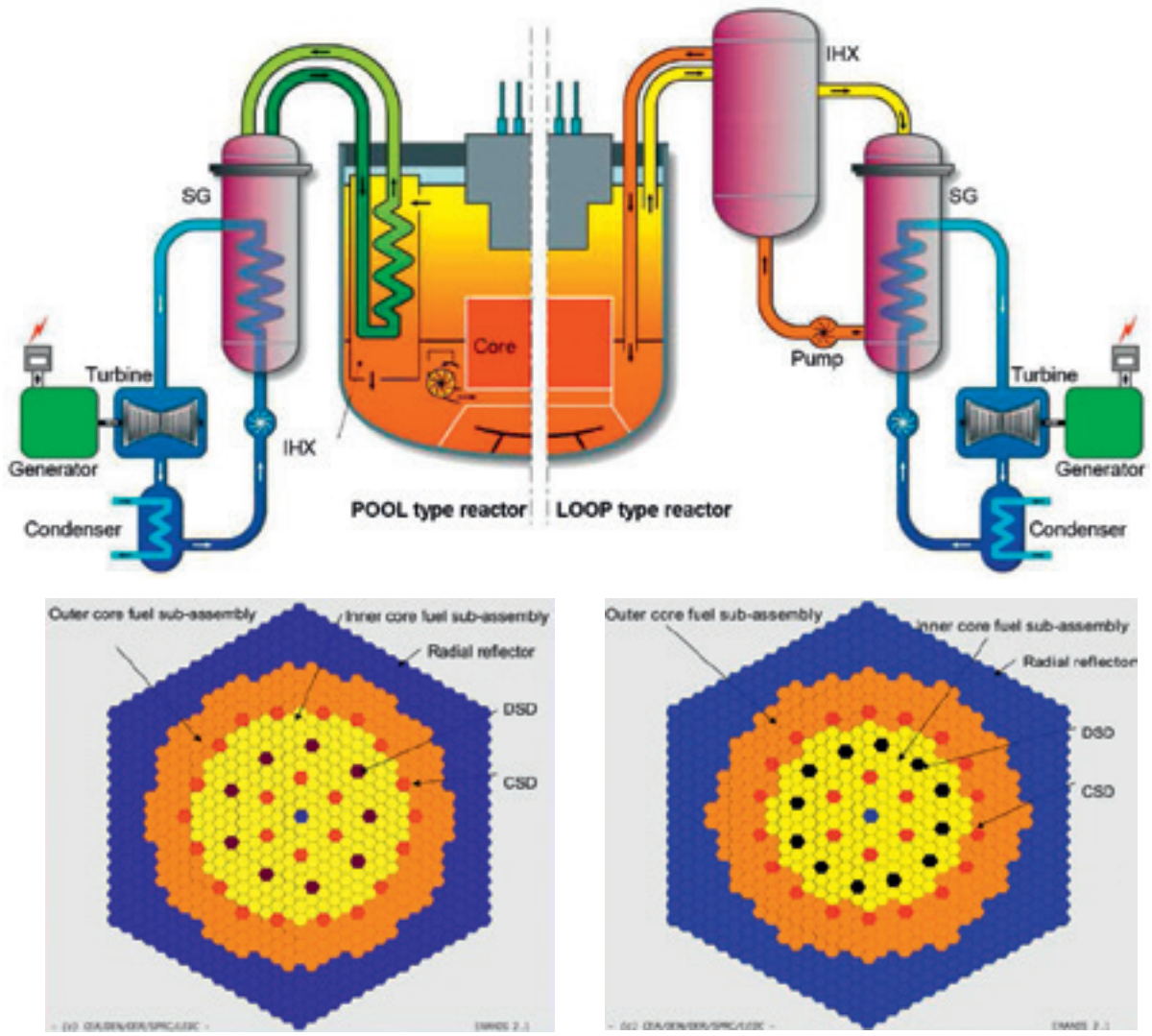

Oxide core [16] Carbide core [16]

Figure 2: Schematic diagram of reactor architectures of the two ESFR working horses [18] and the SFR reference core with oxide fuel and carbide fuel, no blanket case. IHX stands for Intermediate Heat Exchanger, SG stands for Steam Generator, CSD stands for Control and Shutdown device; DSD stands for Diverse Shutdown System. [16]

	SFR Design Concepts as in [10]			ESFR	
Design Parameters	**JSFR[3]**	**KALIMER[4]**	**SMFR[5]**	**Oxide**	**Carbide**
Power Rating, MWe	1,500	600	50	1500	
Thermal Power, MWt	3,570	1,525	125	3600	
Plant Efficiency, %	42	42	~38	42	
Core outlet coolant temperature, oC	550	545	~510	545	
Core inlet coolant temperature, oC	395	370	~355	395	
Main steam temperature, oC	503	495	480	470	
Main steam Pressure, MPa	16.7	16.5	20	18.5	
Cycle length, years	1.5–2.2	1.5	30	2050 EFPD	1600 EFPD
Fuel reload batch, batches	4	4	1	5	3
Core Diameter, m	5.1	3.5	1.75	4.72	4.10
Core Height, m	1.0	0.8	1.0	1.0	0.8
Fuel Type	MOX(TRU bearing)	Metal(U-TRU-10%Zr Alloy),	Metal(U-TRU-10%Zr Alloy),	(U,Pu)O2	(U,Pu)C
Pu content, %	13.8	24.9	15.0	14.05-16.35	17.80-24.50
Burn-up, GWd/t	150	79	~87	100	144
Breeding ratio	1.0–1.2	1.0	1.0	-	-

Table 1: ESFR reference cores characteristics compared with the SFR systems mentioned in [10]. MOX Stands for Mixed Oxides, TRU stands for Transuranium elements, HM stands for Heavy Metal, EFPD stands for Effective Full Power Days.

[3] JAEA Sodium Fast Reactor. The system foresees a loop design [10].
[4] "Korea Advanced Liquid Metal Reactor": Korean pool-type SFR design [10].
[5] US pool-type Small Modular SFR design [10].

	Oxide Core	Carbide Core
Pu content (inner fuel region) (%)	14.05	17.8
Pu content (outer fuel region) (%)	16.35	24.5
Pu mass per item	> 1SQ[6]	> 1SQ

Table 2: Main characteristics of the ESFR reference cores fresh fuel assemblies [6].

Pu Isotope	^{238}Pu	^{239}Pu	^{240}Pu	^{241}Pu	^{242}Pu
%	3.60	47.76	29.89	8.29	10.46

Table 3: Pu composition for ESFR fresh fuel assemblies (all considered core configurations) [17].

In the course of the project the original core options ("reference cores") have subsequently been subject to further analysis and new variants were put on the table for consideration ("CONF-2" cores, from now on referred to as "optimized cores"[7]). As long as PR is considered, the major design variation of all optimized cores is the availability of an axial blanket (i.e. a fertile zone containing depleted UO2) beneath the active part of the fuel element. The plutonium composition of the optimized cores fresh fuel assemblies is the same of the reference ones, reported in Table 3. The main differences between the optimized and reference cores characteristics are shown in Table 5.

As with the reference cores, also the oxide optimized core was investigated for MA management. In this paper, one homogeneous (HOM4' – foreseeing 4% MA content in the Fresh FAs) and two heterogeneous (HET1' and HET2') will be analyzed. As in the case of the reference cores, the HET1' and HET2' options foresee the same core of the optimized oxide core (including the same fresh fuel assemblies) plus additional radial blanket assemblies around it. The HET1' core configuration foresees radial blanket assemblies made of 85% depleted UO_2 and 15% MA. The HET2' core configuration foresees radial blanket assemblies made of 80% depleted UO_2 and 20% MA. The project partners investigated the possibility to perform MA management only within the oxide optimized core type. The fuel elements (HOM4' configuration) and radial blanket (HET1' and HET2' configuration) MA composition are the same of the reference oxide core, reported in Table 4.

Figure 3 summarizes all the ESFR core options considered in this paper.

Isotope	^{237}Np	^{241}Am	^{242m}Am	^{243}Am	^{242}Cm	^{243}Cm	^{244}Cm	^{245}Cm	^{246}Cm
%	16.86	60.62	0.24	15.70	0.02	0.07	5.14	1.26	0.09

Table 4: MA composition of the ESFR assemblies in case of MA transmutation (HOM4, HET2, HET1, HOM4', HET2' configurations) [17].

	Oxide Core		Carbide Core	
	Reference Core	Optimized Core	Reference Core	Optimized Core
Number of Inner core S/A	225	225	168	225
Number of Outer Core S/A	228	228	246	228
Active Core Height (m)	1.0	1.0	0.8	1.0
Number of fuel pins per sub-assembly	271	271	331	271
Outer clad diameter (mm)	10.73	10.73	8.0	8.5
Inner clad diameter (mm)	9.73	9.73	7.0	7.5
Fuel pellet diameter (mm)	9.43	9.43	6.87	7.37
Fuel pellet material	(U, Pu)O_2	(U, Pu)O_2	(U, Pu)C	(U, Pu)C
Inner Core Fuel Content (%)	14.05	14.76	17.8	14.05
Outer Core Fuel Content (%)	16.35	17.15	24.5	18.35

Table 5: Comparison of ESFR reference and optimized cores characteristics [20].

[6] The IAEA defines the significant quantity (SQ) as the approximate amount of NM for which the possibility of manufacturing a nuclear explosive device cannot be excluded. A SQ for Pu, containing less than 80% ^{238}Pu, is 8 kg [19].

[7] The optimization process was not driven by PR&PP considerations.

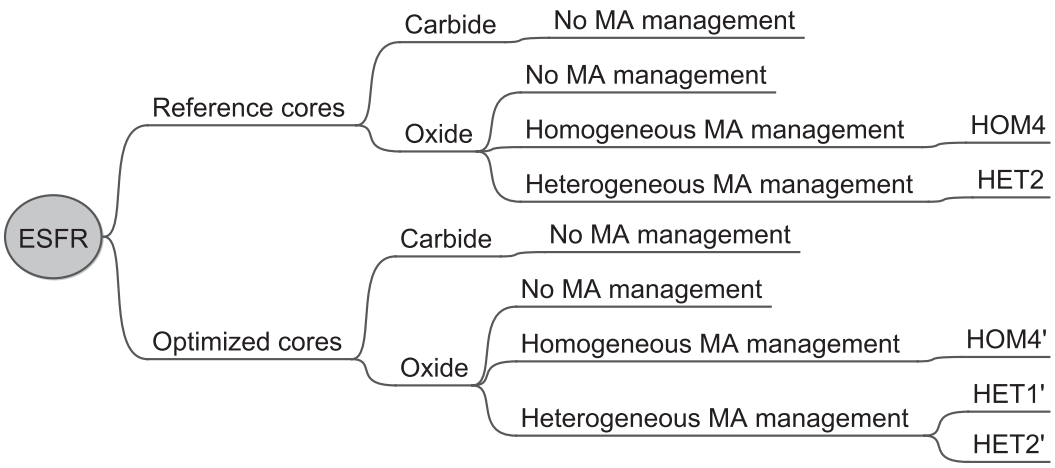

Figure 3: ESFR core configuration options analyzed in this paper.

4. ESFR PR relevant system elements and potential adversary targets

As defined in [7], "PR relevant system elements" are defined as a "collection of facilities inside the identified nuclear energy system (NES) where nuclear material diversion/acquisition and/or processing, as well as theft or radiological sabotage could take place", and proliferation targets are "nuclear material that can be diverted or equipment/processes that can be misused to process undeclared nuclear materials or can be replicated in an undeclared facility".

4.1 ESFR relevant system elements

Figure 4 shows the basic system elements for both pool and loop type 'working horses'[8]. Although the in vessel fuel handling systems of the reactors are different for pool and loop reactor types, both designs share the same conceptual system elements.

Since both the pool and loop configuration share the same core options, from now on the analysis will be valid for both types.

4.2 Targets for the reference cores

The possible ESFR nuclear material diversion targets for the reference cores are the Fresh FAs, spent FAs and - if present – radial blanket assemblies. Figure 5 shows the possible nuclear material target types (in red) in the core configurations here considered. Hereafter no distinction between inner and outer core is made and representative values are used.

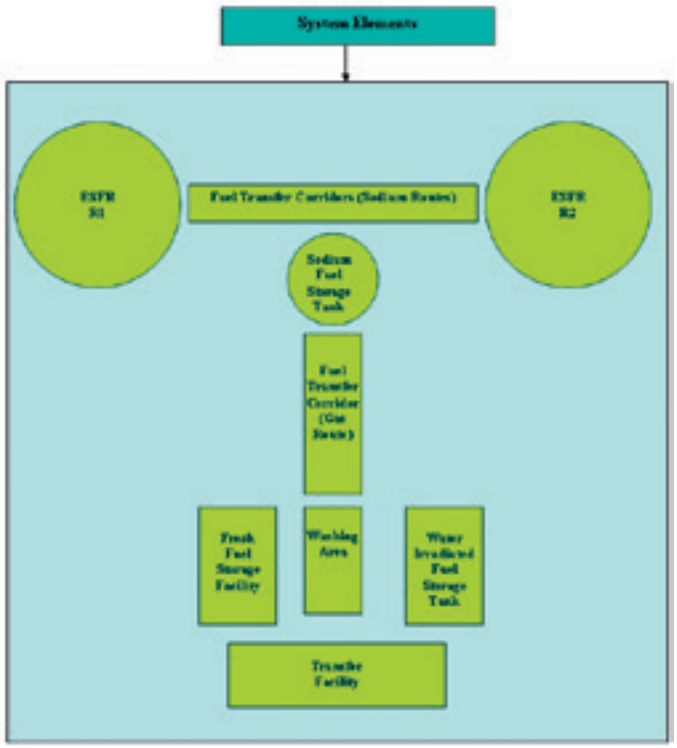

Figure 4: ESFR system elements [6].

The ESFR fuel assemblies have a much higher fissile material content compared to typical light water reactors[9]. This makes these assemblies, especially the fresh ones, an attractive target for a potential diversion strategy.

All fresh FAs, all spent FAs and the spent (irradiated) HET2 oxide radial blanket assemblies (BAs) contain plutonium. The plutonium quality in the targets will differ depending on the target type.

Where present, the fresh oxide HET2 radial BAs are plutonium-free and will not considered in the analysis.

[8] In case MA-bearing fuel is considered, there might be the need of adding a disassembly shop after the washing area or in the transfer facility allowing transport to the reprocessing plant. This would be required also for assembling the FAs with MA. This would add an additional system elements to the ones presented in Figure 4 [6].

[9] Typically, a LWR spent fuel assembly contains less than 1 SQ of Pu (see e.g. [21]) and the ESFR assemblies here considered always have more than 2 SQ of Pu per assembly (see section 6.1).

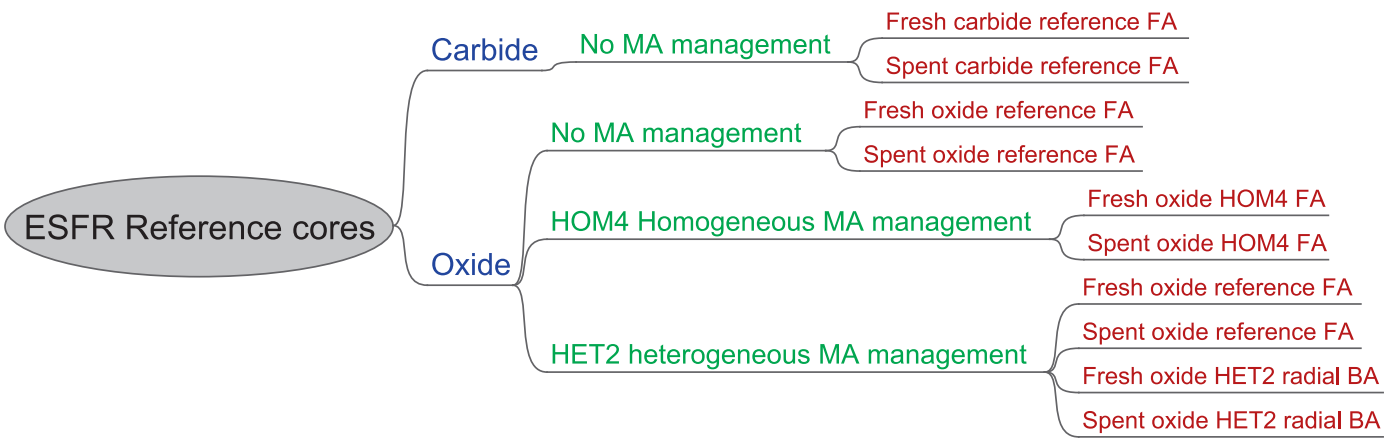

Figure 5: Reference cores nuclear material diversion targets [6].

An additional potential adversary target is represented by the undeclared nuclear material production (by misusing the ESFR system) via the irradiation of fertile material in the reactor core [10].

4.3 Targets for the optimized cores

The identified nuclear material diversion targets for the optimized cores are reported in Figure 6.

The optimized cores foresee the presence of a depleted uranium lower axial blanket in the carbide and oxide fresh FA. When the optimized carbide and oxide fresh FAs are irradiated, the plutonium quality in the axial blanket and in the rest of the FA will differ substantially; after irradiation the lower axial blanket in the spent FA can be cut from the rest of the assembly in order to be processed separately. For this reason, Figure 6 shows also the lower axial

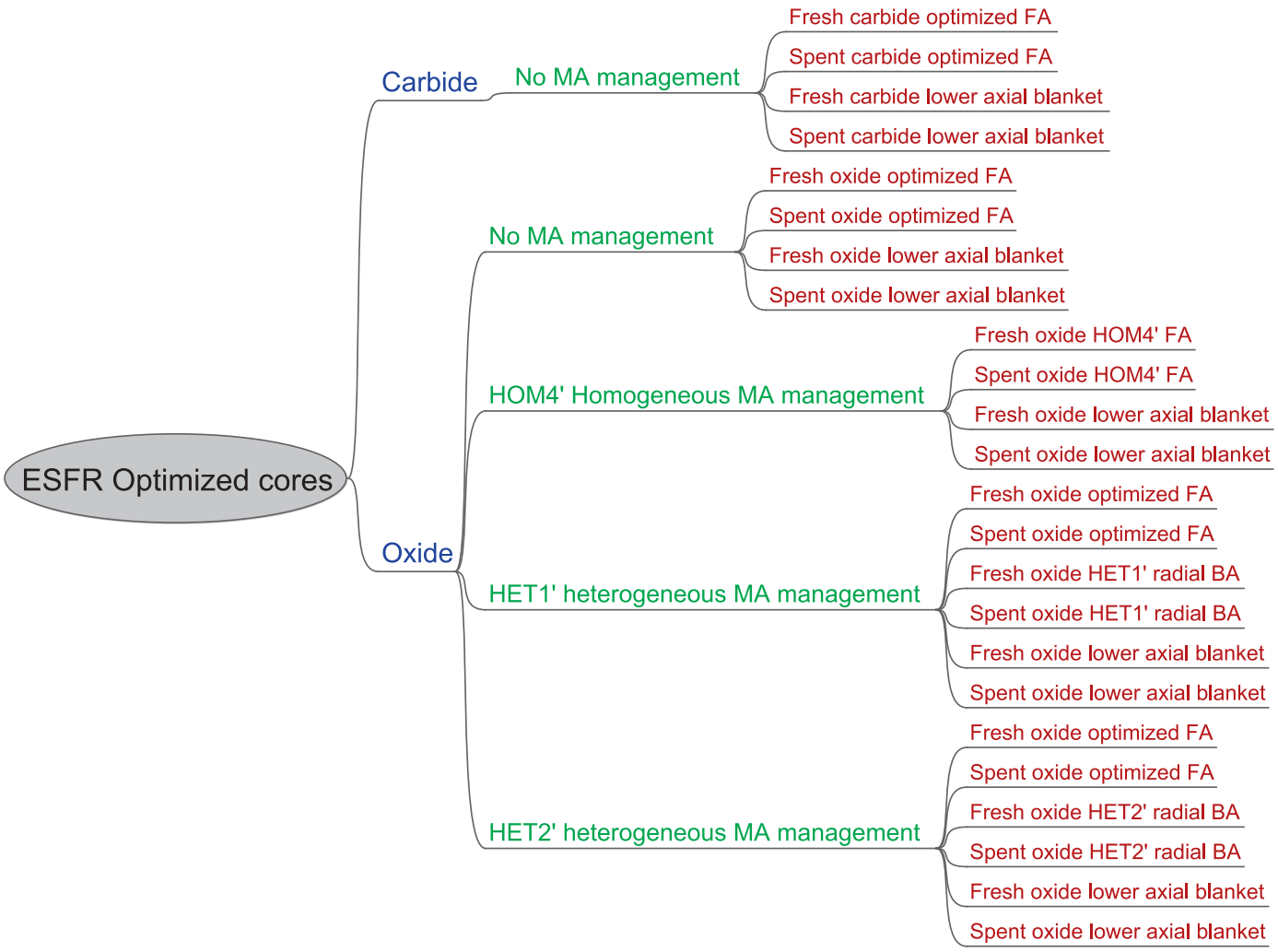

Figure 6: Optimized cores diversion targets [6].

blanket in the carbide and oxide spent FAs as an additional potential adversary target to the already mentioned ones, even if in order to divert the axial blanket material, the diverter has to divert the full ESFR spent FA.

As for the reference cores, the carbide and oxide optimized FA, the oxide HOM4' FA and all the spent FAs - including the spent (irradiated) HET1' and HET2' radial BAs - contain plutonium.

Fresh oxide HET1' and HET2' radial BAs and all the fresh lower axial blankets are plutonium-free and will not be considered in the analysis here presented.

As with the reference cores, another potential adversary target is represented by the undeclared nuclear material production via the irradiation of fertile material in the reactor core [10].

5. ESFR Cores material type analysis

The CP-ESFR PR study concentrated its efforts on the analysis of the different proposed core options. In order to understand the impact that the different options might have on the overall proliferation resistance of the system, the analysis has been focused on estimating the nuclear material attractiveness of selected alternatives. Although the PR&PP methodology Fissile Material Type measure is built having in mind the final product to be used in the fabrication stage, the proposed plutonium categories were felt to be too coarse to be able to discriminate between the available alternatives, and therefore additional metrics from literature studies have been investigated and applied to the ESFR data. In particular, the chosen literature metrics adopted the ones proposed by the INPRO PR methodology [7], Pellaud [11], Kessler et al. [12], and Bathke et al. [13]. Table 6 reports the characteristics considered by the material type measures used in this analysis, together with the related assumed high level proliferation pathways and scenarios.

The analysis here reported concentrates on the proliferation attractiveness of the material contained in the CP-ESFR reference and optimized cores' nuclear material diversion targets for the various considered core options. The main objective of the analysis is to identify the impact of the various core options to the proliferation resistance of the system in terms of nuclear material diversion. The following paragraphs briefly present the measures used and the outcome of their application to the ESFR core options.

5.1 GIF PR&PP Evaluation Methodology, Fissile Material Type measure

The fissile material type (MT) measure is one of the six measures identified by the GIF PR&PP Evaluation Methodology [7]. It categorizes plutonium in three categories according to the fraction of Pu fissile isotopes [7]:

- Weapon Grade (WG) Pu: Nominally 94% fissile Pu isotopes;
- Reactor Grade (RG) Pu: Nominally 70% fissile Pu isotopes;
- Deep Burn (DB) Pu: Nominally 43% fissile Pu isotopes.

Table 7 reports the fissile material type measure according to [7] for the reference cores' targets.

According to the PR&PP Fissile Material Type measure as defined in [7], there is no substantial PR difference between the considered core alternatives (all targets – fresh and irradiated ones - contain reactor-grade plutonium). From Table 7 it can be seen that all the targets exhibit a medium proliferation resistance score, including the spent oxide HET2 radial BA. Remarkably, the latter exhibits the lowest concentration of Pu fissile isotopes of all the considered diversion targets.

Table 8 reports the same analysis done for the optimized cores options diversion targets. Compared to the reference cores options, the optimized cores provide a wider

Study	Bare sphere critical mass	Heat generation rate	Spontaneous neutron emission	Dose rate	Implicit acquisition pathway assumption
GIF PRPP MT	NO	NO	NO	NO	State processes diverted material to obtain separated Pu
INPRO PR UR2	NO	YES	YES	YES	State processes diverted material to obtain separated Pu
Pellaud	YES	NO	YES	NO	State processes diverted material to obtain separated Pu
Kessler	YES	YES	NO	NO	State processes diverted material to obtain separated Pu
Bathke (FOM_1)	YES	YES	NO	YES	Technically advanced State processes diverted material to obtain separated Pu Subnational groups don't perform chemical separation of the acquired material
Bathke (FOM_2)	YES	YES	YES	YES	Developing State processes diverted material to obtain separated Pu

Table 6: Characteristics considered by the considered material type measures, together with the related assumed proliferation pathways.

Core option	target	Fissile isotopes ($^{239}Pu+^{241}Pu$)% in Pu	Estimated Measure Value	PR Qualitative Descriptor
Carbide reference	Fresh carbide reference FA	56.05	RG-Pu	Medium
	Spent carbide reference FA	68.41	RG-Pu	Medium
Oxide reference	Fresh oxide reference FA	56.05	RG-Pu	Medium
	Spent oxide reference FA	67.69	RG-Pu	Medium
Oxide HOM4	Fresh oxide HOM4 FA	56.05	RG-Pu	Medium
	Spent oxide HOM4 FA	63.82	RG-Pu	Medium
Oxide HET2	Fresh oxide reference FA	56.05	RG-Pu	Medium
	Spent oxide reference FA	67.69	RG-Pu	Medium
	Spent oxide HET2 radial BA	48.74	RG-Pu	Medium

Table 7: Fissile Material Type measure for the reference cores' diversion targets in the selected core options according to metrics and scales in [7]. Data taken from [6].

Core option	Target	Fissile isotopes ($^{239}Pu+^{241}Pu$)% in Pu	Estimated Measure Value	PR Qualitative Descriptor
Carbide optimized	Fresh carbide optimized FA	56.05	RG-Pu	Medium
	Spent carbide optimized FA – axial blanket included	63.47	RG-Pu	Medium
	Axial blanket in spent carbide optimized FA	96.68	WG-Pu	Low
Oxide optimized	Fresh oxide optimized FA	56.05	RG-Pu	Medium
	Spent oxide optimized FA – axial blanket included	62.54	RG-Pu	Medium
	Axial blanket in spent oxide optimized FA	96.73	WG-Pu	Low
Oxide HOM4'	Fresh oxide HOM4' FA	56.05	RG-Pu	Medium
	Spent oxide HOM4' FA – axial blanket included	57.31	RG-Pu	Medium
	Axial blanket in spent oxide HOM4' FA	96.73	WG-Pu	Low
Oxide HET1'	Fresh oxide optimized FA	56.05	RG-Pu	Medium
	Spent oxide optimized FA – Axial blanket included	62.54	RG-Pu	Medium
	Axial blanket in spent oxide optimized FA	96.73	WG-Pu	Low
	Spent oxide HET1' radial BA	62.35	RG-Pu	Medium
Oxide HET2'	Fresh oxide optimized FA	56.05	RG-Pu	Medium
	Spent oxide optimized FA – axial blanket included	62.54	RG-Pu	Medium
	Axial blanket in spent oxide optimized FA	96.73	WG-Pu	Low
	Spent oxide HET2' radial BA	49.84	RG-Pu	Medium

Table 8: Fissile material type measure for the optimized cores' diversion targets according to metrics and scales in [7]. Data taken from [6].

selection of potential diversion targets, and if the reference cores do not present major differences in terms of the targets' plutonium composition, in the optimized cores' options the introduction of a lower axial blanket region in the FA leads to the appearance of weapon-grade plutonium among the potential diversion choices for a potential proliferator. However, it has to be noticed that the diversion of this nuclear material would imply the diversion of an entire spent optimized FA. Moreover, the axial blanket in the single FA is far from containing one significant quantity of plutonium[10], and the acquisition of 1 SQ of WG-Pu would therefore imply the diversion of several spent FA. As with the reference cores, the various optimized cores' configuration are substantially similar in terms of the fissile material type available to a potential proliferator.

5.2 INPRO PR Methodology, User Requirement 2 (UR2)

User Requirement (UR) 2 of the INPRO (International Project on Innovative Nuclear Reactors and Fuel Cycles) PR manual states that "the attractiveness of nuclear material and nuclear technology in an innovative nuclear system for a nuclear weapons program should be low"[11]. UR2 has 4 related indicators (IN) foreseeing 13 evaluation parameters (EP) [9]. Of them, this study used 3 indicators and nine related evaluation parameters[12]. Table 9 reports UR2 indicators and evaluation parameters as used in this analysis, with an overview of the associated metrics and PR qualifiers.

According to the INPRO PR manual, each evaluation parameter is to be evaluated via a five-range scale: Very Weak (VW), Weak (W), Moderate (M), Strong (S) and Very Strong (VS). in this context, very weak has the meaning of a very weak proliferation barrier, and very strong has the meaning of a very strong proliferation barrier[13].

[10] See Figure 8.

[11] [9], p. 45.

[12] The study quantified only the indicators and parameters applicable to the plutonium contained in the ESFR targets.

[13] While Table 9 reports a flavor of how the scale is related to the PR qualifiers, for a more detailed description of the INPRO PR scales associated to each EP see [9].

Indicator	Evaluation Parameter	Metric considered	PR qualifier
IN2.1 (Material quality)	EP2.1.1 (Material type / category)	Unirradiated direct use NM (UDU), irradiated direct use NM (IDU), low-enriched uranium (LEU), natural uranium (NU) or depleted uranium (DU)	UDU is related to a VW barrier to proliferation, DU is related to a VH barrier to proliferation
	EP2.1.2 (Isotopic composition)	Relative ^{239}Pu isotopic content	The higher the relative isotopic content, the weaker the proliferation barrier
	EP2.1.3 (Radiation field)	"Dose rate (mSv/hr) at 1 m from the surface of the nuclear material to be diverted"[14]	The lower the dose rate, the weaker the proliferation barrier
	EP2.1.4 (Heat generation)	Relative ^{238}Pu isotopic content	The lower the relative isotopic content, the weaker the proliferation barrier
	EP2.1.5 (Spontaneous neutron generation rate)	Relative isotopic content of the even isotopes of plutonium (^{240}Pu and ^{242}Pu)	The lower the relative isotopic content, the weaker the proliferation barrier
IN2.2 (Material quantity)	EP2.2.1a (Mass of item)	Mass of the item to be diverted	The lower the mass, the weaker the proliferation barrier
	EP2.2.2 (Number of items for SQ[15])	The number of items to be diverted to acquire 1 SQ of NM	The lower the number of items to be diverted for acquire 1 SQ of NM, the weaker the proliferation barrier
	EP2.2.3 (No. of SQ - material stock or flow)	Throughput of the facility in terms of significant quantities of nuclear material in a given period of time	The higher the throughput, the weaker the proliferation barrier
IN2.3 (Material classification)	EP2.3.1 (Chemical/physical form)	The form of the nuclear material	The closer the form to the final target one, the weaker the proliferation barrier

Table 9: INPRO PR UR2 indicators and evaluation parameters as used in this analysis, adapted from [9].

EP2.1.1 Material type/ category

Core Option	Target	VW	W	M	S	VS	MT type
Carbide reference	Fresh carbide reference FA	■					UDU
	Spent carbide reference FA		■				IDU
Oxide reference	Fresh oxide reference FA	■					UDU
	Spent oxide reference FA		■				IDU
Oxide HOM4	Fresh oxide HOM4 FA	■					UDU
	Spent oxide HOM4 FA		■				IDU
Oxide HET2	Fresh oxide reference FA	■					UDU
	Spent oxide reference FA		■				IDU
	Spent oxide HET2 radial BA		■				IDU

UDU: Un-irradiated Direct Use Material
IDU: Irradiated Direct Use Material

EP2.1.2 Isotopic composition

VW	W	M	S	VS	Pu-239/Pu (%)
			■		47.76
	■				62.96
			■		47.76
	■				62.41
			■		47.76
	■				58.82
			■		47.76
	■				62.41
			■		48.57

EP2.1.3 Radiation field

VW	W	M	S	VS	Dose (mGy/hr)
■					145
				■	4.63E+06
	■				173
				■	4.13E+06
			■		3330
				■	3.86E+06
	■				173
				■	4.13E+06
				■	2.29E+06

EP2.1.4 Heat generation rate

Core Option	Target	VW	W	M	S	VS	Pu-238/Pu (%)
Carbide reference	Fresh carbide reference FA		■				3.60
	Spent carbide reference FA		■				1.37
Oxide reference	Fresh oxide reference FA		■				3.60
	Spent oxide reference FA		■				1.94
Oxide HOM4	Fresh oxide HOM4 FA		■				3.60
	Spent oxide HOM4 FA		■				6.68
Oxide HET2	Fresh oxide reference FA		■				3.60
	Spent oxide reference FA		■				1.94
	Spent oxide HET2 radial BA				■		37.79

EP2.1.5 Spontaneous neutron gen. rate

VW	W	M	S	VS	(Pu-240+Pu-242)/Pu (%)
	■				40.35
	■				30.22
	■				40.35
	■				30.37
	■				40.35
	■				29.50
	■				40.35
	■				30.37
	■				13.47

EP2.2.1a Mass of an item (kg)

VW	W	M	S	VS	Mass of one item (kg)
			■		500 - 750
			■		500 - 750
			■		500 - 750
			■		500 - 750
			■		500 - 750
			■		500 - 750
			■		500 - 750
			■		500 - 750
			■		500 - 750

EP2.2.2 No. of items for SQ

Core Option	Target	VW	W	M	S	VS	No. of SQ in FA
Carbide reference	Fresh carbide reference FA	■					2.90
	Spent carbide reference FA	■					2.52
Oxide reference	Fresh oxide reference FA	■					3.45
	Spent oxide reference FA	■					4.83
Oxide HOM4	Fresh oxide HOM4 FA	■					3.45
	Spent oxide HOM4 FA	■					5.26
Oxide HET2	Fresh oxide reference FA	■					3.45
	Spent oxide reference FA	■					4.83
	Spent oxide HET2 radial BA	■					0.83

EP2.2.3 No. of SQ (material stocks or flow)

VW	W	M	S	VS	No of SQ in NES
■					>100
■					>100
■					>100
■					>100
■					>100
■					>100
■					>100
■					>100
	■				69.72

EP2.3.1 Chemical/ physical form

VW	W	M	S	VS	Form
		■			Pu compounds
			■		Spent Fuel
		■			Pu compounds
			■		Spent Fuel
		■			Pu compounds
			■		Spent Fuel
		■			Pu compounds
			■		Spent Fuel
			■		Spent Fuel

Figure 7: Comparison of the cases with respect to nuclear material attractiveness study in INPRO (for the working horses' cores) [14].

[14] [9], p. 47.
[15] Significant Quantity.

Core option	Target	EP2.1.1 Material type/ category					EP2.1.2 Isotopic composition					EP2.1.3 Radiation field				
		VW	W	M	S	VS	MT type	VW	W	M	S	VS	Pu-239/Pu (%)	VW	W	M	S	VS	Dose (mGy/hr)
Carbide optimized	Fresh carbide optimized FA - Axial blanket included	■					UDU				■		47.76		■				129
	Spent carbide optimized FA - Axial blanket included		■				IDU		■				55.70					■	4.10E+06
	Axial blanket in spent carbide optimized FA						IDU						96.58						6.60E+05
Oxide optimized	Fresh oxide optimized FA - Axial blanket included	■					UDU				■		47.76		■				176
	Spent oxide optimized FA - Axial blanket included		■				IDU		■				57.84					■	3.97E+06
	Axial blanket in spent oxide optimized FA						IDU						96.64						5.50E+05
Oxide HOM4'	Fresh oxide HOM4' FA - Axial blanket included	■					UDU				■		47.76				■		3340
	Spent oxide HOM4' FA - Axial blanket included		■				IDU		■				52.59					■	3.39E+06
	Axial blanket in spent oxide optimized FA						IDU						96.64						5.50E+05
Oxide HET1'	Fresh oxide optimized FA - Axial blanket included	■					UDU				■		47.76		■				176
	Spent oxide optimized FA - Axial blanket included		■				IDU		■				57.84					■	3.97E+06
	Axial blanket in spent oxide optimized FA						IDU						96.64						5.50E+05
	Spent oxide HET1' radial BA						IDU						62.11						2.07E+06
Oxide HET2'	Fresh oxide optimized FA - Axial blanket included	■					UDU				■		47.76		■				176
	Spent oxide optimized FA - Axial blanket included		■				IDU		■				57.84					■	3.97E+06
	Axial blanket in spent oxide optimized FA						IDU						96.64						5.50E+05
	Spent oxide HET2' radial BA						IDU				■		49.51					■	2.51E+06

UDU: Un-irradiated Direct Use Material
IDU: Irradiated Direct Use Material

Core option	Target	EP2.1.4 Heat generation rate					EP2.1.5 Spontaneous neutron gen. rate					EP2.2.1a Mass of an item (kg)					
		VW	W	M	S	VS	Pu-238/Pu (%)	VW	W	M	S	VS	(Pu-240+Pu-242)/Pu (%)	VW	W	M	S	VS	Mass of one item (kg)
Carbide optimized	Fresh carbide optimized FA - Axial blanket included		■				3.60		■				40.35				■		500 - 750
	Spent carbide optimized FA - Axial blanket included		■				2.75		■				33.78				■		500 - 750
	Axial blanket in spent carbide optimized FA		■				0.01		■				3.30				■		500 - 750
Oxide optimized	Fresh oxide optimized FA - Axial blanket included		■				3.60		■				40.35				■		500 - 750
	Spent oxide optimized FA - Axial blanket included		■				2.68		■				34.78				■		500 - 750
	Axial blanket in spent oxide optimized FA		■				0.01		■				3.26				■		500 - 750
Oxide HOM4'	Fresh oxide HOM4' FA - Axial blanket included		■				3.60		■				40.35				■		500 - 750
	Spent oxide HOM4' FA - Axial blanket included		■				5.57		■				37.12				■		500 - 750
	Axial blanket in spent oxide optimized FA		■				0.01		■				3.26				■		500 - 750
Oxide HET1'	Fresh oxide optimized FA - Axial blanket included		■				3.60		■				40.35				■		500 - 750
	Spent oxide optimized FA - Axial blanket included		■				2.68		■				34.78				■		500 - 750
	Axial blanket in spent oxide optimized FA		■				0.01		■				3.26				■		500 - 750
	Spent oxide HET1' radial BA				■		26.74		■				10.91				■		500 - 750
Oxide HET2'	Fresh oxide optimized FA - Axial blanket included		■				3.60		■				40.35				■		500 - 750
	Spent oxide optimized FA - Axial blanket included		■				2.68		■				34.78				■		500 - 750
	Axial blanket in spent oxide optimized FA		■				0.01		■				3.26				■		500 - 750
	Spent oxide HET2' radial BA				■		34.96		■				15.20				■		500 - 750

Core option	Target	EP2.2.2 No. of items for SQ					EP2.2.3 No. of SQ (material stocks or flow)					EP2.3.1 Chemical/ physical form					
		VW	W	M	S	VS	No. of SQ in FA	VW	W	M	S	VS	No of SQ in NES	VW	W	M	S	VS	Form
Carbide optimized	Fresh carbide optimized FA - Axial blanket included	■					2.57	■					>100			■			Pu compounds
	Spent carbide optimized FA - Axial blanket included	■					3.18	■					>100				■		Spent Fuel
	Axial blanket in spent carbide optimized FA		■				0.11(in ax. blanket)			■			49.83				■		Spent Fuel
Oxide optimized	Fresh oxide optimized FA - Axial blanket included	■					3.52	■					>100			■			Pu compounds
	Spent oxide optimized FA - Axial blanket included	■					4.34	■					>100				■		Spent Fuel
	Axial blanket in spent oxide optimized FA		■				0.13 (in ax. blanket)		■				58.89				■		Spent Fuel
Oxide HOM4'	Fresh oxide HOM4' FA - Axial blanket included	■					3.52	■					>100			■			Pu compounds
	Spent oxide HOM4' FA - Axial blanket included	■					3.82	■					>100				■		Spent Fuel
	Axial blanket in spent oxide optimized FA		■				0.13 (in ax. blanket)		■				58.89				■		Spent Fuel
Oxide HET1'	Fresh oxide optimized FA - Axial blanket included	■					3.52	■					>100			■			Pu compounds
	Spent oxide optimized FA - Axial blanket included	■					4.34	■					>100				■		Spent Fuel
	Axial blanket in spent oxide optimized FA		■				0.13 (in ax. blanket)		■				58.89				■		Spent Fuel
	Spent oxide HET1' radial BA	■					1.07	■					89.88				■		Spent Fuel
Oxide HET2'	Fresh oxide optimized FA - Axial blanket included	■					3.52	■					>100			■			Pu compounds
	Spent oxide optimized FA - Axial blanket included	■					4.34	■					>100				■		Spent Fuel
	Axial blanket in spent oxide optimized FA		■				0.13 (in ax. blanket)		■				58.89				■		Spent Fuel
	Spent oxide HET2' radial BA	■					1.68	■					141.12				■		Spent Fuel

Figure 8: Comparison of the optimized cores' targets with respect to nuclear material attractiveness study as in INPRO [6].

Figure 7 shows the outcome of the application of INPRO's PR UR2 to the reference cores' possible diversion targets, and Figure 8 shows the outcome of the same analysis applied to the optimized cores' possible diversion targets. Not surprisingly, the fresh fuel assemblies (which contain plutonium) present the weakest barriers to nuclear proliferation of all the possible diversion targets available to a potential proliferator. It has also to be noticed that according to the indicators used in this section the presence of an axial blanket does not seem to increase the proliferation attractiveness of the system. The main reason for this outcome – counterintuitive given the fact that the spent axial blanket region contain WG-Pu and the other targets contain RG-Pu – is to be found in the binning of EP2.1.2, which foresees only two PR qualifiers, a weak PR score if the ^{239}Pu/Pu ratio is above 50% and strong PR score otherwise. The binning implicitly considers any plutonium composition having more than 50% ^{239}Pu on the same level of attractiveness for a potential proliferator.

When MA management core options are considered, the indicators do not highlight any particular difference in the overall material quality of the available diversion targets. In particular, the spent oxide HET2' radial BAs present the highest proliferation barrier of the lot. If from a material quality point of view the HOM4', HET1' and HET2' options seem to be equivalent, the possibility to recycle minor actinides in the blanket (HET1' and HET2' options) instead of recycling them in fresh fuel elements (HOM4 and HOM4' options) would avoid incurring in "safeguardability"[16] issues for the fresh fuel elements [10]. On the other hand, it has to be noticed that the presence of a radial blanket would open up potential misuse scenarios that might worsen the overall PR of the reactor core.

According to the INPRO material quality indicator, there is no substantial difference between diversion targets in the oxide and the carbide options[17].

[16] Along the lines of [7] Safeguardability is here defined as "the ease with which a system can be effectively [and efficiently] put under international safeguards" ([7], p. 2).

[17] The only minor difference is in the radiation field Evaluation Parameter for the reference cores' fresh fuel (Figure 7, EP2.1.3), where the carbide's fresh FA exhibits a VW barrier to proliferation and the oxide's fresh FA exhibits a W barrier. The actual numerical differences in the dose (145 mGy/h versus 173 mGy/h) shows that the difference is just given by the INPRO binning, and does not have any practical significance.

5.3 Material type according to Pellaud and Kessler studies

Pellaud [11] focusses on the spontaneous neutron emission rate of the plutonium to be used in a nuclear military programme. Historically the plutonium composition has been categorised in terms of ^{240}Pu abundance as reported in Table 10. The table also reports Pellaud's assessment of the usability of each category for building a nuclear weapon device. It is worth noticing that although the reported categorization is based on ^{240}Pu concentration, Pellaud performs his analysis on the global neutron emission of the plutonium sample given a certain burn-up, without limiting himself to assess the concentration of one isotope. By analysing only plutonium isotopics, Pellaud assumes a high-level acquisition pathway in which the proliferant State processes the acquired nuclear material to obtain separated plutonium. In case the State shouldn't have a declared reprocessing phase already producing separated plutonium (e.g. a PUREX[18] type reprocessing facility), his analysis implicitly assumes that plutonium is separated by either misusing a declared reprocessing facility operating via a co-extraction process to separate pure Pu or processing it in a clandestine facility.

Category	^{240}Pu abundance range (%)	Usability for a nuclear weapon
Super-grade (SG)	< 3	Best quality
Weapon-grade (WG)	3-7	Standard material
Fuel-grade (FG)	7-18	Practically usable
Reactor-grade (RG)	18-30	Conceivably usable
MOX-grade	>30	Practically unusable

Table 10: Pellaud's assessment of the usability of various Pu categories. Adapted from [11].

Kessler [12] tackles the problem from a different angle: given that an implosion-type nuclear explosive device requires the use of high-potential organic explosive and that this explosive surrounds the plutonium core, the heat generated by plutonium needs to be compatible with what can be tolerated by the explosive. Starting from this assumption, Kessler analyses various plutonium compositions varying the concentration of the contained ^{238}Pu isotope, responsible of most of the heat generated by the Pu mixture. Through various calculations he ends up setting the threshold for ^{238}Pu concentration to around 9%: over this value Kessler suggests that the heat generated by the plutonium core would

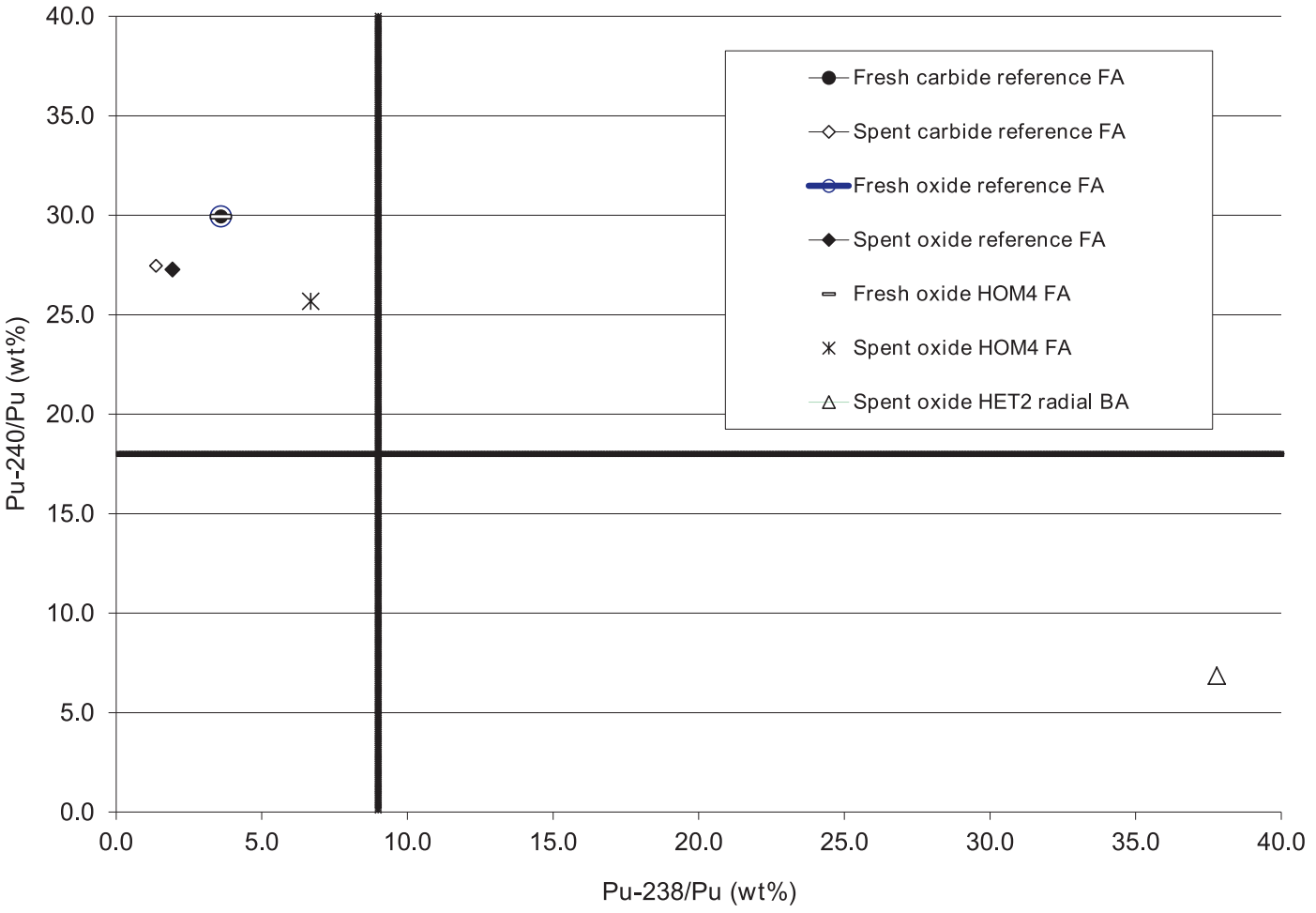

Figure 9: Reference, HOM4 and HET2 core options' diversion targets characterized according to Pellaud's [11] and Kessler's [12] material type's measures [6]. The fresh and spent oxide reference FA are present in both the reference and the HET2 core options.

[18] "Plutonium and Uranium Recovery by EXtraction"

be too high to be handled even for a technologically advanced State, and therefore the plutonium could be considered to be denatured. It is worth noting that in current nuclear fuel cycles this 9% threshold is far from being reached. As Pellaud, Kessler implicitly assumes an acquisition pathway in which the proliferant State processes the acquired nuclear material to separate plutonium and doesn't limit his analysis to the contribution of only one isotope, but computes the total heat generation rate of the plutonium sample. This is done on different plutonium isotopics.

Pellaud and Kessler's considered metrics have been computed for the targets available in the reference and optimized core options here considered. The results for the reference cores' targets are reported in Figure 9 and the results for the optimized cores' diversion targets are reported in Figure 10. The Y-axis shows the metric considered by Pellaud and the X-axis the one considered by Kessler.

As can be seen from Figure 9 and Figure 10, the results can be grouped in three main categories: the majority of the considered targets cannot be considered to be attractive according to Pellaud but they do according to Kessler. The axial blanket in spent oxide and carbide optimized FAs result to be attractive according to both metrics (Pellauds' and Kessler's) and spent oxide HET2, HET1' and HET2' radial BAs are attractive according to Pellaud but not according to Kessler. It has to be noticed that the high percentage of ^{238}Pu in the spent radial blanket assemblies is due to the presence of 15% (HET1' option)or 20% (HET2 and HET2' options) of minor actinides in the fresh blanket assemblies. As with the PR&PP material type measure, Pellaud and Kessler's measures seem to put in evidence that the irradiated axial blanket has the potential of increasing the attractiveness of the nuclear system to the eyes of a potential diverter.

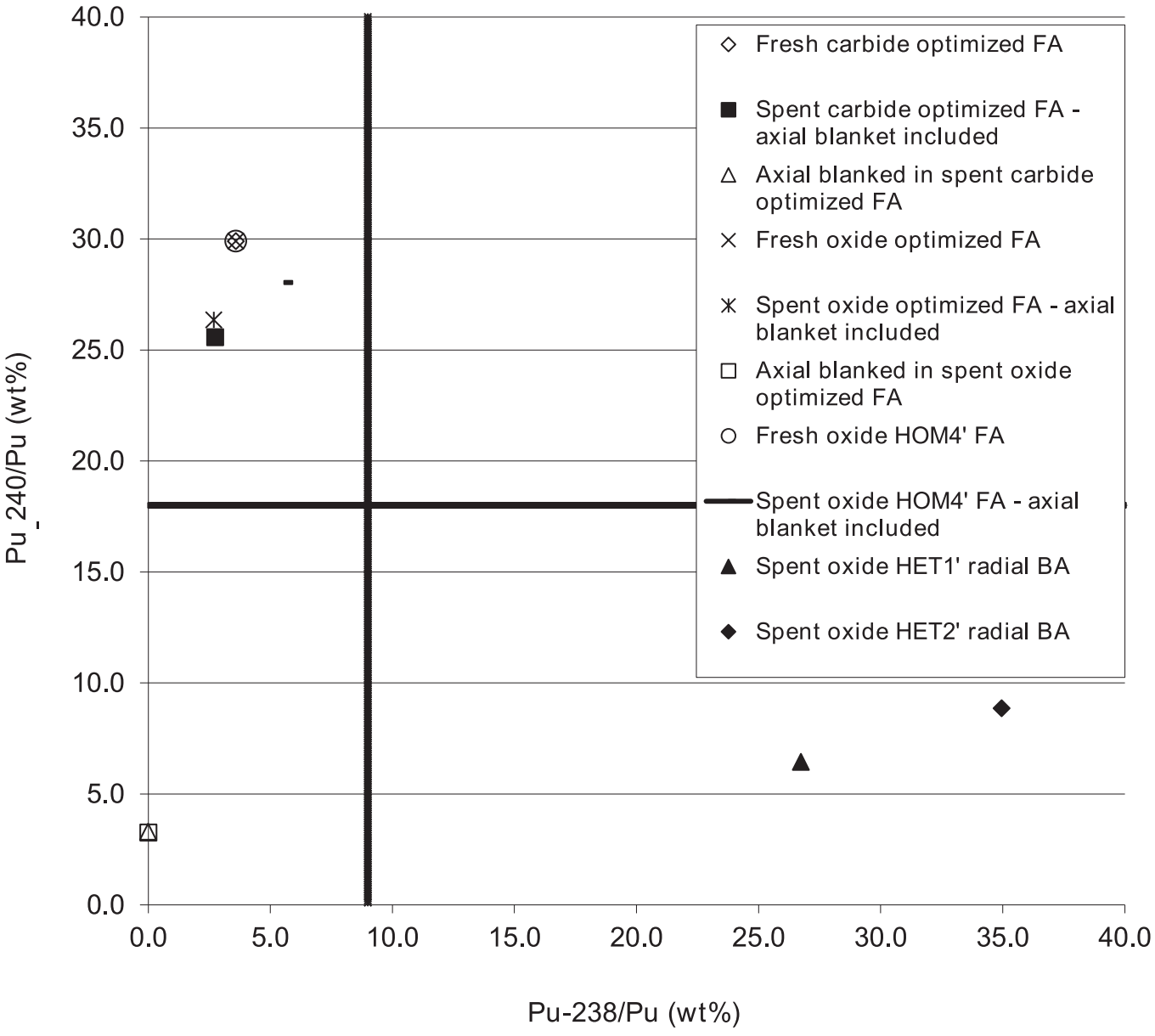

Figure 10: Optimized, HOM4', HET1' and HET2' core options' diversion targets characterized according to Pellaud's [11] and Kessler's [12] material type's measures [6]. The fresh and spent oxide optimized FAs are present in the optimized, HET1' and HET2' core options.

5.4 Material type according to Bathke et al. figures of merit

Bathke et al. [13] tries to analyze the nuclear proliferation attractiveness of the separated nuclear materials foreseen by advanced reprocessing options currently investigated for future deployment. The objective is to understand whether these options represent a real advance in nuclear proliferation resistance and if nuclear safeguards could be relaxed on some of the mixtures there produced. The study foresees several different figures of merit, relating to different proliferation scenarios. Figure 11 shows the four figures of merit considered by Bathke et al. [13], where M is the mixture's bare sphere critical mass in metal form in kg, N is the mass of a fuel assembly, h is the mixture's heat generation rate in W/kg, D is the dose rate of 0.2 M or 0.2 N evaluated at 1 m from the surface in rad/h and S is the intrinsic fission neutron production rate in n/s/kg [13].

A FOM value above 2 would represent a very attractive material (very low proliferation resistance), a FOM between 1 and 2 would represent a medium attractiveness and a FOM below 1 would represent an unattractive material (and therefore a high proliferation resistance).

Table 11 summarizes the Figures of merit, the potential proliferators associated with them and the resulting underlying scenarios.

Table 12 shows the figure of merit FOM11 and FOM21 applied to the plutonium isotopic composition of the reference cores' targets, and Table 13 does the same but taking into consideration not only the plutonium isotopic but the mixture made of both plutonium and minor actinides.

Table 14 shows the figure of merit FOM11 and FOM21 applied to the plutonium isotopic composition of the optimized cores' targets, and Table 15 does the same but taking into consideration not only the plutonium isotopic but the mixture made of both plutonium and minor actinides.

$$FOM_1^1 = 1 - \log_{10}\left(\frac{M}{800} + \frac{Mh}{4500} + \frac{M}{50}\left[\frac{D}{500}\right]^{\frac{1}{\log_{10} 2}}\right) \quad (1)$$

$$FOM_1^2 = 1 - \log_{10}\left(\frac{M}{800} + \frac{Mh}{4500} + \frac{N}{10}\left[\frac{D}{500}\right]^{\frac{1}{\log_{10} 2}}\right) \quad (2)$$

$$FOM_2^1 = 1 - \log_{10}\left(\frac{M}{800} + \frac{Mh}{4500} + \frac{MS}{6.8(10)^6} + \frac{M}{50}\left[\frac{D}{500}\right]^{\frac{1}{\log_{10} 2}}\right) \quad (3)$$

$$FOM_2^2 = 1 - \log_{10}\left(\frac{M}{800} + \frac{Mh}{4500} + \frac{MS}{6.8(10)^6} + \frac{N}{10}\left[\frac{D}{500}\right]^{\frac{1}{\log_{10} 2}}\right) \quad (4)$$

Figure 11: The four Figures of merit considered by [13]. Eq. (1) and (3) apply to mixtures, and eq. (2) and (4) apply to full fuel assemblies.

Actor	FOM_1^1 eq. (1)	FOM_1^2 eq. (2)	FOM_2^1 eq. (3)	FOM_2^2 eq.(4)
Sub-national group	Diversion of best possible reprocessed product, no additional chemical separation	Diversion of best possible material and wait until sufficient decay occurred for separating plutonium	N/A	N/A
Technically advanced State	State processes acquired material to obtain separated plutonium	Not realistic	N/A	N/A
Developing State	N/A	N/A	State processes acquired material to obtain separated plutonium	State diverts best possible material and waits until sufficient decay occurred for separating plutonium

Table 11: FOMs, potential proliferators and resulting underlying scenarios [22].

Core option	Target	If MA is separated from Pu					
		M (kg)	h (W/kg)	D (rad/h)	S (n/s/kg)	FOM_1	FOM_2
Carbide reference	Fresh carbide reference FA	15.30	2.37E+01	8.02E-02	6.08E+05	2.00	0.83
	Spent carbide reference FA	13.44	1.11E+01	3.76E-02	3.84E+05	2.30	1.09
Oxide reference	Fresh oxide reference FA	15.42	2.37E+01	8.08E-02	5.23E+05	2.00	0.89
	Spent oxide reference FA	13.40	1.43E+01	4.44E-02	4.02E+05	2.23	1.07
Oxide HOM4	Fresh oxide HOM4 FA	15.42	2.37E+01	8.08E-02	5.23E+05	2.00	0.89
	Spent oxide HOM4 FA	13.28	4.10E+01	1.03E-01	5.25E+05	1.86	0.93
Oxide HET2	Fresh oxide reference FA	15.42	2.37E+01	8.08E-02	5.23E+05	2.00	0.89
	Spent oxide reference FA	13.40	1.43E+01	4.44E-02	4.02E+05	2.23	1.07
	Spent oxide HET2 radial BA	11.04	2.16E+02	4.01E-01	1.20E+06	1.27	0.60

Table 12: FOM results for different diversion targets in the reference core cases (separated Pu only) [6].

Core option	Target	If MA is not separated from Pu (Pu+MA Mixture)					
		M (kg)	h (W/kg)	D (rad/h)	S (n/s/kg)	FOM_1	FOM_2
Carbide reference	Fresh carbide reference FA	15.35	2.44E+01	1.90	6.03E+05	1.99	0.83
	Spent carbide reference FA	14.15	2.74E+01	1.68E+01	1.50E+08	1.98	-1.49
Oxide reference	Fresh oxide reference FA	15.41	2.44E+01	1.92	6.04E+05	1.99	0.83
	Spent oxide reference FA	14.28	3.09E+01	1.89E+01	6.14E+07	1.94	-1.11
Oxide HOM4	Fresh oxide HOM4 FA	17.43	6.55E+01	38.70	9.55E+07	1.56	-1.39
	Spent oxide HOM4 FA	15.00	7.60E+01	4.91E+01	1.37E+08	1.56	-1.48
Oxide HET2	Fresh oxide reference FA	15.41	2.44E+01	1.92	6.04E+05	1.99	0.83
	Spent oxide reference FA	14.28	3.09E+01	1.89E+01	6.14E+07	1.94	-1.11
	Spent oxide HET2 radial BA	39.48	2.05E+02	4.65E+02	4.24E+08	0.61	-2.39

Table 13: FOM results for different diversion targets in the reference core cases (Pu and MA mixture)[19] [6].

Core option	Target	If MA is separated from Pu					
		M (kg)	h (w/kg)	D (Rad/h)	s (n/s/kg)	FOM_1	FOM_2
Carbide optimized	Fresh carbide optimized FA – Axial Blanket included	15.37	2.37E+01	8.06E-02	5.98E+05	2.00	0.84
	Spent carbide optimized FA – axial blanket included	14.17	1.87E+01	6.16E-02	4.98E+05	2.12	0.95
	Axial blanket in spent carbide optimized FA	10.27	2.19E+00	6.45E-03	3.60E+04	2.75	2.14
Oxide optimized	fresh oxide optimized FA – axial blanket included	15.37	2.37E+01	8.06E-02	6.09E+05	2.00	0.83
	Spent oxide optimized FA – axial blanket included	14.11	1.89E+01	6.10E-02	4.98E+05	2.11	0.95
	Axial blanket in spent oxide optimized FA	10.25	2.18E+00	6.42E-03	3.57E+04	2.75	2.15
Oxide HOM4'	Fresh oxide HOM4' FA- axial blanket included	15.37	2.37E+01	8.06E-02	6.09E+05	2.00	0.83
	Spent oxide HOM4' FA – axial blanket included	14.33	3.47E+01	6.80E-02	5.89E+05	1.89	0.86
	Axial blanket in spent oxide optimized FA	10.25	2.18E+00	6.42E-03	3.57E+04	2.75	2.15
Oxide HET1'	fresh oxide optimized FA – axial blanket included	15.37	2.37E+01	8.06E-02	6.09E+05	2.00	0.83
	Spent oxide optimized FA – axial blanket included	14.11	1.89E+01	6.10E-02	4.98E+05	2.11	0.95
	Axial blanket in spent oxide optimized FA	10.25	2.18E+00	6.42E-03	3.57E+04	2.75	2.15
	Spent oxide HET1' radial BA	10.82	1.54E+02	1.95E-01	8.41E+05	1.42	0.76
Oxide HET2'	fresh oxide optimized FA – axial blanket included	15.37	2.37E+01	8.06E-02	6.09E+05	2.00	0.83
	Spent oxide optimized FA – axial blanket included	14.11	1.89E+01	6.10E-02	4.98E+05	2.11	0.95
	Axial blanket in spent oxide optimized FA	10.25	2.18E+00	6.42E-03	3.57E+04	2.75	2.15
	Spent oxide HET2' radial BA	11.20	2.00E+02	2.62E-01	1.11E+06	1.29	0.63

Table 14: FOM results for different diversion targets in the optimized core options (separated Pu only) [6].

[19] Spent fuel parameters are computed assuming a 10 years cooling time.

Core option	Target	If MA is not separated from Pu					
		M (kg)	h (w/kg)	D (Rad/h)	s (n/s/kg)	FOM_1	FOM_2
Carbide optimized	Fresh carbide optimized FA – Axial Blanket included	16.47	2.44E+01	2.05E+00	6.04E+05	1.96	0.80
	Spent carbide optimized FA – axial blanket included	15.03	2.42E+01	7.85E+00	8.74E+06	2.00	-0.29
	Axial blanket in spent carbide optimized FA	10.27	2.23E+00	4.68E-02	3.44E+04	2.75	2.16
Oxide optimized	fresh oxide optimized FA – axial blanket included	16.47	2.44E+01	2.04E+00	6.04E+05	1.96	0.80
	Spent oxide optimized FA – axial blanket included	15.02	2.43E+01	8.31E+00	8.53E+06	2.00	-0.28
	Axial blanket in spent oxide optimized FA	10.26	2.21E+00	4.51E-02	3.40E+04	2.75	2.16
Oxide HOM4'	Fresh oxide HOM4' FA – axial blanket included	17.49	6.50E+01	3.37E+01	9.46E+07	1.56	-1.39
	Spent oxide HOM4' FA – axial blanket included	17.41	7.02E+01	3.05E+01	1.18E+08	1.53	-1.48
	Axial blanket in spent oxide optimized FA	10.26	2.21E+00	4.51E-02	3.40E+04	2.75	2.16
Oxide HET1'	fresh oxide optimized FA – axial blanket included	16.47	2.44E+01	2.04E+00	6.04E+05	1.96	0.80
	Spent oxide optimized FA – axial blanket included	15.02	2.43E+01	8.31E+00	8.53E+06	2.00	-0.28
	Axial blanket in spent oxide optimized FA	10.26	2.21E+00	4.51E-02	3.40E+04	2.75	2.16
	Spent oxide HET1' radial BA	30.03	1.91E+02	2.05E+02	3.75E+08	0.87	-2.22
Oxide HET2'	fresh oxide optimized FA – axial blanket included	16.47	2.44E+01	2.04E+00	6.04E+05	1.96	0.80
	Spent oxide optimized FA – axial blanket included	15.02	2.43E+01	8.31E+00	8.53E+06	2.00	-0.28
	Axial blanket in spent oxide optimized FA	10.26	2.21E+00	4.51E-02	3.40E+04	2.75	2.16
	Spent oxide HET2' radial BA	31.98	2.11E+02	2.96E+02	4.13E+08	0.78	-2.29

Table 15: FOM results for different diversion targets in the optimized core options (Pu and MA mix) [6].

As it can be seen, almost all the FOM1 values are above 1, making all the potential targets attractive to a proliferant State. The only exceptions are the spent oxide HET1' and HET2' radial BAs, if minor actinides were not to be separated from the plutonium. Adding an axial blanket enables more choice for a potential diverter, and these additional targets result in being very attractive according to both figures of merit[20].

5.5 Summary of the material type estimates and overall discussion

The major difference between the optimized cores and the original working horses is the presence of a depleted uranium axial blanket in the driver assemblies. This proved to be sensitive when proliferation resistance is considered. The plutonium isotopic composition in the axial blanket at the end of the irradiation period is particularly attractive for a potential proliferator, being of weapon-grade quality. It has to be noticed that the axial blanket is not a separate item, but is embedded in the irradiated ESFR fuel assembly: in order to divert it, the entire assembly needs to be diverted and only at a subsequent step it could be chopped out and separated from the rest of the assembly. In addition the amount of weapon-grade plutonium in each item is very low, and a proliferator would need to divert at least 8 full irradiated spent fuel assemblies for acquiring one significant quantity. The diversion of 8 spent fuel assemblies would be extremely difficult to conceal effectively, and therefore this scenario would be realistic only in an overt diversion (breakout) strategy.

The analysis conducted by estimating the above-proposed material type measures highlighted how the various core options tended to be roughly equivalent in terms of proliferation resistance. In general the most attractive targets proved to be the fresh fuel assemblies and the irradiated axial blanket.

When minor actinides management was foreseen, neither the homogeneous nor the heterogeneous option proved to influence the attractiveness of the potential diversion targets. The homogeneous and the heterogeneous options have both advantages and disadvantages:

The homogeneous option might improve the radiation barrier of the fresh fuel, making it more difficult to divert. Anyhow, it has to be noticed that the proliferation pathway implied by the diversion of ESFR fresh fuel assemblies would foresee the fabrication of a nuclear weapon device using reactor grade plutonium. The presence of minor actinides in the fresh fuel targets would increase the PR of the system, but it would not be realistic to think that this would stop a proliferant State accepting the challenge of proliferating with reactor-grade plutonium from proliferating adopting this strategy. In addition, the presence of minor actinides in the fresh fuel assemblies would create additional problems for both handling and safeguarding the items, influencing both the operator and the safeguards inspectorate (for a more detailed analysis see [22]).

[20] It has to be recalled that the plutonium resulting from the breeding of the axial blanket is physically contained in the cores spent fuel assemblies.

The heterogeneous option has the advantage to avoid additional problems in handling and safeguarding the fresh fuel assemblies, and at the same time ensures a very proliferation resistant irradiated blanket composition. Indeed, the irradiated blanket assemblies always score among the least attractive targets for a potential proliferator. The main reason is to be found in the high amount of ^{238}Pu in the final composition of the irradiated blanket's plutonium vector guaranteed by the transformations occurring in the minor actinides irradiation. On the other hand, the presence of a radial blanket might allow misuse scenarios that would not have been possible in a core configured without it.

Given the effect of the presence of minor actinides in the radial blanket, in a homogeneous minor actinide management scheme it could be interesting to investigate the possibility to extend the presence of minor actinides to the axial blanket part of the assembly. In this way, there might be the possibility to increase the proliferation resistance of the most sensitive target without deteriorating the overall handling and safeguardability of the fresh fuel items.

6. ESFR general proliferation resistance considerations for the GIF PR&PP proliferation strategies

The analysis so far focused on the analysis of the nuclear material characterization of the potential diversion targets offered by selected ESFR core options. According to [7] there are four main proliferation strategies:

Concealed diversion: diversion of at least 1 SQ of nuclear material without being detected by nuclear safeguards.

- Concealed production of nuclear material: undeclared production of at least 1 SQ of nuclear material without being detected by nuclear safeguards.
- Breakout: overt diversion or production of of at least 1 SQ of nuclear material, with no effort for going undetected.
- Production in clandestine facilities: undeclared production of at least 1 SQ of nuclear material in undeclared – and therefore unsafeguarded – nuclear facilities.

The following paragraphs briefly discuss the potential impact of the core options under analysis on the above strategies, along the lines of [15].

6.1 Concealed diversion

The oxide reference fresh core foresees a load of 11.6 tons of Pu and the carbide one foresees a load of 8.5 tons of Pu [23]. Each fresh oxide reference FA contains an average of 25.6 kg of Pu and each fresh carbide reference FA contains an average of 20.5 kg of Pu[21], resulting respectively in 3.2 and 2.6 significant quantities (SQs) of Pu. The number of significant quantities in the fuel assemblies does not change significantly with burn-up, resulting in all the ESFR reference FAs (either fresh or irradiated, oxide or carbide) containing more than 1 SQ of reactor-grade plutonium. Within the reference cores, the fresh oxide reference FA and the fresh carbide reference FA are the most attractive for a potential proliferation, due to their lower radiation emission. The fresh ESFR fuel assemblies would represent a more attractive diversion target than typical spent light water reactor FAs mainly thanks to the higher quantity of SQ per assembly9 and the absence of fission products. The Spent oxide and carbide reference FA would still represent a more attractive diversion target than a typical LWR spent FA due to the formers' higher Pu content.

As highlighted by [10], "handling methods for fresh fuel assemblies may depend significantly on minor actinide content (homogeneous recycle or heterogeneous recycle concentrated minor actinide targets)"[22]. MA-bearing fresh fuel, as in the case of fresh oxide HOM4 FAs, has a higher radiation emission, making the handling of the fuel assemblies more complicated. Although the higher radiological barrier might increase the proliferation resistance[23] of the fresh oxide HOM4 FAs compared to the oxide reference FAs, the formers are more difficult to fabricate and might bring in new measurement challenges for the safeguards inspectors. Moreover, depending on MA content, the ESFR system might need an on-site assembly shop which, despite radiation levels, may provide avenues for concealed introduction of fertile materials [6]. This, combined with a more complicated safeguardability, would potentially enable an easier concealed diversion of nuclear material.

The presence of MA in the fertile radial blanket assemblies (as in the case of the fresh oxide HET2 radial BAs) might constitute a proliferation resistance feature and might provide additional technical difficulty to potential proliferators. Thanks to the presence of Np in the MA composition, the irradiation of the fresh oxide HET2 radial BA results in a very high ^{238}Pu content. Thanks to the heat generated by ^{238}Pu, it constitutes an important proliferation barrier in terms of nuclear material attractiveness.

Both ESFR oxide and carbide optimized core options foresee the presence of a lower axial blanket in the fresh optimized FA made of depleted uranium. This, when irradiated, will result in weapon-grade Pu. The amount of WG-Pu contained in each spent oxide (carbide) optimized FA is very small, and several FAs would have to be diverted to obtain one SQ of Pu (8 spent oxide optimized FAs or 10 spent carbide optimized FAs). The amount of FAs needed to divert one significant quantity of weapon-grade plutonium makes this scenario very likely to be detected by safeguards verifications.

[21] These values are calculated using the data in [23].

[22] [10], Section 4.1.

[23] Although PR might be increased by the higher radiological barrier, its effectiveness in deterring a potential proliferator from diverting the target is debatable. For a discussion on this topic see [22].

Core option	Most attractive target (NM quality)	Most attractive target (overall)
Carbide reference	Fresh carbide reference FA	
Oxide reference	Fresh oxide reference FA	
HOM4	Fresh oxide HOM4 FA	
HET2	Fresh oxide reference FA	
Carbide optimized	Axial blanket in spent carbide optimized FA	Fresh carbide optimized FA
Oxide optimized	Axial blanket in spent oxide optimized FA	Fresh oxide optimized FA
HOM4'	Axial blanket in spent oxide HOM4' FA	Fresh oxide optimized FA
HET1'	Axial blanket in spent oxide optimized FA	Fresh oxide optimized FA
HET2'	Axial blanket in spent oxide optimized FA	Fresh oxide optimized FA

Table 16: Most attractive diversion targets for a concealed diversion strategy for the analyzed core options.

Table 16 summarizes the most attractive diversion targets for a concealed diversion strategy in the analyzed core options of Figure 3.

Irrespective of the core option, the sodium environment in many system elements represents a challenge to nuclear safeguards activities. Due to the sodium being visually opaque, new methods might be needed to identify and monitor fuel assemblies.

6.2 Concealed production of nuclear material (misuse)

There are multiple possibilities for misusing a system, and therefore there are many different possible pathway combinations. Generally a misuse strategy has the objective to produce a better-than-available fissile material quality (in this case weapon-grade plutonium) or a higher quantity of a given (already available) material quality.

For the carbide and oxide reference, oxide HOM4 and oxide HET2 core options, producing undeclared fissile material by irradiating fertile material in inner, outer and blanket regions of the ESFR core might be a potentially attractive misuse strategy. The fertile material might be introduced either by replacing a FA in the inner or outer core region with a fertile target assembly or by putting it just above or beneath the active part of an ordinary FA.

For the carbide and oxide optimized, HOM4', HET1' and HET2' cores, the plutonium available in the irradiated axial blanket is already weapon-grade, making the concealed production of nuclear material aimed at producing a higher quantity of high-quality nuclear material. The ESFR axial blanket is distributed over all the fresh fuel assemblies, resulting in having only a small part of the assembly containing weapon-grade plutonium. This would require the diversion of several assemblies to acquire one significant quantity of weapon-grade plutonium. Trying to misuse the optimized reactor core to end up with a single element containing one or more significant quantities might represent a potentially attractive scenario. From this point of view, the ESFR system doesn't present peculiarities making it substantially different from other existing sodium fast reactors, and therefore its behavior in a misuse scenario would be similar to any other SFR.

6.3 Breakout

Fresh carbide and oxide reference FAs contain on average 3.2 and 2.6 SQ of plutonium respectively. Thus, a breakout scenario would see the availability of a huge amount of significant quantities readily available for diversion. However this material would be reactor grade Pu and not weapon-grade Pu, i.e. less than ideal for a weapon programme. The major concern posed by a breakout strategy would be the huge production capability of Pu of any desired quality, and the key parameter to assess would be its proliferation time.

When the optimized core options are considered, in addition of the potential given by the reference core options, the proliferator would have a huge inventory of weapon-grade plutonium in the FA's axial blanket ready to be diverted and further processed. This would pose a serious proliferation concern to be carefully investigated and mitigated. The possibility to include an adequate fraction of MA in the axial blanket might increase the overall proliferation resistance of the system when an overt diversion strategy is considered.

6.4 Production in clandestine facilities

As highlighted by [10] and recalled in [15] the sodium fast reactor technology does not seem to be the most suitable one to be replicated in a clandestine facility. The intrinsic difficulties connected with the presence of a sodium environment, together with the overkilling dimensions of a fully-fledged commercial power reactor makes the ESFR a very unlikely candidate for clandestine replication.

7. Conclusions

Within the CP-ESFR project, 25 European partners developed R&D solutions for a European Sodium Fast Reactor concept. In this framework, a specific task led by JRC-ITU, with contributions of AREVA, EdF and ENEA addressed

proliferation resistance issues The aim of this task was to propose an approach to evaluate the level of protection of a given nuclear power plant (NPP) design with respect to nuclear proliferation.

Following the GIF White Paper Structure [10], information has been collected for the two CP-ESFR working horses and related core concepts with emphasis on features relevant for PR. Both loop and pool working horses share the same core options. A detailed material type PR analysis of the available potential diversion targets of selected core options has been carried out, together with high-level considerations on the PR of the various core options with respect to the four proliferation strategies foreseen by the GIF PR&PP EM (concealed diversion, concealed misuse, breakout and undeclared production of nuclear material in clandestine facilities).

From a PR point of view the two working horses options (pool or loop) are equivalent, provided that they are considered with the same core option, i.e. oxide (with or without MA) or carbide. The main common features of the considered core options are the following:

- Use of reactor grade Pu as feed;
- High fuel burn-up;
- Possibility of including MA in the fuel for MA management.

All the reference core options (carbide reference, oxide reference, HOM4, HET2) are mainly equivalent from a material type point of view. In the case of the HOM4 and HET2 core options, the addition of MA to the fuel and/or blankets might constitute a proliferation resistance feature and might provide additional technical difficulty to potential proliferators. This is remarkably true in the case of radial blanket fuel elements (HET2), where the produced plutonium would contain a very high fraction of ^{238}Pu, making it less than ideal for a nuclear military programme in light of its high heat generation.

Also the optimized core options (carbide and oxide optimized, HOM4', HET1' and HET2') are mainly equivalent among themselves. When compared to the reference, HOM4 and HET2 options, the main difference is the presence of an axial blanket in the optimized spent fuel assemblies. This, when irradiated, contains weapon-grade plutonium. Given the size of the foreseen axial blanket region at least 8 spent oxide optimized FAs (or 10 spent carbide optimized FAs) need to be diverted to obtain 1 SQ of weapon-grade plutonium. In case of a breakout proliferation strategy, where an overt diversion is among the proliferator's possibilities, the presence of weapon-grade plutonium in the FAs' axial blanket, readily available for diversion and further processing would represent a major proliferation concern. When homogeneous minor actinides management is considered, the extension of the presence of minor actinides to the axial blanket might prove to be effective in increasing the proliferation resistance of the most sensitive diversion target without degrading the overall system's safeguardability.

Beyond the potential attractiveness of the existing nuclear material diversion targets, the possibility to misuse the reactor to irradiate fertile targets for the concealed production of undeclared Pu remains, and needs to be addressed with appropriate safeguards measures and controls. In case of an overt (breakout) misuse strategy, a Sodium Fast Reactor core physics will allow a huge Pu production capability of any desired quality.

8. Acknowledgments

The CP-ESFR project was carried out under the aegis of the 7th Framework Programme in the area of Advanced Nuclear Systems. Although led by JRC-ITU, the project activities summarized in this paper saw the contribution and the review of several people from many organizations. Thanks are due to D. VERRIER (AREVA), L. VAN DEN DURPEL (AREVA); F. BEAUDOIN (EDF), C. MEUWISSE (EDF); F. PADOANI (ENEA), P. PEERANI (JRC-ITU) and F. SEVINI (JRC-ITU).

The authors would also like to thank R. JUNGWIRTH (JRC-ITU) and L.K. KIM (JRC-ITU) for the precious comments and discussions on this work.

The work is entirely based on the JRC Science and Policy Report EUR 26996.

9. References

[1] The Collaborative Project for a European Sodium fast Reactor (CP-ESFR). http://www.cp-esfr.eu/.

[2] Fiorini, G.L. et al. European Commission — 7th Framework Programme, The Collaborative Project on European Sodium Fast Reactor (CP ESFR). In *Proceedings of ICAPP'09*. 2009.

[3] Vasile, A., Fiorini, G.L., et al. The Collaborative Project for a European Sodium Fast Reactor — CP ESFR. In *Proceedings of ICAPP'2011*. 2011.

[4] European Commission. Seventh Framework Programme (FP7) - Tomorrow's Answers Start Today. http://ec.europa.eu/research/fp7/pdf/fp7-factsheets_en.pdf.

[5] Fiorini, G.L. and Vasile, A. European Commission–7th Framework Programme: The Collaborative Project on European Sodium Fast Reactor (CP ESFR). *Nuclear Engineering and Design*, volume 241, no. 9:pp. 3461–3469, 2011.

[6] Fatih, A., Renda, G., Cojazzi, G.G.M., Peerani, P., and Sevini, F. *Considerations of Proliferation Resistance Concerns*. Technical Report SP3.2.5 D5, CP-ESFR, 2012.

[7] PRPP Working Group. *Evaluation Methodology for Proliferation Resistance and Physical Protection of Generation IV Nuclear Energy Systems — Revision 6*. Generation IV International Forum (GIF), 2011.

[8] PRPP Working Group. *Addendum to the Evaluation Methodology for Proliferation Resistance and Physical Protection of Generation IV Nuclear Energy Systems*. GIF/PRPPWG/2006/005-A. Generation IV International Forum (GIF), 2007.

[9] International Atomic Energy Agency (IAEA). *Guidance for the Application of an Assessment Methodology for Innovative Nuclear Energy Systems, INPRO Manual — Proliferation Resistance Volume 5 of the Final Report of Phase 1 of the International Project on Innovative Nuclear Reactors and Fuel Cycles (INPRO)*. IAEA-TECDOC-1575 Rev.1. IAEA, 2008.

[10] PRPP Working Group and System Steering Committees of the Generation IV International Forum. *Proliferation Resistance and Physical Protection of the Six Generation IV Nuclear Energy Systems*. GIF/PRPPWG/2011/002. GIF, 2011.

[11] Pellaud, B. Proliferation aspects of plutonium recycling. *Comptes Rendus Physique*, volume 3, no. 7:pp. 1067–1079, 2002.

[12] Kessler, G., Broeders, C., Hoebel, W., Goel, B., and Wilhelm, D. A new scientific solution for preventing the misuse of reactor-grade plutonium as nuclear explosive. *Nuclear Engineering and Design*, volume 238, no. 12:pp. 3429–3444, 2008.

[13] Bathke, C.G., Ebbinghaus, B.B., Collins, B.A., Sleaford, B.W., Hase, K.R., Robel, M., Wallace, R.K., Bradley, K.S., Ireland, J.R., Jarvinen, G.D., Bradley, K.S., Ireland, J.R., Johnson, M.W., Prichard, A.W., and Smith, B.W. The attractiveness of materials in advanced nuclear fuel cycles for various proliferation and theft scenarios. *Nuclear Technology*, volume 179, no. 1:pp. 5–30, 2012.

[14] Alim, F., Cojazzi, G.G.M., and Renda, G. The collaborative project on the European sodium fast reactor and its proliferation resistance evaluation. In *Proceedings of the European Nuclear Conference 2012, Manchester, 9-12 December 2012*. 2012.

[15] Alim, F., Cojazzi, G.G.M., and Renda, G. Proliferation Resistance Considerations within the Collaborative Project for a European Sodium Fast Reactor. In *Proceedings of the 35th ESARDA ANNUAL MEETING*. 2013.

[16] Buiron, L. *CP ESFR Working Horses Core Concept Definition*. Technical Report SP2.1.2.D1, CP-ESFR, 2009.

[17] Martín-Fuertes, F., Pérez-Martín, S., Álvarez-Velarde, F., Villamarín, D., Krepel, J., Mikityuk, K., Corsetti, E., Polidoro, F., Vimercati, G., Ochoa, R., García-Herranz, N., Aragonés, J.M., Scholer, A.C., and Verrier, D. *Transmutation options assessment*. Technical Report SP2.1.4.D1, CP-ESFR, 2011.

[18] Villedieu, A., Augem, J.M., Genot, J.S., Lavallez, R., and Prèle, G. *Comparison between Pool and Loop Type Work Horses Concepts*. Technical Report SP4.1.D3, CP-ESFR, 2010.

[19] International Atomic Energy Agency (IAEA). *IAEA Safeguards Glossary*. Number 3 in International Nuclear Verification Series. IAEA, 2002.

[20] Sunderland, R., Sheth, V., Buiron, L., Tetart, P., Massara, S., Tsige-Tamirat, H., Rineiski, A., Vezzoni, B., Gabrielli, F., Marchetti, M., Zhang, D., Flad, M., Maschek, W., Krepel, J., Sun, K., and Mikityuk, K. *ESFR cores with optimized characteristics interim report*. Technical Report SP2.1.5.D1, CP-ESFR, 2012.

[21] The National Academy of Science (NAS). *The Spent Fuel Standard for Disposition of Excess Weapon Plutonium - Application to Current DOE Options*. The National Academy Press (NAP), 2000.

[22] Renda, G., Alim, F., Cojazzi, G.G.M., and Peerani, P. Material Type and Safeguardability Considerations for Innovative Sodium Fast Reactors Fuel including Different Minor Actinides Compositions. In *Proceedings of the INMM-53rd Annual Meeting*. 2012.

[23] Krepel, J., Mikityuk, K., Huml, O., Tsige-Tamirat, H., Ammirabile, L., Blanchet, D., and Polidoro, F. *Working Horses ESFR Core Concepts Calculations Neutronic and Thermal-hydraulic Characteristics*. Technical Report SP2.1.2.D2, CP-ESFR, 2010.

LC-AB-14-052-EN-N